Distribution Agreement

In presenting this thesis or dissertation as a partial fulfillment of the requirements for an advanced degree from Emory University, I hereby grant to Emory University and its agents the non-exclusive license to archive, make accessible, and display my thesis or dissertation in whole or in part in all forms of media, now or hereafter known, including display on the world wide web. I understand that I may select some access restrictions as part of the online submission of this thesis or dissertation. I retain all ownership rights to the copyright of the thesis or dissertation. I also retain the right to use in future works (such as articles or books) all or part of this thesis or dissertation.

Signature:

4/20/2022

Jillian Dunbar Date

Exploring the Temperature and Rainfall Influence on Malaria Prevalence in Ethiopia due to Climate Change

By

Jillian Dunbar

Master of Public Health

Epidemiology

_____

Dr. Christine Moe

Committee Chair

Exploring the Temperature and Rainfall Influence on Malaria Prevalence in Ethiopia due to Climate Change

By

Jillian Dunbar

B.S., The University of Alabama, 2020

B.A., The University of Alabama, 2020

Thesis Committee Chair

Christine Moe, Ph.D.

An abstract of

A thesis submitted to the Faculty of the

Rollins School of Public Health of Emory University

in partial fulfillment of the requirements for the degrees of

Master of Public Health

in Epidemiology

2022

Abstract

Exploring the Temperature and Rainfall Influence on Malaria Prevalence in Ethiopia due to Climate Change

By Jillian Dunbar

INTRODUCTION: Climate change is a continuing phenomenon that is negatively impacting the environment of pathogens, vectors, and humans. As many factors are influenced by climate change, the uncertainty surrounding the future burden of infectious diseases, particularly vector-borne diseases, intensifies. The impact of rainfall changes on malaria is ambiguous as it has been difficult for researchers to predict increases and decreases of rainfall in specific areas, and the current rainfall patterns are essential to understand the extent of rainfall changes. The temperature has been easier to assess—temperature increases are strongly linked to creating optimal environmental conditions for Plasmodium to develop faster and increase transmission; yet, as temperatures continue to increase the mosquito itself becomes negatively impacted by the heat. OBJECTIVE: The objective of this research was to explore the effect of two important climatic variables—temperature and rainfall—on the prevalence of malaria in Ethiopia. Comparing data from 2011 and 2015 allowed for a short-term observation of the impact of climate change on the prevalence of malaria in nine geographic regions. METHODS: Descriptive and analytical methods were used to address the research question. Plotting rainfall and temperature across varying time scales was used to visualize temporal changes in average rainfall and temperature; R^2 values for lines of best fit were applied to these plots. A log-binomial regression model was used to examine the prevalence rate of individuals testing positive for a malaria antigen test with every one-millimeter increase in rainfall or with every one-degree increase in temperature. RESULTS: Changes in both temperature and rainfall patterns were observed in Ethiopia from 1981 to 2019—rainfall and temperature generally increased in most regions. Minimal changes in rainfall and temperature were observed between 2011 and 2015 within the same regions; though, larger differences were seen between the geographic regions in Ethiopia. There was a statistically significant association between temperature and cluster prevalence ratios in 2011 for three antigens, but only one antigen in 2015. There were no significant associations between rainfall and cluster prevalence ratios in either year. CONCLUSION: For certain species of Plasmodium, increasing average temperature may be reducing the prevalence ratios of malaria. Overall, more research needs to be conducted to determine the significance of long-term climate change on the prevalence of malaria in Ethiopia. Furthermore, the impact of climate change on the burden of malaria on a larger geographic scale needs to be investigated.

Exploring the Temperature and Rainfall Influence on Malaria Prevalence in Ethiopia due to Climate Change

By

Jillian Dunbar

B.S., The University of Alabama, 2020

B.A., The University of Alabama, 2020

Thesis Committee Chair:

Christine Moe, Ph.D.

A thesis submitted to the Faculty of the

Rollins School of Public Health of Emory University

in partial fulfillment of the requirements for the degrees of

Master of Public Health

in Epidemiology

2022

Acknowledgements

This thesis would not have been possible without the help and support from mentors, family, and friends.

To my thesis advisor, Dr. Christine Moe, for providing me with invaluable guidance and support every week for months leading up to the submission of this thesis. Your knowledge and input were critical in shaping this project.

To Stephen Hilton, for assisting me with the R coding for the maps and statistical analysis of my results section. I greatly appreciate the support and help to troubleshoot the many errors I came across. Your knowledge of all things mapping was an irreplaceable source of help!

To Dr. Marissa Grossman and Ian Hennessee for your insight on malaria and for helping me plan my next steps during the analysis and discussion of the research.

To Dr. Gabriel Ponce de Leon and the members of the Malaria Indicator Surveys in 2011 and 2015, for allowing me to work with this data and for collecting all the data in the first place for my research questions. This project would not have been possible without the data collected through their tireless efforts.

To my parents and my sister for their endless support and confidence in me. I would not be at Emory without their constant love and guidance. Thank you for always being there for me!

To Emily, for listening to all the problems that seemed to arise with this thesis and reading parts of it too. The moral support and edits were much appreciated. To Toba, for supplying me with all the coffee while I am currently writing this section of my thesis.

Abbreviations

ACT → Artemisinin-Based Combination Therapy

An. → *Anopheles*

C → Celsius

CDC → Centers for Disease Control and Prevention

CHIRPS → Climate Hazards Center Infrared Precipitation with Station

ChPvMSP1 → Chimeric *P. vivax* Merozoite Protein 1

DALY → Disability-Adjusted Life Years

DBS → Dried Blood Spot

EA → Enumeration Areas

F → Fahrenheit

GBD → Global Burden of Disease

GPS → Global Positioning System

GST → Glutathione-S-Transferase

IgG → Immunoglobulin G

IPT → Intermittent Preventive Therapy

IRS → Individual Residual Spray

ITN → Insecticide-Treated Bed Nets

LMIC → Low- and Middle-Income Country

MBD → Mosquito Borne Disease

MDG → Millennium Development Goals

MERG → Monitoring and Evaluation Working Group

MFI → Mean Fluorescence Intensity

MIS → Malaria Indicator Survey

Mosq# Sal → Mosquito Salivary Peptide

P. → *Plasmodium*

PfAMA1→ *P. falciparum* Apical Membrane Antigen 1 (N-Terminal Region)

PfCSP → *P. falciparum* Circumsporozoite

PfETRAMP5Ag1 → *P. falciparum* Etramp 5 Antigen 1

PfGLURPR0 → *P. falciparum* Glutamate-Rich Protein, Ro Fragment

PfLSA1 → *P. falciparum* Liver Stage Antigen 1

PfMPS1 → *P. falciparum* Merozoite Protein 1

PfSEA1 → *P. falciparum* Schizont Egress Antigen

PmMSP1 → *P. malariae* Merozoite Protein 1

PoMSP1 → *P. ovale* Merozoite Protein 1

PvAMA1 → *P. vivax* Apical Membrane Antigen 1

PvMSP1 → *P. vivax* Merozoite Protein 1

RBC → Red Blood Cells

RDT → Rapid Diagnostic Test

RPC → Representative Concentration Pathway

SNNPR → Southern Nations, Nationalities, And People's Region

$\boldsymbol{T_{max}}$ **→** Maximum Temperature

UNDP → United Nations Development Programme

UNICEF → United National Children's Fund

WHO → World Health Organization

Glossary of Terms

Anopheles → a taxonomic genus within the family *Culicidae*; any of a genus (*Anopheles*) of mosquitoes that can carry and transmit various diseases, esp. malaria. [1]

Anthropophilic → in parasitology, anthropophilia is a preference of a parasite for humans over other animals. Contrasting to parasites that prefer non-human hosts—are described as zoophilic.[2]

CHIRPS → Climate Hazards Group InfraRed Precipitation with Station data (CHIRPS) is a 35+ year quasi-global rainfall data set. Spanning 50°S-50°N (and all longitudes) and ranging from 1981 to near-present, CHIRPS incorporates our in-house climatology, CHPclim, 0.05° resolution satellite imagery, and in-situ station data to create gridded rainfall time series for trend analysis and seasonal drought monitoring. [3]

CHIRTS → CHIRTSmax is a global 2-m maximum temperature (Tmax) product that directly combines satellite and station-based estimates of Tmax to produce routinely updated data to support the monitoring of temperature extremes. The basic idea behind CHIRPS was to produce a data set suitable for monitoring weather extremes in areas with limited in situ observations. [4]

Climate → weather of a specific region averaged over a long period of time; climate change refers to long-term changes. The average course or condition of the weather at a place usually over a period of years as exhibited by temperature, wind velocity, and precipitation. [5],[6]

Duffy Glycoprotein → a receptor for chemicals that are secreted by blood cells during inflammation. It also serves as a receptor for *P. vivax*; red blood cells that lack the Duffy antigens are relatively resistant to invasion by *P. vivax*. [7]

Enumeration Areas → An enumeration area is a unit of land delineated for the purpose of enumerating housing units and populations without omission and duplication. An EA usually consists of 150– 200 households in rural areas and 150–200 housing units in urban centers. [8]

Gametocyte → Some of the infected blood cells leave the cycle of asexual multiplication. Instead of replicating, the merozoites in these cells develop into sexual forms of the parasite, called gametocytes, that circulate in the bloodstream. When a mosquito bites an infected human, it ingests the gametocytes, which develop further into mature sex cells called gametes. [9]

---

[1] "Anopheles." *ANOPHELES | Definition in the Cambridge English Dictionary*, https://dictionary.cambridge.org/us/dictionary/english/anopheles.
[2] "Anthropophilic." *Biology Articles, Tutorials & Dictionary Online*, 1 Mar. 2021, https://www.biologyonline.com/dictionary/anthropophilic.
[3] "CHIRPS: Rainfall Estimates from Rain Gauge and Satellite Observations." *Climate Hazards Center - UC Santa Barbara*, USAID, https://www.chc.ucsb.edu/data/chirps.
[4] "CHIRTSmonthly." *Climate Hazards Center - UC Santa Barbara*, USAID, https://www.chc.ucsb.edu/data/chirtsmonthly.
[5] "Climate Definition & Meaning." *Merriam-Webster*, Merriam-Webster, https://www.merriam-webster.com/dictionary/climate.
[6] "What Is the Difference between Weather and Climate Change?" *What Is the Difference between Weather and Climate Change? | U.S. Geological Survey*, https://www.usgs.gov/faqs/what-difference-between-weather-and-climate-change#:~:text=Weather%20refers%20to%20short%20term,refers%20to%20long%2Dterm%20changes.
[7] Dean L. Blood Groups and Red Cell Antigens [Internet]. Bethesda (MD): National Center for Biotechnology Information (US); 2005. Chapter 9, The Duffy blood group. Available from: https://www.ncbi.nlm.nih.gov/books/NBK2271/
[8] *Malaria Indicator Surveys - Access to Malaria Indicator ...* https://www.malariasurveys.org/documents/Ethiopia_MIS_2015.pdf.
[9] "Malaria Parasite Life Cycle." *PATH's Malaria Vaccine Initiative*, 20 May 2021, https://www.malariavaccine.org/malaria-and-vaccines/vaccine-development/life-cycle-malaria-parasite.

Hypnozoite → The sporozoites pass quickly into the human liver. Hypnozoites are dormant forms in the life cycles of certain *Plasmodium* species; they are associated with the latency and relapse in human malarial infections caused by *Plasmodium ovale* and *P. vivax.* [10]

Kebele → a small administrative unit in Ethiopia. [11]

Malaria Lifecycle → The malaria parasite develops both in humans and in the female *Anopheles* mosquitoes. The parasite also changes through several life stages even while in the human host, presenting different antigens at different stages of its life cycle. [12]

Merozoite → the parasite is released from the liver in the form of merozoites. They travel through the heart and reach the lungs, settling in the lung capillaries. Eventually, the merozoites enter the blood phase of their development. In the bloodstream, the merozoites invade RBCs and multiply again until the cells burst. Then they invade more erythrocytes. This cycle is repeated, causing fever each time parasites break free and invade blood cells. [13]

National Ethiopian Malaria Indicator Survey → evaluates the coverage of key malaria control interventions and assesses progress toward national strategic goals. [14]

Nephrotic Syndrome → a kidney disorder that causes the body to pass too much protein into the urine. This syndrome has been reported in the infection by *P. falciparum*, but it is usually rare. [15],[16]

Plasmodium → a protozoan parasite that are the causative organisms of malaria. *Plasmodium* infects the red blood cells in mammals, typical in tropical and temperate zones. The parasite is transmitted by the bite of the female *Anopheles* mosquito. Five species cause human malaria: *P. vivax*, *P. ovale*, *P. falciparum*, *P. malariae*, and *P. knowlesi*.[17]

Schizont → The sporozoites multiply asexually in the liver cells over the next 7 to 10 days, causing no symptoms. The sporozoites mature into schizonts in the liver; the schizonts contain hemozoin-an insoluble iron-which is formed as they feed on hemoglobin from the RBCs. [18]

---

[10] Markus, Miles B. "Malaria: origin of the term "hypnozoite"." *Journal of the history of biology* vol. 44,4 (2011): 781-6. doi:10.1007/s10739-010-9239-3

[11] "Kebele Definition and Meaning: Collins English Dictionary." *Kebele Definition and Meaning | Collins English Dictionary*, HarperCollins Publishers Ltd, https://www.collinsdictionary.com/us/dictionary/english/kebele.

[12] "Malaria Parasite Life Cycle." *PATH's Malaria Vaccine Initiative*, 20 May 2021, https://www.malariavaccine.org/malaria-and-vaccines/vaccine-development/life-cycle-malaria-parasite.

[13] Baer K, Klotz C, Kappe SH, et al. Release of hepatic *Plasmodium yoelii* merozoites into the pulmonary microvasculature. *PLoS Pathogens*. 2007;(11): e171.

[14] *Ethiopia Malaria Indicator Survey (MIS) - Carter Center*. https://www.cartercenter.org/resources/pdfs/news/health_publications/malaria/Ethiopia_MIS-2007_Technical_Summary.pdf.

15 "Nephrotic Syndrome." Mayo Clinic, Mayo Foundation for Medical Education and Research, 23 Feb. 2022, https://www.mayoclinic.org/diseases-conditions/nephrotic-syndrome/symptoms-causes/syc-20375608#:~:text=Nephrotic%20syndrome%20is%20a%20kidney,excess%20water%20from%20your%20blood.

16 Silva, Geraldo Bezerra da Junior et al. "Kidney involvement in malaria: an update." Revista do Instituto de Medicina Tropical de Sao Paulo vol. 59 (2017): e53. doi:10.1590/S1678-9946201759053

[17] "Plasmodium." *Encyclopedia Britannica*, Encyclopedia Britannica, Inc., https://www.britannica.com/science/Plasmodium-protozoan-genus.

[18] "Malaria Parasite Life Cycle." *PATH's Malaria Vaccine Initiative*, 20 May 2021, https://www.malariavaccine.org/malaria-and-vaccines/vaccine-development/life-cycle-malaria-parasite.

Sporozoite → Malaria infection begins when an infected female *Anopheles* mosquito bites a person, injecting *Plasmodium* parasites, in the form of sporozoites, into the bloodstream. [19]

Trophozoite → When the sporozoites reach the liver cells of the human host they transform into trophozoites. The trophozoite is the active, amoeboid cell form of the *Plasmodium*. It loses its apical complex and surface coat. The trophozoite invades the vacuole of the hepatocyte where they go through schizogonic development. [20]

Vector-Borne Diseases → Vector-borne diseases are human illnesses caused by parasites, viruses, and bacteria that are transmitted by vectors. Vectors are living organisms that can transmit infectious pathogens between humans, or from animals to humans. Many of these vectors are bloodsucking insects, which ingest disease-producing microorganisms during a blood meal from an infected host and later transmit it to a new host after the pathogen has replicated. [21]

Weather → short-term atmospheric conditions. The state of the atmosphere with respect to heat or cold, wetness or dryness, calm or storm, clearness or cloudiness. [22],[23]

Zoophilic → having an attraction to or preference for animals; especially, the preference of an insect, preferring animals to humans as a source of food. [24]

---

[19] "Malaria Parasite Life Cycle." *PATH's Malaria Vaccine Initiative*, 20 May 2021, https://www.malariavaccine.org/malaria-and-vaccines/vaccine-development/life-cycle-malaria-parasite.
[20] "Trophozoite." *Biology Articles, Tutorials & Dictionary Online*, 26 Feb. 2021, https://www.biologyonline.com/dictionary/trophozoite.
[21] "Vector-Borne Diseases." *World Health Organization*, World Health Organization, https://www.who.int/news-room/fact-sheets/detail/vector-borne-diseases.
[22] "What Is the Difference between Weather and Climate Change?" *What Is the Difference between Weather and Climate Change? | U.S. Geological Survey*, https://www.usgs.gov/faqs/what-difference-between-weather-and-climate-change#:~:text=Weather%20refers%20to%20short%20term,refers%20to%20long%2Dterm%20changes.
[23] "Weather Definition & Meaning." *Merriam-Webster*, Merriam-Webster, https://www.merriam-webster.com/dictionary/weather.
[24] "Zoophilic Definition & Meaning." *Merriam-Webster*, Merriam-Webster, https://www.merriam-webster.com/dictionary/zoophilic#:~:text=Definition%20of%20zoophilic,as%20a%20source%20of%20food.

TABLE OF CONTENTS

LIST OF FIGURES AND TABLES

LITERATURE REVIEW

Infectious Disease: Malaria

Overview of Malaria: Malaria is a disease caused by the parasite genus *Plasmodium*, with multiple species, including *falciparum, malariae, vivax, ovale,* and *knowlesi.* The parasite is transmitted to humans through the bite of an *Anopheles* mosquito, and this is the only species of mosquito that can spread malaria[25]. The disease severity depends on the species of *Plasmodium* the individual is infected with; however, the outcome can range from as little as fatigue and fever to death[26]. Currently, there are around 430 *Anopheles* species, but only 30-40 of these species can transmit malaria; the other species either do not frequently bite humans or the vectors are unable to sustain the parasite[27]. Apart from Antarctica, *Anopheles* mosquitoes are found on every continent. Historically, malaria has had well-defined geographical boundaries--different species of *Plasmodium* surviving in their respective geographical environments. However, as humidity, temperature, rainfall, and other climatic characteristics shift due to climate change, the geographic distribution of malaria-causing *Anopheles* species has been changing, and in some areas, the disease has been reintroduced in regions where malaria was previously eradicated[28]. Increasing temperature and humidity provide beneficial growth conditions for the parasite in the mosquitoes. The two most effective malaria mosquito vectors in Africa are *An. gambiae* and *An. funestus*. These two species tend to be anthropophilic, meaning they prefer to feed on humans, as opposed to zoophilic mosquitoes, which would rather feed on cattle, amphibians, birds, primates, and other animals[29].

[25] "Causes." *Stanford Health Care (SHC) - Stanford Medical Center*, 16 Jan. 2019, https://stanfordhealthcare.org/medical-conditions/primary-care/malaria/causes.html.
[26] "Symptoms." *Stanford Health Care (SHC) - Stanford Medical Center*, 16 Jan. 2019, https://stanfordhealthcare.org/medical-conditions/primary-care/malaria/symptoms.html.
[27] "CDC - Malaria - about Malaria - Biology." Centers for Disease Control and Prevention, Centers for Disease Control and Prevention, 16 July 2020, https://www.cdc.gov/malaria/about/biology/index.html.
[28] "CDC - Malaria - about Malaria - Biology." Centers for Disease Control and Prevention, Centers for Disease Control and Prevention, 16 July 2020, https://www.cdc.gov/malaria/about/biology/index.html.
[29] "CDC - Malaria - about Malaria - Biology." Centers for Disease Control and Prevention, Centers for Disease Control and Prevention, 16 July 2020, https://www.cdc.gov/malaria/about/biology/index.html.

Species of *Plasmodium:* Four of the five species of *Plasmodium* are found in parts of Africa; *P. knowlesi* is exclusively found throughout Southeast Asia and will not be further discussed in this paper. *P. falciparum* is one of the species that predominate throughout Africa, causing severe malaria because of its typical rapid amplification of the parasite in the bloodstream of its host which results in severe anemia. Furthermore, this parasite is known to block blood vessels and blood flow which, if this happens in the brain, the consequent cerebral malaria can be fatal[30]. *P. vivax* is only found in certain parts of Africa, including Ethiopia[31]. This species, along with *P. ovale*, are threatening because they have a dormant phase which can cause the infection to be latent for numerous months or years after the infecting mosquito bite[32]. Moreover, *P. ovale* is alarming because even individuals who are negative for the Duffy glycoprotein are susceptible to *P. ovale*. Individuals who are negative for the Duffy glycoprotein lack the receptor necessary for *P. vivax* to attach to their red blood cells (RBCs)[33]; however, *P. ovale* has found a way to still infect the RBCs regardless of an individual's lack of the Duffy glycoprotein. Lastly, *P. malariae* is found worldwide, and if left untreated, the parasite will cause a chronic infection, typically lasting the rest of the individual's life. In certain individuals, *P. malariae* will cause their kidneys to eliminate too much protein in their urine: nephrotic syndrome[34].

[30] "CDC - Malaria - about Malaria - Biology." *Centers for Disease Control and Prevention*, Centers for Disease Control and Prevention, 16 July 2020, https://www.cdc.gov/malaria/about/biology/index.html.
[31] Twohig, Katherine A., et al. "Growing Evidence of Plasmodium Vivax across Malaria-Endemic Africa." *PLOS Neglected Tropical Diseases*, Public Library of Science, https://journals.plos.org/plosntds/article?id=10.1371%2Fjournal.pntd.0007140.
[32] "CDC - Malaria - about Malaria - Biology." *Centers for Disease Control and Prevention*, Centers for Disease Control and Prevention, 16 July 2020, https://www.cdc.gov/malaria/about/biology/index.html.
[33] Dean, Laura. "The Duffy Blood Group." *Blood Groups and Red Cell Antigens [Internet].*, U.S. National Library of Medicine, 1 Jan. 1970, https://www.ncbi.nlm.nih.gov/books/NBK2271/#:~:text=The%20Duffy%20glycoprotein%20is%20a,vivax.
[34] "Nephrotic Syndrome." *Mayo Clinic*, Mayo Foundation for Medical Education and Research, 30 Jan. 2020, https://www.mayoclinic.org/diseases-conditions/nephrotic-syndrome/symptoms-causes/syc-20375608#:~:text=Nephrotic%20syndrome%20is%20a%20kidney,excess%20water%20from%20your%20blood.

Lifecycle in the Human Body: The lifecycle of *Plasmodium* is quite complex but necessary to understand for interpreting antigen diagnostic test results. The first important step occurs when a female *Anopheles* mosquito takes its blood meal from a human while simultaneously injecting the human with the sporozoite phase of the parasite (Figure 1: Step 1, infective stage). From the bloodstream, the sporozoites travel to the human liver, where the parasite infects these cells (Figure 1: Step 2). The parasite can remain dormant in the liver cells for months to years depending on the species of *Plasmodium* (the parasite is called "hypnozoites" at this phase) (Figure 1: Step 3). Once the parasite is ready to leave the liver, it forms a mature schizont which allows the parasite to rupture the liver cell as merozoites and head back into the human's bloodstream (Figure 1: Step). The entire stage of *Plasmodium's* transformations in the liver is known as the exoerythrocytic cycle (Figure 1: Stage A). Once back in the bloodstream, the parasite finds RBCs to infect (Figure 1: Step 5). The parasite in the infected RBCs then forms an immature trophozoite, also known as the ring stage[35] (Figure 2). The parasite's lifecycle can then proceed in one of two ways: i) the

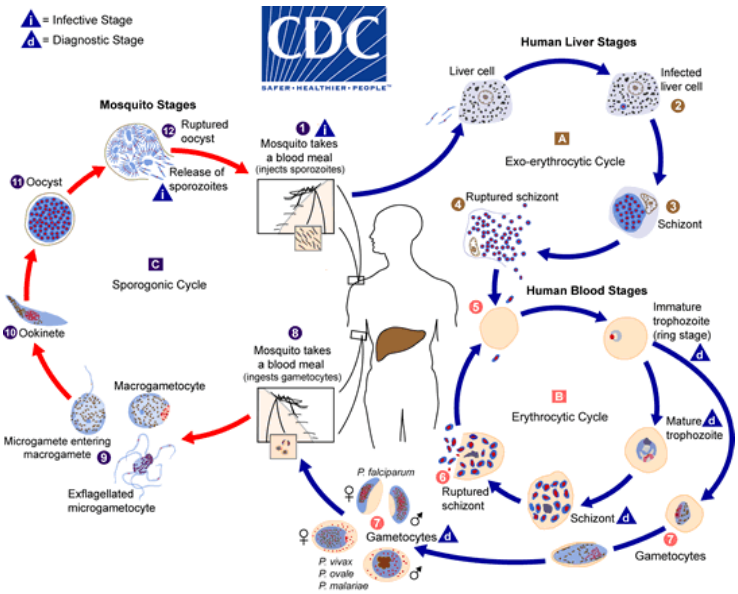

Figure 1: Lifecycle of the *Plasmodium* genus. (29)

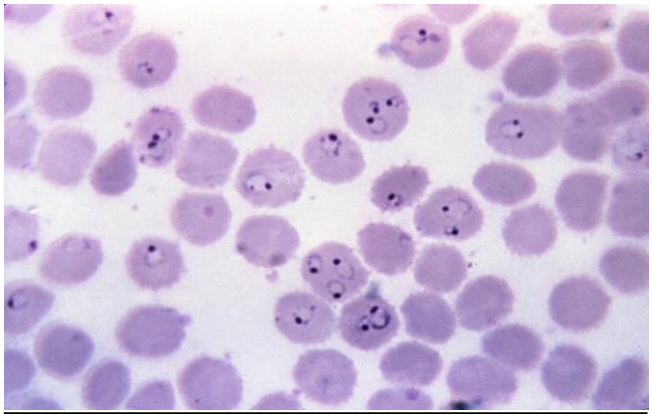

Figure 2: Micrograph of *P. falciparum* trophozoite stage (ring stage). (35)

[35] Glenn, Steven. "Free Picture: Photo Micrograph, Ring Form, Plasmodium Falciparum, Trophozoites, Cells, Infection." *PIXNIO*, 18 Sept. 2016, https://pixnio.com/science/microscopy-images/malaria-plasmodium/micrograph-depicts-a-number-of-ring-form-plasmodium-falciparum-trophozoites.

erythrocytic cycle (Figure 1: Stage B): the parasite will form a mature trophozoite which transforms into more schizonts to then rupture the RBC and infect more RBCs as merozoites, thus repeating the cycle (Figure 1: Step 6), or ii) the sexual erythrocytic stage: the immature trophozoite will form gametocytes (Figure 1: Step 7) which will be ingested by the next mosquito that takes a blood meal from the infected human host (Figure 1: Step 8). Another lifecycle of *Plasmodium* occurs in the mosquito, the sporogonic cycle (Figure 1: Stage C), which readies the parasite and mosquito to infect another human[36].

The Global Burden of Malaria: Around the world, malaria remains one of the high-burden diseases, with an even larger impact on low- and middle-income countries (LMIC). According to the Global Burden of Disease Collaborative Network, the estimated number of global deaths from malaria in 2011 was 755,546 deaths. The age group with the highest number of deaths was those under 5 years of age: 476,352 deaths. The overall number of malaria deaths in 2015 was somewhat reduced to 662,166 deaths; the same age group, those under 5 years of age, was still the age group impacted the most by malaria-related deaths with 395,030 deaths[37]. Sub-Saharan Africa accounted for 90.4% of the deaths from malaria, as estimated by world regions, in 2011, and 89.4% of the total number of deaths from malaria, as estimated by world regions, in 2015[38]. Although Africa is the continent with the most cases and deaths related to malaria compared to the rest of the world, it is also the region that has made the most progress in reducing malaria deaths by 51.7% between 2000 and 2015[39].

The Burden of Malaria in Ethiopia: Ethiopia is included in the long list of sub-Saharan countries where malaria is highly endemic. Great efforts have been made over the past decades to reduce the burden of

[36] "CDC - Malaria - about Malaria - Biology." Centers for Disease Control and Prevention, Centers for Disease Control and Prevention, 16 July 2020, https://www.cdc.gov/malaria/about/biology/index.html.
[37] Global Burden of Disease Collaborative Network. Global Burden of Disease Study 2017 (GBD 2017) Results. Seattle, United States: Institute for Health Metrics and Evaluation (IHME), 2018.
[38] Global Burden of Disease Collaborative Network. Global Burden of Disease Study 2016 (GBD 2016) Results. Seattle, United States: Institute for Health Metrics and Evaluation (IHME), 2017.
[39] Roser, Max, and Hannah Ritchie. "Malaria." Our World in Data, 12 Nov. 2019, https://ourworldindata.org/malaria.

disease from malaria[40],[41],[42]. These efforts have resulted in a decline, but malaria still persists as a major public health problem in the country. Approximately 75% of the Ethiopian territory is considered endemic to malaria which places more than 60 million individuals at risk for infection[43],[44]. Public health interventions initiated in order to achieve the malaria Millennium Development Goal by 2015 assisted in reducing malaria incidence and mortality through 1) early diagnosis and treatment of cases using artemisinin-based combination therapy (ACT), 2) prevention and control of malaria among pregnant woman using intermittent preventive therapy (IPT), and 3) use of vector control methods including insecticide-treated bed nets (ITNs), and indoor residual spray (IRS)[45],[46]. These efforts successfully reduced both the number of deaths and disability-adjusted life years (DALYs) lost from malaria. Regardless of the progress which has been made in Ethiopia, malaria remains an enormous public health burden in the country[47]. Comparatively, the incidence of malaria in 2011 was 116.13 per 100,000 people vs. 52.77 per 100,000 people in 2015[48]. The death rate from malaria in 2011 was 13.12 per 100,000 people vs. 7.38 per 100,000 people in 2015[49]. These numbers demonstrate the progress that malaria initiatives have contributed to in reducing malaria incidence and mortality in Ethiopia. However, just as quickly as this progress has been made, it can quickly disappear from the impact of climate change.

[40] "Malaria - Eradication, Prevention, through Innovation & Data." *Bill & Melinda Gates Foundation*, https://www.gatesfoundation.org/our-work/programs/global-health/malaria.
[41] Published: Mar 02, 2021. "The President's Malaria Initiative and Other U.S. Government Global Malaria Efforts." *KFF*, 9 Aug. 2021, https://www.kff.org/global-health-policy/fact-sheet/the-u-s-government-and-global-malaria/.
[42] Tizifa, Tinashe A, et al. "Prevention Efforts for Malaria." *Current Tropical Medicine Reports*, Springer International Publishing, 2018, https://www.ncbi.nlm.nih.gov/pmc/articles/PMC5879044/.
[43] Federal democratic Republic of Ethiopia Ministry of Health. Ethiopian national malaria indicator survey 2011: technical summary Ethiopian: Ministry of Health of Ethiopia; 2012.
[44] Girum, Tadele et al. "Burden of malaria in Ethiopia, 2000-2016: findings from the Global Health Estimates 2016." *Tropical diseases, travel medicine and vaccines* vol. 5 11. 12 Jul. 2019, doi:10.1186/s40794-019-0090-z
[45] United Nations. The Millennium Development Goals Report 2015. New York: United Nations. p. 2015.
[46] Aregawi M, Lynch M, Bekele W, Kebede H, Jima D, Taffese HS, et al. Time series analysis of trends in malaria cases and deaths at hospitals and the effect of antimalarial interventions, 2001–2011, Ethiopia. PLoS ONE. 2014;9: e106359.
[47] Girum, T., Shumbej, T. & Shewangizaw, M. Burden of malaria in Ethiopia, 2000-2016: findings from the Global Health Estimates 2016. Trop Dis Travel Med Vaccines 5, 11 (2019). https://doi.org/10.1186/s40794-019-0090-z
[48] Global Burden of Disease Collaborative Network. Global Burden of Disease Study 2019 (GBD 2019) Results. Seattle, United States: Institute for Health Metrics and Evaluation (IHME), 2021.
[49] "Data Catalog." *The World Bank*, https://datacatalog.worldbank.org/search/dataset/0037712.

Climate Change: Temperature and Rainfall

Overview of Climate Change: Weather is constantly changing; it refers to the short-term atmospheric conditions—perhaps in relation to the temperature, humidity, or precipitation[50],[51]. Unlike the weather, though, the term "climate" refers to weather patterns of a specific region averaged over a long period of time[52],[53]. The average course or condition of the weather at a place usually over a period of years can be characterized by temperature, wind velocity, and precipitation. Typically, the average conditions—or the climate—of a region have consistent patterns and characteristics observed over long-term regional or even global spaces[54]. Thus, climate change is defined as any long-term change in the typical weather patterns that have defined the earth's local, regional, and global climates. These changes we are observing, such as global warming, stem from human activities[55]. Many behaviors contribute to climate change, but the most significant is that of burning fossil fuels, causing greenhouse gas concentrations to increase, and thus increase the earth's temperature[56]. The earth's average temperature has increased by nearly 1.5° Fahrenheit (F) over the last century[57]. Even the smallest changes in average temperature can result in large, possibly dangerous, shifts in climate and weather around the globe[58]. This rise in temperature has already been linked to regional extreme changes in rainfall—more flooding or more

[50] "What Is the Difference between Weather and Climate Change?" *What Is the Difference between Weather and Climate Change? | U.S. Geological Survey*, https://www.usgs.gov/faqs/what-difference-between-weather-and-climate-change#:~:text=Weather%20refers%20to%20short%20term,refers%20to%20long%2Dterm%20changes.
[51] "Weather Definition & Meaning." *Merriam-Webster*, Merriam-Webster, https://www.merriam-webster.com/dictionary/weather.
[52] "Climate Definition & Meaning." *Merriam-Webster*, Merriam-Webster, https://www.merriam-webster.com/dictionary/climate.
[53] "What Is the Difference between Weather and Climate Change?" *What Is the Difference between Weather and Climate Change? | U.S. Geological Survey*, https://www.usgs.gov/faqs/what-difference-between-weather-and-climate-change#:~:text=Weather%20refers%20to%20short%20term,refers%20to%20long%2Dterm%20changes.
[54] "Overview: Weather, Global Warming and Climate Change." NASA, NASA, 24 August 2021, https://climate.nasa.gov/resources/global-warming-vs-climate-change/.
[55] "Causes of Climate Change." *EPA*, Environmental Protection Agency, https://www.epa.gov/climatechange-science/causes-climate-change.
[56] "The Causes of Climate Change." *NASA*, NASA, 7 Mar. 2022, https://climate.nasa.gov/causes/.
[57] "Global Warming of 1.5 ºC." *Intergovernmental Panel on Climate Change*, https://www.ipcc.ch/sr15/.
[58] "Climate Change: Basic Information." EPA, Environmental Protection Agency, 17 Jan. 2017, https://19january2017snapshot.epa.gov/climatechange/climate-change-basic-information_.html.

droughts—as well as increased severity and frequency of heat waves[59],[60],[61]. There is concern about the potential impacts of climate change on human health. There are many different ways in which climate change can have negative impacts, and these effects of climate change on vector-borne diseases and human health is one area of concern where researchers are focusing their efforts[62].

General Impacts of Climate Change on Malaria: As our earth continues to experience drastic changes in weather patterns as a result of climate change, there are questions about how variations in temperatures and changes in precipitation may affect malaria transmission[63]. Just how the changes from climate change will impact the transmission of vector-borne infections, like malaria, is not fully understood. However, it is hypothesized that the variations in climatic conditions, like increased temperatures, increased rainfall patterns, and increased humidity will profoundly influence the longevity of the mosquito vector and the ability of the malaria parasite to develop inside the mosquito, which in turn would increase malaria transmission. Thus, there is potential for climate change to reverse the great progress which has been made around the globe, and specifically in Africa to reduce malaria transmission and disease.

The world's temperature has significantly risen since the 1880s when climate records started being recorded. In 2020, the temperature for the year was 2.3° F above average, the highest it has ever been in the past 141 years[64]. Using modeling to look at the future implications of vector-borne disease transmission due to climate change has revealed an increased transmission rate of mosquito-borne diseases and a widening geographical distribution[65]. An article by Reiter et al. modeled the vectorial

[59] "Climate Change Widespread, Rapid, and Intensifying." *Intergovernmental Panel on Climate Change*, IPCC, https://www.ipcc.ch/2021/08/09/ar6-wg1-20210809-pr/.
[60] "Impacts of Climate Change." *EPA*, Environmental Protection Agency, https://www.epa.gov/climatechange-science/impacts-climate-change.
[61] "Mapped: How Climate Change Affects Extreme Weather around the World." *Carbon Brief*, 8 Oct. 2021, https://www.carbonbrief.org/mapped-how-climate-change-affects-extreme-weather-around-the-world.
[62] "Climate Change: Basic Information." EPA, Environmental Protection Agency, 17 Jan. 2017, https://19january2017snapshot.epa.gov/climatechange/climate-change-basic-information_.html.
[63] "Climate Change and Malaria Transmission." *Taylor & Francis*, https://www.tandfonline.com/doi/abs/10.1080/00034983.1996.11813087.
[64] NCEI.Monitoring.Info@noaa.gov. "Global Climate Report - Annual 2020." *Global Climate Report - Annual 2020 | National Centers for Environmental Information (NCEI)*, https://www.ncdc.noaa.gov/sotc/global/202013.
[65] Reiter, P. "Climate change and mosquito-borne disease." *Environmental health perspectives* vol. 109 Suppl 1, Suppl 1 (2001): 141-61. doi:10.1289/ehp.01109s1141

capacity of *Anopheles* as a way to express transmission risk. The researchers described the vectorial capacity as:

$$\frac{m * a^2 * p^n}{-log_e(p)}$$

where *m* is the mosquito density per human, *a* is the average number of bites per day for each mosquito, *p* is the probability of a mosquito surviving through any one day, and *n* is the extrinsic incubation period—the time taken for the pathogen to develop in the mosquito until the insect becomes infective. The only factor directly affected by a climate variable is *n*, which is inversely related to temperature[66]. The article concluded that in tropical and subtropical locations, where malaria is currently unstable, transmission is more sensitive to climatic factors, so the impact of rising temperature could be significant.

A long-term increase in average rainfall may promote higher mosquito populations in areas that are currently arid but reduce them in areas that are currently ideal for mosquito breeding and development due to a potential increase in flooding. Lower rainfall could reduce mosquito breeding patterns in arid areas, as appears to have happened in recent years on the southern edge of the Sahara[67], but promote mosquito prevalence in regions that may experience a reduction in flooding due to a decrease in precipitation creating optimal conditions for mosquito survival. Increased temperatures could facilitate transmission in humid areas but reduce it if associated with low humidity. The abundance of factors involved is complex, and the overall impact on malaria endemicity and stability is difficult to predict. Additionally, climate change will induce other ecologic changes, which could lead to agricultural and economic changes that may affect human behavior and exposure to mosquitoes and consequently increase or decrease transmission potential. These other factors, which influence the changes in malaria spread in

[66] Reiter, P. "Climate change and mosquito-borne disease." *Environmental health perspectives* vol. 109 Suppl 1, Suppl 1 (2001): 141-61. doi:10.1289/ehp.01109s1141

[67] Mouchet J, Faye O, Juivez J, Manguin S. Drought and malaria retreat in the Sahel, West Africa [letter]. Lancet 348:1735–1736 (1996).

current endemic areas, [68],[69], and reemergence in regions that have controlled transmission or eliminated malaria previously[70], make the outcome even more uncertain and challenging for modeling the future transmission of malaria.

Climate Change in Ethiopia: The varying topographical and climatic features in Ethiopia contribute to the seasonal and unstable malaria transmission patterns. Normally, the peak of malaria prevalence occurs after the main rainfall season: July, August, and September of each year[71]. If climate change were to increase the amount of rainfall that occurs within the rainy seasons or increase the length of the rainy season or the number of days with rain, mosquito populations would flourish during this time—meaning the seasonality of mosquito prevalence may increase. Zogo et al. identified the breeding habitats of *Anopheles* mosquitoes in Cote d'Ivoire; they found *Anopheles* breeding and larvae developing in rice paddies (61%), followed by edges of rivers and streams (12%) during the rainy season. In the dry season, rice paddies (57%) and puddles (27%) were the most abundant breeding habitats for *Anopheles*[72]. Increased temperatures contribute to the *Plasmodium* parasites developing and surviving in the mosquito and transmitting malaria to the human host. The older females are the ones able to transmit malaria; once the mosquito ingests the parasite, it takes about nine days when temperatures are around 85° F for the parasite to transform into a sporozoite, a phase which is necessary to infect a human. When temperatures are too cold, 59° F for *P. vivax* and 68° F for *P. falciparum,* the development of the parasite cannot occur[73].

---

[68] "Climate Change and Malaria - a Complex Relationship." *United Nations*, United Nations, https://www.un.org/en/chronicle/article/climate-change-and-malaria-complex-relationship.
[69] Zhou, Guofa et al. "Association between climate variability and malaria epidemics in the East African highlands." *Proceedings of the National Academy of Sciences of the United States of America* vol. 101,8 (2004): 2375-80. doi:10.1073/pnas.0308714100
[70] Baldari, M et al. "Malaria in Maremma, Italy." *Lancet (London, England)* vol. 351,9111 (1998): 1246-7. doi:10.1016/S0140-6736(97)10312-9
[71] Belay, B., Gelana, T. & Gebresilassie, A. Malaria prevalence, knowledge, attitude, and practice among febrile patients attending Chagni health center, Northwest Ethiopia: a cross-sectional study. Trop Dis Travel Med Vaccines 7, 20 (2021). https://doi.org/10.1186/s40794-021-00146-2
[72] Zogo, Barnabas, et al. "Identification and Characterization of Anopheles Spp. Breeding Habitats in the Korhogo Area in Northern Côte D'Ivoire: A Study Prior to a BTI-Based Larviciding Intervention - Parasites & Vectors." *BioMed Central*, BioMed Central, 27 Mar. 2019, https://parasitesandvectors.biomedcentral.com/articles/10.1186/s13071-019-3404-0#:~:text=Rice%20paddies%20(61%25)%2C%20followed,breeding%20habitats%20for%20Anopheles%20spp.
[73] "CDC - Malaria - about Malaria - Biology." Centers for Disease Control and Prevention, Centers for Disease Control and Prevention, 16 July 2020, https://www.cdc.gov/malaria/about/biology/index.html.

Malaria transmission is more intense in warm and humid areas, and climate change is widening the geographical distribution of these favorable climatic conditions, such as in Ethiopia. In a model of temperature-dependent malaria transmission, the model developed maps with estimates for Africa to illustrate: i) baseline climate conditions for current endemic and seasonal transmission patterns (Figure 3), and ii) projected future climate change models for representative concentration pathways (RCP) 4.5 and RCP 8.5 in 2030 (Figure 4), and iii) in 2050 (Figure 5), and iv) in 2080[74] (Figure 6).

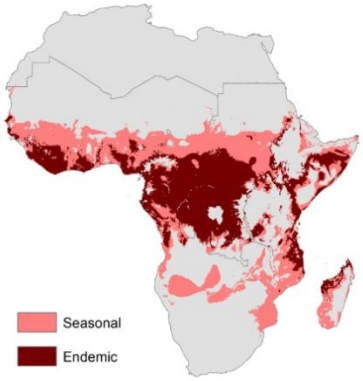

Figure 3: Modeled endemic and season malaria transmission under current climate conditions. 74

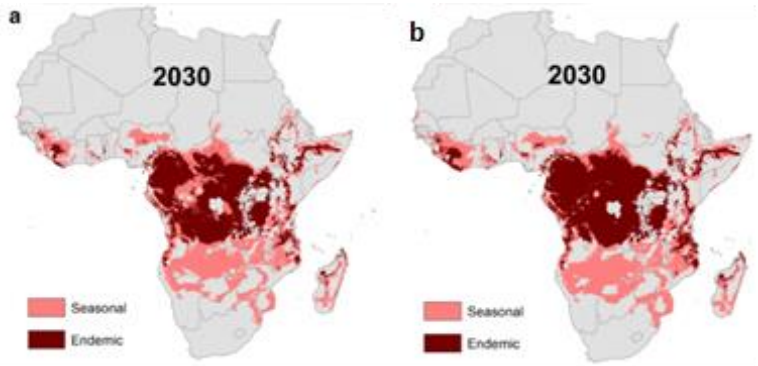

Figure 4: Modeled endemic and season malaria transmission in 2030 under a) RCP 4.5 b) RCP 8.5. 74

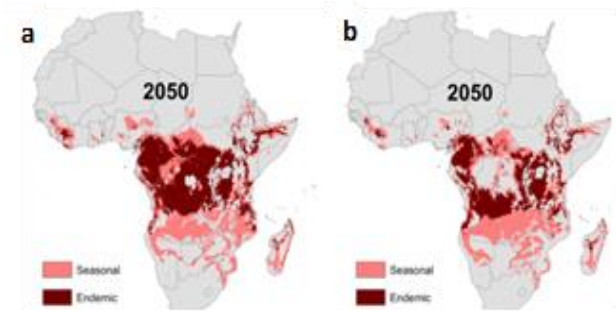

Figure 5: Modeled endemic and season malaria transmission in 2050 under a) RCP 4.5 b) RCP 8.5. 74

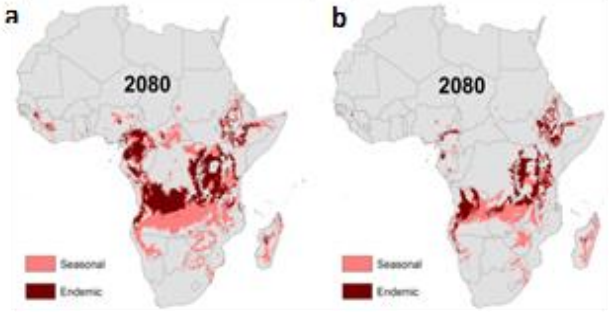

Figure 6: Modeled endemic and season malaria transmission in 2080 under a) RCP 4.5 b) RCP 8.5. 74

[74] Ryan, S.J., Lippi, C.A. & Zermoglio, F. Shifting transmission risk for malaria in Africa with climate change: a framework for planning and intervention. *Malar J* 19, 170 (2020). https://doi.org/10.1186/s12936-020-03224-6

The RCPs are scenarios that include time series of emissions and concentrations of the full suite of greenhouse gases (GHGs), aerosols, chemically active gases, as well as, land use and land cover[75]. The word representative signifies that each RCP provides only one of many possible scenarios that would lead to the specific radiative forcing characteristics (the net change of radiative flux at the top of the atmosphere due to a change in an external driver of climate change—typically measured with carbon dioxide). The term pathway emphasizes that not only the long-term concentration levels are of interest, but also the trajectory that was taken over time to reach that outcome[76]. As the figures demonstrate, certain countries in Africa will experience reduced transmission suitability. These models predict that Ethiopia will have an increase in both seasonal and endemic malaria transmission in the coming decades.

Impacts of Rainfall on Malaria Burden: The impact of rainfall on malaria is ambiguous for two reasons. The first is that climate change can result in either extreme rainfall or extreme drought, and geographically it is still uncertain which locations will experience increased or decreased rainfall. Particularly in Ethiopia, the country has complex patterns of topography and therefore rainfall—higher elevations receive more rainfall compared to the low elevation arid regions. In some areas, spring and summer rains have declined by 15-20% since the mid-1970s[77]. Secondly, even if research or modeling can determine which areas will experience increases and decreases in rainfall, it is still uncertain what are the thresholds of impact. This means researchers do not know how much of an increase or decrease in rainfall certain areas will experience, and what amount of precipitation would signify a significant change in rainfall that would lead to significant changes in the environment that would affect vector breeding and survival. Some areas with heavy rainfall provide mosquitoes with good breeding conditions due to more areas with standing water. Yet, in other regions, heavy rainfall can wash out the breeding sites and reduce

[75] Moss, Richard H., et al. "Expert Meeting Report Scenarios - IPCC." *Intergovernmental Panel on Climate Change*, WMO & UNEP, https://archive.ipcc.ch/pdf/supporting-material/expert-meeting-report-scenarios.pdf.
76 Moss, Richard H., et al. "The next Generation of Scenarios for Climate Change Research and Assessment." Nature, vol. 463, no. 7282, 2010, pp. 747–756., https://doi.org/10.1038/nature08823.
77 "A Climate Trend Analysis of Ethiopia." USAID, Famine Early Warning System Network, https://www.usaid.gov/sites/default/files/documents/1860/A%20Climate%20Trend%20Analysis%20of%20Ethiopia.pdf.

the prevalence of malaria as mosquito populations are wiped out[78]. In general, though, increases in rainfall are beneficial for mosquitos by increasing the atmospheric humidity from the rainfall, which allows mosquitoes to enhance their flight activity and host-seeking behavior[79],[80]. Furthermore, increases in rainfall provide more standing water in the environment which mosquitoes take advantage of for their egg deposition and the following immature development stage[81]. Little information is available about the direct effects of rainfall on *Plasmodium*. One study in China explored the impact of rainfall on the prevalence of *P. falciparum* malaria after an increase in rainfall. The results indicated that a 10 mm increase in weekly rainfall was strongly correlated with an increasing number of malaria cases. Though, whether the association was from the rainfall impact on the vector or on the parasite was not determined[82].

Impacts of Temperature on Malaria Burden: Rising temperatures experienced in Ethiopia, and in other countries around the globe, will impact malaria transmission by affecting the growth cycle of the *Plasmodium* parasite in the mosquito. The rise in temperature creates a more optimal environmental condition for the parasite to develop faster and increase transmission[83]. A study by Siraj et al. described how malaria moved up in elevation with temperature increases in Ethiopia and Colombia[84],[85]. The research team tracked the year-to-year temperature variations from 1990 to 2005. They found that malaria infection rates tended to increase as temperatures increased since the *Plasmodium* parasite reproduced

78 WHO, Fact Sheet 192: El Nino and its health impact, (2002)
79 Shaman, Jeffrey, and Jonathan F Day. "Reproductive phase locking of mosquito populations in response to rainfall frequency." PloS one vol. 2,3 e331. 28 Mar. 2007, doi: 10.1371/journal.pone.0000331
80 Reinhold, Joanna M et al. "Effects of the Environmental Temperature on Aedes aegypti and Aedes albopictus Mosquitoes: A Review." Insects vol. 9,4 158. 6 Nov. 2018, doi:10.3390/insects9040158
81 Shaman, Jeffrey, and Jonathan F Day. "Reproductive phase locking of mosquito populations in response to rainfall frequency." *PLoS one* vol. 2,3 e331. 28 Mar. 2007, doi : 10.1371/journal.pone.0000331
82 Bi, Yan, et al. "Impact of Climate Variability on Plasmodium Vivax and Plasmodium Falciparum Malaria in Yunnan Province, China - Parasites & Vectors." *BioMed Central*, BioMed Central, 17 Dec. 2013, https://parasitesandvectors.biomedcentral.com/articles/10.1186/1756-3305-6-357#:~:text=falciparum%20malaria%20cases%20were%20significantly,association%20between%20humidity%20and%20P.
83 T.H. Jetten, W.J. Martens, W. Takken, "Model simulations to estimate malaria risk under climate change", Journal of Medical Entomology, 33(3) (1996): p.361-71.
84 Siraj, A S et al. "Altitudinal changes in malaria incidence in highlands of Ethiopia and Colombia." Science (New York, N.Y.) vol. 343,6175 (2014): 1154-8. doi:10.1126/science.1244325
85 Pascual, M et al. "Malaria resurgence in the East African highlands: temperature trends revisited." Proceedings of the National Academy of Sciences of the United States of America vol. 103,15 (2006): 5829-34. doi:10.1073/pnas.0508929103

faster inside vector mosquitoes when it was warmer, thus increasing the likelihood of infection when the mosquito bites someone[86]. Since *Plasmodium* is reproducing at a faster rate inside the mosquito, when the mosquitoes take a blood meal, the likelihood of infection is greatly increased. This is because of the quantity of *Plasmodium* in the salivary glands of the mosquitoes; the higher number of *Plasmodium* increases the risk of transmission. However, while higher temperature benefits the parasite, if temperatures get too high it harms the mosquito. The impact of high temperatures, ranging between 90-100° F, also depends on the species of *Anopheles* and the other climatic factors, like humidity and precipitation[87]. Though, some research indicates that mosquitoes are already evolving to accommodate these warmer temperatures[88],[89]. Other studies indicate that at higher temperatures, the mosquito experiences significant reductions in egg viability and hatching capability[90]. Temperature stress during the immature mosquito stages can impact adult life characteristics like fecundity, survival, and body size[91]. The temperature in the adult stage directly influences female longevity and flying power[92]. Lastly, mosquitoes tend to be the most active and bite more when the temperature is above 80° F; however, if the temperature gets too high (i.e., 90-100° F), their activity declines rapidly[93]. Thus, this benefit of higher temperature to the parasite, but harmful to the vector, creates uncertainty around the potential impact of warmer temperatures on the overall malaria burden.

---

[86] Irfan, Umair. "As Temperatures Climb, so Does Malaria." *Scientific American*, Scientific American, 7 Mar. 2014, https://www.scientificamerican.com/article/as-temperatures-climb-so-does-malaria/#:~:text=Infection%20rates%20tend%20to%20increase,mosquito%20bites%20someone%2C%20Pascual%20explained.

[87] Mordecai, Erin A., et al. "Thermal Biology of Mosquito-Borne Disease." *Ecology Letters*, vol. 22, no. 10, 2019, pp. 1690–1708., https://doi.org/10.1111/ele.13335.

[88] Mordecai, Erin A., et al. "Thermal Biology of Mosquito-Borne Disease." *Ecology Letters*, vol. 22, no. 10, 2019, pp. 1690–1708., https://doi.org/10.1111/ele.13335.

[89] Couper, Lisa I et al. "How will mosquitoes adapt to climate warming?." *eLife* vol. 10 e69630. 17 Aug. 2021, doi:10.7554/eLife.69630

[90] Bellone, Rachel, and Anna-Bella Failloux. "The Role of Temperature in Shaping Mosquito-Borne Viruses Transmission." *Frontiers*, Frontiers, 1 Jan. 1AD, https://www.frontiersin.org/articles/10.3389/fmicb.2020.584846/full.

91 Agyekum, Thomas P et al. "A Systematic Review of the Effects of Temperature on Anopheles Mosquito Development and Survival: Implications for Malaria Control in a Future Warmer Climate." International journal of environmental research and public health vol. 18,14 7255. 7 Jul. 2021, doi:10.3390/ijerph18147255

[92] Bellone, Rachel, and Anna-Bella Failloux. "The Role of Temperature in Shaping Mosquito-Borne Viruses Transmission." *Frontiers*, Frontiers, 1 Jan. 1AD, https://www.frontiersin.org/articles/10.3389/fmicb.2020.584846/full.

[93] "How Does Weather Affect Mosquito Activity?" *Preventive Pest Control*, 5 July 2016, https://www.preventivepestcontrol.com/weather-affect-mosquito-activity/#:~:text=Warm%2C%20Moist%20Weather%2D%20a%20Mosquito's%20Friend&text=They%20are%20most%20active%20in,active%20and%20hence%20more%20transmissible.

Antigen Testing for Malaria

Overview of Antigen Testing: Since 2008, over 290 rapid diagnostic test (RDT) products have been evaluated through the World Health Organization's Malaria RDT Product Testing Programme[94]. These test kits work by detecting *Plasmodium* antigens in individual blood specimens. RDTs are useful alternatives to the traditional method of diagnosing malaria through microscopic examination of blood smears. Many sites, especially in Africa, lack quality reagents, good microscopes, and laboratory technicians with experience in identifying the parasite[95]. Thus, the RDTs are used in many clinical settings and programs to understand the malaria burden. Unfortunately, as malaria continues to be transmitted, the parasite is mutating, and this results in these RDTs losing their sensitivity and specificity for malaria diagnosis. In Eritrea, a country directly north of Ethiopia, local health care workers and the WHO determined up to 80% of the *Plasmodium* in the area have mutations that have caused them to stop producing the two proteins detected by the rapid diagnostic tests: histidine-rich protein (HRP) 2 and HRP3[96]. The WHO team conducted a similar survey in Ethiopia as well and established that the prevalence of *Plasmodium* with these mutations was not as high in Ethiopia, but what they did find was still "really concerning levels."[97] These antigens are solely used for the diagnosis of *P. falciparum* infection and not for other species of *Plasmodium.* The majority of the RDTs, procured globally, target this antigen for malaria diagnosis[98]. It serves as a reminder, though, that the other species of *Plasmodium* can also evolve and render current antigen test kits useless.

[94] "CDC - Malaria - Malaria Worldwide - How Can Malaria Cases and Deaths Be Reduced? - Diagnosis and Treatment." *Centers for Disease Control and Prevention*, Centers for Disease Control and Prevention, 23 July 2018, https://www.cdc.gov/malaria/malaria_worldwide/reduction/dx_tx.html.
[95] "CDC - Malaria - Malaria Worldwide - How Can Malaria Cases and Deaths Be Reduced? - Diagnosis and Treatment." *Centers for Disease Control and Prevention*, Centers for Disease Control and Prevention, 23 July 2018, https://www.cdc.gov/malaria/malaria_worldwide/reduction/dx_tx.html.
[96] Page, Michael Le. "Parasite Evolution Is Making It Harder to Detect and Treat Malaria." *New Scientist*, New Scientist, 29 Sept. 2021, https://www.newscientist.com/article/2291463-parasite-evolution-is-making-it-harder-to-detect-and-treat-malaria/.
[97] Page, Michael Le. "Parasite Evolution Is Making It Harder to Detect and Treat Malaria." *New Scientist*, New Scientist, 29 Sept. 2021, https://www.newscientist.com/article/2291463-parasite-evolution-is-making-it-harder-to-detect-and-treat-malaria/.
[98] Kong, A., Wilson, S.A., Ah, Y. *et al.* HRP2 and HRP3 cross-reactivity and implications for HRP2-based RDT use in regions with *Plasmodium falciparum hrp2* gene deletions. *Malar J* **20,** 207 (2021). https://doi.org/10.1186/s12936-021-03739-6

Specific Antigens used for Malaria Diagnosis: Overall, 12 different *Plasmodium* antigens have been used for malaria diagnostic testing. The following section provides a brief description of these various *Plasmodium* antigens. The glutathione-S-transferase (GST MFI) test serves as an internal control antigen. The *P. falciparum* merozoite protein 1 (PfMSP1 MFI) is acquired naturally during infection of *P. falciparum* and serves as a potential vaccine target for antibodies[99]. The *P. falciparum* apical membrane antigen 1 (N-terminal region) (PfAMA1 MFI) is a low-abundance type I integral membrane protein which is synthesized in the mature blood stages; it accumulates in the micronemes, secretory organelles, of developing merozoites[100],[101],[102]. The protein *P. falciparum* circumsporozoite (PfCSP MFI) is a surface protein in the sporozoite phase; it is the leading candidate for a vaccine targeting pre-erythrocytic malaria[103]. The next targeted protein was the *P. falciparum* glutamate-rich protein, Ro fragment (PfGLURPr0 MFI). This protein is associated with RBCs infected with mature schizonts; the Ro fragment refers to the nonrepetitive N-terminal of GLURP[104]. The *P. falciparum* liver stage antigen 1 (PfLSA1 MFI) is only expressed within infected hepatocytes; it is thought to have a role in merozoite release from the liver[105]. *P. falciparum* schizont egress antigen (PfSEA1 MFI) is another potential vaccine antigen target; it is released in schizont-infected RBCs and is necessary for replication in the blood[106]. The last target for *P. falciparum* is the *P. falciparum* ETRAMP 5 antigen 1 (PfEtramp5Ag1 MFI), this antigen is a good detection of current or recent exposure to malaria[107]. *P. vivax* merozoite protein 1 (PvMSP1 MFI),

[99] Jäschke, Anja et al. "Merozoite Surface Protein 1 from Plasmodium falciparum Is a Major Target of Opsonizing Antibodies in Individuals with Acquired Immunity against Malaria." *Clinical and vaccine immunology: CVI* vol. 24,11 e00155-17. 6 Nov. 2017, doi:10.1128/CVI.00155-17

[100] Healer, Julie et al. "Functional analysis of Plasmodium falciparum apical membrane antigen 1 utilizing interspecies domains." *Infection and immunity* vol. 73,4 (2005): 2444-51. doi:10.1128/IAI.73.4.2444-2451.2005

[101] Bannister, L. H., J. M. Hopkins, A. R. Dluzewski, G. Margos, I. T. Williams, M. J. Blackman, C. H. Kocken, A. W. Thomas, and G. H. Mitchell. 2003. Plasmodium falciparum apical membrane antigen 1 (PfAMA-1) is translocated within micronemes along subpellicular microtubules during merozoite development. J. Cell Sci. 116:3825–3834.

[102] Healer, J., S. Crawford, S. Ralph, G. McFadden, and A. F. Cowman. 2002.Independent translocation of two micronemal proteins in developing Plas-modium falciparum merozoites. Infect. Immun. 70:5751–5758

[103] Singh, Susheel K, et al. "The Plasmodium Falciparum Circumsporozoite Protein Produced in Lactococcus Lactis Is Pure and Stable." *Journal of Biological Chemistry*, PlumX Metrics, Jan. 2020, https://www.jbc.org/article/S0021-9258(17)48336-0/fulltext.

[104] Theisen, M et al. "The glutamate-rich protein (GLURP) of Plasmodium falciparum is a target for antibody-dependent monocyte-mediated inhibition of parasite growth in vitro." *Infection and immunity* vol. 66,1 (1998): 11-7. doi:10.1128/IAI.66.1.11-17.1998

[105] Hillier, Collette J et al. "Process development and analysis of liver-stage antigen 1, a pre-erythrocyte-stage protein-based vaccine for Plasmodium falciparum." *Infection and immunity* vol. 73,4 (2005): 2109-15. doi:10.1128/IAI.73.4.2109-2115.2005

[106] Park, Sangshin et al. "Impact of maternally derived antibodies to Plasmodium falciparum Schizont Egress Antigen-1 on the endogenous production of anti-PfSEA-1 in offspring." *Vaccine* vol. 37,35 (2019): 5044-5050. doi: 10.1016/j.vaccine.2019.06.084

[107] van den Hoogen, Lotus L., et al. "Selection of Antibody Responses Associated with Plasmodium Falciparum Infections in the Context of Malaria Elimination." *Frontiers*, Frontiers, 1 Jan. 1AD, https://www.frontiersin.org/articles/10.3389/fimmu.2020.00928/full.

similar to PfMSP1 MFI antigen, is a vaccine candidate for *P. vivax* and is mainly expressed during the trophozoites stage[108]. The second *P. vivax* target is the *P. vivax* apical membrane antigen 1 (PvAMA1 MFI), this protein serves an important role in hepatocyte and erythrocyte invasion during the sporozoites and merozoites stages respectively[109]. The last *P. vivax* protein is the chimeric *P. vivax* merozoite protein 1 (chPvMSP1 MFI), including additional B and T cell epitopes. This protein is required for the invasion of the parasite into the RBCs and is highly expressed on the RBC merozoites; this makes it a suitable candidate for a vaccine target[110]. Since the immunoglobulin G (IgG) does not always respond to the presence of the chPvMSP1 MFI, this test utilizes additional recognition from B and T cell epitopes for the detection of malaria with this antigen[111]. There is only one antigen test for *P. malariae, P. malariae* merozoite protein 1 (PmMSP1 MFI). The surface antigen is present within the RBC stages of *Plasmodium* species. *P. ovale* used the same protein as *P. malariae—P. ovale* merozoite protein 1 (PoMSP1 MFI). Finally, a mosquito salivary peptide (Mosq# sal MFI) is used as a biomarker for bite exposure and malaria infection based on the level of salivary peptide present in the blood sample[112].

The 12 antigens assessed for IgG antibody detection can be categorized into 3 groups: "short-term" *P. falciparum*, "long-term" *P. falciparum, P. vivax, P. ovale*, and *P. malariae* antibodies. Short-term antibodies were more likely to have been acquired in the past year and included antibodies to PfCSP, PfETR5Ag1, PfGLURP-R0, PfLSA1, and PfSEA1[113],[114]. Long-term *P. falciparum* antibodies, acquired at

[108] Punnath, Kishore et al. "Acquired antibody responses against merozoite surface protein-1_{19} antigen during *Plasmodium falciparum* and *P. vivax* infections in South Indian city of Mangaluru." *Journal of parasitic diseases: official organ of the Indian Society for Parasitology*, vol. 45,1 1-15. 21 Oct. 2020, doi:10.1007/s12639-020-01288-4

[109] Igonet, Sébastien, et al. "Cross-Reactivity Studies of an Anti-Plasmodium Vivax Apical Membrane Antigen 1 Monoclonal Antibody: Binding and Structural Characterization." Journal of Molecular Biology, Academic Press, 16 Dec. 2006, https://www.sciencedirect.com/science/article/pii/S0022283606017049?casa_token=TbBY5HwACNYAAAAA%3A1LzNgKijGoo63lZdUjY1auFRwwoXzaN-TI-eX6pyKiaaq9pMCnT8ik3IQtjN89YYckw99vBFBsJA.

[110] Shen, Fei-Hu et al. "A Chimeric Plasmodium vivax Merozoite Surface Protein Antibody Recognizes and Blocks Erythrocytic P. cynomolgi Berok Merozoites *In Vitro*." *Infection and immunity* vol. 89,2 e00645-20. 19 Jan. 2021, doi:10.1128/IAI.00645-20

[111] Egan, A et al. "Characterization of human T- and B-cell epitopes in the C terminus of Plasmodium falciparum merozoite surface protein 1: evidence for poor T-cell recognition of polypeptides with numerous disulfide bonds." *Infection and immunity* vol. 65,8 (1997): 3024-31. doi:10.1128/iai.65.8.3024-3031.1997

[112] Londono-Renteria, Berlin et al. "Identification and Pilot Evaluation of Salivary Peptides from *Anopheles albimanus* as Biomarkers for Bite Exposure and Malaria Infection in Colombia." *International journal of molecular sciences* vol. 21,3 691. 21 Jan. 2020, doi:10.3390/ijms21030691

[113] Helb DA, Tetteh KK, Felgner PL, et al. Novel serologic biomarkers provide accurate estimates of recent Plasmodium falciparum exposure for individuals and communities. Proc Natl Acad Sci U S A 2015; 112: E4438–47.

[114] Ondigo BN, Hodges JS, Ireland KF, et al. Estimation of recent and long-term malaria transmission in a population by antibody testing to multiple Plasmodium falciparum antigens. J Infect Dis 2014 ; 210 :1123–32.

any time in life, included antibodies to PfAMA1 and PfMSP1[115],[116]. *P. vivax* antibodies to these antigens, PvAMA1, PvMSPS1, and chPvMSP1, are all considered long-term. Both PoMPS1 and PmMSP1 are considered long-term *P. ovale* and *P. malariae* antibodies, respectively. Although the long-term antibodies generally persist longer than the short-term antibodies, the short-term antibodies can last for years, especially in adults[117].

Standard Malaria Indicator Survey: The Malaria Indicator Survey (MIS) is a survey that is available for nearly 30 countries worldwide[118]. The MIS was developed by the Monitoring and Evaluation Working Group (MERG) of Roll Back Malaria, an international partnership developed to coordinate global efforts to fight malaria[119],[120]. A standardized household survey collects national and regional or provincial data from a representative sample of respondents. Through household sampling, blood samples are collected from enrolled study participants at their place of residence. All participants read the informed consent form in the appropriate local language(s), and verbal informed consent is obtained from the participants. For children less than 5 years of age, parents' consent is obtained on their behalf before blood samples are collected. The dried blood spot (DBS) samples are analyzed for the *Plasmodium* antigen markers of infection. The MIS package includes questionnaires, manuals, and guidelines that are based on Demographic and Health Surveys materials[121].

[115] Drakeley CJ, Corran PH, Coleman PG, et al. Estimating medium- and long-term trends in malaria transmission by using serological markers of malaria exposure. Proc Natl Acad Sci U S A 2005; 102:5108–13.
[116] Ondigo BN, Hodges JS, Ireland KF, et al. Estimation of recent and long-term malaria transmission in a population by antibody testing to multiple Plasmodium falciparum antigens. J Infect Dis 2014 ; 210 :1123–32.
[117] Helb DA, Tetteh KK, Felgner PL, et al. Novel serologic biomarkers provide accurate estimates of recent Plasmodium falciparum exposure for individuals and communities. Proc Natl Acad Sci U S A 2015; 112: E4438–47.
[118] "The DHS Program." The DHS Program - Malaria Indicators Survey (MIS), https://dhsprogram.com/methodology/survey-types/mis.cfm.
[119] "Endmalaria.org." *Roll Back Malaria Partnership to End Malaria*, https://endmalaria.org/sites/default/files/RBM-WG-MERG-TORs_0.pdf.
[120] "Surveillance, Monitoring and Evaluation." Surveillance, Monitoring and Evaluation | RBM Partnership to End Malaria, https://endmalaria.org/our-work-working-groups/monitoring-and-evaluation.
[121] "The DHS Program." *The DHS Program - Malaria Indicators Survey (MIS)*, https://dhsprogram.com/methodology/survey-types/mis.cfm.

THESIS OBJECTIVES

Building on the previous work of the Plucinski et al.[122] and Moriarty[123], climate change data and malaria antigen test results were used to examine the impact of climate change, in terms of rainfall and temperature, on the proportion of positive malaria antigen detections in blood specimens collected from geographically representative samples of the Ethiopian population at two-time points, 2011 and 2015. This thesis explored the association between the variation in region-specific climate change and malaria prevalence across Ethiopia. Two variables were explored as indicators of climate change. For rainfall, precipitation amounts were averaged across monthly, seasonal, and decadal time frames and compared to malaria prevalence across the nine geographic regions. Second, for temperature, monthly and decadal averages were calculated and examined as predictors of malaria prevalence across nine geographic regions in Ethiopia.

This thesis has three overall objectives:

Objective 1: Examine if climate change is occurring in Ethiopia by comparing decadal patterns of rainfall and temperature from 1981 to 2019 using open-source datasets.

Objective 2: Describe changes in rainfall, temperature, and malaria prevalence (as measured by antigen detection tests) between 2011 and 2015.

Objective 3: Examine the association between rainfall changes and temperature changes and the prevalence of positive malaria antigen tests in 2011 and 2015.

[122] Plucinski MM, Candrinho B, Chambe G, Muchanga J, Muguande O, Matsinhe G, et al. (2018) Multiplex serology for impact evaluation of bed net distribution on burden of lymphatic filariasis and four species of human malaria in northern Mozambique. PLoS Negl Trop Dis 12(2): e0006278. https://doi.org/10.1371/journal. pntd.0006278

[123] Moriarty, Leah, "Epidemiology of Malaria and Other Diseases of Public Health Importance and Implications for Interventions in High Transmission Settings in Sub-Saharan Africa." Dissertation, Georgia State University, 2021. https://scholarworks.gsu.edu/sph_diss/42

To achieve these objectives, six specific aims were defined:

Aim 1.1: Calculate the decadal, yearly, and seasonal averages for rainfall in each of the nine regions of Ethiopia and compare the decadal patterns between 1981 to 2019 to assess the impacts of climate change.

Aim 1.2: Calculate the yearly average temperature in each of the nine regions of Ethiopia and compare those yearly patterns between 1981 to 2019 to assess the influence of climate change.

Aim 2.1: Compare average monthly (August through December) and seasonal rainfall between 2011 and 2015 in each of the nine regions of Ethiopia.

Aim 2.2: Compare the monthly average temperature (August through December) between 2011 and 2015 in each of the nine regions of Ethiopia.

Aim 2.3: Compare the prevalence rates of positive antigen tests for each of the 12 malaria antigen tests between 2011 and 2015 in each of the nine regions of Ethiopia.

Aim 3.1: Examine the association between climate change (rainfall and temperature) and the prevalence of positive malaria antigen tests.

MANUSCRIPT

Abstract

INTRODUCTION: Climate change is a continuing phenomenon that is negatively impacting the environment of pathogens, vectors, and humans. As many factors are influenced by climate change, the uncertainty surrounding the future burden of infectious diseases, particularly vector-borne diseases, intensifies. The impact of rainfall changes on malaria is ambiguous as it has been difficult for researchers to predict increases and decreases of rainfall in specific areas, and the current rainfall patterns are essential to understand the extent of rainfall changes. The temperature has been easier to assess—temperature increases are strongly linked to creating optimal environmental conditions for Plasmodium to develop faster and increase transmission; yet, as temperatures continue to increase the mosquito itself becomes negatively impacted by the heat. OBJECTIVE: The objective of this research was to explore the effect of two important climatic variables—temperature and rainfall—on the prevalence of malaria in Ethiopia. Comparing data from 2011 and 2015 allowed for a short-term observation of the impact of climate change on the prevalence of malaria in nine geographic regions. METHODS: Descriptive and analytical methods were used to address the research question. Plotting rainfall and temperature across varying time scales was used to visualize temporal changes in average rainfall and temperature; R^2 values for lines of best fit were applied to these plots. A log-binomial regression model was used to examine the prevalence rate of individuals testing positive for a malaria antigen test with every one-millimeter increase in rainfall or with every one-degree increase in temperature. RESULTS: Changes in both temperature and rainfall patterns were observed in Ethiopia from 1981 to 2019—rainfall and temperature generally increased in most regions. Minimal changes in rainfall and temperature were observed between 2011 and 2015 within the same regions; though, larger differences were seen between the geographic regions in Ethiopia. There was a statistically significant association between temperature and cluster prevalence ratios in 2011 for three antigens, but only one antigen in 2015. There were no significant associations between rainfall and cluster prevalence ratios in either year. CONCLUSION: For certain

species of Plasmodium, increasing average temperature may be reducing the prevalence ratios of malaria. Overall, more research needs to be conducted to determine the significance of long-term climate change on the prevalence of malaria in Ethiopia. Furthermore, the impact of climate change on the burden of malaria on a larger geographic scale needs to be investigated.

Introduction

Antigen testing for malaria is the most common way to assess the burden of the disease in Africa where microscopes and reagents are not easily accessible. Through this type of testing, organizations like the World Health Organization (WHO), the East Africa International Center of Excellence for Malaria Research, the United National Children's Fund (UNICEF), and the United Nations Development Programme (UNDP)[124],[125], have been able to monitor the prevalence of malaria in various regions of Africa and evaluate the success of their intervention programs. Between 1990 and 1997, the mortality from malaria was reduced from 22 malaria deaths per 10,000 population to 16 malaria deaths per 10,000 population in sub-Saharan Africa[126]. While there has been much success in reducing the caseload and mortality related to malaria, a new threat has been amplifying which could undo all the work and accomplishments that have been made thus far. As a result of climate change, our earth continues to experience drastic changes in weather patterns, including rainfall and temperature. Consequently, these extreme weather events—increased temperatures and large variations in precipitation amounts—will result in fluctuations in malaria transmission[127]. The temperature of the world has significantly risen since the 1880s when temperature, and other climate variables, started being recorded. In 2020, the temperature

[124] "Four International Organizations Unite to Roll Back Malaria | Meetings Coverage and Press Releases." *United Nations*, United Nations, https://www.un.org/press/en/1998/19981029.sag15.html.
[125] "East Africa International Center of Excellence for Malaria Research." *National Institute of Allergy and Infectious Diseases*, U.S. Department of Health and Human Services, https://www.niaid.nih.gov/research/east-africa-international-center-excellence-malaria-research.
[126] Carter, Richard, and Kamini N Mendis. "Evolutionary and historical aspects of the burden of malaria." *Clinical microbiology reviews* vol. 15,4 (2002): 564-94. doi:10.1128/CMR.15.4.564-594.2002
[127] "Climate Change and Malaria Transmission." *Taylor & Francis*, https://www.tandfonline.com/doi/abs/10.1080/00034983.1996.11813087.

for the year was 2.3° F above average, the highest it has ever been in the past 141 years[128]. Using modeling to examine the implications of climate change on vector-borne disease transmission suggests an increased transmission rate of mosquito-borne diseases and a widening geographical distribution[129].

The impact of rainfall on malaria is ambiguous for two reasons. The first is that climate change can result in either extreme rainfall or extreme drought. Particularly in Ethiopia, the country has complex patterns of topography and therefore rainfall—higher elevations receive more rainfall as compared to the low arid regions. In some areas, spring and summer rains have declined by 15-20% since the mid-1970s[130]. Secondly, if research or modeling can determine which areas will experience increases in rainfall it is uncertain what are the thresholds of impact. Some areas with heavy rainfall help provide mosquitoes with good breeding conditions with standing water. Yet, in other regions, the heavy rainfall can wash out the breeding sites and reduce the prevalence of malaria as mosquito populations are wiped out[131].

Building on the previous work of the Plucinski et al.[132] and Moriarty[133], climate change data and malaria antigen test results were used to examine the impact of climate change, in terms of rainfall and temperature, on the proportion of positive malaria antigen detections in blood specimens collected from geographically representative samples of the Ethiopian population at two-time points, 2011 and 2015. This thesis seeks to address the key limitations in region-specific climate change and malaria data, to see the true extent of climate change variability and its influence on malaria in the country. Through the proposed methodology, this thesis work will attempt to demonstrate the past and current trends of malaria

[128] NCEI.Monitoring.Info@noaa.gov. "Global Climate Report - Annual 2020." *Global Climate Report - Annual 2020 | National Centers for Environmental Information (NCEI)*, https://www.ncdc.noaa.gov/sotc/global/202013.
[129] Reiter, P. "Climate change and mosquito-borne disease." *Environmental health perspectives* vol. 109 Suppl 1, Suppl 1 (2001): 141-61. doi:10.1289/ehp.01109s1141
[130] "A Climate Trend Analysis of Ethiopia." *USAID*, Famine Early Warning System Network, https://www.usaid.gov/sites/default/files/documents/1860/A%20Climate%20Trend%20Analysis%20of%20Ethiopia.pdf.
[131] WHO, Fact Sheet 192: El Nino and its health impact, (2002)?
[132] Plucinski MM, Candrinho B, Chambe G, Muchanga J, Muguande O, Matsinhe G, et al. (2018) Multiplex serology for impact evaluation of bed net distribution on burden of lymphatic filariasis and four species of human malaria in northern Mozambique. PLoS Negl Trop Dis 12(2): e0006278. https://doi.org/10.1371/journal. pntd.0006278
[133] Moriarty, Leah, "Epidemiology of Malaria and Other Diseases of Public Health Importance and Implications for Interventions in High Transmission Settings in Sub-Saharan Africa." Dissertation, Georgia State University, 2021. https://scholarworks.gsu.edu/sph_diss/42

prevalence in Ethiopia regarding climate change broken down into various regions in the country. There are two climate change factors—rainfall and temperature—being explored as influential variables on the malaria prevalence in Ethiopia. First, temporal trends in average and extreme rainfall measurements were examined on monthly, seasonal, and decadal scales. Secondly, temporal trends in average and extreme temperature were examined on a monthly and decadal scale.

This project examined three main research questions motivating this project:

> Research Question 1: Did climate change impact temperature and rainfall in each of the nine regions of Ethiopia between 2011 and 2015
>
> Research Question 2: Did the proportion of positive malaria antigen test results change between 2011 and 2015?
>
> Research Question 3: After adjusting for age, bed net utilization, and region, do climate factors—rainfall and temperature—explain differences in the prevalence of positive malaria antigen tests between 2011 and 2015?

The Centers for Disease Control and Prevention is involved in malaria antigen testing through the Ethiopia Malaria Indicator Survey (MIS). Two MIS datasets were collected in 2011 and 2015, and these data were used in this project. The first dataset was collected from October to December 2011, and the second set of data was collected from September 30th to December 10th, 2015. These dates coincide with the high malaria transmission season in the country. The MIS was a cross-sectional, multi-stage, representative household survey that produced national and sub-national estimates for malaria-endemic and malaria-prone areas of Ethiopia. Malaria is endemic in Ethiopia, and the country has experienced outbreaks of malaria after both heavy rainfall events and extreme drought events. This research is important for estimating the burden of malaria in Ethiopia by region. However, it is necessary to combine this prevalence data with climate data to understand how the malaria burden is changing in response to

global warming and climate change. If this research demonstrates a negative impact of climate change on the malaria burden in Ethiopia, then this serves as evidence to advocate for further research on the impact of climate change on other vector-borne diseases and allocation of funding and resources to areas that will be disproportionately affected by increasing malaria transmission.

This thesis had three overall objectives:

Objective 1: Examine if climate change is occurring in Ethiopia by comparing patterns of rainfall and temperature from 1981 to 2019 using open-source datasets.

Objective 2: Describe changes in malaria prevalence (as measured by antigen detection tests) between 2011 and 2015.

Objective 3: Examine the association between rainfall changes and temperature changes and the prevalence of positive malaria antigen tests in 2011 and 2015.

To achieve these objectives, six specific aims were defined:

Aim 1.1: Calculate the decadal, yearly, and seasonal averages for rainfall in each of the nine regions of Ethiopia and compare the decadal patterns between 1981 to 2019 to assess the impacts of climate change.

Aim 1.2: Calculate the yearly average temperature in each of the nine regions of Ethiopia and compare those yearly patterns between 1981 to 2019 to assess the influence of climate change.

Aim 2.1: Compare average monthly (August through December) and seasonal rainfall between 2011 and 2015 in each of the nine regions of Ethiopia.

Aim 2.2: Compare the monthly average temperature (August through December) between 2011 and 2015 in each of the nine regions of Ethiopia.

Aim 2.3: Compare the prevalence rates of positive antigen tests for each of the 12 malaria antigen tests between 2011 and 2015 in each of the nine regions of Ethiopia.

Aim 3.1: Examine the association between climate change (rainfall and temperature) and the prevalence of positive malaria antigen tests.

Methods

Dataset #1: Ethiopian MIS 2011: The study data were obtained from the 2011 Ethiopia Malaria Indicator Survey (MIS). This data was conducted from October to December 2011, these dates coincide with the high malaria transmission season in the country. The MIS was a cross-sectional, multi-stage, representative household survey that produced national and sub-national estimates for malaria-endemic and malaria-prone areas of Ethiopia. Using a two-stage cluster sampling methodology, enumeration areas (EA), the sampling unit, were selected proportional to population size as estimated by the Ethiopian Central Statistics Agency, and 25 households were randomly selected per enumeration area. A total of 13,274 individuals were surveyed in 10,444 selected households. Every child less than 5 years of age in each selected household and all persons in every fourth household were eligible for malaria testing. Survey enumerators recorded the global positioning system (GPS) coordinates of each household. Before enrollment in the MIS, participants were read the informed consent form in the appropriate local language, and verbal informed consent was obtained from the participants. For children less than 5 years of age, parents' consent was obtained on their behalf before blood samples were collected. Demographic, socioeconomic, malaria prevention, and malariometric data (the endemic level of malarial infection in a population) were also collected in the selected households.

Blood Sample: Dried blood spot samples were collected during the national MIS survey in 2011. Whole blood from a single finger prick from consenting individuals (with or without fever) was collected for *Plasmodium* infection identification by RDT and microscopy, hemoglobin testing, and for collection of DBS samples. Whatman 903 (GE Healthcare, Pittsburgh, PA) filter paper cards were used for DBS

collection. These were air-dried, individually packed in a plastic bag together with a desiccant, and stored at – 20° Celsius (C) at Ethiopian Public Health Institute (EPHI) before they were sent to the U.S. Centers for Disease Control and Prevention (CDC) in, Atlanta, Georgia, for processing.

Ethics: The study protocol was approved by the National Ethics Committee of Ethiopia as well as Emory University and PATH institutional review boards. Additional ethical clearance for the study was obtained from the College of Health Science of Addis Ababa University (AAUMPF 03-008). The survey protocol underwent human subject review at the CDC and received non-research determination (Human Subjects Research Tracking no. 2015-244). Laboratory assays for antigen and IgG antibody detection were conducted at the CDC in Atlanta, and researchers did not have access to identifying information.

Study Area and Population: The study locations were limited to areas below 2500 m elevation, with 55.7% of the households surveyed from areas below 2000 m in elevation, with the remaining 44.3% from areas between 2000 and 2500 m in elevation.

Multiplex Antigen and IgG Detection Assays: Reagent preparation and multiplex bead-based antigen detection[134] and IgG detection assay[135] were performed as described elsewhere. Briefly, a 6-mm punch equivalent to 10 µL of whole blood was used from each dried blood spot, with blood eluted overnight to a 1:20 concentration in blocking buffer (phosphate-buffered saline containing 0.5% bovine serum albumin, 0.05% Tween 20, 0.02% sodium azide, 0.5% polyvinyl alcohol, 0.8% polyvinylpyrrolidone, and 3-µg/mL *Escherichia coli* extract).

A 1:200 dilution of serum was used for the multiplex IgG detection assay to detect antibodies to a panel of 12 *Plasmodium* antigens. For *P. falciparum,* the following were tested: circumsporozoite protein (PfCSP), early transcribed membrane protein 5 antigen 1 (PfETR5Ag1), glutamate-rich protein

[134] Plucinski MM, Herman C, Jones S, et al. Screening for Pfhrp2/3-deleted Plasmodium falciparum, non-falciparum, and low-density malaria infections by a multiplex antigen assay. J Infect Dis 2019; 219:437–47.
[135] Assefa A, Ali Ahmed A, Deressa W, et al. Multiplex serology demonstrates cumulative prevalence and spatial distribution of malaria in Ethiopia. Malar J 2019; 18:246.

(PfGLURP-R0), liver-stage antigen 1 (PfLSA1), schizont egress antigen-1 (PfSEA1), apical membrane antigen 1 N terminal region (PfAMA1), and merozoite surface protein 1 19-kD region (PfMSP1); for *P. vivax*: PvAMA1, PvMSP1, and a chimeric form of the PvMSP1 antigen with additional T- and B-cell epitopes (chPvMSP1); for *P. malariae*: PmMSP1; for *P. ovale*: PoMSP1. The threshold assay signal was dichotomized into antigen or IgG positive or negative as appropriate, based on the log-normal mean plus 3 standard deviations of a panel of 92 known negative blood samples from US residents for all assays. For both antigen detection and IgG assays, each assay plate included a buffer blank and positive and negative controls to ensure appropriate assay data collection.

Dataset #2: Ethiopian MIS 2015: The study data were obtained from the 2015 Ethiopia Malaria Indicator Survey (MIS). This data was conducted from September 30th to December 10th in 2015, these dates coincide with the high malaria transmission season in the country. The MIS utilized the same two-staged cluster-randomized sampling technique as mentioned with the MIS 2011 data. A total of 10,261 individuals were surveyed in 4,730 selected households. The same protocol for identifying eligible households and enrollment was implemented in this study as seen in 2011.

Blood collection: Blood collection was performed in the exact same manner as seen in the MIS 2011 data.

Ethics: The study protocol was approved by the same organizations and entities that approved the MIS 2011 data.

Study Area and Population: The study locations were limited to areas below 2500 m elevation, with 85% of samples collected from areas below 2000 m in elevation, with the remaining 15% from areas between 2000 and 2500 m in elevation.

Multiplex Antigen and IgG Detection Assays: Refer to the MIS 2011 data regarding reagent preparation and antigen and IgG detection assays.

Study-specific Antigens: MIS 2011 and MIS 2015: For these particular studies, 14 different antigen tests were conducted on blood samples collected from participants in two-cross sectional surveys. The glutathione-S-transferase (GST MFI) test serves as an internal control antigen. The *P. falciparum* merozoite protein 1 (PfMSP1 MFI) is acquired naturally during infection of *P. falciparum* and serves as a potential vaccine target for antibodies[136]. The *P. falciparum* apical membrane antigen 1 (N-terminal region) (PfAMA1 MFI) is a low-abundance type I integral membrane protein which is synthesized in the mature blood stages; it accumulates in the micronemes, secretory organelles, of developing merozoites[137],[138],[139]. The protein *P. falciparum* circumsporozoite (PfCSP MFI) is a surface protein in the sporozoite phase; it is the leading candidate for a vaccine targeting pre-erythrocytic malaria[140]. The next targeted protein was the *P. falciparum* glutamate-rich protein, Ro fragment (PfGLURPr0 MFI). This protein is associated with RBCs infected with mature schizonts; the Ro fragment refers to the nonrepetitive N-terminal of GLURP[141]. The *P. falciparum* liver stage antigen 1 (PfLSA1 MFI) is only expressed within infected hepatocytes; it is thought to have a role in merozoite release from the liver[142]. *P. falciparum* schizont egress antigen (PfSEA1 MFI) is another potential vaccine antigen target; it is released in schizont infected RBCs and is necessary for replication in the blood[143]. The last target for *P. falciparum* is the *P. falciparum* ETRAMP 5 antigen 1 (PfEtramp5Ag1 MFI), this antigen is a good

[136] Jäschke, Anja et al. "Merozoite Surface Protein 1 from Plasmodium falciparum Is a Major Target of Opsonizing Antibodies in Individuals with Acquired Immunity against Malaria." *Clinical and vaccine immunology: CVI* vol. 24,11 e00155-17. 6 Nov. 2017, doi:10.1128/CVI.00155-17

[137] Healer, Julie et al. "Functional analysis of Plasmodium falciparum apical membrane antigen 1 utilizing interspecies domains." *Infection and immunity* vol. 73,4 (2005): 2444-51. doi:10.1128/IAI.73.4.2444-2451.2005

[138] Bannister, L. H., J. M. Hopkins, A. R. Dluzewski, G. Margos, I. T. Williams, M. J. Blackman, C. H. Kocken, A. W. Thomas, and G. H. Mitchell. 2003. Plasmodium falciparum apical membrane antigen 1 (PfAMA-1) is translocated within micronemes along subpellicular microtubules during merozoite development. J. Cell Sci. 116:3825–3834.

[139] Healer, J., S. Crawford, S. Ralph, G. McFadden, and A. F. Cowman. 2002.Independent translocation of two micronemal proteins in developing Plasmodium falciparum merozoites. Infect. Immun. 70:5751–5758

[140] Singh, Susheel K, et al. "The Plasmodium Falciparum Circumsporozoite Protein Produced in Lactococcus Lactis Is Pure and Stable." *Journal of Biological Chemistry*, PlumX Metrics, Jan. 2020, https://www.jbc.org/article/S0021-9258(17)48336-0/fulltext.

[141] Theisen, M et al. "The glutamate-rich protein (GLURP) of Plasmodium falciparum is a target for antibody-dependent monocyte-mediated inhibition of parasite growth in vitro." *Infection and immunity* vol. 66,1 (1998): 11-7. doi:10.1128/IAI.66.1.11-17.1998

[142] Hillier, Collette J et al. "Process development and analysis of liver-stage antigen 1, a pre-erythrocyte-stage protein-based vaccine for Plasmodium falciparum." *Infection and immunity* vol. 73,4 (2005): 2109-15. doi:10.1128/IAI.73.4.2109-2115.2005

[143] Park, Sangshin et al. "Impact of maternally derived antibodies to Plasmodium falciparum Schizont Egress Antigen-1 on the endogenous production of anti-PfSEA-1 in offspring." *Vaccine* vol. 37,35 (2019): 5044-5050. doi: 10.1016/j.vaccine.2019.06.084

detection of current or recent exposure to malaria[144]. *P. vivax* merozoite protein 1 (PvMSP1 MFI), similar to PfMSP1 MFI antigen, is a vaccine candidate for *P. vivax* and is mainly expressed during the trophozoites stage[145]. The second *P. vivax* target is the *P. vivax* apical membrane antigen 1 (PvAMA1 MFI), this protein serves an important role in hepatocyte and erythrocyte invasion during the sporozoites and merozoites stages respectively[146]. The last *P. vivax* protein is the chimeric *P. vivax* merozoite protein 1 (chPvMSP1 MFI), including additional B and T cell epitopes. This protein is required for the invasion of the parasite into the RBCs and is highly expressed on the RBC merozoites; this makes it a suitable candidate for a vaccine target[147]. Since the immunoglobulin G (IgG) does not always respond to the presence of the chPvMSP1 MFI, this test utilized additional recognition from B and T cell epitopes for the detection of malaria with this antigen[148]. There is only one antigen test for *P. malariae, P. malariae* merozoite protein 1 (PmMSP1 MFI). The surface antigen is present within the RBC stages of *Plasmodium* species. *P. ovale* used the same protein as *P. malariae—P. ovale* merozoite protein 1 (PoMSP1 MFI). Finally, a mosquito salivary peptide (Mosq# sal MFI) is used as a biomarker for bite exposure and malaria infection based on the level of salivary peptide present in the blood sample[149].

The 12 antigens assessed for IgG antibody detection can be categorized into two groups: "short-term" *P. falciparum*, and "long-term" *P. falciparum, P. vivax, P. ovale,* and *P. malariae* antibodies. Short-term antibodies were more likely to have been acquired in the past year and included antibodies to PfCSP,

---

[144] van den Hoogen, Lotus L., et al. "Selection of Antibody Responses Associated with Plasmodium Falciparum Infections in the Context of Malaria Elimination." *Frontiers*, Frontiers, 1 Jan. 1AD, https://www.frontiersin.org/articles/10.3389/fimmu.2020.00928/full.

[145] Punnath, Kishore et al. "Acquired antibody responses against merozoite surface protein-1_{19} antigen during *Plasmodium falciparum* and *P. vivax* infections in South Indian city of Mangaluru." *Journal of parasitic diseases: official organ of the Indian Society for Parasitology*, vol. 45,1 1-15. 21 Oct. 2020, doi:10.1007/s12639-020-01288-4

[146] Igonet, Sébastien, et al. "Cross-Reactivity Studies of an Anti-Plasmodium Vivax Apical Membrane Antigen 1 Monoclonal Antibody: Binding and Structural Characterization." Journal of Molecular Biology, Academic Press, 16 Dec. 2006, https://www.sciencedirect.com/science/article/pii/S0022283606017049?casa_token=TbBY5HwACNYAAAAA%3A1LzNgKijGoo63lZdUjY1auFRwwoXzaN-TI-eX6pyKiaaq9pMCnT8ik3IQtjN89YYckw99vBFBsJA.

[147] Shen, Fei-Hu et al. "Chimeric Plasmodium vivax Merozoite Surface Protein Antibody Recognizes and Blocks Erythrocytic P. cynomolgi Berok Merozoites *In Vitro*." *Infection and immunity* vol. 89,2 e00645-20. 19 Jan. 2021, doi:10.1128/IAI.00645-20

[148] Egan, A et al. "Characterization of human T- and B-cell epitopes in the C terminus of Plasmodium falciparum merozoite surface protein 1: evidence for poor T-cell recognition of polypeptides with numerous disulfide bonds." *Infection and immunity* vol. 65,8 (1997): 3024-31. doi:10.1128/iai.65.8.3024-3031.1997

[149] Londono-Renteria, Berlin et al. "Identification and Pilot Evaluation of Salivary Peptides from *Anopheles albimanus* as Biomarkers for Bite Exposure and Malaria Infection in Colombia." *International journal of molecular sciences* vol. 21,3 691. 21 Jan. 2020, doi:10.3390/ijms21030691

PfETR5Ag1, PfGLURP-R0, PfLSA1, and PfSEA1[150],[151]. Long-term *P. falciparum* antibodies, acquired at any time in life, included antibodies to PfAMA1 and PfMSP1[152],[153]. *P. vivax* antibodies to these antigens, PvAMA1, PvMSPS1, and chPvMSP1, were all considered long-term. Both PoMPS1 and PmMSP1 are considered long-term *P. ovale* and *P. malariae* antibodies respectively. Although the long-term antibodies generally persist longer than the short-term antibodies, the short-term antibodies can last for years, especially in adults[154].

Dataset #3: Ethiopian Annual Rainfall: The Rainfall dataset in Ethiopia was obtained from the Ki-Data, Kimetrica Data Publishing open-source website. This dataset contained data on the average monthly rainfall in the 11 regions and administrative councils that make up Ethiopia from January 1981 to December 2019[155]. The dataset included information on many of the regions in Ethiopia: Afar, Amhara, Benishangul Gumuz, Dire Dawa, Harari, Oromiya, SNNPR, Somali, and Tigray. This dataset provided mean rainfall for all 12 months of each year between 1981 to 2019. For the yearly averages, the 12 months' mean rainfall values were averaged together for the yearly rainfall average value. Similarly, any decadal averages were calculated by the averages of all 12 months for the 10-year period. Additionally, any seasonal averages for 2011 and 2015 were calculated with the appropriate monthly averages (mean rainfall average for February to May (Belg), mean rainfall average for June to September (Kiremt), and mean rainfall average for October to January (Bega)) for those two years. Many of the regions were further broken down into administrative councils (admin2 variable); since the analysis was at the regional

[150] Helb DA, Tetteh KK, Felgner PL, et al. Novel serologic biomarkers provide accurate estimates of recent Plasmodium falciparum exposure for individuals and communities. Proc Natl Acad Sci U S A 2015; 112: E4438–47.
[151] Ondigo BN, Hodges JS, Ireland KF, et al. Estimation of recent and long-term malaria transmission in a population by antibody testing to multiple Plasmodium falciparum antigens. J Infect Dis 2014 ; 210 :1123–32.
[152] Drakeley CJ, Corran PH, Coleman PG, et al. Estimating medium- and long-term trends in malaria transmission by using serological markers of malaria exposure. Proc Natl Acad Sci U S A 2005; 102:5108–13.
[153] Ondigo BN, Hodges JS, Ireland KF, et al. Estimation of recent and long-term malaria transmission in a population by antibody testing to multiple Plasmodium falciparum antigens. J Infect Dis 2014 ; 210 :1123–32.
[154] Helb DA, Tetteh KK, Felgner PL, et al. Novel serologic biomarkers provide accurate estimates of recent Plasmodium falciparum exposure for individuals and communities. Proc Natl Acad Sci U S A 2015; 112: E4438–47.
[155] "Ki-Data." *Conflict Model-Ethiopia - Eth-Rainfall-Monthly.csv*, https://data.kimetrica.com/dataset/conflict_model/resource/92077aa6-edf2-4533-afc4-837959da4594?view_id=2b38dfc4-edf7-4bbb-bc29-c24eed0d8dcc.

level, each administrative council value during the same month and the same year was averaged together, aiding in creating a large sample size for these total rainfall (mm) average values.

Dataset #4: Ethiopian Annual Temperature: The Temperature dataset in Ethiopia was obtained from the Ki-Data, Kimetrica Data Publishing open-source website. The dataset contained data on the average monthly temperatures in the 11 regions and administrative councils that make up Ethiopia from January 1981 to December 2019[156]. Similarly, the dataset included information on many of the regions in Ethiopia: Afar, Amhara, Benishangul Gumuz, Dire Dawa, Harari, Oromiya, SNNPR, Somali, and Tigray. This dataset provided a temperature mean variable for all 12 months for each year listed between 1981 to 2019. For the yearly averages, the 12 months temperature mean values were averaged together for the yearly temperature average value. Many of the regions were further broken down into administrative councils (admin2 variable); since the analysis was at the regional level, each administrative council value during the same month and the same year was averaged together, aiding in creating a large sample size for these temperature average values (° C).

Dataset #5: Ethiopian Population: The Population dataset in Ethiopia was obtained from the Ki-Data, Kimetrica Data Publishing open-source website. The dataset contained data on the total population in the 11 regions and administrative councils that make up Ethiopia from 2000 to 2020[157]. The population dataset contained regional subcategorization of Ethiopia: Afar, Amhara, Benishangul Gumuz, Dire Dawa, Harari, Oromiya, SNNPR, Somali, and Tigray. This dataset only contained population values from 2000 to 2020. Again, many of the regions were further broken down into subregions (admin2 variable); since the analysis was at the regional level, each subregional value during the same year was summed together, calculating a more accurate estimate of the true population in these regions. For example, the population in Oromiya was given at the following subregional levels: Adama, Arsi, Bale, Borena, Burayu, East

[156] "Ki-Data." *Conflict Model-Ethiopia - Eth-Temperature.csv*, https://data.kimetrica.com/dataset/conflict_model/resource/8e54320f-8ef5-46ba-be58-f9fa5b3a1012.
[157] "Ki-Data." *Conflict Model-Ethiopia - Eth-Population.csv*, https://data.kimetrica.com/dataset/conflict_model/resource/fcf0ade4-eab0-4cd2-ac04-7cc65ea67ccf.

Hararge, East, Shewa, East Wellega, Guji, Horo Gudru Wellega, Ilu Aba Bora, Jimma, Jimma Sp., North Shewa, Qeleme Wellega, South West Shewa, West Arsi, West Hararge, West Shewa, and West Wellega. All the population values for these subregional locations were summed together for the entire population value in 2011 and, again in 2015.

Dataset #6: Ethiopian Monthly Rainfall: The Climate Hazards Center InfraRed Precipitation with Station data (CHIRPS) dataset for Ethiopia was also obtained from the Climate and Hazards Center at UC Santa Barbara. The CHIRPS incorporates a 0.05° resolution satellite imagery with in-situ station data to create gridded rainfall time series for trend analysis and seasonal drought monitoring[158].

Dataset #7: Ethiopian Monthly Temperature: The CHIRTSmax dataset for Ethiopia was obtained from the Climate and Hazards Center at UC Santa Barbara. The data is a global 2-m maximum temperature (Tmax) product that directly combines satellite and station-based estimates of Tmax to produce routinely updated data to support the monitoring of temperature extremes. The result is a monthly estimate of the daily maximum temperature for the 2011 and 2015 time period[159].

Dataset #8: Ethiopian Shapefile of Administrative Boundaries: The shapefile for Ethiopia was obtained from The Humanitarian Data Exchange. The dataset is a part of the Ethiopia Data grid and provided the subnational administrative boundaries: Ethiopia administrative level 0-3 boundary shapefiles[160].

Ethiopian Regions Included: Based on the data from the CDC datasets, the data from Ki-Data, Kimetrica Data Publishing, and the data from the Climate and Hazards Center at UC Santa Barbara, the number of overlapping region locations in Ethiopia was reduced to nine regions: Afar, Amhara, Benishangul Gumuz, Dire Dawa, Harari, Oromiya, Southern Nations, Nationalities, and People's Region (SNNPR), Somali,

[158] "CHIRPS: Rainfall Estimates from Rain Gauge and Satellite Observations." *Climate Hazards Center - UC Santa Barbara*, US AID, https://www.chc.ucsb.edu/data/chirps.
[159] "Introduction to CHIRTSmax." *Climate Hazards Center - UC Santa Barbara*, US AID, https://www.chc.ucsb.edu/data/chirtsmonthly.
[160] "Ethiopia - Subnational Administrative Boundaries." *Humanitarian Data Exchange*, United Nations Office for the Coordination of Humanitarian Affairs Services, https://data.humdata.org/dataset/cod-ab-eth.

and Tigray. These nine regions are presented in Figure 7[161] and their populations in 2011 and 2015 and region areas are highlighted in Table 1. The population growth is also presented (Table 1: Difference).

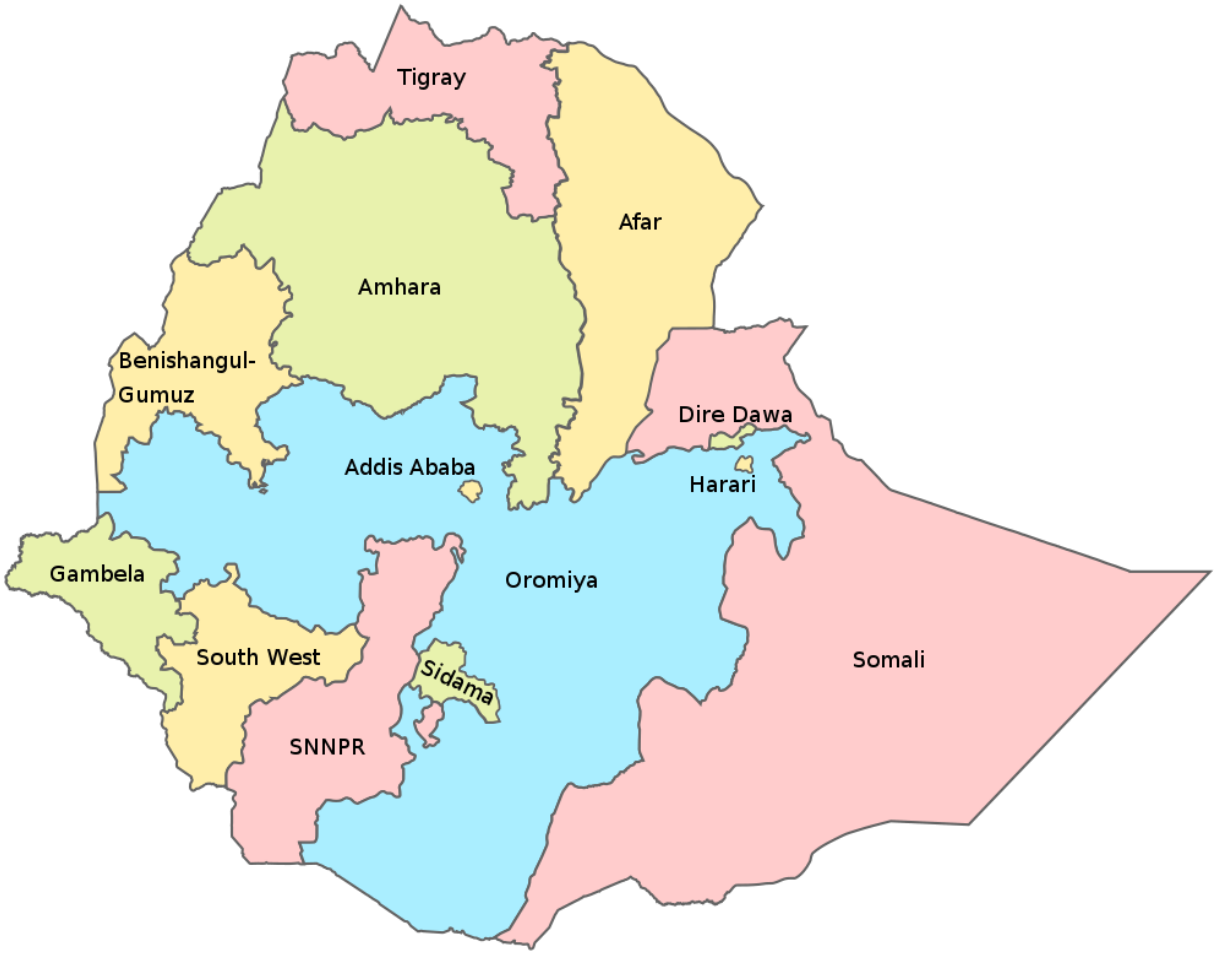

Figure 7: Regional States and Charted Cities of Ethiopia: Afar, Amhara, Benishangul Gumuz, Dire Dawa, Harari, Oromiya, SNNPR, Somali, and Tigray are of research importance to this study. 161

[161] "File: Regions of Ethiopia En.svg." *Wikimedia Commons*, https://commons.wikimedia.org/wiki/File:Regions_of_Ethiopia_EN.svg.

Table 1: Population of Ethiopia in 2011 and 2015 by Region with Region Area (Km^2) and Difference

Regions	Area (Km^2)	2011 Population	2015 Population	Difference
Afar	72,053	1,737,060	2,061,197	324,137
Amhara	154,709	19,699,988	21,271,284	1,571,296
Benishangul Gumuz	50,699	1,019,056	1,237,326	218,270
Dire Dawa	1,559	409,504	460,391	50,887
Harari	334	218,598	241,840	23,242
Oromiya	284,538	32,726,110	37,142,128	4,416,018
SNNPR	105,476	18,111,019	20,452,286	2,341,267
Somali	279,252	5,478,651	6,371,112	892,461
Tigray	84,722	5,111,568	5,636,546	524,978

Descriptive and Analytical Methods: Data cleaning and statistical analyses were performed by using RStudio (Version 1.4.1717; 2009-2021 RStudio, PBC). After importing the MIS 2011 and MIS 2015 datasets into RStudio, along with the Annual Rainfall and Annual Temperature datasets, the sample sizes of these datasets were reduced by removing any regions that were not similar between all four files, or any entries that did not have a region record. For the Annual Temperature and Annual Rainfall datasets,

all administrative council subcategories inside a region were averaged together for the entire year to create the average yearly total rainfall values or temperature values between 1981 through 2019 for each of the nine regions. Next, any data not from 2011 or 2015 in these files were removed to calculate the average yearly total rainfall and temperature values, along with the monthly average total rainfall and temperature values and the seasonal average total rainfall and temperature values: February to May (Belg), June to September (Kiremt), and October to January (Bega), again at the regional level for all nine regions. This data was then exported to Microsoft® Excel® 2016 MSO (Version 2203 Build 16.0.15028.20152) 32-bit to create the graphical representation of the values of rainfall and temperature over the various time frames.

The average yearly total rainfall graphs for the entire 1981 to 2019 period by regions were created with scatter plots. The average yearly temperature graphs for the entire 1981 to 2019 period by regions were also created with scatter plots, because a more obvious trend was observed with these graphs a linear line of best fit was placed over the individual points, and an R^2 value was calculated. The average decadal total rainfall graphs were stratified into four decades: 1981-1989, 1990-1999, 2000-2009, and 2010-2019. These graphs were made with clustered columns. The same clustered column graphs were used to depict the yearly average temperature and yearly average total rainfall in 2011 and 2015, and the difference between the two years (2015-2011 = difference). Furthermore, the seasonal average of total rainfall and the seasonal average of temperature were constructed with the same clustered columns.

Back in RStudio, independent-samples t-tests were used to statistically analyze the maximum rainfall total average from 1981 to 2019 and the minimum rainfall total average from 1981 to 2019. These two average values were compared statistically, to determine if the difference between the maximum rainfall and minimum rainfall values were statistically significantly different from each other. The same test was used to determine if the difference between the maximum temperature and minimum temperatures values between 1981 to 2019 were statistically significantly different from each other. This statistical test was done at the regional level in Ethiopia. The same independent-samples t-tests were used to compare the

short-term climate change between 2011 and 2015. This was done for rainfall and temperature at the country level and the regional level. The rainfall analysis was further subcategorized by 2011 and 2015 rainfall values during Kiremt, the heavy rainfall season in Ethiopia.

For the malaria antigen test detection, these datasets: MIS 2011 and MIS 2015, were examined in RStudio. The proportions of positive antigen test results for each of the 12 investigated antigens were calculated, first removing any missing values from the antigen columns independently. Similarly, the proportions were exported from RStudio into Microsoft Excel to create clustered columns graphs to represent the proportion of positive antigen detection between 2011 and 2015, along with the difference in percentages for each antigen within each region. For each antigen within each region, a two-proportions z-test was performed to observe if the difference in the proportion of positive antigen detection between 2011 and 2015 was statistically significant.

The difference in rainfall and temperature between 2011 and 2015 was not as notable as the difference seen across the select regions of Ethiopia, mainly since there is only a four-year gap between these data points. To account for expected trends over extended periods of time, an analysis of each unique geographic region in Ethiopia was conducted to address how larger discrepancies in climatic patterns would relate to malaria prevalence in Ethiopia. Potentially, if a higher malaria prevalence was seen in warmer and wetter regions as opposed to colder and drier regions, then as climate change continues to exacerbate, we may expect to see an increase in malaria prevalence within a singular region across a longer time period. The average Bega total rainfall values from 2011 and 2015 were calculated for each region. These were matched with the previously calculated proportion of positive antigen tests for each of the 12 antigens. The same calculation was done for the average Kiremt total rainfall values from 2011 and 2015 matched with the same antigen proportions. For rainfall, an exponential trend line was added to the scatter plots. This analysis was repeated for the average Bega Temperatures and average Kiremt temperatures for 2011 and 2015 matched to the proportion of positive antigen detection for all 12 antigens. The scatterplots were created with the best fit from a polynomial curve for temperature.

Then, while ascertaining the demographic information for 2011 and 2015, any missing data for my confounding variables—age, bed net utilization, and region—were removed from the data sets. Sex was also reported in the demographic tables and any missing sex information removed the individual from the data. To calculate the number of households used, instead of individual numbers, the GPS latitude and longitudes were used to determine the number of distinct values for these two columns. The average age of the region was calculated and reported with the standard deviation of the value.

From the Monthly Rainfall, Monthly Temperature, and Shapefile of Administrative Boundaries the files were properly formatted in RStudio with the packages: "sf" and "raster". The Monthly Rainfall and Monthly Temperature files, which contained all data points for Africa, were reduced to just Ethiopia by masking the Shapefile of Administrative (Ethiopian) Boundaries on the climate variable datasets. Data for each month (August through December) was plotted for both 2011 and 2015.

Additionally, variables in the MIS 2011 and MIS 2015 were used to create cluster locations; the district, zone, and kebele columns were combined to create a new variable "Unique_ID". The following variables were also calculated at the new cluster level for modeling purposes:

- Bed net utilization at the cluster level (average number of bed nets used)
- Age of the cluster (average age)
- Latitude of the cluster (average of latitude)
- Longitude of the cluster (average of longitude)
- Cluster prevalence of PfMSP1 (summation of positive tests/total number tested)
- Cluster prevalence of PvMSP1 (summation of positive tests/total number tested)
- Cluster prevalence of PmMSP1 (summation of positive tests/total number tested)
- Cluster prevalence of PoMSP1 (summation of positive tests/total number tested)

The cluster prevalence of the four antigens was plotted with the cluster latitude and longitude on the Shapefile of Ethiopia with the administrative boundaries. The different plots were then layered together

so that the cluster prevalence of each antigen was overlayed on the monthly (August through December) rainfall and temperature gradient in Ethiopia.

Finally, the exact rainfall and temperature values at the cluster latitude and longitude points were extracted and combined with the MIS 2011 and MIS 2015 datasets. A log-binomial regression model was performed in RStudio, which modeled the potential association between rainfall and temperature in 2011/2015 with the antigen prevalence ratios at the cluster level in 2011/2015 after controlling for average cluster age, the average number of bed nets used, and region location. Four antigen tests were assessed using this model to estimate the prevalence of each of the four pathogenic species of *Plasmodium*. The 12 antigen tests that were conducted identified infection multiple times for the same individual, for example, a person infected with *P. falciparum* should in theory test positive for seven of the 12 antigen tests. To ensure the model does not overinflate the prevalence of species with a larger number of antigen testing, the four tests that detected a protein consistent across all species were chosen. The four antigen tests chosen detected merozoite protein 1, the only antigen marker consistent across all four species. Therefore, the log-binomial regression model was applied to each of the four explored antigens for August through December in 2011 and 2015.

Results

Objective 1: Climate Change Exposure #1: Rainfall

1981 to 2019 Long-term Rainfall Observations

In most of Ethiopia, there was a general trend that rainfall had been increasing from 1981 to 2019. An average of the nine different region's rainfall revealed that Ethiopia's driest year was 1984 with only 54.70 mm of rainfall, while the wettest year was 2019 with 81.93 mm of rainfall. However, there was tremendous variability in rainfall at the regional level. As a result, the nine regions' yearly average rainfall was observed. The minimum and maximum rainfall measurements between 1981 and 2019 are

reported along with the year in which they occurred (Table 2). Generally, most regions experienced an increase in rainfall, with the minimum measurement occurring in the 1980s and the maximums occurring after 2000. However, two regions—Dire Dawa and Harari—did not fit this pattern. They experienced a decrease in rainfall during this time frame. As depicted in Figure 2, there is a large range of minimum (17.79 mm in Somali and 84.94 mm in SNNPR) and maximum values (11.36 mm in Oromiya and 134.46 mm in SNNPR). Due to the regional variability, each region is further discussed in detail below.

Table 2: Maximum and Minimum Rainfall Measurements during 1981 to 2019 for each Region of Ethiopia

Region	Year of Minimum Rainfall	Minimum mean total yearly rainfall (mm)	Year of Maximum Rainfall	Maximum mean total yearly rainfall (mm)	P-value**
Afar	1984	20.40	1998	46.00	<0.001*
Amhara	1984	69.58	1998	104.53	<0.01*
Benishangul Gumuz	1986	83.13	2008	114.31	0.21
Dire Dawa	2015	32.90	2010	82.20	0.04*
Harari	2015	43.23	1996	84.99	0.12
Oromiya	2002	81.42	2019	11.36	<0.001*
SNNPR	1984	84.94	2019	134.46	<0.0001*
Somali	1984	17.79	1997	47.63	<0.0001*
Tigray	1984	43.14	1986	76.02	0.02*

** P-values calculated from an Independent-samples T-test
* Significant difference between the minimum mean total yearly rainfall and the maximum mean total yearly rainfall at a 95% confidence interval.

Afar: The rainfall distribution in Afar between 1981 to 2019 had much more variability in the average yearly rainfall (Appendix A: Figure A1.1); however, when examining the decadal average rainfall in the region (1981-1989), (1990-1999), (2000-2009), and (2010-2019) no consistent pattern in average rainfall was observed, suggesting that climate change is impacting the consistency of rainfall in Afar, Ethiopia (Appendix A: Figure A1.2). The average decadal rainfall was highest between 1981 and 1989 with 37.71 mm of rainfall. Among the seasonal averages in Afar (Belg (February – May, light rain season), Kiremt

(June – September, heavy rain season), and Bega (October – January, dry season), the decrease in rainfall between 2011 and 2015 was only notable during Kiremt (-21.38 mm of rainfall). The other rainfall seasons Belg and Bega were not substantially different between the two years observed (Appendix A: Figure A1.3). From 1981 to 2019, the minimum and maximum total average rainfall values were in 1984 and 1998, respectively. An independent-samples t-test revealed the average rainfall in 1984, 20.40 mm, and the average rainfall in 1998, 46.00 mm, were statistically significantly different from each other (p-value < 0.001, df = 118) (Table 2).

Amhara: The rainfall distribution in Amhara between 1981 to 2019 had a lot of variability in the average yearly rainfall. The maximum rainfall occurred in 1998 with 104.53 mm of rainfall, and the minimum rainfall occurred in 1984 with 69.58 mm of rainfall (Appendix A: Figure A2.1). Observing the decadal averages from (1981-1989), (1990-1999), (2000-2009), and (2010-2019) revealed an inconsistency with the rainfall averages. Each decade appeared to increase, decrease, and then increase again with the total average rainfall, suggesting that climate change could be causing fluctuations in rainfall patterns (Appendix A: Figure A2.2). Among the seasonal averages in Amhara, the decrease in rainfall between 2011 and 2015 was only notable during Kiremt (-36.35 mm of rainfall). The other rainfall seasons, Belg and Bega, were not substantially different between the two years observed (Appendix A: Figure A2.3). From 1981 to 2019, the minimum and maximum total average rainfall values were seen in 1984 and 1998. An independent-samples t-test indicated the average rainfall in 1984, 69.58 mm, and the average rainfall in 1998, 104.53 mm, were statistically significantly different from each other (p-value < 0.01, df = 286) (Table 2).

Benishangul Gumuz: The rainfall distribution in Benishangul Gumuz between 1981 to 2019 revealed instability in the yearly rainfall distribution. Yet, the overall trend for Benishangul Gumuz suggested an increase in rainfall over the time period (Appendix A: Figure A3.1). This pattern is emphasized in the decadal average rainfall distribution. Each decade, the average rainfall amount increased from 96.80 mm in 1981-1989, then 98.63 mm from 1990-1999, 99.79 mm in 2000-2009, and lastly, 103.73 mm in 2010-

2019. This more consistent increasing pattern may indicate climate change impacts are affecting this region through a more predictable increase in rainfall over each decade (Appendix A: Figure A3.2). Among the seasonal averages in Benishangul Gumuz, this region experienced different trends in rainfall, as there was an increase in rainfall in each rainfall season. The most notable increase in rainfall between 2011 and 2015 occurred in Kiremt (+13.49 mm). The other rainfall seasons, Belg and Bega, also had an increased amount of rainfall between the two years observed, 7.86 and 9.69 mm, respectively (Appendix A: Figure A3.3). From 1981 to 2019, the minimum and maximum total average rainfall values were seen in 1986 and 2008. An independent-samples t-test indicated the average rainfall in 1986, 83.13 mm, and the average rainfall in 2008, 114.31 mm, were not statistically significantly different from each other (p-value = 0.21, df = 70) (Table 2). Perhaps a larger sample size of rainfall measurements in more administrative councils in Benishangul Gumuz would have produced a significant difference between the maximum and minimum total average yearly rainfall (mm) measurements.

Dire Dawa: The rainfall distribution in Dire Dawa between 1981 to 2019 showed two different baselines for the average rainfall. From 1981 to about 2000, the average rainfall each year remained around the same amount. However, after 2005, each year had an increased or decreased amount of rainfall as compared to the previous year (Appendix A: Figure A4.1). The decadal average graph demonstrates an inconstant pattern in the average rainfall indicating that climate change was impacting the consistency of rainfall in Dire Dawa, Ethiopia (Appendix A: Figure A4.2). Comparing the seasonal averages in Dire Dawa, the decrease in rainfall between 2011 and 2015 was only notable during Kiremt (-43.26 mm of rainfall). The other rainfall seasons, Belg and Bega, were not substantially different between the two years observed (Appendix A: Figure A4.3). From 1981 to 2019, the minimum and maximum total average rainfall values were seen in 2015 and 2010. An independent-samples t-test indicated the average rainfall in 2015, 32.90 mm, and the average rainfall in 2010, 82.80 mm, were statistically significantly different from each other (p-value = 0.04, df = 22) (Table 2).

Harari: The rainfall distribution in Harari between 1981 to 2019 followed a similar pattern to Dire Dawa in that there were two different sets of average rainfall baselines. From 1981 to 1995, the average rainfall each year was relatively the same. Yet, after the maximum rainfall in 1996 with 84.99 mm of rainfall, the amount of rainfall each year began to fluctuate drastically year after year (Appendix A: Figure A5.1). The decadal average rainfall demonstrated a cyclical pattern of low rainfall (at 61.75 and 61.79) and high rainfall (65.60 and 66.32) alternately (Appendix A: Figure A5.2). Among the seasonal averages in Harari, the decrease in rainfall between 2011 and 2015 was only notable during Kiremt (-48.80 mm of rainfall). The other rainfall seasons, Belg and Bega, were not substantially different between the two years observed (Appendix A: Figure A5.3). From 1981 to 2019, the minimum and maximum total average rainfall values were seen in 2015 and 1996. An independent-samples t-test indicated the average rainfall in 2015, 43.23 mm, and the average rainfall in 1996, 84.99 mm, were not statistically significantly different from each other (p-value = 0.12, df = 22) (Table 2). Perhaps a larger sample size of rainfall measurements in more administrative councils in Harari would have produced a significant difference between the maximum and minimum total average yearly rainfall (mm) measurements.

Oromiya: The rainfall distribution in Oromiya between 1981 to 2019 had consistent variability throughout the entire time period 1981 to 2019. The maximum rainfall, however, occurred in the last year of data collection, 2019, with 111.36 mm. This is greatly increased from the lowest rainfall average in Oromiya at 81.42 mm in 2002 (Appendix A: Figure A6.1). Observing the decadal averages from (1981-1989), (1990-1999), (2000-2009), and (2010-2019) revealed an inconsistency with the rainfall averages. In each decade, the average amounts of rainfall appeared to increase, decrease, and then increase again, illustrating fluctuations in the overall rainfall patterns (Appendix A: Figure A6.2). Among the seasonal averages in Oromiya, the decrease in rainfall between 2011 and 2015 was only notable during Kiremt (-44.87 mm of rainfall). The other rainfall seasons, Belg and Bega, were not substantially different between the two years observed (Appendix A: Figure A6.3). From 1981 to 2019, the minimum and maximum total average rainfall values were seen in 2002 and 2019. An independent-samples t-test showed the average

rainfall in 2002, 81.42 mm, and the average rainfall in 2019, 111.36 mm, were statistically significantly different from each other (p-value < 0.001, df = 478) (Table 2).

SNNPR: The rainfall distribution in SNNPR between 1981 to 2019 appears to remain relatively consistent throughout the time frame. However, in the 1990s and the 2010s decades, there was a notable increase in the average yearly rainfall amounts. Especially toward the end of the time period (2015-2019), an obvious curve trending upward was seen, marking the maximum value of rainfall in the region at 134.46 mm in 2019 (Appendix A: Figure A7.1). These same patterns were also observed in the decadal average rainfall patterns. The average rainfall in 2010-2019 was the highest reported in SNNPR since 1981-1989, with the second-highest decade of rainfall occurring in 1990-1999 (Appendix A: Figure A7.2). Among the seasonal averages in SNNPR, the decrease in rainfall between 2011 and 2015 was only notable during Kiremt (-30.22 mm of rainfall). The other rainfall seasons, Belg and Bega, were not substantially different between the two years observed (Appendix A: Figure A7.3). From 1981 to 2019, the minimum and maximum total average rainfall values were seen in 1984 and 2019. An independent-samples t-test indicated the average rainfall in 1984, 84.94 mm, and the average rainfall in 2019, 134.46 mm, were statistically significantly different from each other (p-value < 0.0001, df = 382) (Table 2).

Somali: The rainfall distribution in Somali between 1981 to 2019 shows a rather inconsistent pattern of average yearly rainfall. The baseline rainfall can be seen around the high 20s to low 30s mm of rainfall. Every few years, however, the rainfall amount increased to the upper 30s or higher. The maximum average rainfall occurred in 1997 with 47.62 mm of rainfall (Appendix A: Figure A8.1). The average decadal rainfall between (1981-1989), (1990-1999), and (2000-2009) indicated a consistent decrease in rainfall suggesting greater drought in the region. However, the last decade (2010-2019) had a large increase in the average rainfall, suggesting a climatic change resulting in flooding in the region (Appendix A: Figure A8.2). Examining the seasonal averages in Somali, the trend for rainfall was different than in many of the other regions in Ethiopia. The decreases in Bega and Kiremt were rather small and not notable (-5.66 and -4.94 mm respectively). The biggest trend in the rainfall pattern was an increase in

rainfall during Belg, +11.13 mm (Appendix A: Figure A8.3). From 1981 to 2019, the minimum and maximum total average rainfall occurred in 1984 and 1997, respectively. An independent-samples t-test demonstrated the average rainfall in 1984, 17.79 mm, and the average rainfall in 1997, 47.63 mm, were statistically significantly different from each other (p-value < 0.0001, df = 214) (Table 2).

Tigray: The rainfall distribution in Tigray between 1981 to 2019 illustrated a range of variability in rainfall from 1981 to 1994, which then leveled out between 1995 to 2000, followed by another period of instability from 2001 until 2019 (Appendix A: Figure A9.1). Minimum rainfall occurred in 1990 with only 43.08 mm of rainfall, and maximum rainfall was reported in 1986 with 76.02 mm of rainfall. Examining the decadal average of rainfall in Tigray, the graphs illustrate a continual increase in average rainfall from (1981-1989), (1990-1999), (2000-2009), and (2010-2019) (Appendix A: Figure A9.2). Inspecting the seasonal averages in Tigray, the decrease in rainfall between 2011 and 2015 was only notable during Kiremt (-27.90 mm of rainfall). The other rainfall seasons, Belg and Bega, were not substantially different between the two years observed (Appendix A: Figure A9.3). From 1981 to 2019, the minimum and maximum total average rainfall values were reported in 1984 and 1986, respectively. An independent-samples t-test demonstrated that the average rainfall in 1984, 43.14 mm, and the average rainfall in 1986, 76.02 mm, were statistically significantly different from each other (p-value = 0.02, df = 142) (Table 2).

Objective 1: Climate Change Variable #2: Temperature

1981 to 2019 Long-term Temperature Observations

In most of Ethiopia, there was a general trend that temperature had been increasing from 1981 to 2019. An average of the nine different region's temperature measurements revealed that Ethiopia's coldest year was 1989 at 21.76° C, while the hottest year was 2015 at 23.38° C. However, there was significant variability in temperature at the regional level. As a result, the nine regions' yearly average temperature measurements were observed. The minimum and maximum temperature measurements between 1981 and

2019 were reported along with the year in which they occurred (Table 3). Generally, all the regions experienced an increase in temperature, with the minimum measurement occurring in the 1980s and the maximum occurring in 2015 (*one in 2009). However, as depicted in Figure 3, there was a large range of minimum (26.96° C in Afar and 18.59° C in Oromiya) and maximum values (28.72° C in Afar and 20.24° C in Oromiya). Due to the regional variability, each region is further discussed in detail below.

Table 3: Maximum and Minimum Temperature Measurements during 1981 to 2019 for each Region of Ethiopia

Region	Year of Minimum temperature	Minimum mean yearly temperature (°C)	Year of Maximum temperature	Maximum mean yearly temperature (°C)	P-value**
Afar	1981	26.96	2015	28.72	<0.01*
Amhara	1989	19.42	2015	21.17	<0.001*
Benishangul Gumuz	1989	23.49	2015	25.23	<0.001*
Dire Dawa	1984	22.78	2015	24.46	0.09
Harari	1984	18.69	2015	20.31	<0.01*
Oromiya	1989	18.59	2015	20.24	<0.001*
SNNPR	1989	19.49	2015	21.03	<0.001*
Somali	1984	24.97	2015	26.37	<0.001*
Tigray	1989	21.12	2009	22.88	<0.01*

** P-values calculated from an Independent-samples T-test
* Significant difference between the minimum mean yearly temperature and the maximum mean yearly temperature at a 95% confidence interval.

Afar: The temperature data in Afar between 1981 to 2019 indicated a small, but consistent, increase in temperature during the time period. The minimum temperature was observed in 1981 at 26.96° C, and the highest temperature was observed in 2015 at 28.71° C. The increase in temperature steadily occurred each year (Appendix B: Figure B1). The R^2 value illustrates a good fit of the temperature values over the time period using a linear regression model (R^2 = 0.70). From 1981 to 2019, the minimum and maximum average temperature values were reported in 1981 and 2015. An independent-samples t-test indicated the

average temperature in 1981, 26.96° C, and the average temperature in 2015, 28.72° C, were statistically significantly different from each other (p-value < 0.01, df = 118) (Table 3).

Amhara: The temperature data in Amhara between 1981 to 2019 indicated a small, but consistent, increase in temperature during the time period. The minimum temperature was observed in 1989 at 19.41° C, and the highest temperature was observed in 2015 at 21.17° C. The increase in temperature steadily occurred each year (Appendix B: Figure B2). The R^2 value illustrates a relatively good fit of the temperature values over the time period using a linear regression model (R^2 = 0.66). From 1981 to 2019, the minimum and maximum average temperature values were reported in 1989 and 2015. An independent-samples t-test indicated the average temperature in 1989, 19.42° C, and the average temperature in 2015, 21.17° C, were statistically significantly different from each other (p-value < 0.001, df = 286) (Table 3).

Benishangul Gumuz: The temperature data in Benishangul Gumuz between 1981 to 2019 indicated more variability over the years, with a few outlier values impacting the linear regression fit to the graph. Overall, though, the temperature reported in this region increased throughout the time frame. The minimum temperature was observed in 1989 at 23.49° C, and the highest temperature was observed in 2015 at 25.22° C. The increase in temperature steadily occurred each year in 2000, after experiencing extremely low-temperature outliers from 1989 to 1999 (Appendix B: Figure B3). The R^2 value illustrates a lower fit of the temperature values over the time period using a linear regression model (R^2 = 0.44). This is most likely due to the lower temperature outliers impacting the fit of the model to the data points. From 1981 to 2019, the minimum and maximum average temperature values were reported in 1989 and 2015. An independent-samples t-test indicated the average temperature in 1989, 23.49° C, and the average temperature in 2015, 25.23° C, were statistically significantly different from each other (p-value < 0.001, df = 70) (Table 3).

Dire Dawa: The temperature data in Dire Dawa between 1981 to 2019 indicated a small, but consistent, increase in temperature during the time period. The minimum temperature was observed in 1984 at 22.78° C, and the highest temperature was observed in 2015 at 24.46° C. The increase in temperature steadily occurred each year (Appendix B: Figure B4). The R^2 value illustrates a good fit of the temperature values over the time period using a linear regression model (R^2 = 0.70). From 1981 to 2019, the minimum and maximum average temperature values were reported in 1984 and 2015. An independent-samples t-test indicated the average temperature in 1984, 22.78° C, and the average temperature in 2015, 24.46° C, were not statistically significantly different from each other (p-value = 0.09, df = 22) (Table 3).

Harari: The temperature data in Harari between 1981 to 2019 observed a small, but consistent, increase in temperature during the time period. The minimum temperature was observed in 1984 at 18.69° C, and the highest temperature was observed in 2015 at 20.31° C. The increase in temperature steadily occurred each year (Appendix B: Figure B5). The R^2 value illustrates a good fit of the temperature values over the time period using a linear regression model (R^2 = 0.69). From 1981 to 2019, the minimum and maximum average temperature values were reported in 1984 and 2015. An independent-samples t-test indicated the average temperature in 1984, 18.69° C, and the average temperature in 2015, 20.31° C, were statistically significantly different from each other (p-value < 0.01, df = 22) (Table 3).

Oromiya: The temperature data in Oromiya between 1981 to 2019 indicated a small, but consistent, increase in temperature during the time period. The minimum temperature was observed in 1989 at 18.59° C, and the highest temperature was observed in 2015 at 20.24° C. The increase in temperature steadily occurred each year (Appendix B: Figure B6). The R^2 value illustrates a relatively good fit of the temperature values over the time period using a linear regression model (R^2 = 0.66). There were a few outlying values with lower and higher temperatures which most likely reduced the R^2 value. From 1981 to 2019, the minimum and maximum average temperature values were reported in 1989 and 2015. An independent-samples t-test indicated the average temperature in 1989, 18.59° C, and the average

temperature in 2015, 20.24° C, were statistically significantly different from each other (p-value < 0.001, df = 478) (Table 3).

SNNPR: The temperature data in SNNPR between 1981 to 2019 indicated a mostly consistent increase in temperature during the time period. The minimum temperature was observed in 1989 at 19.49° C, and the highest temperature was observed in 2015 at 21.03° C. The increase in temperature, overall, occurred each year (Appendix B: Figure B7). There are a few low-temperature outliers that occurred prior to 2000, and a noteworthy low temperature in 2019 at 20.21° C. These outliers most likely contributed to the lower R^2 value (R^2 = 0.64). The value illustrates a relatively good fit of the temperature values over the time period using a linear regression model. From 1981 to 2019, the minimum and maximum average temperature values were reported in 1989 and 2015. An independent-samples t-test indicated that the average temperature in 1989, 19.49° C, and the average temperature in 2015, 21.03° C, were statistically significantly different from each other (p-value < 0.001, df = 382) (Table 3).

Somali: The temperature data in Somali between 1981 to 2019 indicated a consistent, but rather gradual, increase in temperature, compared to other regions, during the time period. The minimum temperature was observed in 1984 at 24.97° C, and the highest temperature was observed in 2015 at 26.37° C. The increase in temperature steadily occurred each year (Appendix B: Figure B8). The R^2 value illustrates a reasonably good fit of the temperature values over the time period using a linear regression model (R^2 = 0.59). The temperature data points from Somali experienced more fluctuation year-by-year which most likely contributed to the lower R^2 value. From 1981 to 2019, the minimum and maximum average temperature values were reported in 1984 and 2015. An independent-samples t-test indicated the average temperature in 1948, 24.97° C, and the average temperature in 2015, 26.37° C, were statistically significantly different from each other (p-value < 0.001, df = 214) (Table 3).

Tigray: The temperature data in Tigray between 1981 to 2019 indicated a small, but consistent, increase in temperature during the time period. The minimum temperature was observed in 1989 at 21.12° C, and

the highest temperature was observed in 2009 at 22.88° C. The increase in temperature steadily occurred each year (Appendix B: Figure B9). The R^2 value illustrates a relatively good fit of the temperature values over the time period using a linear regression model (R^2 = 0.61). From 1981 to 2019, the minimum and maximum average temperature values were reported in 1989 and 2009. An independent-samples t-test indicated the average temperature in 1989, 21.12° C, and the average temperature in 2009, 22.88° C, were statistically significantly different from each other (p-value < 0.01, df = 142) (Table 3).

Objective 2: Climate Change Exposure #1: Rainfall

2011 and 2015 Short-term Rainfall Observations: After examining the long-term rainfall patterns in the nine regions, we then compared rainfall between 2011 and 2015 because these are the time points when the malaria prevalence data was collected. The difference in rainfall distribution between 2011 and 2015 revealed a decrease in the yearly average rainfall in millimeters (mm) in Afar, Amhara, Dire Dawa, Harari, Oromiya, SNNPR, and Tigray. Two regions, Benishangul Gumuz and Somali experienced an increase in the yearly average rainfall between 2011 and 2015; although, the increased rainfall in Somali was relatively small (Figure 8).

For the entire country of Ethiopia, an independent-samples t-test indicated that the average rainfall in 2011, 81.61 mm, and the average rainfall in 2015, 72.80 mm, were statistically significantly different from each other (p-value = 0.03, df = 1,750) (Table 4). However, the independent-samples t-test for each of the nine individual regions did not report any statistically significant differences between the average rainfall in 2011 and the average rainfall in 2015. Table 4 reports the average yearly rainfall in 2011 and in 2015, along with the calculated p-value from the statistical test for Ethiopia and the nine regions.

Table 4: Total Average Yearly Rainfall Measurements in 2011 and 2015 for Ethiopia, and for each Region

Region	Mean total yearly rainfall in 2011 (mm)	Mean total yearly rainfall in 2015 (mm)	P-value**
Ethiopia	43.14	76.02	0.03*
Afar	30.89	23.48	0.23
Amhara	84.30	72.89	0.28
Benishangul Gumuz	95.24	105.59	0.67
Dire Dawa	49.09	32.90	0.40
Harari	60.81	43.23	0.43
Oromiya	96.34	83.84	0.13
SNNPR	115.73	105.92	0.22
Somali	27.48	27.65	0.97
Tigray	61.65	51.46	0.42

** P-values calculated from an Independent-samples T-test
* Significant difference between the mean total yearly rainfall in 2011 and the mean total yearly rainfall in 2015 at a 95% confidence interval.

While none of the regions show a significant difference in the mean total rainfall during the entire years of 2011 and 2015, further investigation revealed that the largest changes in rainfall occurred during the Kiremt season (June to September). The independent-samples t-test for only the months of June through September in 2011 and 2015, indicated significant differences in the average rainfall for all of Ethiopia and in some specific regions: Oromiya and SNNPR (Table 5). For the significant results, all three locations, Ethiopia, Oromiya, and SNNPR, reported a significant decrease in mean total rainfall between 2011 and 2015.

Table 5: Total Average Yearly Rainfall Measurements in 2011 and 2015 for Ethiopia, and for 2 Regions during Kiremt Rainfall Season in June through September

Region***	Mean total yearly rainfall in 2011 (mm)	Mean total yearly rainfall in 2015 (mm)	P-value**
Ethiopia	149.22	119.25	<0.001*
Oromiya	186.89	142.03	<0.01*
SNNPR	171.23	141.01	<0.01*

*** Only statistically significant results are reported in this table
** P-values calculated from an Independent-samples T-test
* Significant difference between the mean total yearly rainfall in 2011 and the mean total yearly rainfall in 2015 during Kiremt at a 95% confidence interval.

The rainfall changes reported between 2011 and 2015 demonstrate a decrease in the total yearly averages of rainfall. The largest difference seen was in Harari with a decrease of 17.58 mm of rainfall between 2011 and 2015. Only two locations demonstrated an increase in rainfall between 2011 and 2015. The increase reported in Somali was minimal; however, the increase reported in Benishangul Gumuz was much more pronounced at an increase of 10.35mm of rainfall between 2011 and 2015 (Figure 8).

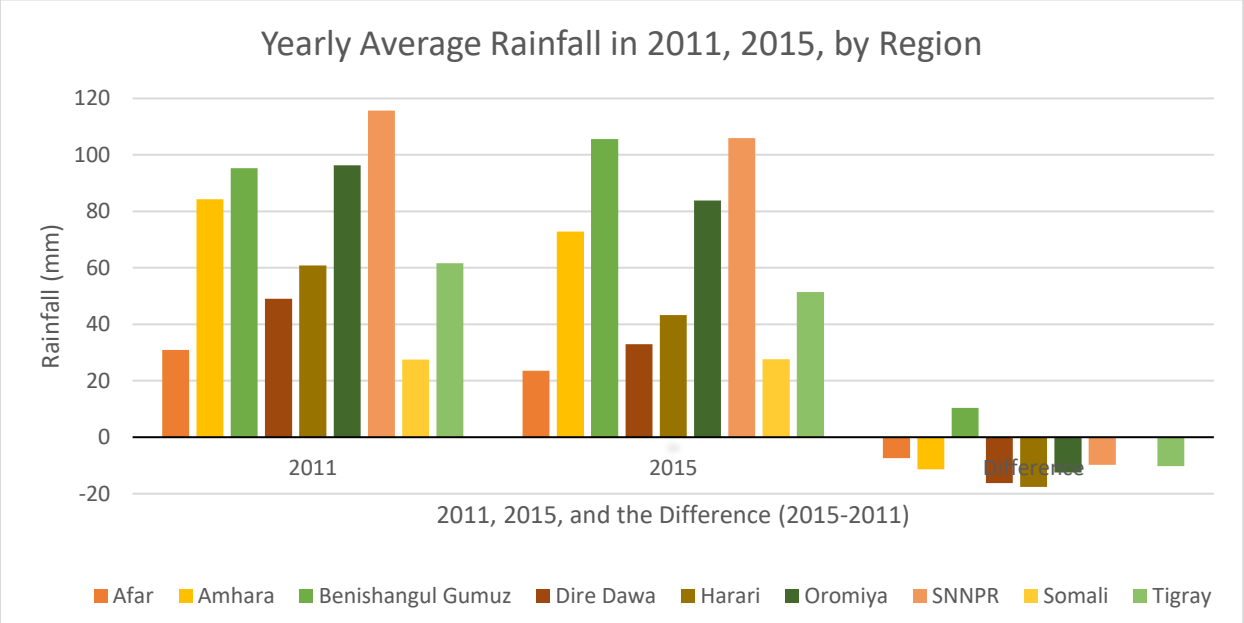

Figure 8: The Yearly Average Rainfall in 2011 and 2015 in Afar, Amhara, Benishangul Gumuz, Dire Dawa, Harari, Oromiya, SNNPR, Somali, and Tigray Regions of Ethiopia

For the seven locations that reported a decrease in rainfall between 2011 and 2015, the change in rainfall was consistently seen in the rainfall season called Kiremt. This rainfall season occurs from June to September and is defined as the heavy rainfall season in Ethiopia. During this specific season, all locations experienced an average decline of -27.63 mm of rainfall between 2011 and 2015 (excluding Benishangul Gumuz which experienced an increase in rainfall during the time period). An example of the seasonal patterns of rainfall in 2011 and 2015 with the difference between the two years is seen in Figure 9, in which Dire Dawa represents the common patterns seen in the other locations in Ethiopia for the seasonal rainfall (apart from Benishangul Gumuz).

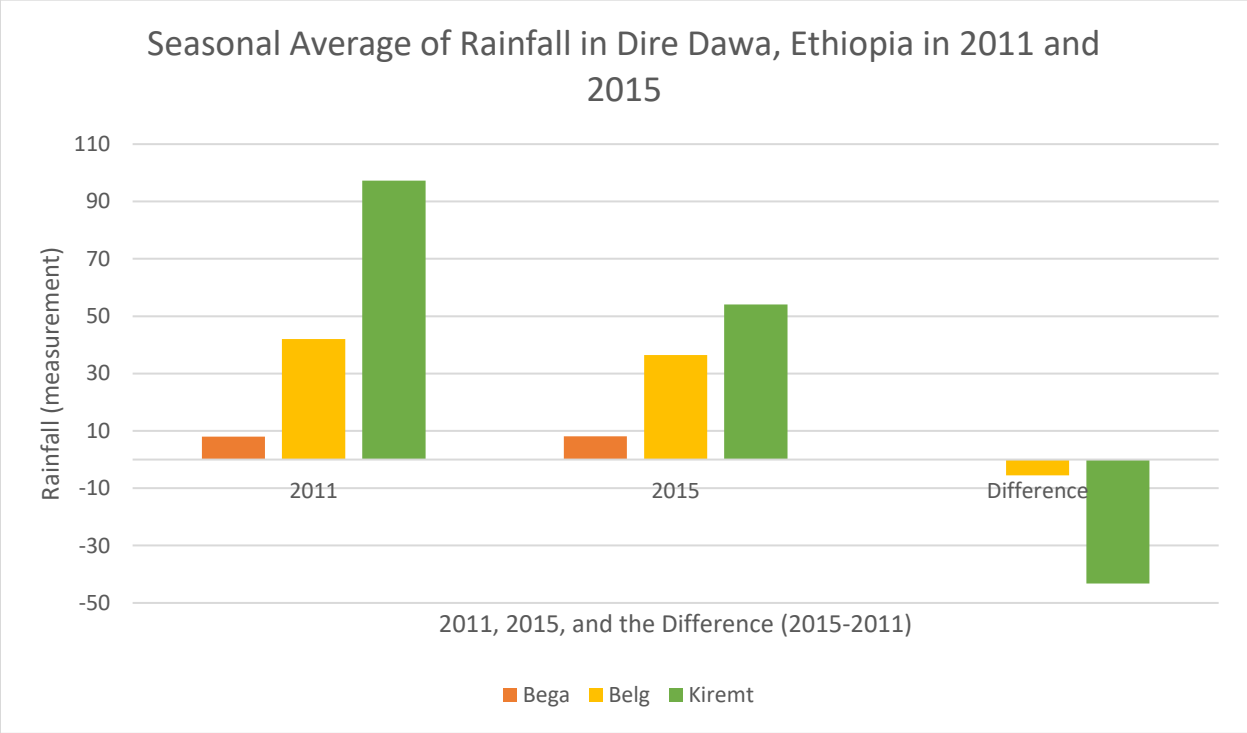

Figure 9: Seasonal Average Rainfall in 2011 and 2015 in Dire Dawa, Ethiopia

Objective 2: Climate Change Exposure #2: Temperature

2011 and 2015 Short-term Temperature Observations: Examining differences in temperature distribution for 2011 and 2015 indicated a consistent increase in the yearly average temperature in each region in Ethiopia (Figure 10). Harari experienced the largest increase in temperature between 2011 and 2015, with

an increase of 0.72° C. The region with the lowest temperature increase was SNNPR with an increase of 0.15° C.

For the entire country of Ethiopia, an independent-samples t-test indicated the average temperature in 2011, 21.98° C, and the average temperature in 2015, 22.38° C, were statistically significantly different from each other (p-value = 0.02, df = 1,750) (Table 6). Analyses at a regional level indicated none of the regions showed a significant difference in the average temperature between 2011 and 2015. Even after controlling for the different rainfall seasons, Kiremt, Bega, and Belg, the difference in average yearly temperatures between 2011 and 2015 was not statistically significant.

Table 6: Average Yearly Temperature Measurements in 2011 and 2015 for Ethiopia, and for each Region

Region	Mean yearly temperature in 2011(°C)	Mean yearly temperature in 2015 (°C)	P-value**
Ethiopia	21.98	22.38	0.02*
Afar	28.15	28.72	0.31
Amhara	20.69	21.17	0.11
Benishangul Gumuz	24.87	25.23	0.51
Dire Dawa	23.76	24.46	0.45
Harari	19.59	20.31	0.15
Oromiya	19.85	20.24	0.06
SNNPR	20.88	21.03	0.56
Somali	25.79	26.37	0.08
Tigray	22.36	22.88	0.36

** P-values calculated from an Independent-samples T-test
* Significant difference between the mean yearly temperature in 2011 and the mean yearly temperature in 2015 at a 95% confidence interval.

The temperature changes between 2011 and 2015 demonstrated an increase in the total yearly averages of temperature. The largest increase in temperature seen was in Harari with an increase of 0.72° C between 2011 and 2015. The smallest increase in temperature was seen in SNNPR with only an increase of 0.15° C (Figure 10).

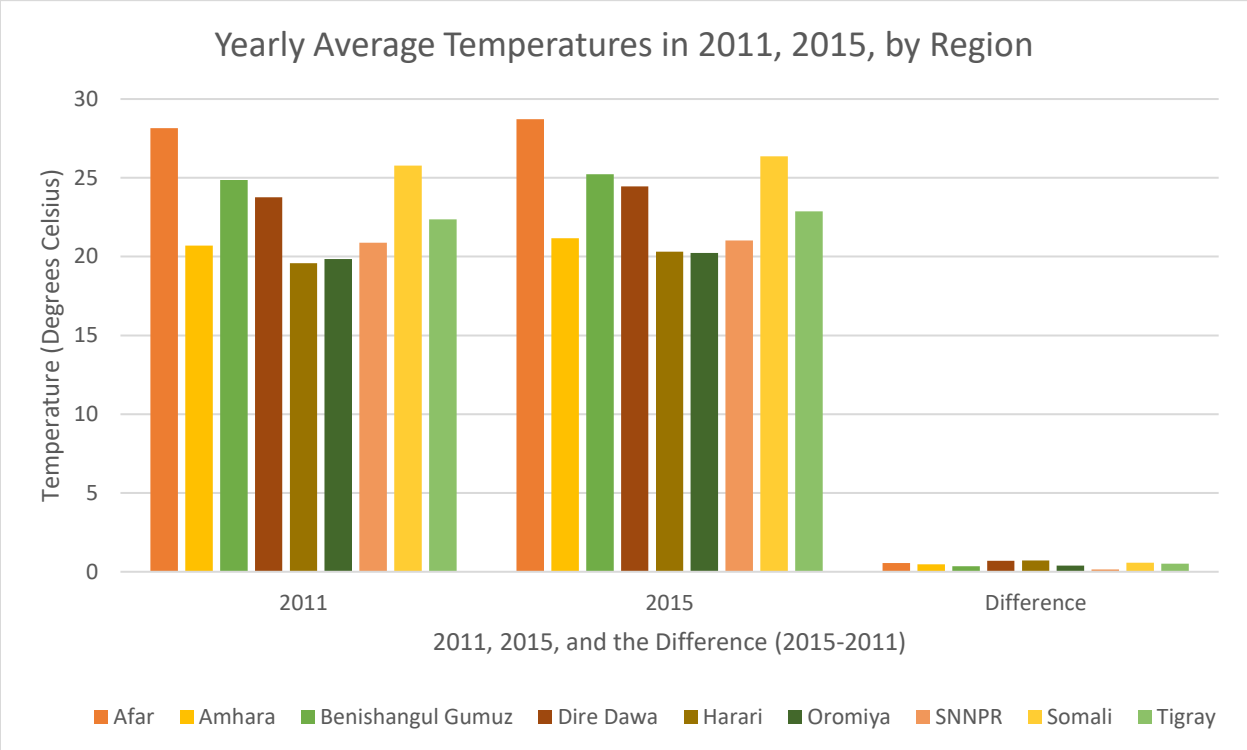

Figure 10: Yearly Average Temperature in 2011 and 2015 in Afar, Amhara, Benishangul Gumuz, Dire Dawa, Harari, Oromiya, SNNPR, Somali, and Tigray Regions of Ethiopia

For all nine regions which experienced an increase in temperature between 2011 and 2015, the change in temperature was consistently seen in the rainfall season called Belg. This rainfall season occurs from February to May and is defined as the light rainfall season in Ethiopia. During this specific season, all regions experienced an average increase in temperature of 0.71° C between 2011 and 2015 (excluding SNNPR which experienced a decrease in temperature during the time period). An example of the seasonal patterns of temperature in 2011 and 2015 with the difference between the two years is seen in Figure 11, in which Tigray represents the common patterns seen in the other locations in Ethiopia for the seasonal temperature (except for SNNPR).

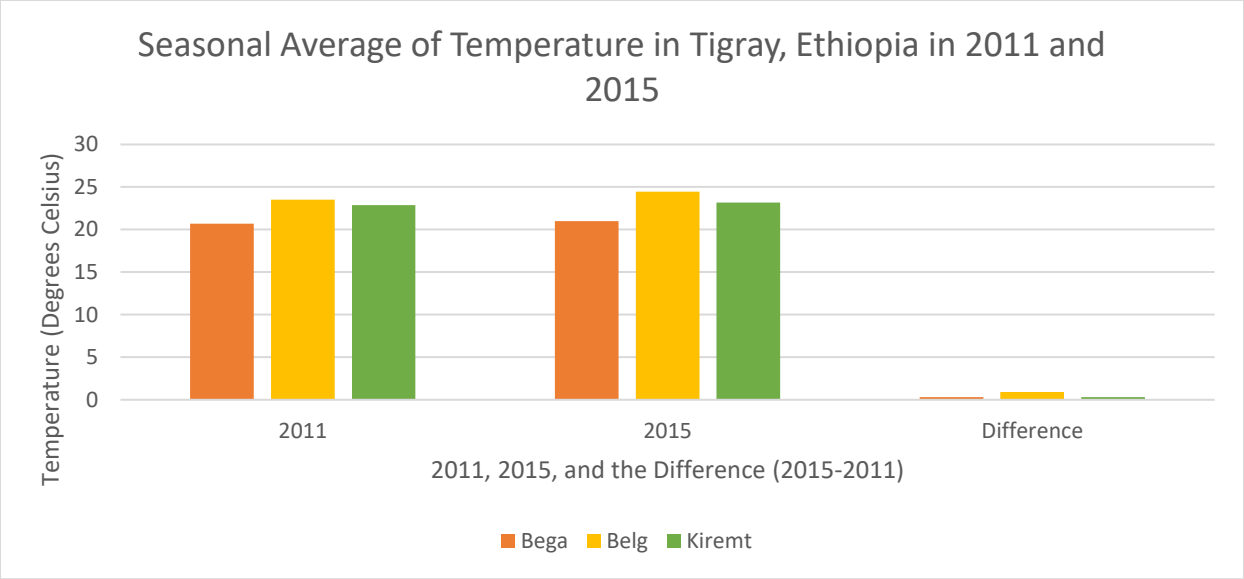

Figure 11: Seasonal Average Temperature in 2011 and 2015 in Tigray, Ethiopia

The following figure represents solely the differences in temperature seen between 2011 and 2015. The change in the y-axis allows a stronger observation of the differences in temperature change seen between the rainfall seasons in Ethiopia. As the figure represents, the rainfall season Belg experienced the highest increase in temperature between the two years as compared to the other rainfall seasons: Bega and Kiremt (Figure 12).

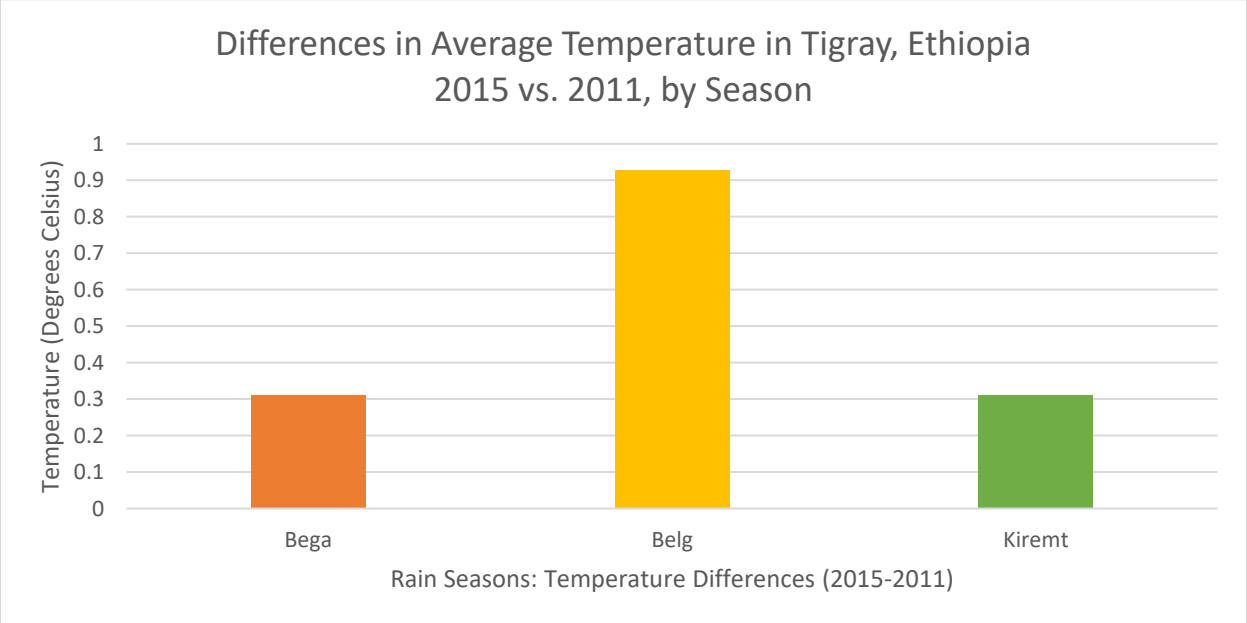

Figure 12: Seasonal Average Temperature Differences between 2011 and 2015 in Tigray.

Objective 2: Malaria Antigen Diagnostic Test Outcomes

Comparing 2011 and 2015 Malaria Prevalence by Antigen Diagnostic Test

Ethiopia: For the entire country of Ethiopia, the prevalence of malaria was statistically significantly higher in 2015 as compared to 2011, for all 12 of the antigen diagnostic tests (Table 7). The largest differences in malaria prevalence were seen with antigen diagnostic tests for *P. falciparum* and *P. vivax.*

Table 7: Comparing Proportion of Positive Malaria Diagnostic Tests for 12 *Plasmodium* Antigens, 2011 vs. 2015, Ethiopia

Antigen	2011	2015	Difference	P-value**
PfMSP1	0.19	0.3	0.11	<0.001*
PfAMA1	0.17	0.28	0.11	<0.001*
PfCSP	0.05	0.09	0.04	<0.001*
PfGLURP	0.04	0.07	0.03	<0.001*
PfLSA1	0.02	0.03	0.01	<0.01*
PfSEA1	0.07	0.2	0.13	<0.001*
PfETR5Ag1	0.08	0.12	0.04	<0.001*
PvMSP1	0.16	0.23	0.07	<0.001*
PvAMA1	0.1	0.16	0.06	<0.001*
chPvMSP1	0.21	0.35	0.14	<0.001*
PmMSP1	0.03	0.09	0.06	<0.001*
PoMSP1	0.02	0.03	0.01	<0.001*

** P-values calculated from a Two-proportions Z-test
* Significant difference between the % positive in 2011 and % positive in 2015 at a 95% confidence interval.

Afar: In the Afar region, for each of the 12 *Plasmodium* antigen tests, there was a lower proportion of positive tests in 2015 compared to 2011. The largest decrease in positive antigen tests was for the *P. falciparum* merozoite protein 1 (PfMSP1pos) with a decrease of 24.90%, whereas, the smallest change in the proportion of positive antigen tests was for the *P. ovale* merozoite protein 1 (PoMSP1pos) with a decrease of 0.92% (Appendix C: Figure C1) (Table 8). Statistically significant differences in positive antigen tests between 2011 and 2015 in Afar were observed for the following antigens: PfMSP1, PfAMA1, PfCSP, PfGLURP, and PvAMA1.

Table 8: Afar Region Comparing Proportion of Positive Malaria Diagnostic Tests for 12 *Plasmodium* Antigens, 2011 vs. 2015

Antigen	2011	2015	Difference	P-value**
PfMSP1	0.57	0.22	-0.35	<0.001*
PfAMA1	0.5	0.19	-0.31	<0.001*
PfCSP	0.1	0.02	-0.08	0.02*
PfGLURP	0.22	0.04	-0.18	<0.001*
PfLSA1	0.09	0.04	-0.05	0.29
PfSEA1	0.13	0.1	-0.03	0.53
PfETR5Ag1	0.15	0.07	-0.08	0.08
PvMSP1	0.21	0.13	-0.08	0.2
PvAMA1	0.16	0.06	-0.1	0.03*
chPvMSP1	0.27	0.22	-0.05	0.51
PmMSP1	0.13	0.06	-0.07	0.09
PoMSP1	0.04	0.03	-0.01	1

** P-values calculated from a Two-proportions Z-test
* Significant difference between the % positive in 2011 and % positive in 2015 at a 95% confidence interval.

Amhara:

The antigen testing in Amhara resulted in an increased proportion of positive test results for all 12 *Plasmodium* antigens between 2011 and 2015. The largest increase in positive antigen tests was for the *P. falciparum* schizont egress antigen (PfSEA1pos) with an increase of 24.13%, whereas, the smallest change in the proportion of positive antigen tests was reported for the *P. falciparum* liver stage antigen 1 (PfLSA1pos) with an increase of 1.69% (Appendix C: Figure C2) (Table 9). For each of the 12 *Plasmodium* antigen tests, there was a statistically significantly higher proportion of positive antigen tests in 2015 as compared to 2011.

Table 9: Amhara Region Comparing Proportion of Positive Malaria Diagnostic Tests for 12 *Plasmodium* Antigens, 2011 vs. 2015

Antigen	2011	2015	Difference	P-value**
PfMSP1	0.2	0.42	0.22	<0.001*
PfAMA1	0.19	0.36	0.17	<0.001*
PfCSP	0.06	0.15	0.09	<0.001*
PfGLURP	0.04	0.13	0.09	<0.001*
PfLSA1	0.02	0.03	0.01	0.04*
PfSEA1	0.09	0.33	0.24	<0.001*
PfETR5Ag1	0.07	0.19	0.12	<0.001*
PvMSP1	0.2	0.36	0.16	<0.001*
PvAMA1	0.14	0.25	0.11	<0.001*
chPvMSP1	0.26	0.49	0.23	<0.001*
PmMSP1	0.03	0.12	0.09	<0.001*
PoMSP1	0.02	0.08	0.06	<0.001*

** P-values calculated from a Two-proportions Z-test
* Significant difference between the % positive in 2011 and % positive in 2015 at a 95% confidence interval.

Benishangul Gumuz: The antigen testing in Benishangul Gumuz resulted in a variety of changes between 2011 and 2015 for the 12 *Plasmodium* antigen tests conducted. Six of the antigen tests showed an increase in positive detections between 2011 and 2015, whereas, the other six antigen tests revealed a decrease in positive detections between the two years. The largest increase in the proportion of positive antigen tests was for the *P. falciparum* apical membrane antigen 1 (N-terminal region) (PvAMA1pos) with an increase of 4.35%, whereas, the largest decrease in the proportion of positive antigen tests was for the *P. falciparum* merozoite protein 1 (PfMSP1pos) with a decrease of 10.69% (Appendix C: Figure C3) (Table 10). There was a statistically significant difference in the proportion of positive antigen tests between 2011 and 2015 for only one antigen: PfMSP1. For the other 11 antigens, the proportion of positive detection in 2011 was not statistically different than the proportion of positive antigen tests in 2015.

Table 10: Benishangul Gumuz Region Comparing Proportion of Positive Malaria Diagnostic Tests for 12 *Plasmodium* Antigens, 2011 vs. 2015

Antigen	2011	2015	Difference	P-value**
PfMSP1	0.57	0.43	-0.14	0.04*
PfAMA1	0.51	0.4	-0.11	0.11
PfCSP	0.1	0.1	0	1
PfGLURP	0.12	0.13	0.01	1
PfLSA1	0.11	0.08	-0.03	0.56
PfSEA1	0.22	0.25	0.03	0.72
PfETR5Ag1	0.22	0.15	-0.07	0.17
PvMSP1	0.2	0.2	0	1
PvAMA1	0.12	0.16	0.04	0.53
chPvMSP1	0.33	0.31	-0.02	0.78
PmMSP1	0.16	0.11	-0.05	0.26
PoMSP1	0.01	0.02	0.01	1

** P-values calculated from a Two-proportions Z-test
* Significant difference between the % positive in 2011 and % positive in 2015 at a 95% confidence interval.

Dire Dawa: The antigen testing in Dire Dawa resulted in a variety of changes between the 12 malaria diagnostic tests conducted. Five of the antigen tests revealed an increase in positive detections between 2011 and 2015, whereas, seven of the antigen tests revealed a decrease in positive detections between the two years. The largest increase in the proportion of positive antigen tests was for the *P. malariae* merozoite protein 1 (PmMSP1pos) with an increase of 4.64%, whereas, the largest decrease in the proportion of positive antigen tests was for the *P. falciparum* schizont egress antigen (PfSEA1pos) with a decrease of 0.13.96% (Appendix C: Figure C4) (Table 11). There was a statistically significant difference in the proportion of positive antigen tests between 2011 and 2015 for only one antigen: chPvMSP1. For the other 11 antigens, the proportion of positive detection in 2011 was not statistically different than the proportion of positive antigen tests in 2015.

Table 11: Dire Dawa Region Comparing Proportion of Positive Malaria Diagnostic Tests for 12 *Plasmodium* Antigens, 2011 vs. 2015

Antigen	2011	2015	Difference	P-value**
PfMSP1	0.09	0.07	-0.02	0.90
PfAMA1	0.13	0	-0.13	0.88
PfCSP	0.03	0.01	-0.02	0.96
PfGLURP	0	0.02	0.02	0.51
PfLSA1	0.01	0.04	0.03	0.66
PfSEA1	0.16	0.06	-0.1	0.09
PfETR5Ag1	0.03	0.05	0.02	0.05
PvMSP1	0.17	0.07	-0.1	0.11
PvAMA1	0.07	0.04	-0.03	0.65
chPvMSP1	0.26	0.09	-0.17	<0.01*
PmMSP1	0	0.04	0.04	0.27
PoMSP1	0	0.01	0.01	1

** P-values calculated from a Two-proportions Z-test
* Significant difference between the % positive in 2011 and % positive in 2015 at a 95% confidence interval.

Harari: The region of Harari was not included in this analysis because the sample size for 2011 (n = 2) was not large enough to examine if there were significant changes between 2011 and 2015 (Appendix C: Figure C5).

Oromiya: The antigen testing in Oromiya resulted in an increased proportion of positive detections for 11 of the 12 malaria diagnostic tests between 2011 and 2015. The largest increase in the proportion of positive antigen tests was for the chimeric *P. vivax* merozoite protein 1, including additional B and T cell epitopes (chPvMSP1pos) with an increase of 24.95%, whereas, the smallest change in the proportion of positive antigen tests was for the *P. falciparum* liver stage antigen 1 (PfLSA1pos) with an increase of 0.42% (Appendix C: Figure C6) (Table 12). There was a statistically significant difference in the proportion of positive antigen tests between 2011 and 2015 for all but one antigen: PfLSA1.

Table 12: Oromiya Region Comparing Proportion of Positive Malaria Diagnostic Tests for 12 *Plasmodium* Antigens, 2011 vs. 2015

Antigen	2011	2015	Difference	P-value**
PfMSP1	0.15	0.23	0.08	<0.001*
PfAMA1	0.12	0.24	0.12	<0.001*
PfCSP	0.04	0.12	0.08	<0.001*
PfGLURP	0.02	0.03	0.01	0.01*
PfLSA1	0.01	0.01	0	0.91
PfSEA1	0.04	0.25	0.21	<0.001*
PfETR5Ag1	0.07	0.11	0.04	0.02*
PvMSP1	0.12	0.19	0.07	<0.001*
PvAMA1	0.07	0.12	0.05	<0.001*
chPvMSP1	0.16	0.4	0.24	<0.001*
PmMSP1	0.02	0.09	0.07	<0.001*
PoMSP1	0.01	0.03	0.02	0.01*

** P-values calculated from a Two-proportions Z-test
* Significant difference between the positive antigen proportions in 2011 and positive antigen proportions in 2015 at a 95% confidence interval.

SNNPR:

In SNNPR, 11 of the 12 malaria diagnostic tests indicated an increase in positive results between 2011 and 2015. The diagnostic test for PoMSP1 decreased in the positive detections between 2011 and 2015 (-1%). The largest increase in the proportion of positive antigen tests was for the *P. falciparum* liver stage antigen 1 (PfSEA1pos) with an increase of 11.34%, whereas, the smallest significant increase in the proportion of positive antigen tests was for the *P. falciparum* glutamate-rich protein, Ro fragment (PfGLURPpos) with an increase of 1.53% (Appendix C: Figure C7) (Table 13). Two antigen tests were not statistically significant in their proportion of positive results between 2011 and 2015; these two antigens were PfLSA1 and PoMSP1. The remaining 10 antigen test results were statistically significantly different from each other between 2011 and 2015. Neither PoMSP1 nor PfLSA1 was statistically different in the proportion of positive results in 2011 compared to the proportion of positive results in 2015.

Table 13: SNNPR Region Comparing Proportion of Positive Malaria Diagnostic Tests for 12 *Plasmodium* Antigens, 2011 vs. 2015

Antigen	2011	2015	Difference	P-value**
PfMSP1	0.2	0.34	0.14	<0.001*
PfAMA1	0.18	0.37	0.19	<0.001*
PfCSP	0.04	0.1	0.06	<0.001*
PfGLURP	0.05	0.09	0.04	<0.01*
PfLSA1	0.02	0.03	0.01	0.2
PfSEA1	0.09	0.22	0.13	<0.001*
PfETR5Ag1	0.08	0.15	0.07	<0.001*
PvMSP1	0.19	0.31	0.12	<0.001*
PvAMA1	0.12	0.23	0.11	<0.001*
chPvMSP1	0.24	0.4	0.16	<0.001*
PmMSP1	0.04	0.13	0.09	<0.001*
PoMSP1	0.03	0.02	-0.01	0.51

** P-values calculated from a Two-proportions Z-test
* Significant difference between the % positive in 2011 and % positive in 2015 at a 95% confidence interval.

Somali:

Each of the 12 malaria diagnostic tests in Somali resulted in a decreased proportion of positive results between 2011 and 2015. The largest decrease in the proportion of positive antigen tests was for the chimeric *P. vivax* merozoite protein 1, including additional B and T cell epitopes (chPvMSP1pos) with a decrease of 12.89%, whereas, the smallest change in the proportion of positive antigen tests was for the *P. falciparum* liver stage antigen 1 (PfLSA1pos) with a decrease of 2.67% (Appendix C: Figure C8) (Table 14). For each of the 12 *Plasmodium* antigen tests, there was a statistically significantly lower proportion of positive antigen tests in 2015 as compared to 2011.

Table 14: Somali Region Comparing Proportion of Positive Malaria Diagnostic Tests for 12 *Plasmodium* Antigens, 2011 vs. 2015

Antigen	2011	2015	Difference	P-value**
PfMSP1	0.19	0.1	-0.09	<0.001*
PfAMA1	0.16	0.09	-0.07	<0.01*
PfCSP	0.07	0.01	-0.06	<0.001*
PfGLURP	0.05	0.02	-0.03	<0.01*
PfLSA1	0.04	0.01	-0.03	<0.01*
PfSEA1	0.1	0.06	-0.04	0.03*
PfETR5Ag1	0.06	0.02	-0.04	<0.01*
PvMSP1	0.11	0.03	-0.08	<0.001*
PvAMA1	0.07	0.01	-0.06	<0.001*
chPvMSP1	0.2	0.08	-0.12	<0.001*
PmMSP1	0.05	0.02	-0.03	0.01*
PoMSP1	0.03	0	-0.03	<0.01*

** P-values calculated from a Two-proportions Z-test
* Significant difference between the % positive in 2011 and % positive in 2015 at a 95% confidence interval.

Tigray: The antigen testing in Tigray resulted in decreased proportions of positive results for nine of the antigen tests between 2011 and 2015, and three increased proportions of positive malaria diagnostic tests. The largest decrease in the proportion of positive antigen tests was for the *P. malariae* merozoite protein 1 (PmMSP1pos) with a decrease of 12.89%, whereas, the largest increase in the proportion of positive antigen tests was for the *P. falciparum* liver stage antigen 1 (PfLSA1pos) with an increase of 1.26% (Appendix C: Figure C9) (Table 15). There was only one statistically significant difference in the proportion of positive antigen tests between 2011 and 2015: PmMSP1. For the other 11 antigens, the proportion of positive tests in 2011 was not statistically different than the proportion of positive tests in 2015.

Table 15: Tigray Region Comparing Proportion of Positive Malaria Diagnostic Tests for 12 *Plasmodium* Antigens, 2011 vs. 2015

Antigen	2011	2015	Difference	P-value**
PfMSP1	0.31	0.31	0	0.95
PfAMA1	0.25	0.26	0.01	0.91
PfCSP	0.06	0.05	-0.01	0.81
PfGLURP	0.07	0.06	-0.01	0.79
PfLSA1	0.01	0.02	0.01	0.5
PfSEA1	0.11	0.11	0	0.94
PfETR5Ag1	0.11	0.07	-0.04	0.19
PvMSP1	0.2	0.23	0.03	0.62
PvAMA1	0.18	0.14	-0.04	0.3
chPvMSP1	0.31	0.3	-0.01	0.76
PmMSP1	0.14	0.04	-0.1	<0.001*
PoMSP1	0.03	0.02	-0.01	0.68

** P-values calculated from a Two-proportions Z-test
* Significant difference between the % positive in 2011 and % positive in 2015 at a 95% confidence interval.

MIS 2011 and 2015 Demographics:

After including potential confounding variables in the data sets for the MIS from 2011 and the MIS from 2015 (age, utilization of bed nets, and region), any sample participant missing this information was subsequently excluded from further analysis. Table 16 presents the 2011 demographic information for the nine Ethiopian regions examined in this analysis. The demographic information for the Ethiopian regions in 2015 was similar (Table 17). Both the sample size and number of unique households in Ethiopia between 2011 and 2015 are quite similar. At the regional level the sample sizes collected between the two years varied, particularly Oromiya, SNNPR, and Tigray had larger sample size differences between 2011 and 2015. The average age of participants in 2011 was 14.3 years old and 15.1 years old in 2015. The sex distribution was roughly 50:50 in Ethiopia and each region between 2011 and 2015. The largest difference between the two years was observed in the bed net utilization. In 2015, both Amhara and Dire Dawa substantially increased the percentage of sample participants reporting bed net utilization. The other regions either decreased their usage or stay the same.

Table 16: Demographic Characteristics for the 2011 MIS Population in Ethiopia

				Sex		Bed Net Utilization
Region	Sample Size	Unique Households	Age, years (mean (SD))	Females	Males	Yes (%)
Ethiopia Total	**4,962**	**2,701**	**14.3 (16.9)**	**2,636**	**2,326**	**2,326 (47)**
Afar	81	59	11.4 (14.5)	47	34	46 (57)
Amhara	1,258	707	15.2 (17.1)	684	574	322 (26)
Benishangul Gumuz	80	44	11.6 (15.0)	45	35	24 (30)
Dire Dawa	75	42	15.7 (19.5)	37	38	24 (32)
Harari	2	2	14.5 (19.1)	1	1	1 (50)
Oromiya	2,209	1307	14.0 (16.6)	1,157	1,052	1,216 (55)
SNNPR	703	371	15.3 (17.9)	377	326	410 (58)
Somali	431	270	12.0 (15.2)	226	205	249 (58)
Tigray	123	100	15.8 (18.5)	62	61	34 (28)

Table 17: Demographic Characteristics for the 2015 MIS Population in Ethiopia

				Sex		Bed Net Utilization
Region	Sample Size	Unique Households	Age, years (mean (SD))	Females	Males	Yes (%)
Ethiopia Total	**4,763**	**2,257**	**15.1 (17.7)**	**2,499**	**2,264**	**1,815 (38)**
Afar	162	94	8.4 (11.8)	74	88	35 (21)
Amhara	801	364	16.8 (18.3)	403	398	311 (39)
Benishangul Gumuz	255	131	15.9 (19.6)	140	115	80 (31)
Dire Dawa	80	45	16.1 (19.2)	50	30	61 (76)
Harari	123	68	12.4 (17.3)	65	58	66 (53)
Oromiya	928	402	15.7 (17.8)	459	469	298 (32)
SNNPR	1,121	540	15.2 (17.1)	603	518	487 (43)
Somali	418	201	11.4 (15.7)	226	192	105 (25)
Tigray	875	439	15.8 (18.5)	479	396	372 (43)

Objective 3: Associations between Rainfall and Temperature with Prevalence of Positive Malaria Antigen Tests

Geographic Comparisons of Climate Change: After observing the temperature and rainfall differences between 2011 and 2015 were smaller than the differences between the regions, the temperatures and

rainfall amounts for both years were averaged together, and the nine different geographical regions were plotted against the various antigen test prevalence. Two graphs were created for each antigen type for the Bega (October to December) season and Kiremt (June to September) season in Ethiopia.

Geographic Comparisons of Rainfall: From the average rainfall graphs, after applying an exponential curve to the nine data points (the nine regions), the R^2 values indicated relatively weak correlations between the percent positive for each antigen test and the average Bega and average Kiremt rainfall (mm) from 2011 and 2015. Apart from two antigens, PfCSP and PoMSP1, all the antigen and rainfall plots indicated a stronger correlation with the Kiremt rainfalls as compared to the Bega rainfalls (Appendix D: Figures D1 through D24). This indicates that the rainfall during the four-month period (June to September) prior to the October to December malaria antigen testing for MIS had a stronger impact than the rainfall during the MIS testing. Although, given the low R^2 values it is clear other factors are contributing to the outcome of the malaria antigen testing in these regions.

The rainfall maps from August through December 2011 and 2015 are presented with latitude and longitude scales on the axis, and the region boundaries are seen in black on the maps. For the region names in Ethiopia refer to Appendix E: Figure E1 (note two regions: Gambela and Addis Ababa are shown on the map but are not included in the analyses). The rainfall maps of August 2011 and August 2015 reveal a decrease in rainfall, particularly in the upper half of the country. The lower half of the country had a similar pattern of less than 100 mm of rainfall during this month for both years (Appendix F: Figures F1 and F2). The September rainfall graphs showed a similar pattern as compared to August—September 2015 showed a smaller distribution of rainfall throughout the country; there was both less rainfall in total and rainfall in fewer places. Rainfall during September for both years was localized to mainly the western side of Ethiopia (Appendix F: Figures F3 and F4). October 2011 and 2015 had similar rainfall patterns for both years. There was a localized increase in rainfall seen in the middle of SNNPR. There was also a decrease in rainfall in 2015 in southern Oromiya as compared to 2011 (Appendix F: Figures F5 and F6). Additionally, the comparison between November 2011 and November 2015 revealed

not only a decrease in the geographic distribution of high rainfall, but the areas that did still experience "high" rainfall showed a 50% reduction in the amount of rainfall from 2011 to 2015: from 400 mm of rainfall to 200 mm of rainfall (Appendix F: Figures F7 and F8). December 2011 and December 2015 rainfall patterns did not show much of a change between the two years. Overall, the country of Ethiopia experiences less than 20 mm of rainfall in December, except for a few locations (Appendix F: Figures F9 and F10).

Geographic Comparisons of Temperature: From the average temperature graphs, after applying a polynomial curve to the nine data points (the nine regions), the R^2 values indicated relatively weak correlations between the percent positive for each antigen test and the average Bega and average Kiremt temperatures (degrees Celsius) from 2011 and 2015. Except for one antigen test, PfCSP, all the antigen and temperature plots indicated a stronger correlation with the Bega temperatures as compared to the Kiremt temperatures (Appendix D: Figures D25 through D48). This indicates that the temperature during the malaria diagnostic testing from October to December for the MIS had a stronger impact on the results of the antigen tests compared to the temperature of the four-month period (June to September) prior to testing. Given the low R^2 values, though, it is clear other factors are contributing to the outcome of the malaria diagnostic tests in these regions.

The temperature maps from August through December 2011 and 2015 are presented with latitude and longitude scales on the axis, and the region boundaries are seen in black on the maps. For the region names in Ethiopia refer to Appendix E: Figure E1. As previously noted, the temperatures between 2011 and 2015, while showing an overall increase in temperatures, reveals a very minute difference between these two years. As such, the temperature maps of August 2011 and August 2015 reveal very similar temperature patterns throughout the various regions. However, there is a wide range of temperatures, with some regions with temperatures as low as 15° C to as high as 45° C (Appendix G: Figures G1 and G2). The September temperature graphs illustrate a similar pattern of limited changes between 2011 and 2015, but still, demonstrate the variability of temperatures ranging from 15° C to 40° C in September (Appendix

G: Figures G3 and G4). October 2011 and 2015 reveal the same geographic distribution of temperature for both years. As compared to September, October starts to demonstrate higher temperatures along the western border of Ethiopia in regions such as Gambela, Benishangul Gumuz, and Amhara (Appendix G: Figures G5 and G6). November 2011 and 2015 were slightly different than the other months in that November 2015 was almost 5° C hotter than November 2011 in the same areas (Appendix G: Figures G7 and G8). December 2011 and 2015 demonstrated the same trend as seen in November. The temperature in December 2015 was nearly 5° C hotter than recorded for December 2011. Furthermore, the lowest temperature recorded was almost 5° C warmer than in the past 4 months (20° C compared to 15° C) (Appendix G: Figures G9 and G10).

Geographic Comparisons of Malaria Prevalence: Next, this part of the results focused on the geographic location of the malaria clusters created from unique identifiers from the individual recorded zone, district, and kebele of the study participants and their samples. In addition, shapefiles of the rainfall and temperatures in the country were mapped to show the variability of monthly weather in the different regions. The regions were identified with a color-coded legend and shown on a latitude and longitude scale for reference (Appendix E: Figure E1).

Next, the cluster prevalence of positive antigen-specific malaria tests was graphed on the shapefile of Ethiopia (Figure 13). In 2011, there was a high prevalence of positive PfMSP1 antigen tests in regions like Tigray, northern Amhara, Afar, and SNNPR. There were many clusters for PfMSP1 in the center of Ethiopia (Oromiya and southern Amhara). However, most of these clusters were less than 20% positive for the PfMSP1 antigen test (Appendix I: Figure I1). In 2015, there was a high prevalence of positive PfMSP1 antigen tests in the same regions as 2011: Tigray, northern Amhara, Afar, and SNNPR. There was also high prevalence in Benishangul Gumuz and a particularly high prevalence cluster in Somali. The low-prevalence clusters in 2015 were more dispersed throughout the country as compared to 2011. These low-prevalence clusters, those under 20%, were more equally distributed among the high-prevalence clusters rather than grouped together among other low prevalence clusters (Appendix I: Figure I2).

Comparing the results from the *P. falciparum* apical membrane antigen 1 test to *P. falciparum* merozoite protein 1 test in 2011, there were fewer high-prevalence clusters for the PfAMA1 test, particularly in the region of SNNPR. There were still high-prevalence clusters observed in Tigray, northern Amhara, Afar, and SNNPR. However, throughout the low-prevalence clusters observed in Oromiya and southern Amhara many of the PfSMP1 clusters that were 20-40% positive in 2011 have shifted to 0-20% positive in similar locations in 2015 (Appendix I: Figure I3). The results from the *P. falciparum* apical membrane antigen 1 test in 2015 illustrated a high prevalence of positive PfMSP1 antigen tests in the same regions as 2011: Tigray, northern Amhara, and SNNPR. There were particularly high prevalence clusters in Somali—90-100% positive in this singular cluster and a few 90-100% positive clusters within Benishangul Gumuz. The low prevalence clusters in 2015 were more dispersed throughout the country as compared to 2011. There was a decrease in the number clusters with 90-100% positive in northern Ethiopia, there is an increase in Benishangul Gumuz of these 90-100% positive clusters, and an increase clusters with 40-60% positive throughout Ethiopia (Appendix I: Figure I4).

In 2011, there was a low prevalence of positive PfCSP antigen tests throughout the entire country. There were a few clusters of PFCSP antigen tests around 50-60% positive but overall, the prevalence of this antigen was much lower among the tested individuals as compared to PfMSP1 and PfAMA1 antigen tests. There was one singular high-prevalence cluster in Oromiya with a prevalence between 90-100% (Appendix I: Figure I5). In 2015, there was a high-prevalence of positive PfCSP antigen tests in SNNPR, Oromiya, Benishangul Gumuz, and Amhara. These areas went from under 20% positive to a prevalence of 40-80% positive. There was an additional high-prevalence cluster (90-100%) along the border of SNNPR and Oromiya (Appendix I: Figure I6).

In 2011, there was a low-prevalence of PfGLURP throughout Ethiopia. There were a few clusters around with a prevalence around 30-50% positive for the PfGLURP antigen tests within Afar and SNNPR but overall, the prevalence was much lower than PfMSP1 and PfAMA1 antigen tests (Appendix I: Figure I7). In 2015, the prevalence of PfGLURP was high in SNNPR, Benishangul Gumuz, Tigray, and Amhara.

These areas went from under 20% positive to between 40-90% positive for PfGLURP antigen tests. There was a high-prevalence cluster (90-100%) within northern SNNPR (Appendix I: Figure I8).

The prevalence of PfLSA1 was typically less than 10% positive in the 2011 clusters. Many of these low-prevalence clusters were concentrated within the center of Ethiopia. Along the borders of Ethiopia, high-prevalence clusters emerged with 60-100% positive. The three 90-100% positive clusters were seen in Afar, Benishangul Gumuz, and SNNPR (Appendix I: Figure I9). In 2015, the cluster prevalence for *P. falciparum* liver stage antigen 1 indicated a novel pattern compared to the previously discussed antigen tests in that PfLSA1 decreased between 2011 and 2015. Apart from one cluster in Somali that was at 90-100% positive, the remaining clusters were no higher than 40% positive for PfLSA1, and most of these clusters were under 10% positive (Appendix I: Figure I10).

The cluster prevalence of PfSEA1 indicated many clusters with a prevalence less than 10% in 2011. Most of these low-prevalence clusters were concentrated within the center of the country. Along the borders of Ethiopia, high-prevalence clusters emerged around 40-80% positive. These high-prevalence clusters were mainly observed in Tigray, northern Amhara, and a few clusters in SNNPR (Appendix I: Figure I11). In 2015, there were many more high-prevalence clusters of PfSEA1 than in 2011. There was a large increase in the number of 40-70% positive clusters in Amhara, Benishangul Gumuz, and SNNPR. There were clusters at 90-100% positive located in Tigray, Somali, and Amhara (Appendix I: Figure I12).

In 2011, there was a relatively low prevalence of PfERT5Ag1 positive tests, with many clusters less than 10% positive. Most of these low-prevalence clusters were concentrated within the center of Ethiopia and interspersed with high-prevalence clusters along Ethiopia's borders. Along those borders, high-prevalence clusters were seen around 50-70% positive. The high prevalence-clusters were observed in Tigray, northern Amhara, and SNNPR (Appendix I: Figure I13). In 2015, there was an increase in the high-prevalence clusters of PfERT5Ag1 positive tests. There was a large increase in the number of clusters between 40-80% positive in Amhara, Benishangul Gumuz, Oromiya, Tigray, and SNNPR. There were also clusters at 90-100% positive located in Tigray, Somali, and Amhara (Appendix I: Figure I14).

We then compared the diagnostic test results for *Plasmodium vivax* (three target antigens) by region for 2011 and 2015. The first antigen test for *P. vivax* is based on the *P. vivax* merozoite protein 1 (PvMSP1). The results from this antigen test indicated a wide range of prevalence of *P. vivax* antibodies. There were many clusters with prevalence under 10% within the center of Ethiopia, but higher prevalence was detected further away from central Ethiopia. Along the borders of Ethiopia, high-prevalence clusters were observed with about 50-70% positive test results. These high-prevalence clusters were in Tigray, northern Amhara, and SNNPR. There were more high-prevalence (90-100%) clusters of PvMSP1 positive tests compared to the previous antigen tests for *P. falciparum* (Appendix I: Figure I15). In 2015, there was an increase in the prevalence of PvMSP1 positive tests in the north of Ethiopia (Tigray and Amhara) whereas the south had a decrease in the prevalence (SNNPR). Tigray and Amhara shifted from clusters with less than 20% positive to clusters around 40-70% positive. In SNNPR, there was a decrease in the number of clusters that were 90-100% positive to more clusters that were around 50-70% positive (Appendix I: Figure I16).

In 2011, the cluster prevalence for the second *P. vivax* antigen test, PvAMA1, was predominately less than 30% positive. There were many prevalence clusters less than 20% within the center of Ethiopia, but higher prevalence was detected further away from central Ethiopia. Along the borders of Ethiopia, high-prevalence clusters were observed at 40-80% positive test results. The high-prevalence clusters were mainly observed in Tigray, northern Amhara, and a few clusters in SNNPR (Appendix I: Figure I17). In 2015, the cluster prevalence consistently shifted higher—from about 20% positive in 2011 to 30-60% positive *P. vivax* antigen tests in 2015. This increase in high-prevalence clusters was mainly reported in Tigray, Amhara, SSNPR, and 1 cluster in Somali at 90-100% positive (Appendix I: Figure I18).

A lower prevalence of positive chimeric *P. vivax* merozoite protein 1, including additional B and T cell epitopes test results was observed in 2011. There were many prevalence clusters less than 20% in the center of Ethiopia, but higher prevalence results were observed further away from the center. Along the borders of Ethiopia, high-prevalence clusters were observed at 50-100% positive. These high prevalence

clusters were mainly detected in western Tigray, northern Amhara, and SNNPR. Approximately five different clusters in east SNNPR right next to each other had a prevalence of 90-100% positive (Appendix I: Figure I19). In 2015, the chPvMSP1 antigen test results indicated a relative decrease in the overall prevalence of the chPvMSP1 antigen in Ethiopia. There were fewer prevalence clusters at 90-100% positive in 2015. There were more clusters at 40-50% positive, but fewer clusters at 60-70% positive (Appendix I: Figure I20).

Next, we compared the diagnostic test results for *Plasmodium malariae* (one target antigen) by region for 2011 and 2015. The 2011 results indicated very low prevalence of positive PmMSP1 antigen tests, less than 10% in most of the tested clusters. Tigray was the region with the most clusters greater than 10%, these clusters ranged between 50-70% positive (Appendix I: Figure I21). In 2015, there was an increase in the relative prevalence of clusters to between 20-40% positive. There were fewer clusters between 50-70% positive, but there were a few more clusters observed between 90-100% for positive PmMSP1 antigen tests, particularly at the northern Somali and Oromiya border (Appendix I: Figure I22).

Lastly, we compared the diagnostic test results for *Plasmodium ovale* (one target antigen) by region for 2011 and 2015. The 2011 results demonstrated very low prevalence of positive PoMSP1 antigen tests, predominately less than 20%, only about four clusters observed were above 20%. These higher clusters were seen in Amhara: one cluster between 30-40% positive and one at 60-70% positive, and SNNPR: one cluster between 40-50% positive and another at 90-100% positive (Appendix I: Figure I23). In 2015, there was a high prevalence of positive PoMPS1 antigen tests. The regions most impacted by this increase were Amhara and Tigray, with a few high-prevalence clusters observed in SNNPR as well. These high prevalence clusters were mainly between 30-70% positive, with three between 90-100% positive (Appendix I: Figure I24).

For the next set of analyses, the temperature shapefiles, or rainfall shapefiles, were overlapped with the cluster prevalence for each of the 12 *Plasmodium* antigen tests conducted in Ethiopia. The relationship with monthly total rainfall during the months of August through December in 2011 and 2015 are

presented in Figures 14 through 25, monthly average temperature during the same months and years are shown in Figures 26 through 37.

Figure 13: Cluster Prevalence legend to reference for the following 24 graphs (12 antigens and 2 climatic factors) (Dark Blue = 0-0.1, Blue = 0.1-0.2, Light Blue = 0.2-0.3, Purple = 0.3-0.4, Light Purple = 0.4-0.5, Pink = 0.5-0.6, Salmon = 0.6-0.7, Orange = 0.7-0.8, Light Orange = 0.8-0.9, Yellow = 0.9-1.0 prevalence).

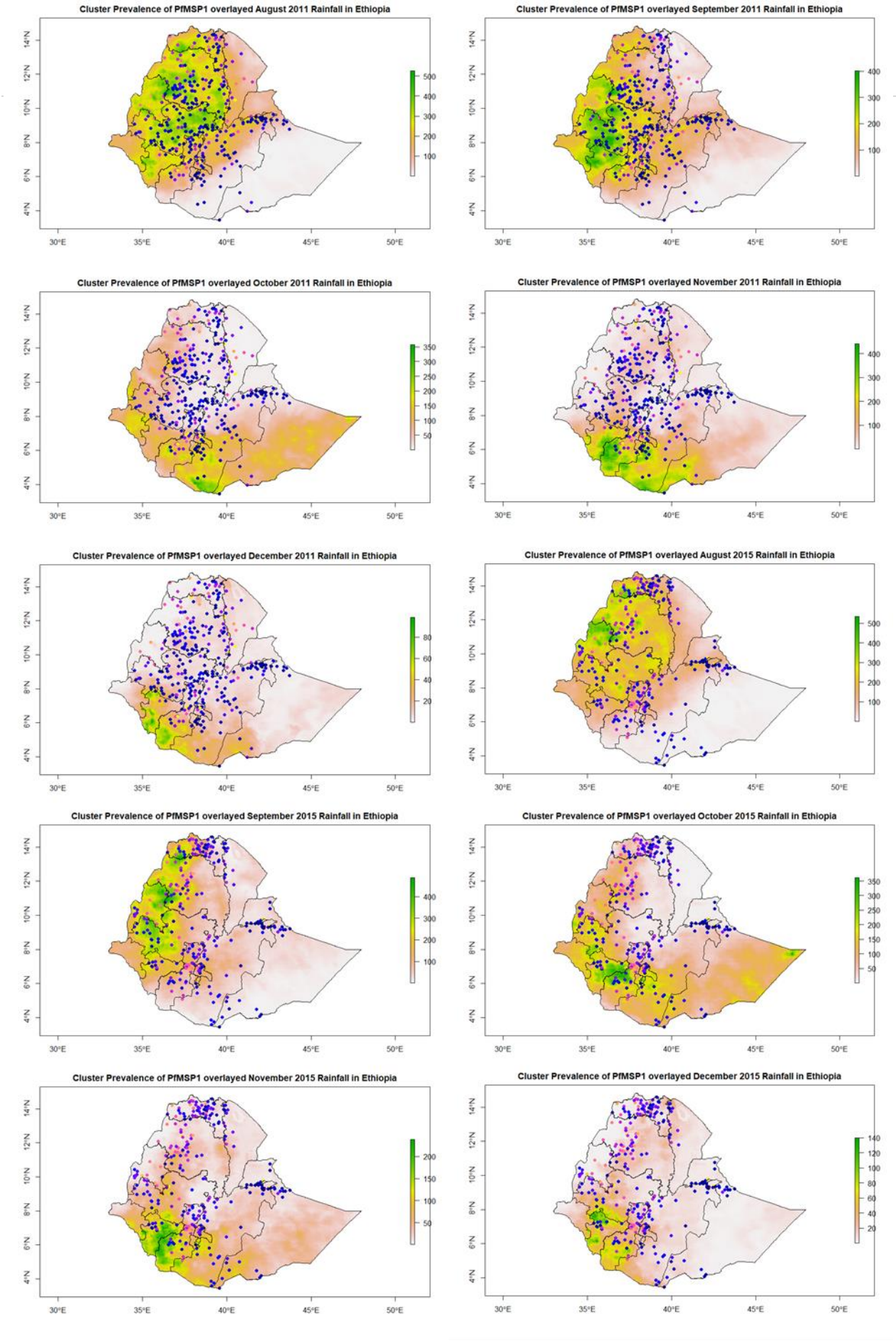

Figure 14: Cluster prevalence of *P. falciparum* merozoite protein 1 in 2011 and 2015 overlayed with the monthly rainfalls from August to December

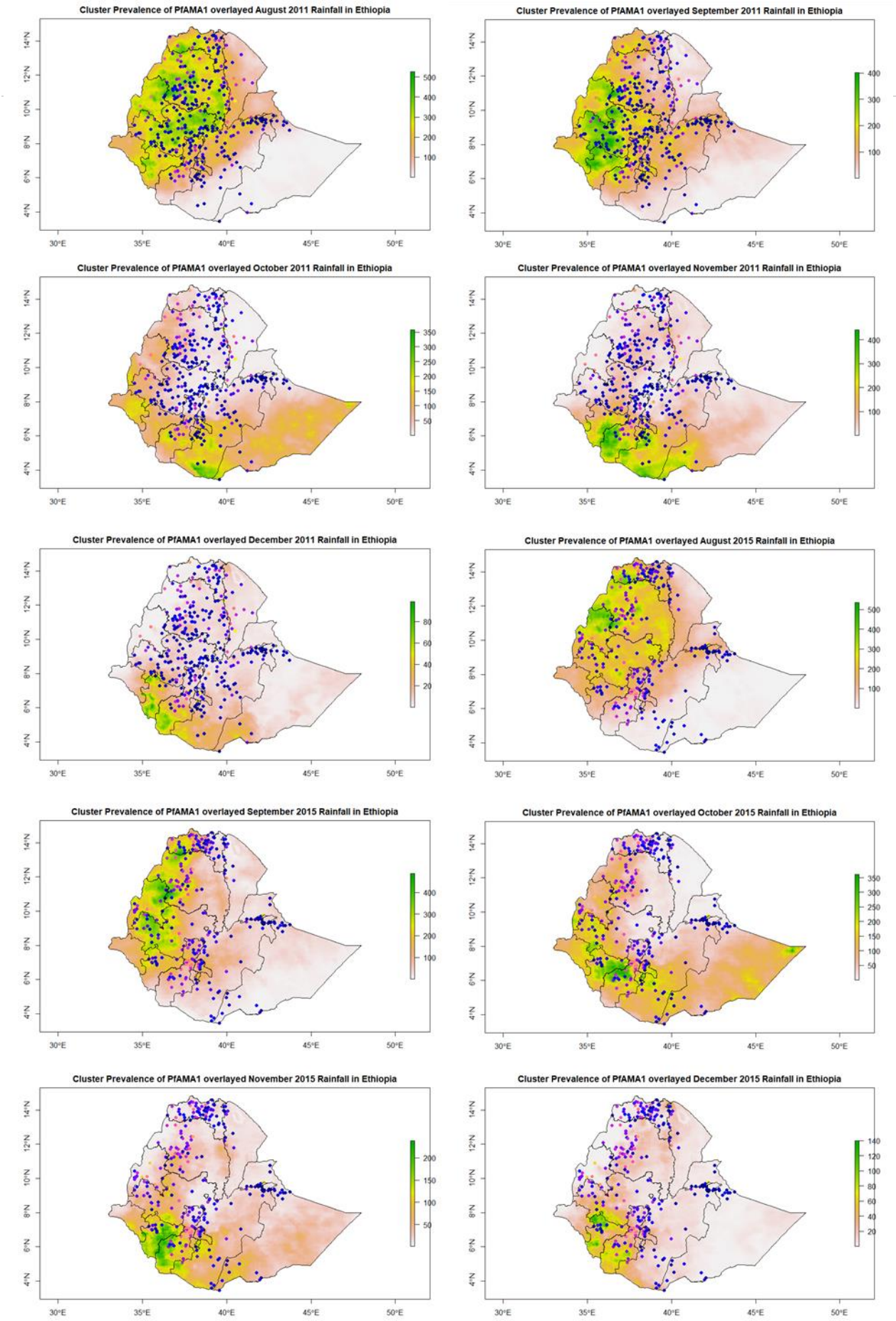

Figure 15: Cluster prevalence of *P. falciparum* apical membrane antigen 1 in 2011 and 2015 overlayed with the monthly rainfalls from August to December

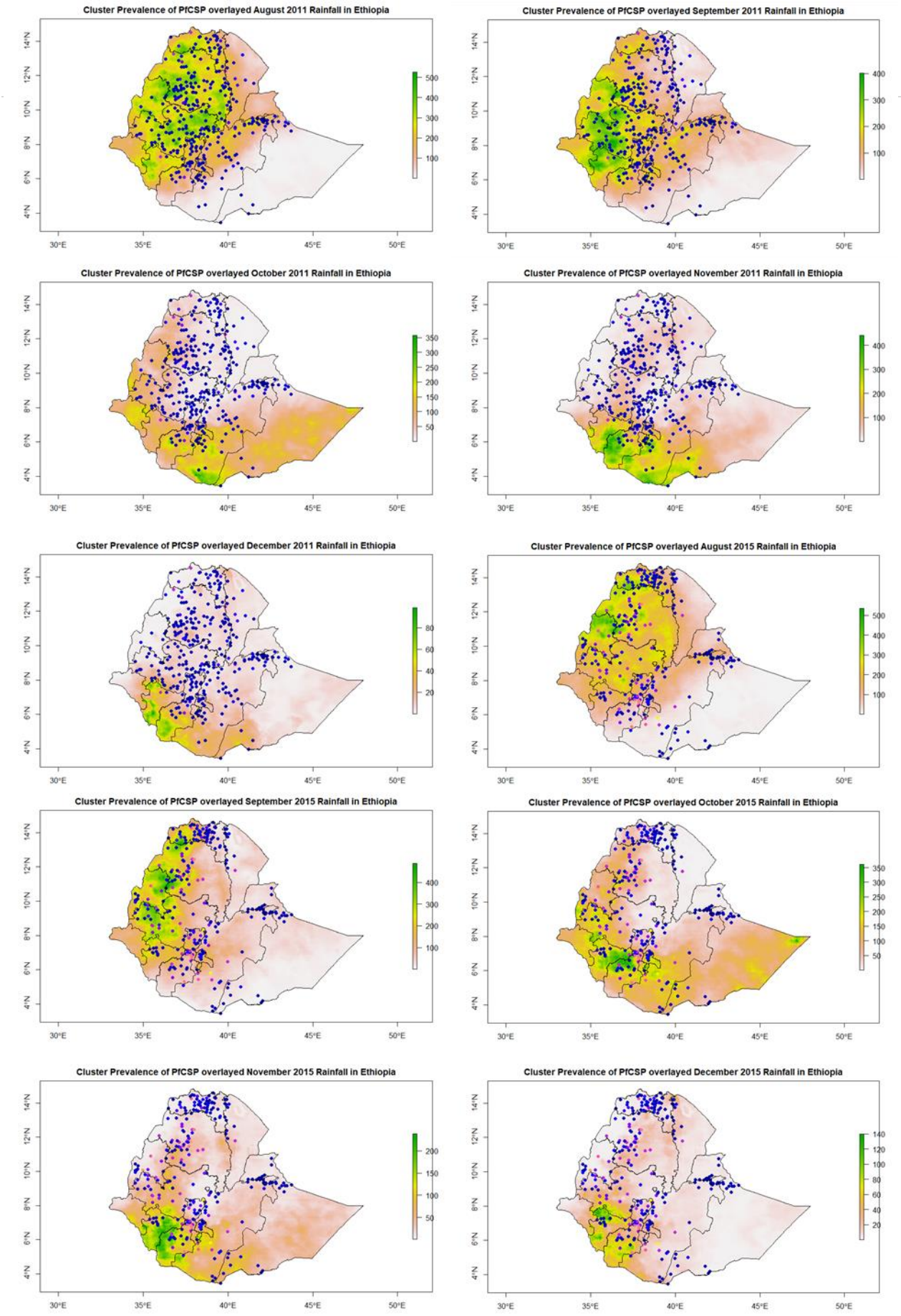

Figure 16: Cluster prevalence of *P. falciparum* circumsporozoite protein in 2011 and 2015 overlayed with the monthly rainfalls from August to December

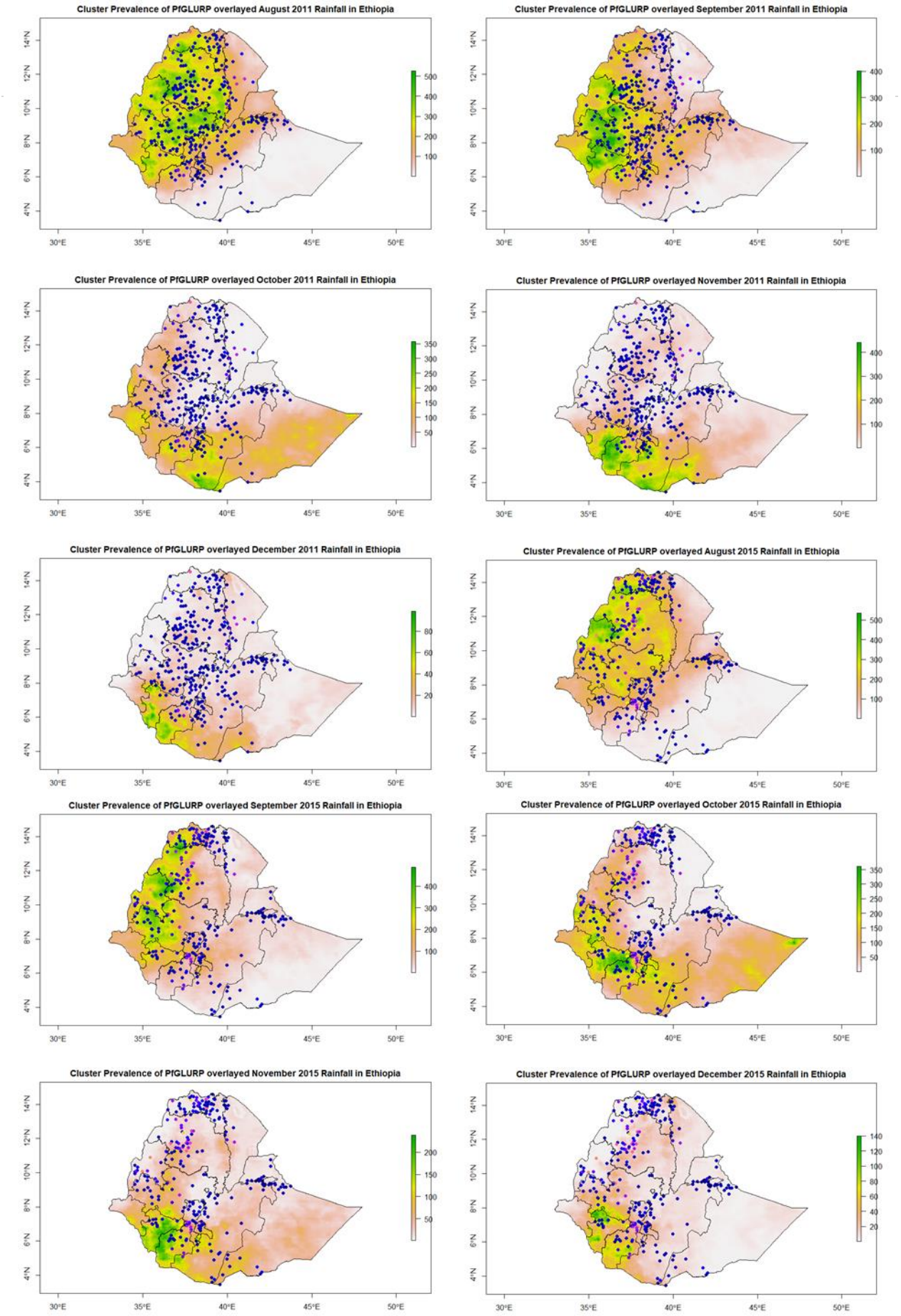

Figure 17: Cluster prevalence of *P. falciparum* glutamate-rich protein, Ro fragment in 2011 and 2015 overlayed with the monthly rainfalls from August to December

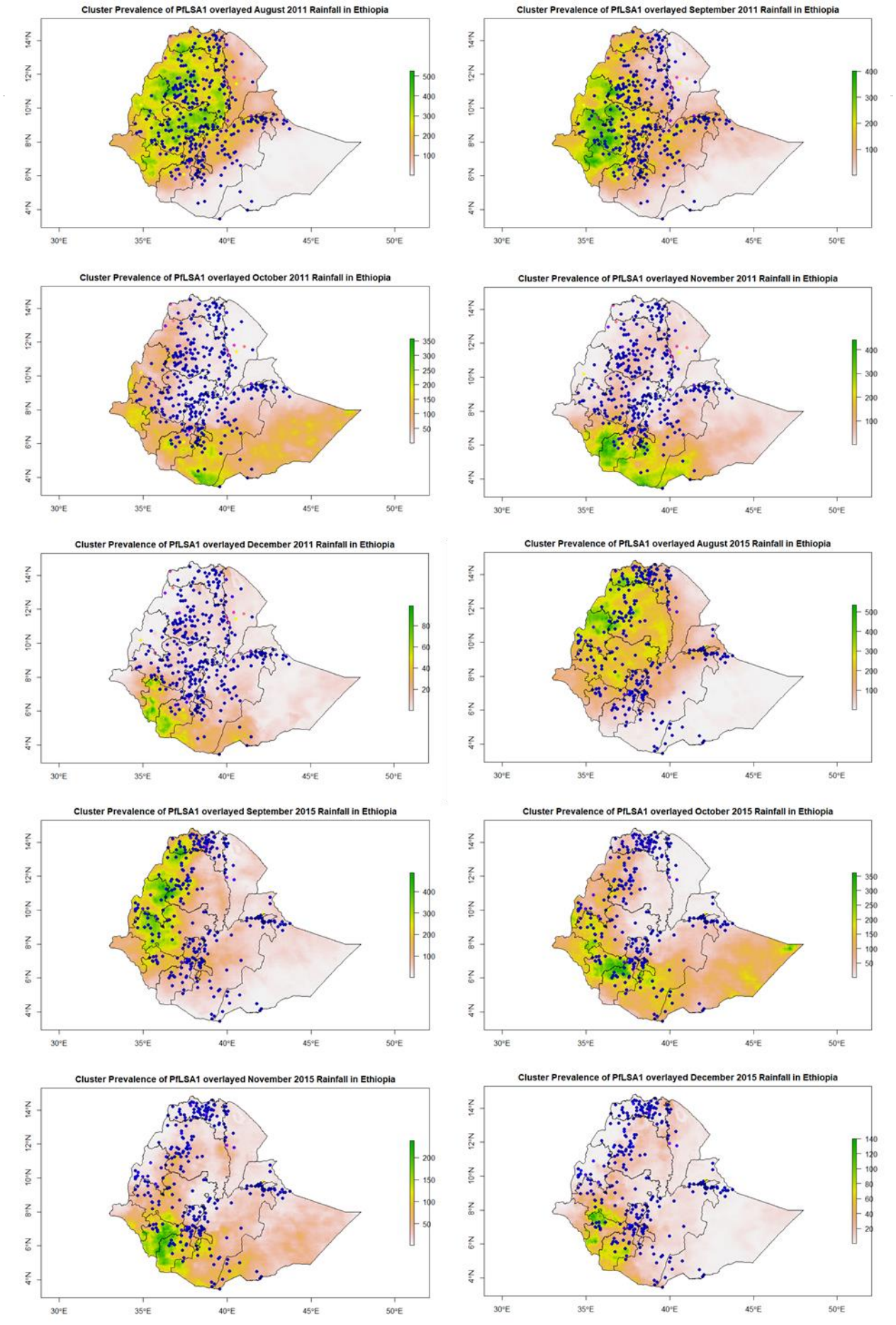

Figure 18: Cluster prevalence of *P. falciparum* liver stage antigen 1 in 2011 and 2015 overlayed with the monthly rainfalls from August to December

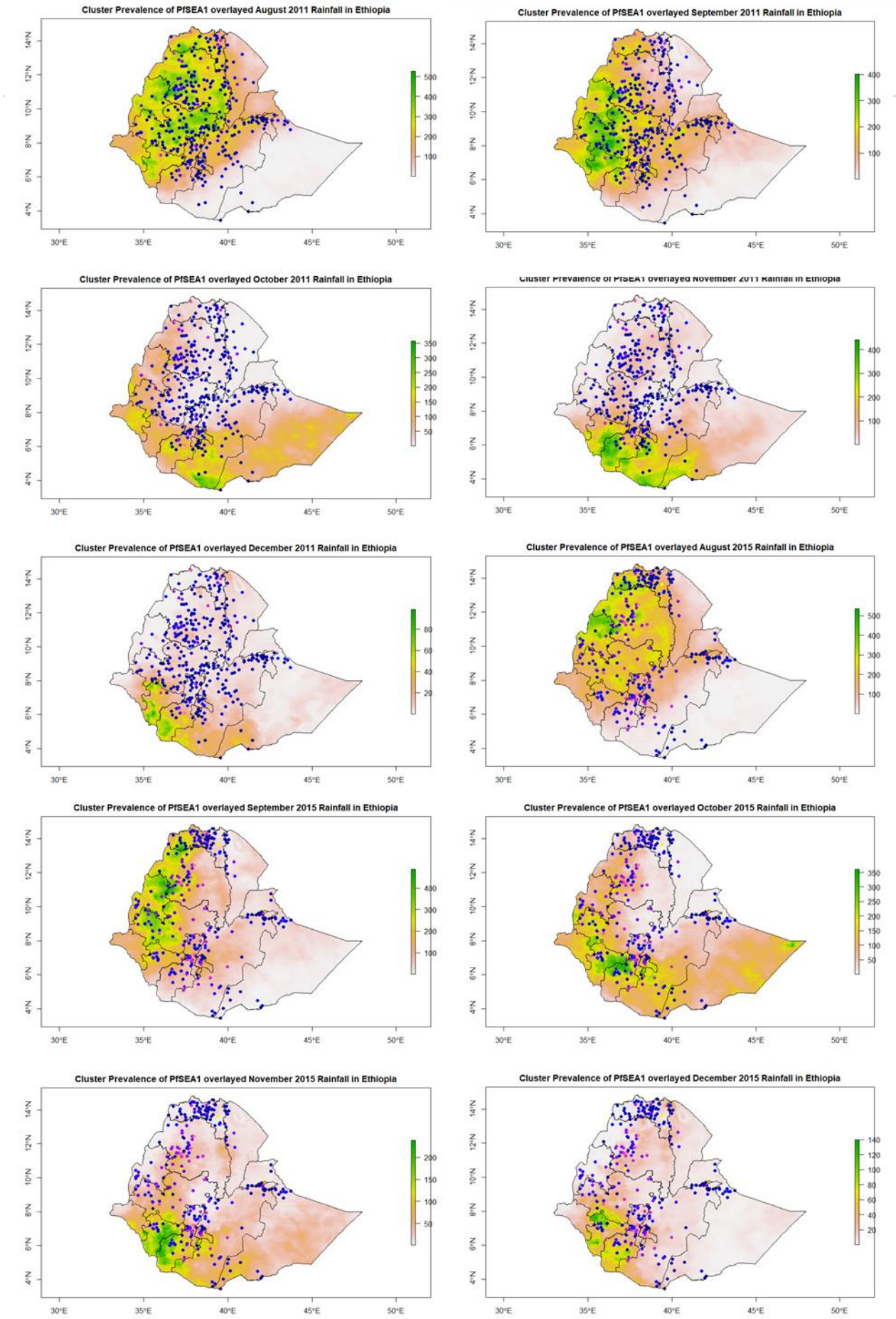

Figure 19: Cluster prevalence of *P. falciparum* schizont egress antigen 1 in 2011 and 2015 overlayed with the monthly rainfalls from August to December

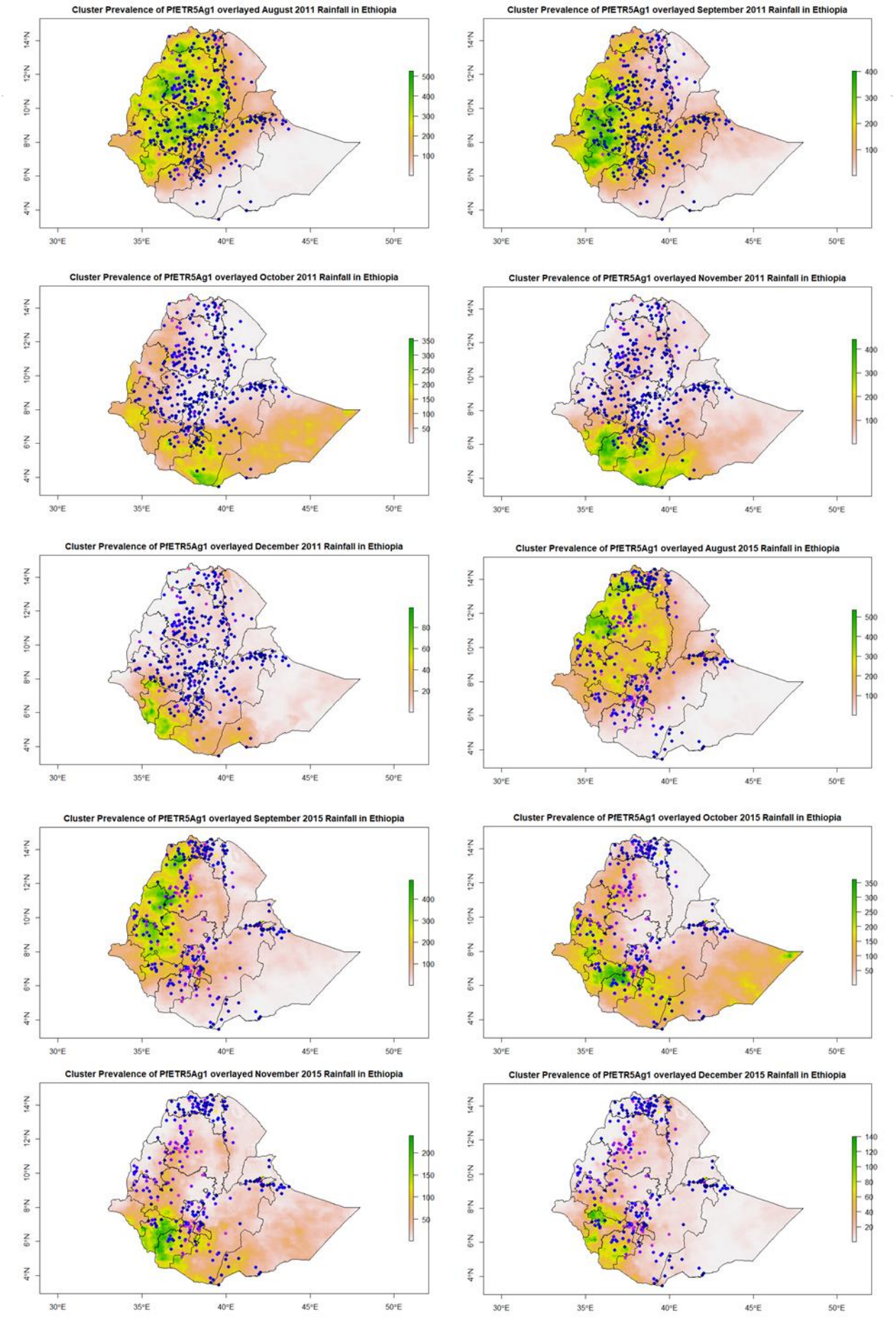

Figure 20: Cluster prevalence of *P. falciparum* ETRAMP5 antigen 1 in 2011 and 2015 overlayed with the monthly rainfalls from August to December

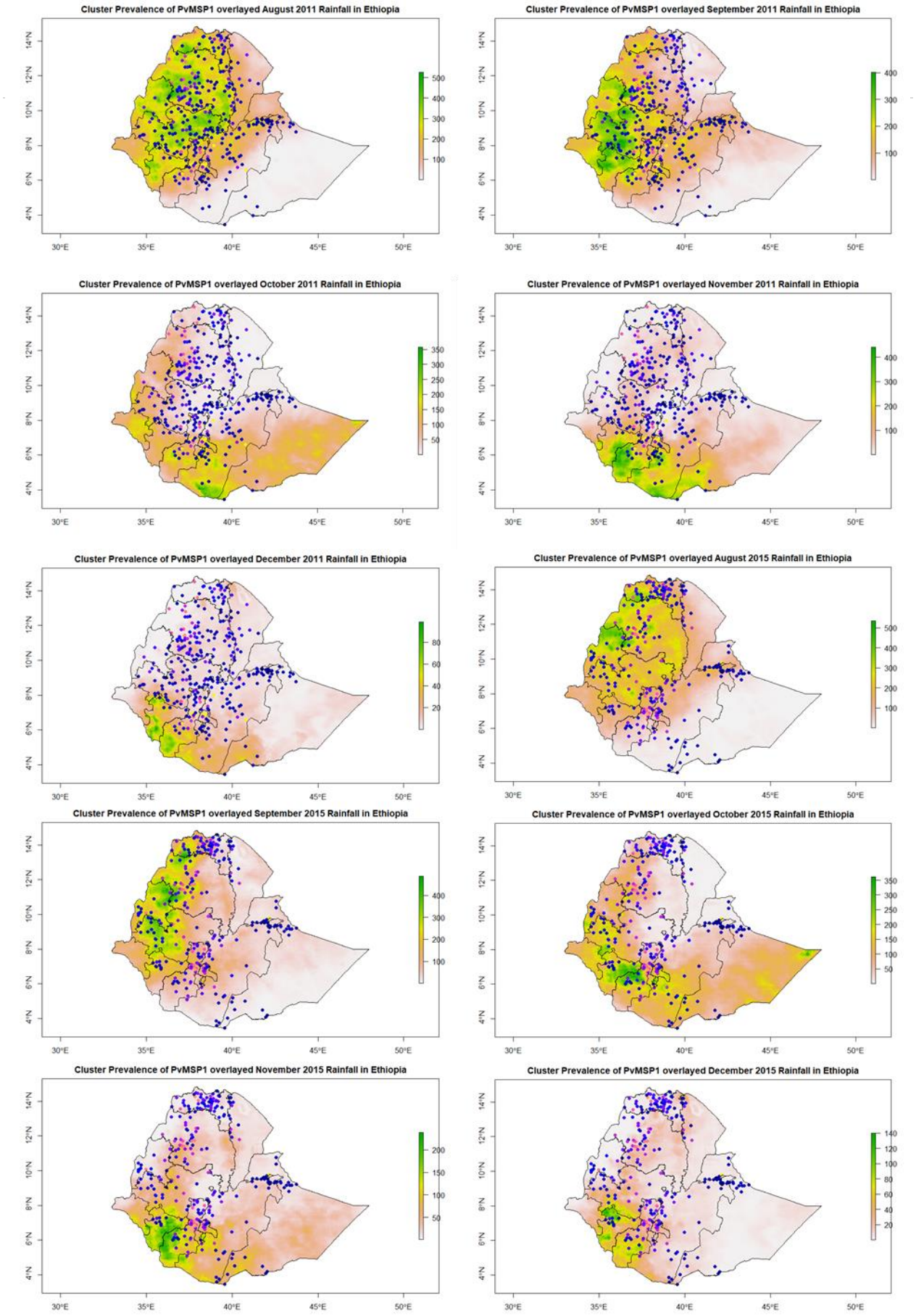

Figure 21: Cluster prevalence of *P. vivax* merozoite protein 1 in 2011 and 2015 overlayed with the monthly rainfalls from August to December

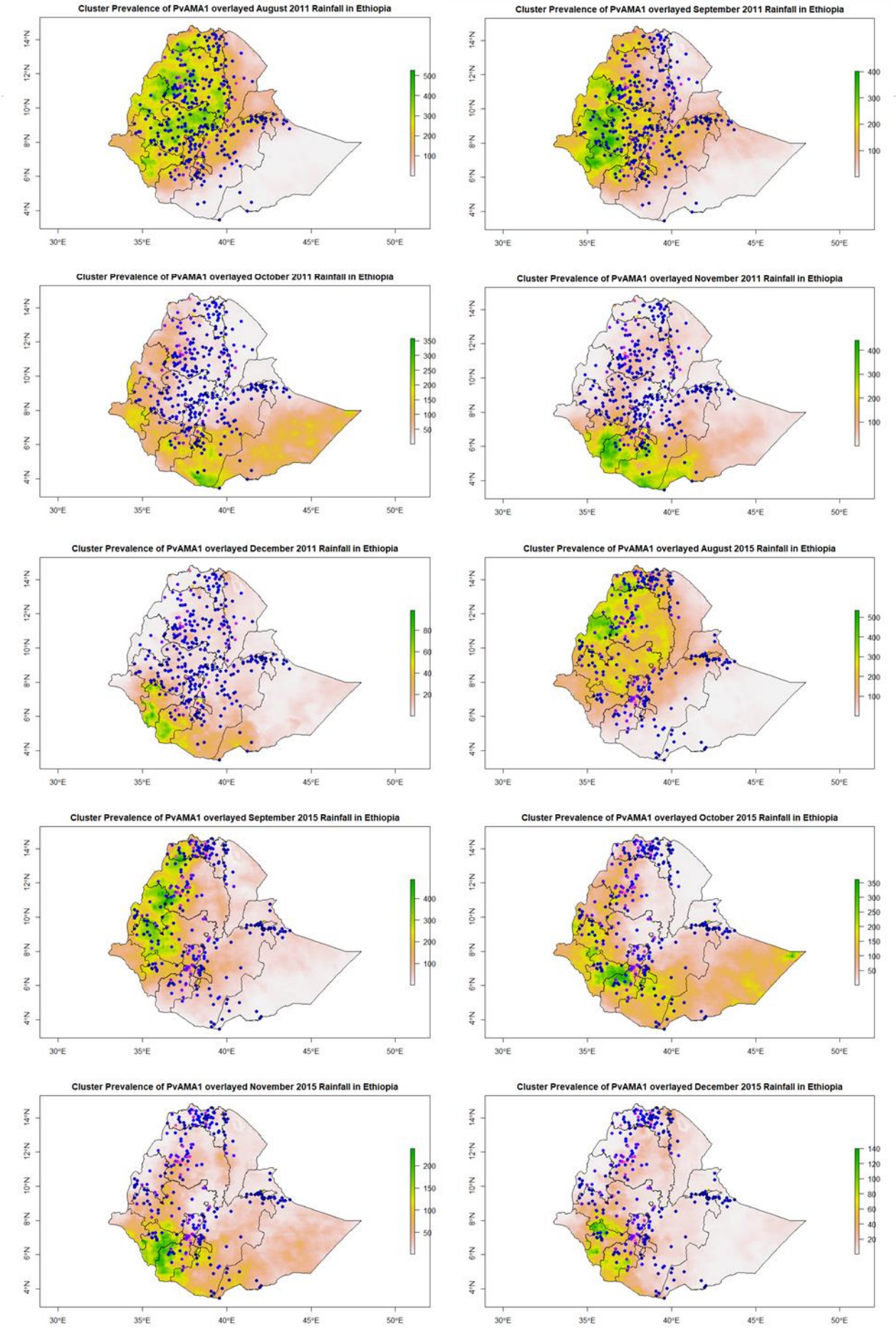

Figure 22: Cluster prevalence of *P. vivax* apical membrane antigen 1 in 2011 and 2015 overlayed with the monthly rainfalls from August to December

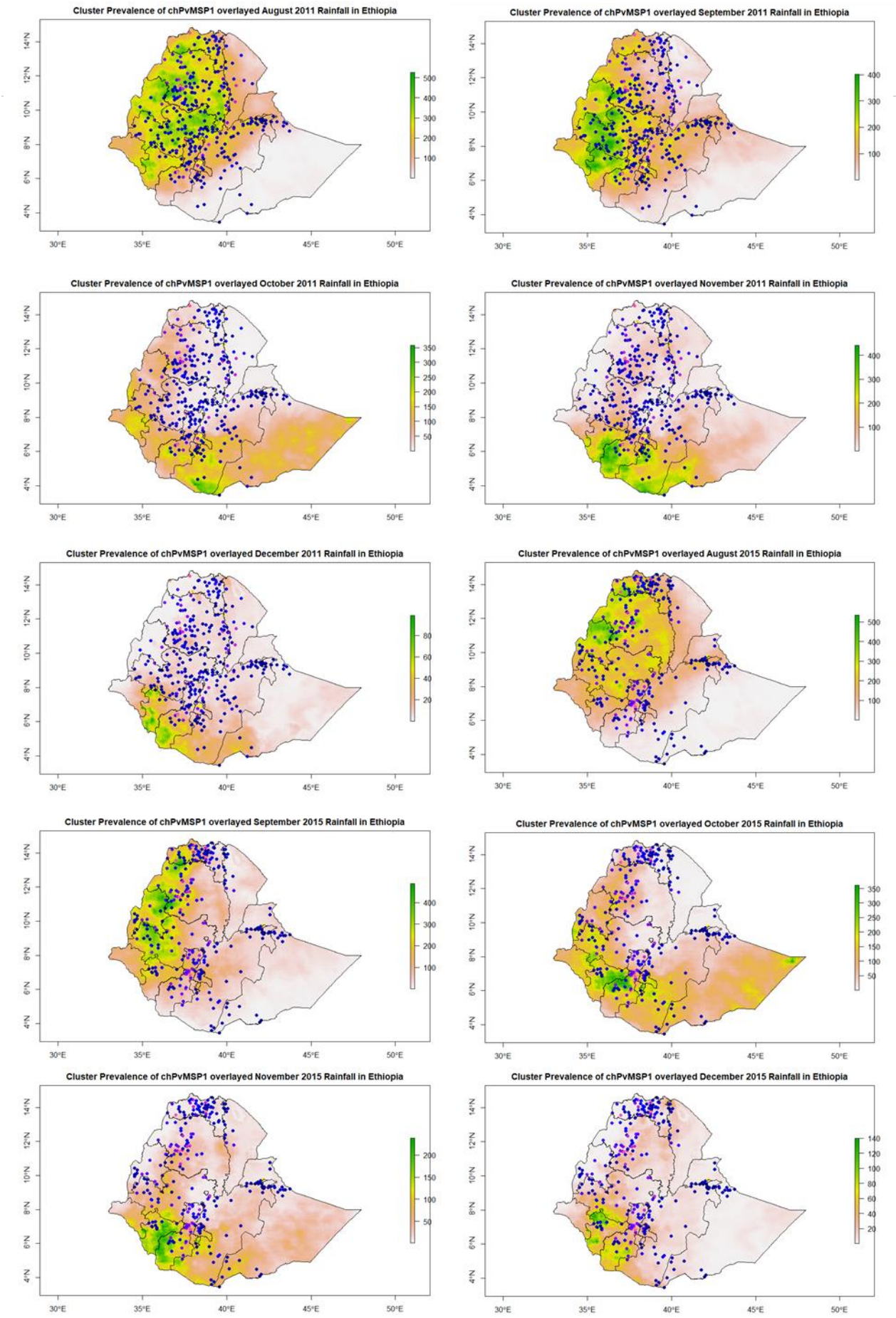

Figure 23: Cluster prevalence of chimeric *P. vivax* merozoite protein 1, including additional B and T cell epitopes in 2011 and 2015 overlayed with the monthly rainfalls from August to December

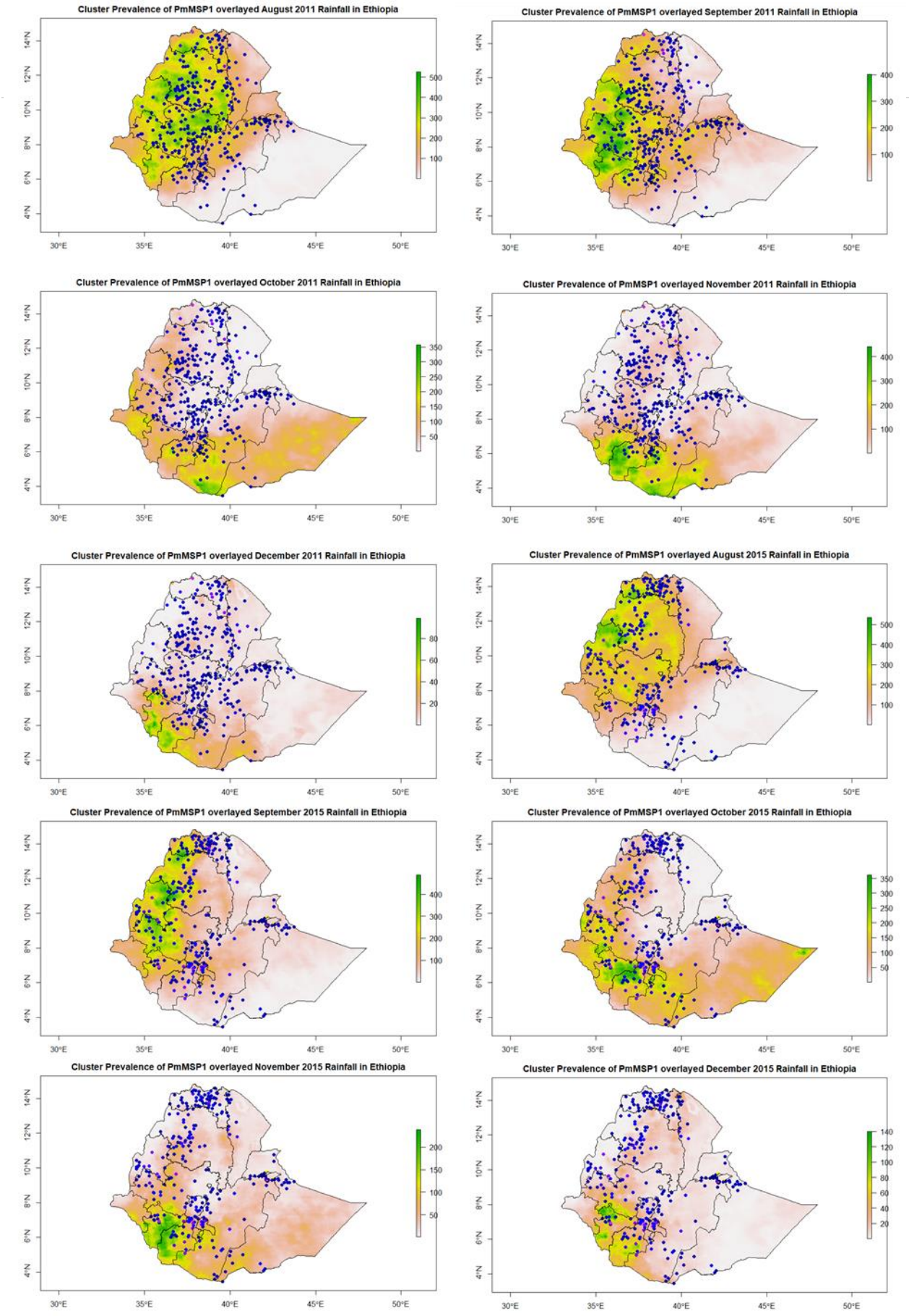

Figure 24: Cluster prevalence of *P. malariae* merozoite protein 1 in 2011 and 2015 overlayed with the monthly rainfalls from August to December

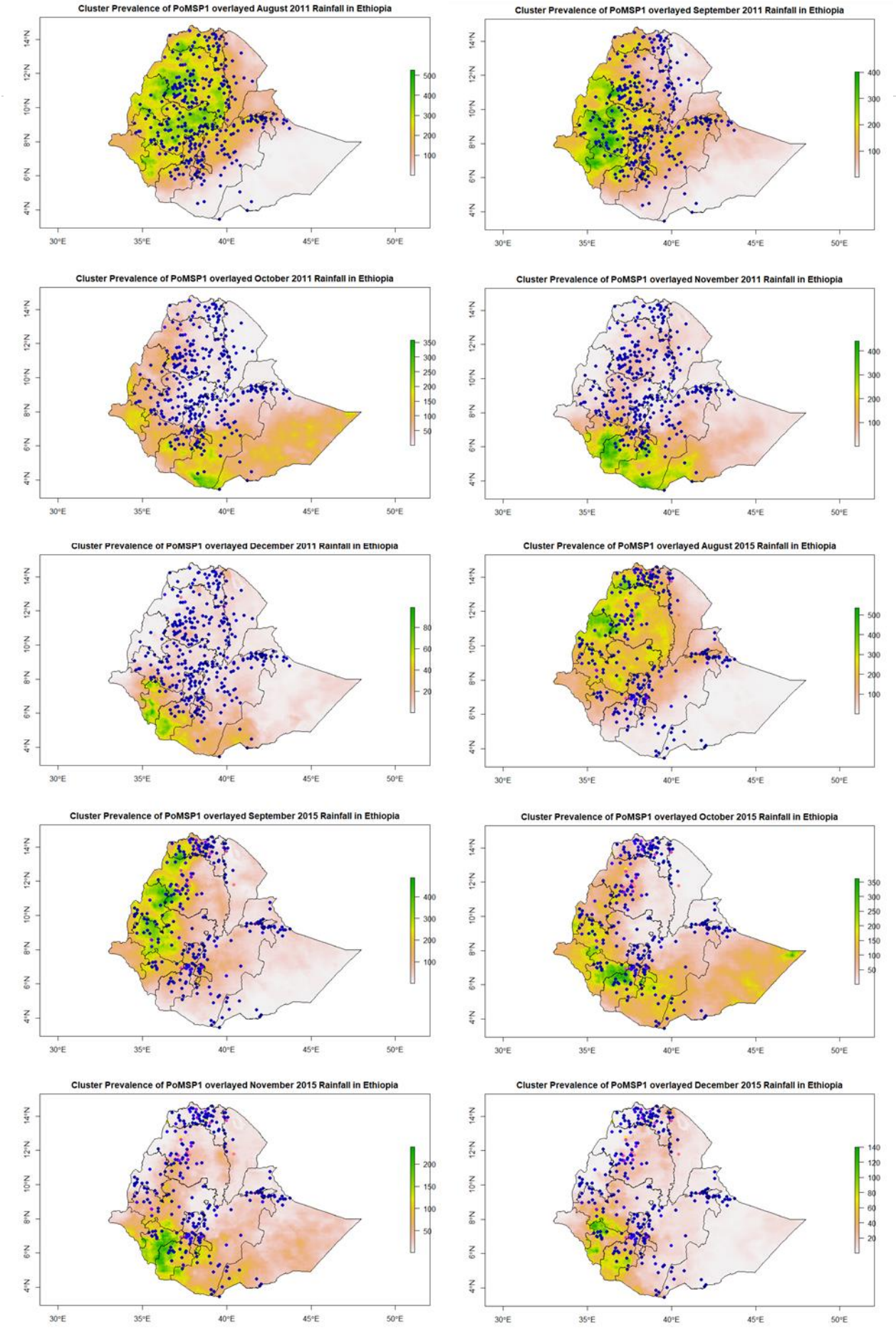

Figure 25: Cluster prevalence of *P. ovale* merozoite protein 1 in 2011 and 2015 overlayed with the monthly rainfalls from August to December

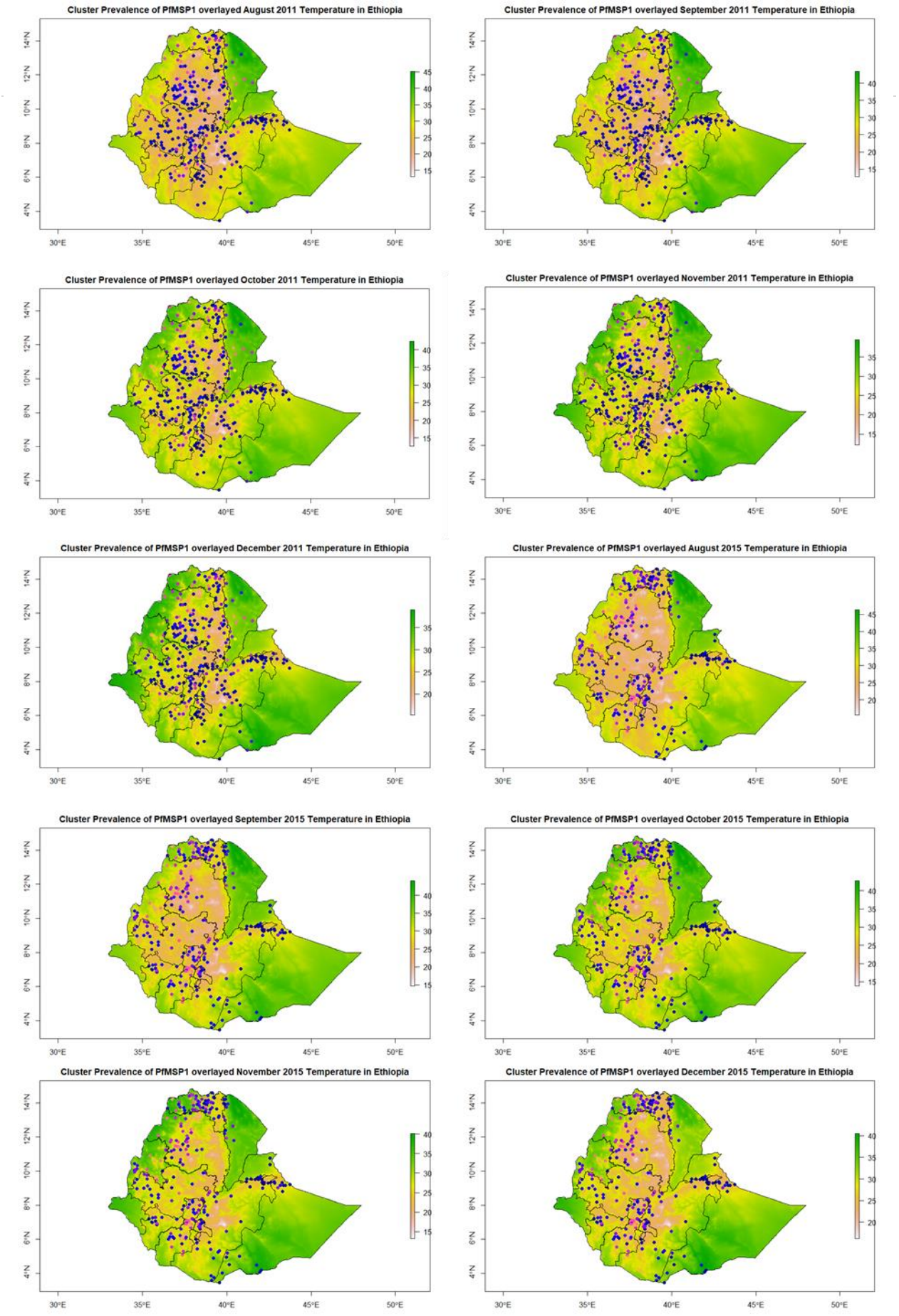

Figure 26: Cluster prevalence of *P. falciparum* merozoite protein 1 in 2011 and 2015 overlayed with the monthly average temperatures from August to December

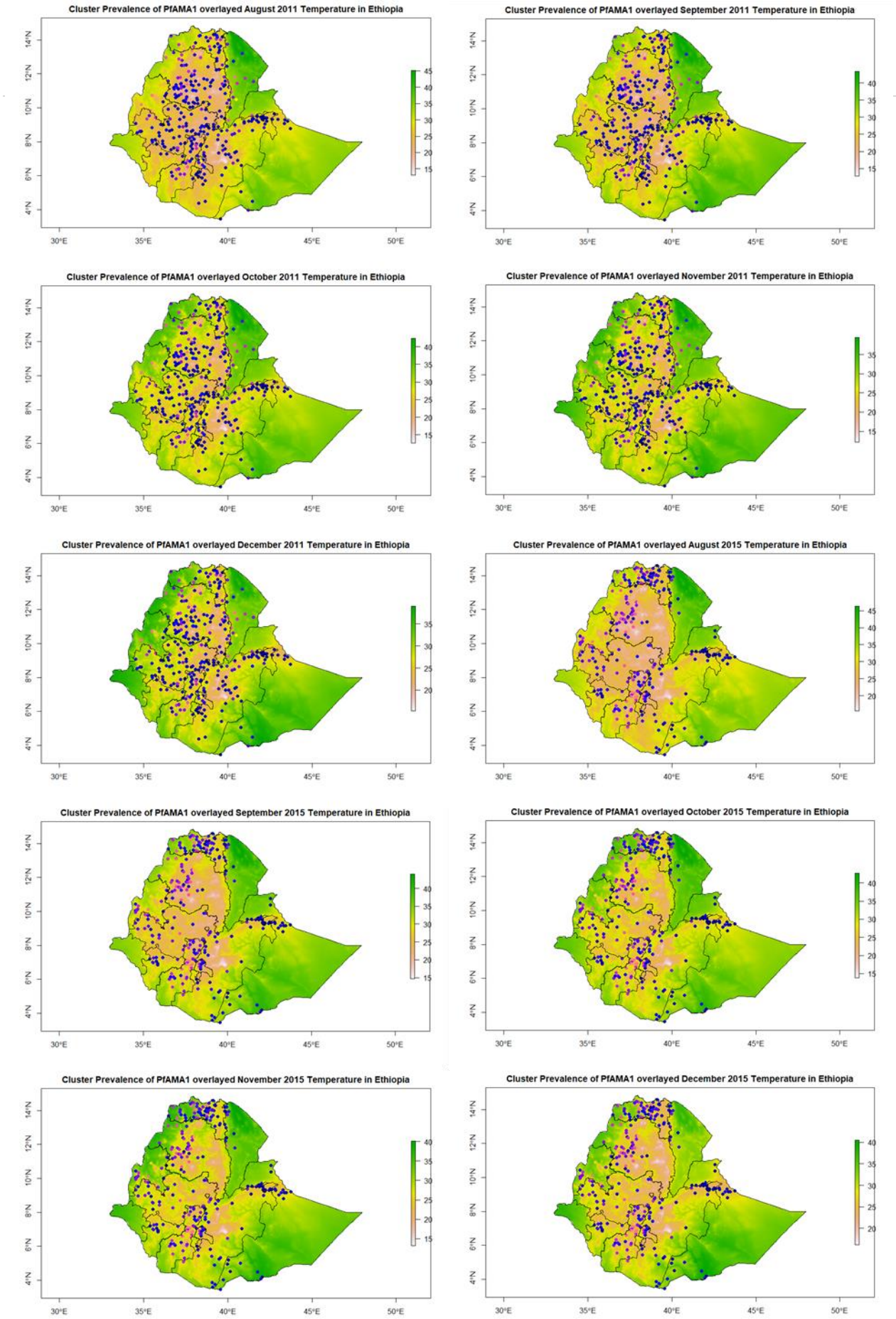

Figure 27: Cluster prevalence of *P. falciparum* apical membrane antigen 1 in 2011 and 2015 overlayed with the monthly average temperatures from August to December

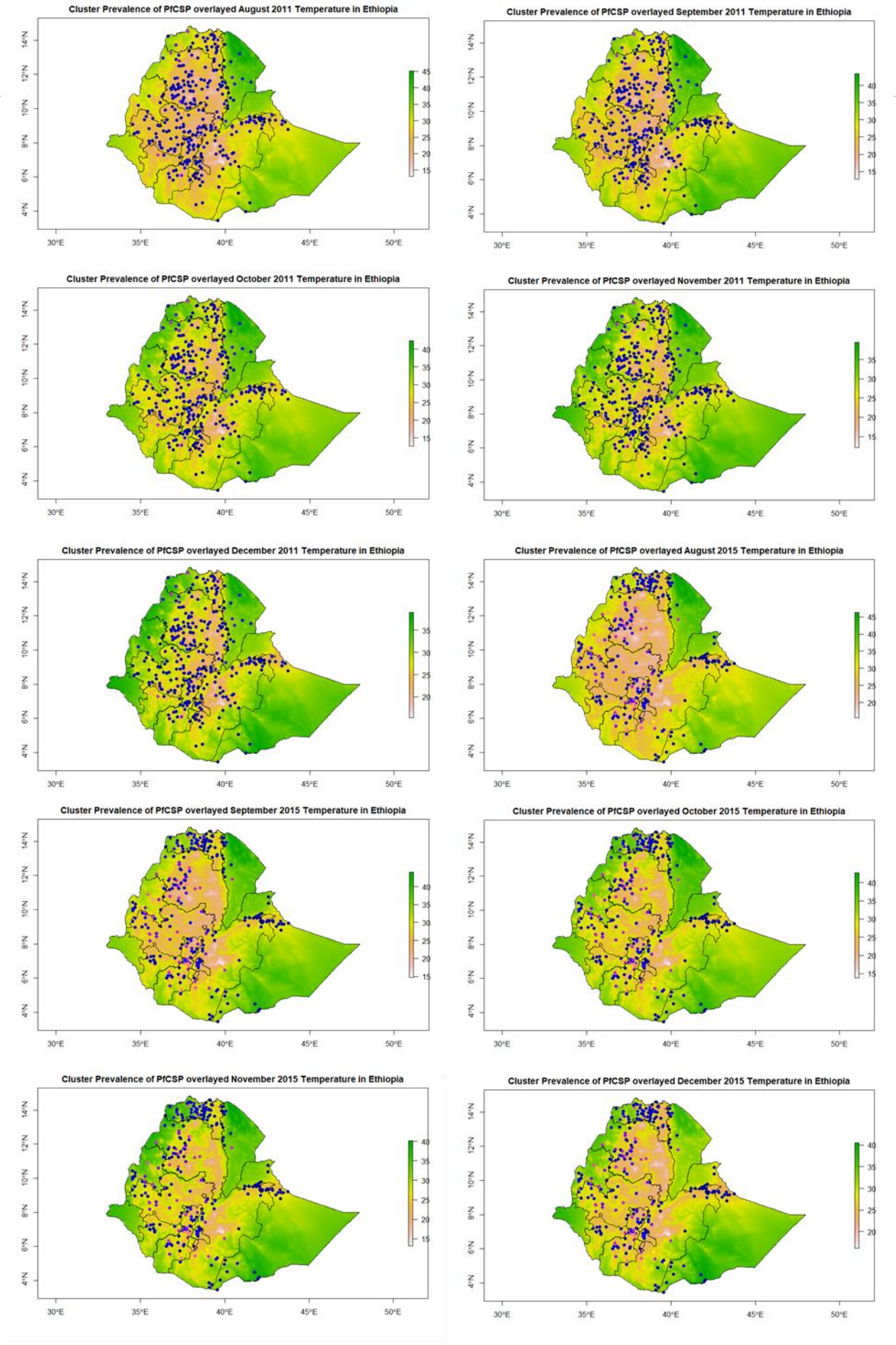

Figure 28: Cluster prevalence of *P. falciparum* circumsporozoite protein in 2011 and 2015 overlayed with the monthly average temperatures from August to December

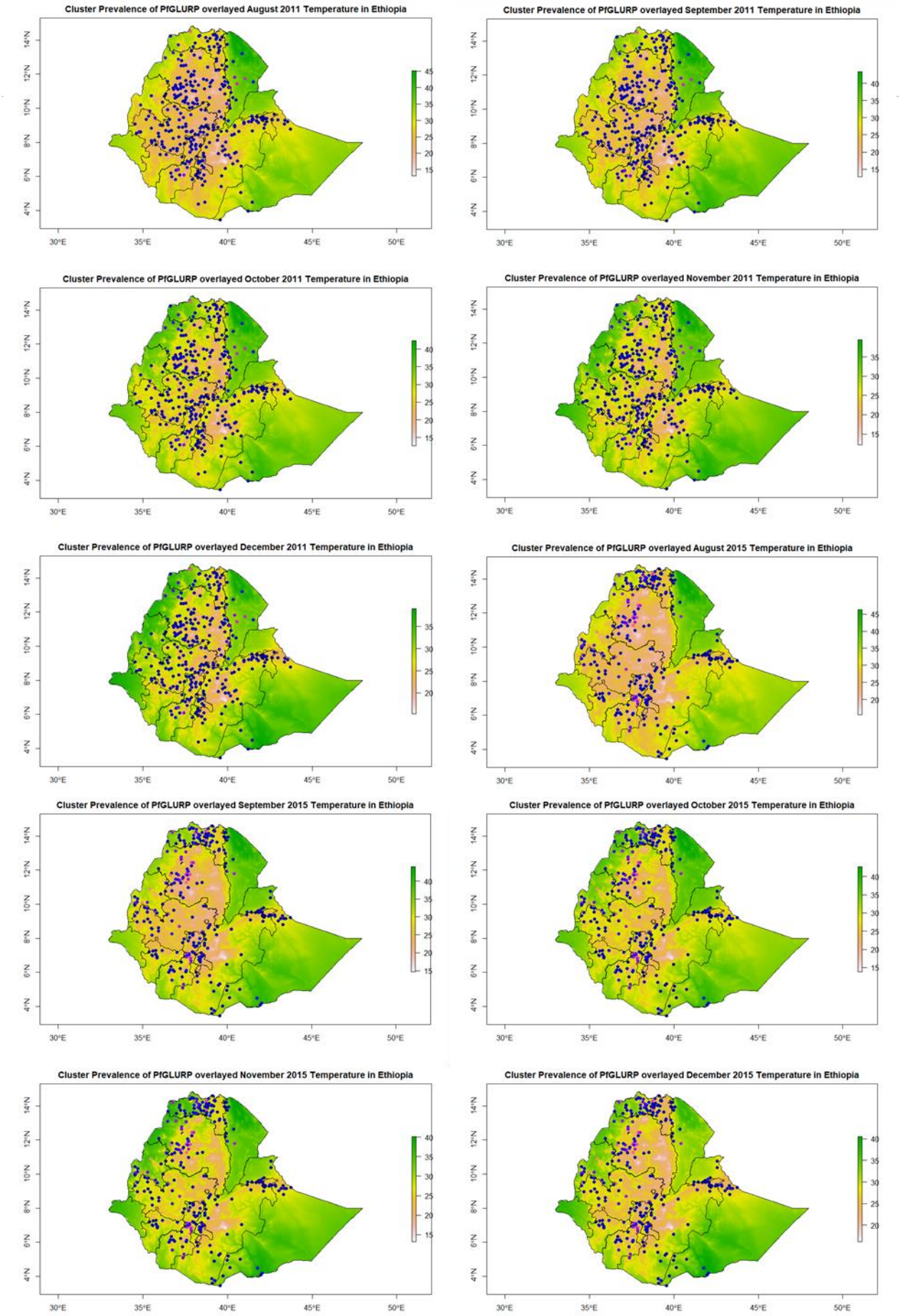

Figure 29: Cluster prevalence of *P. falciparum* glutamate-rich protein, Ro fragment in 2011 and 2015 overlayed with the monthly average temperatures from August to December

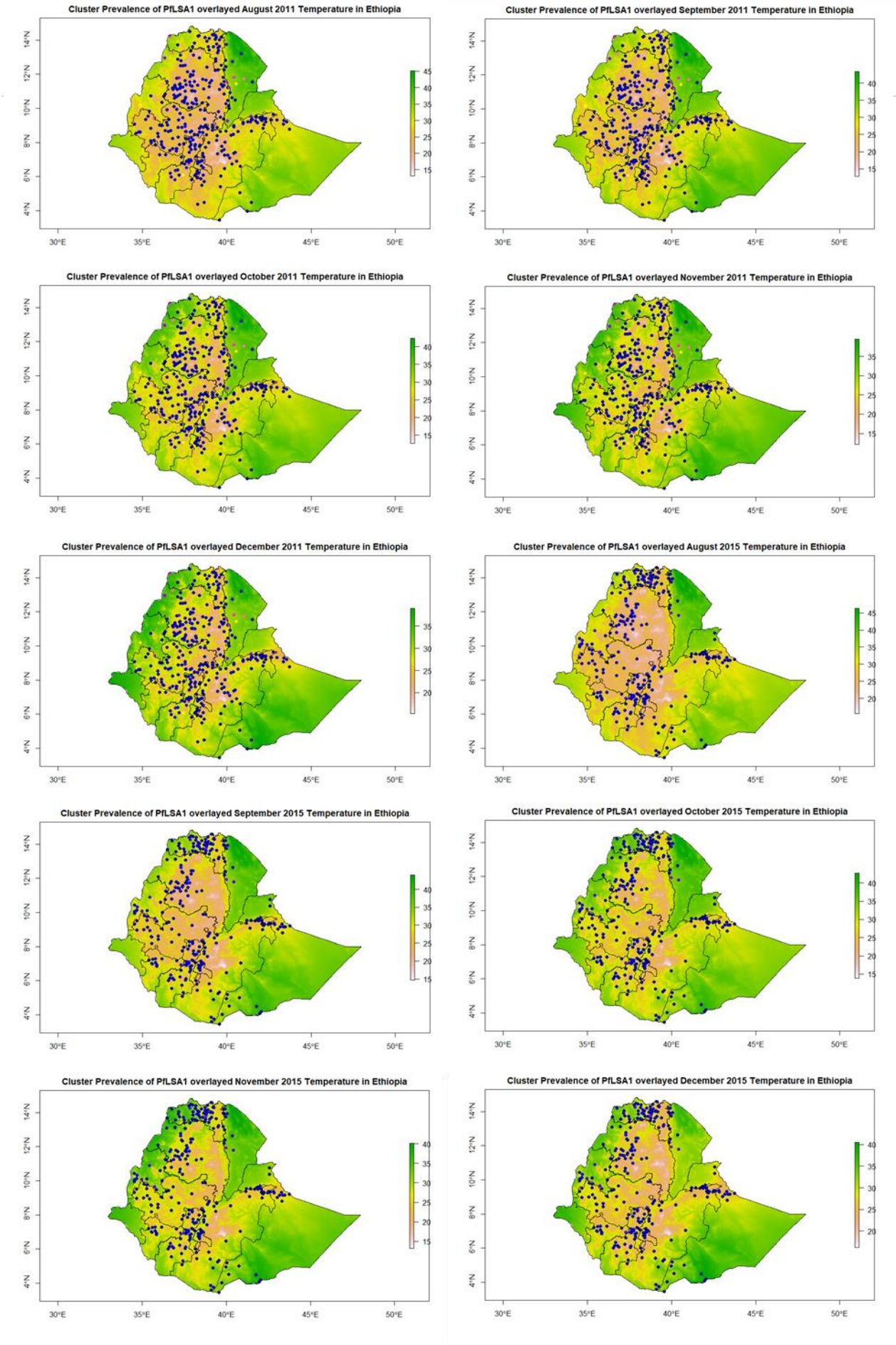

Figure 30: Cluster prevalence of *P. falciparum* liver stage antigen 1 in 2011 and 2015 overlayed with the monthly average temperatures from August to December

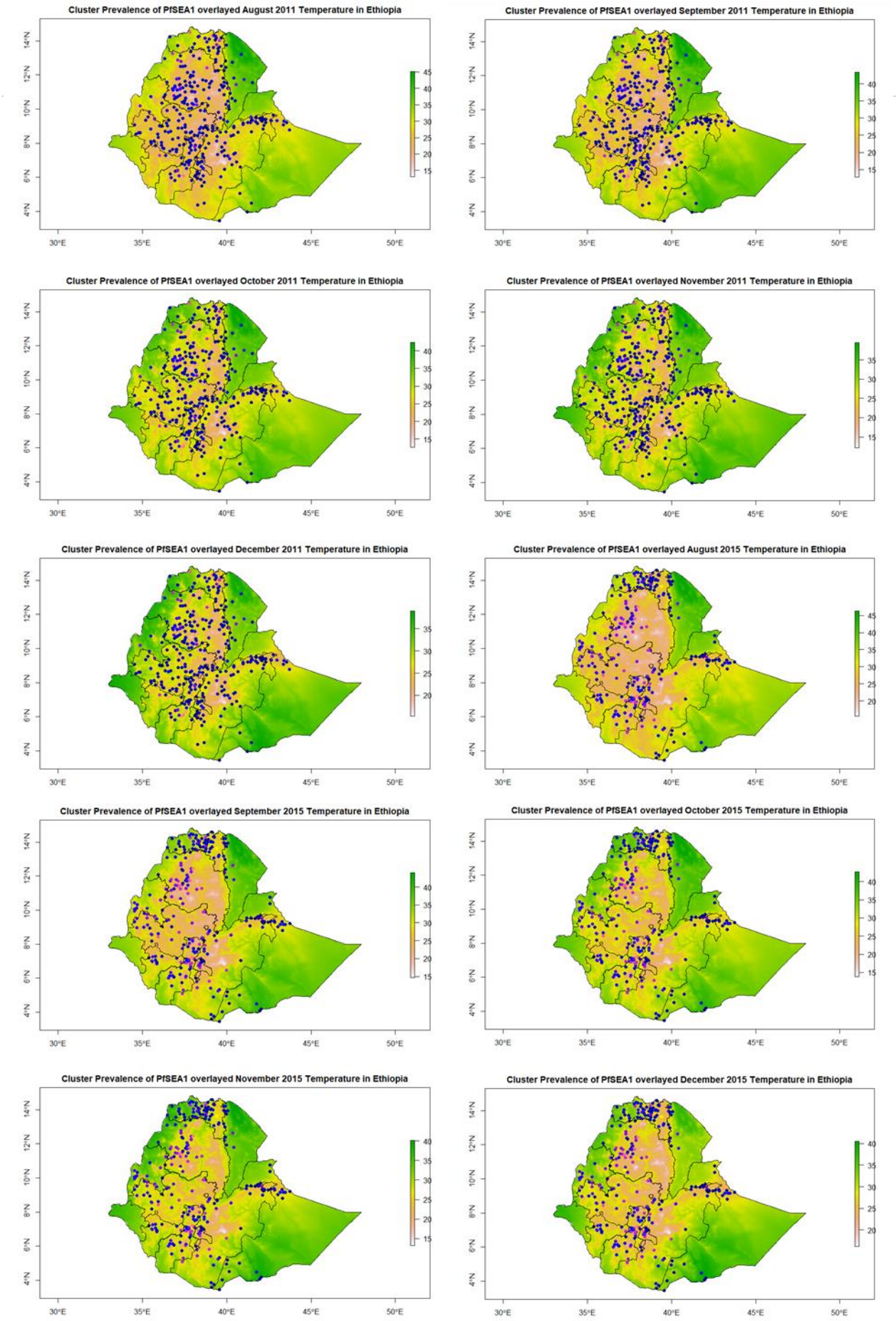

Figure 31: Cluster prevalence of *P. falciparum* schizont egress antigen 1 in 2011 and 2015 overlayed with the monthly average temperatures from August to December

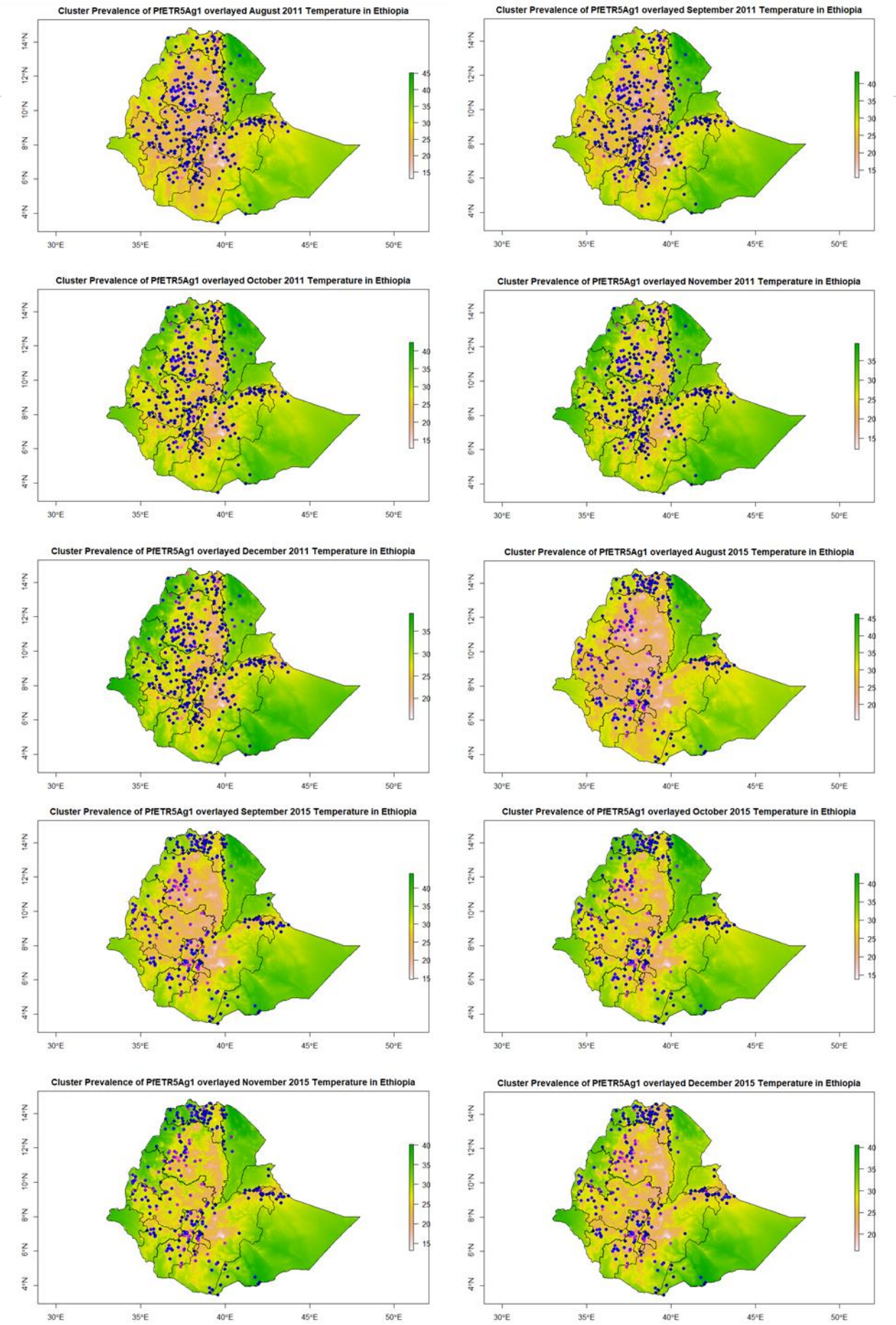

Figure 32: Cluster prevalence of *P. falciparum* ETRAMP5 antigen 1 in 2011 and 2015 overlayed with the monthly average temperatures from August to December

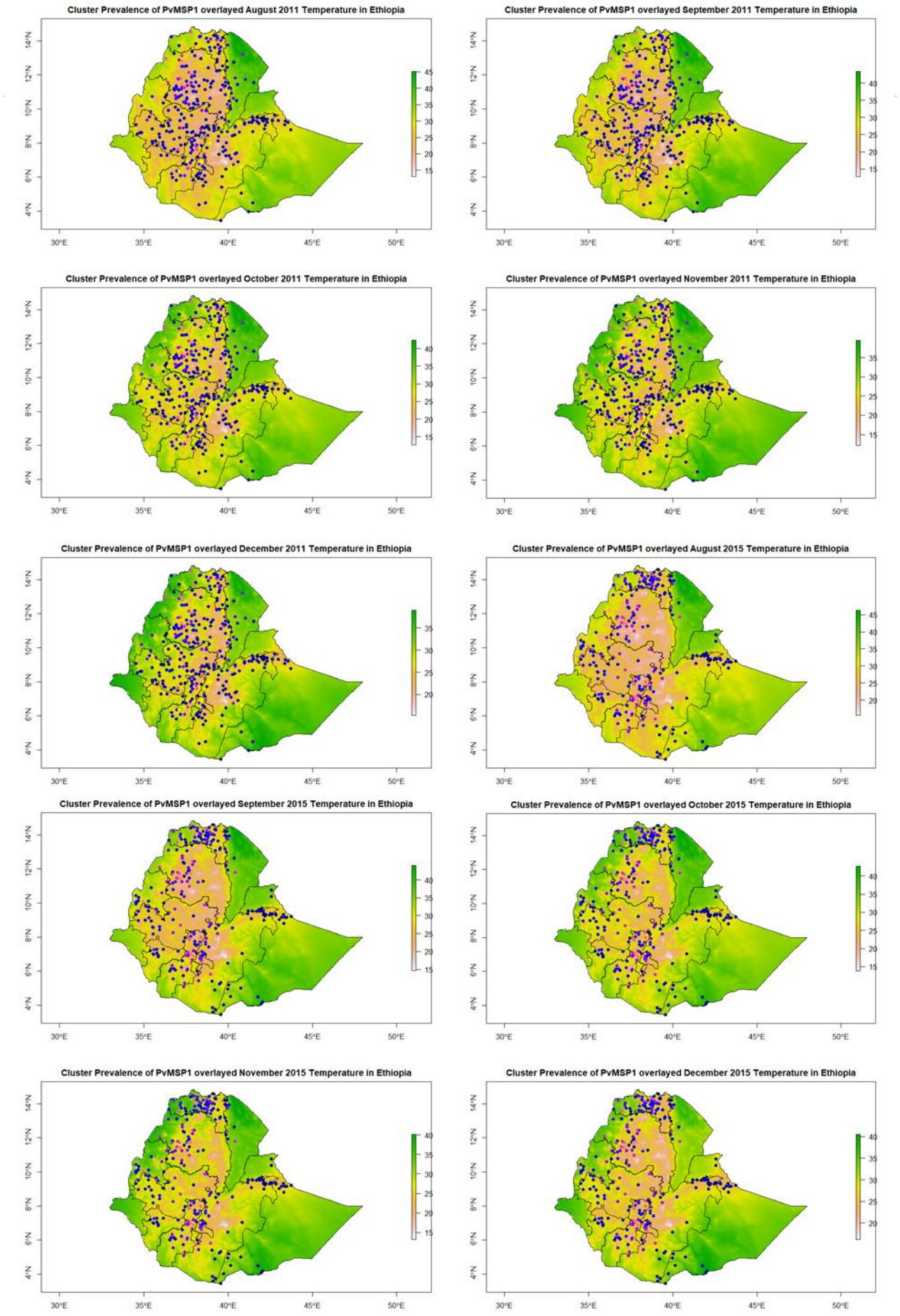

Figure 33: Cluster prevalence of *P. vivax* merozoite protein 1 in 2011 and 2015 overlayed with the monthly average temperatures from August to December

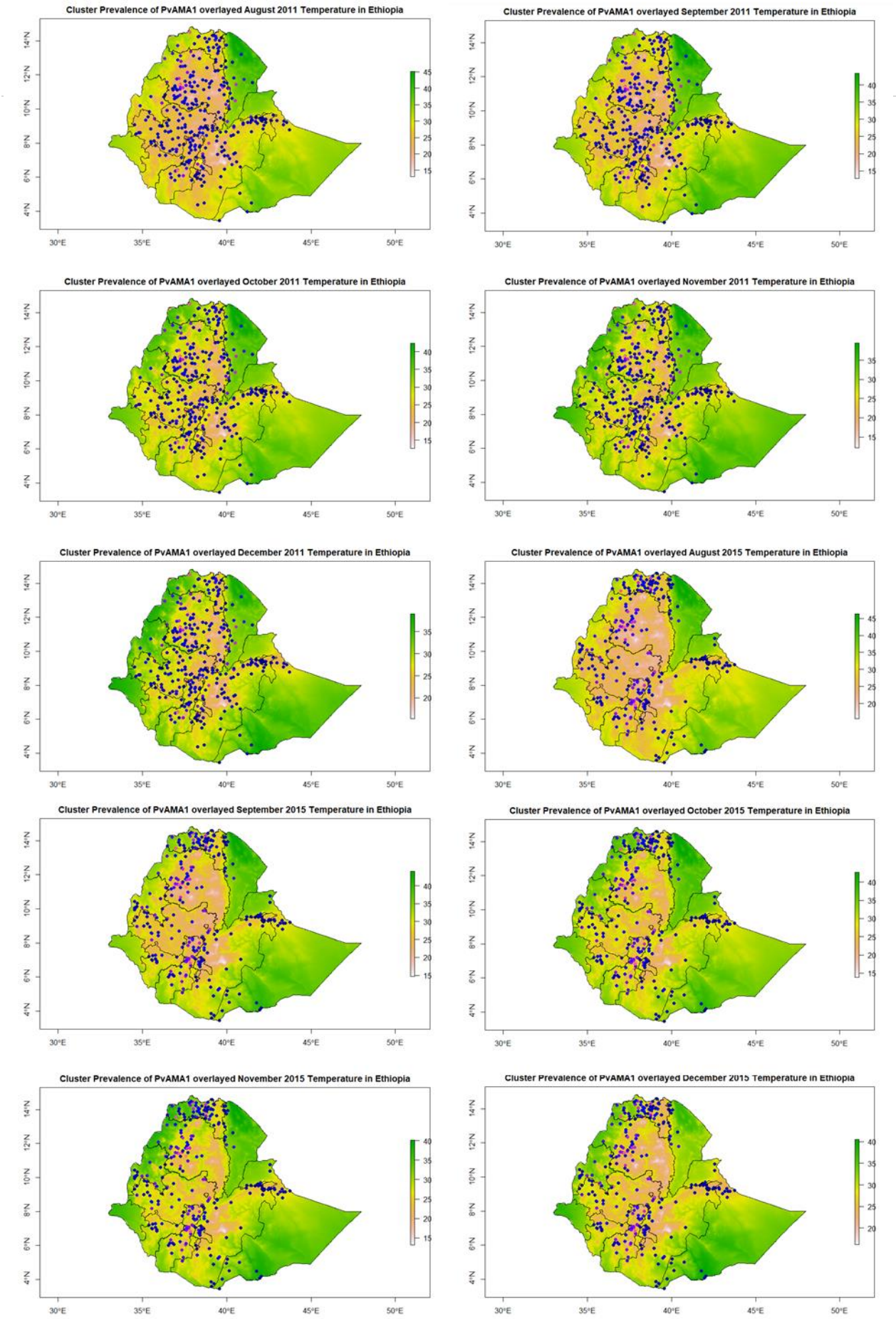

Figure 34: Cluster prevalence of *P. vivax* apical membrane antigen 1 in 2011 and 2015 overlayed with the monthly average temperatures from August to December

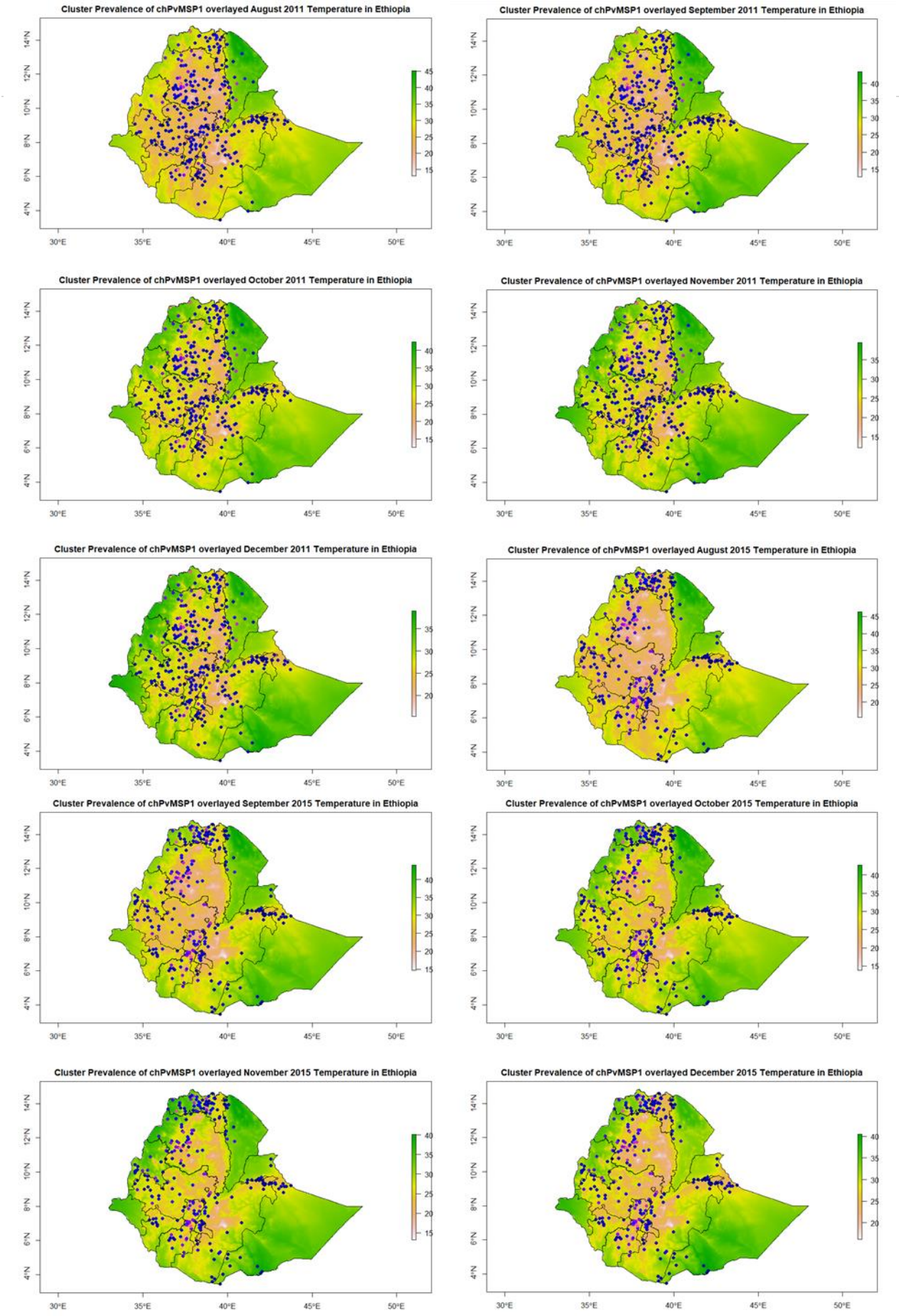

Figure 35: Cluster prevalence of chimeric *P. vivax* merozoite protein 1, including additional B and T cell epitopes in 2011 and 2015 overlayed with the monthly average temperatures from August to December

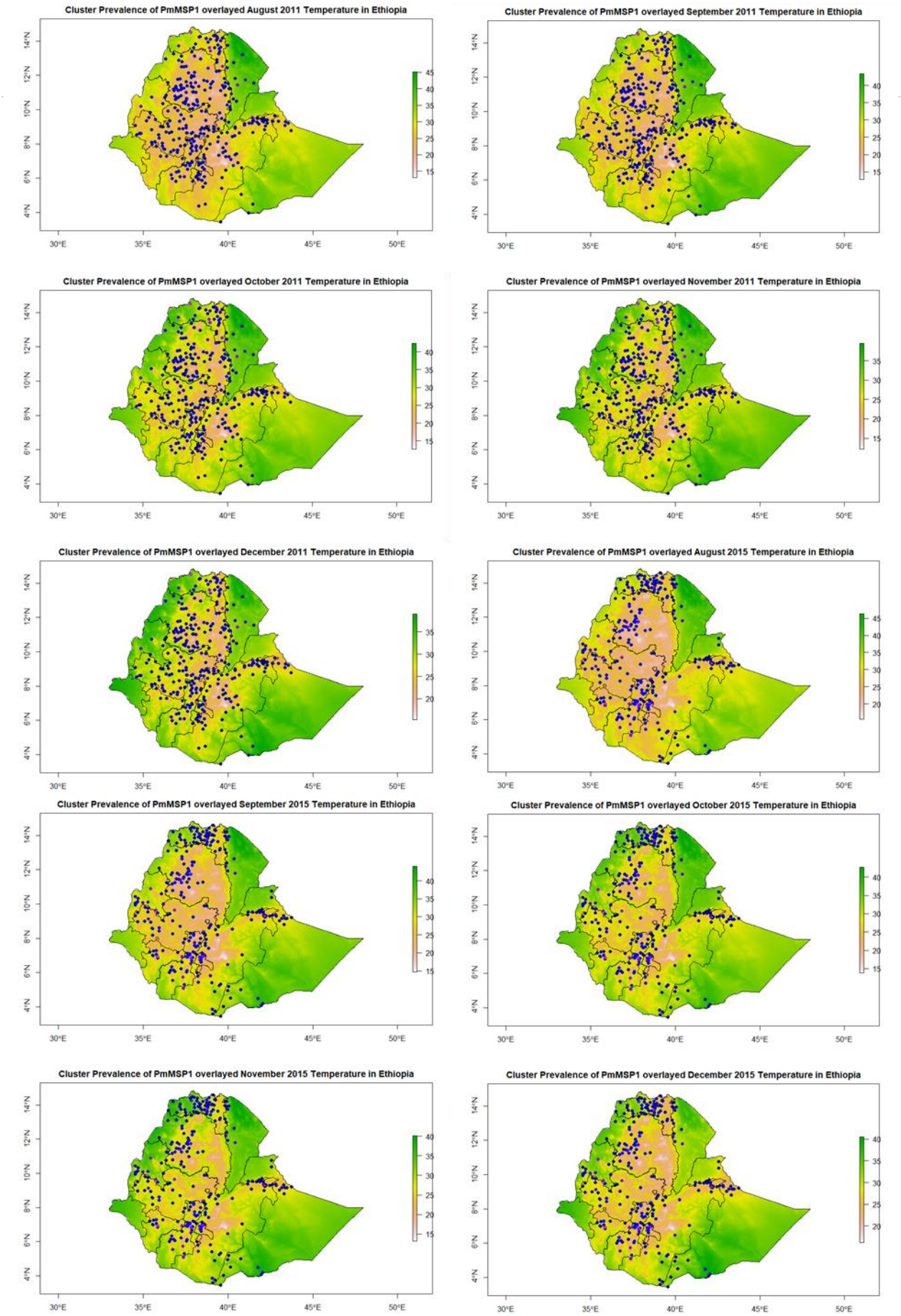

Figure 36: Cluster prevalence of *P. malariae* merozoite protein 1 in 2011 and 2015 overlayed with the monthly average temperatures from August to December

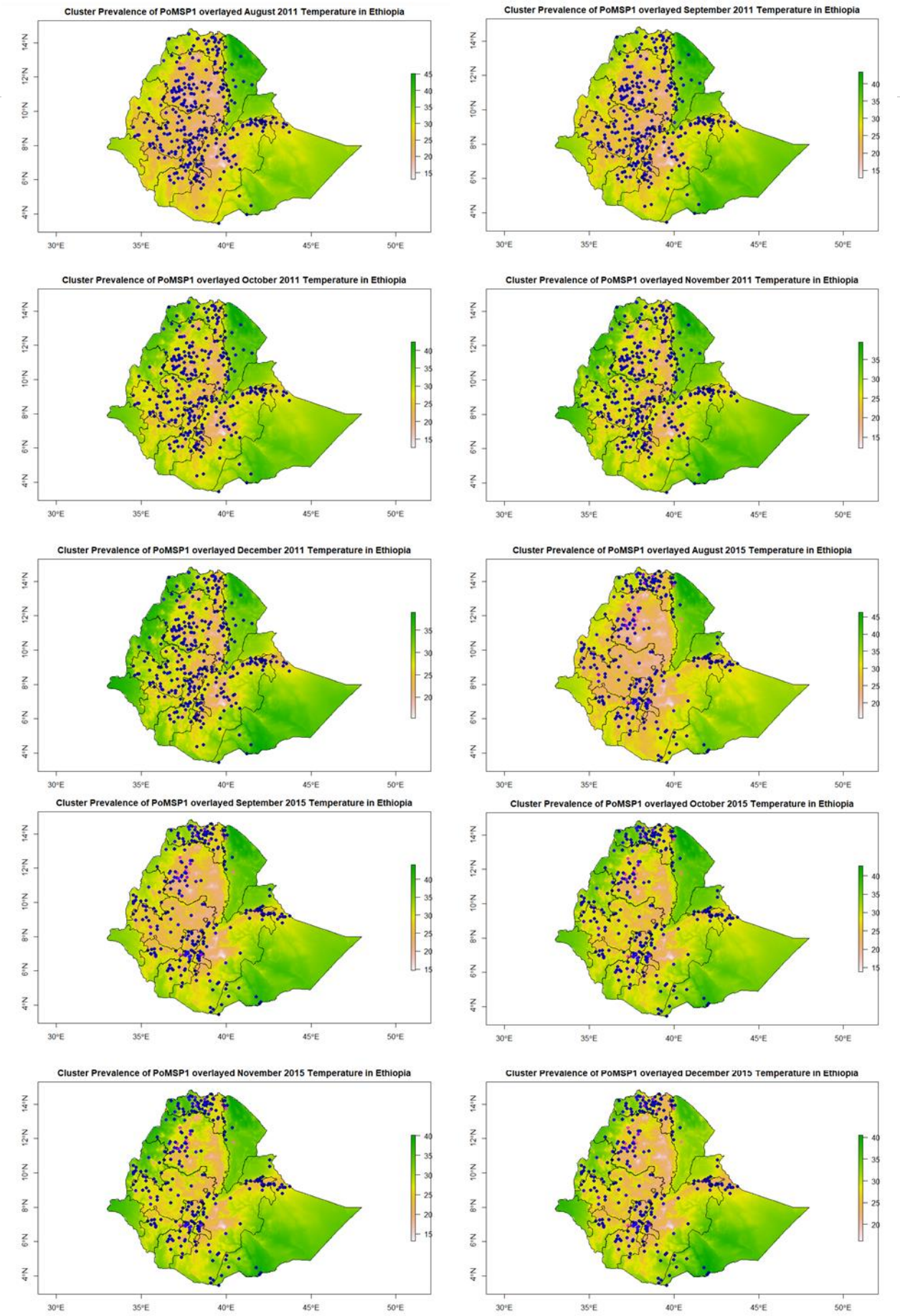

Figure 37: Cluster prevalence of *P. ovale* merozoite protein 1 in 2011 and 2015 overlayed with the monthly average temperatures from August to December

It was challenging to visually observe an association between the cluster prevalence results from the various antigen tests and the climate indicators—temperature and rainfall. Therefore, the next analyses focused on mathematical modeling of the data to determine if there was an association between these climate change factors and the malaria prevalence in Ethiopia. There was no significant result from the model when including an interaction term between the rainfall and temperature variables; the following model was used to examine the relation between climate and demographic predictor variables and the various malaria outcomes (diagnostic antigen test results).

Log-Binomial Regression Model:

$$\ln(\text{cluster prevalence ratio of antigen*}) = \alpha + \beta 1\text{Temperature} + \beta 2\text{Rainfall} + \gamma 1\text{ClusterAverageAge} + \gamma 2\text{ClusterAverageBedNetsUsed} + \gamma 3\text{Region}$$

*Specific Antigen Name

The gold standard for malaria detection is microscopy; however, since the data collected from the MIS were only antigen test results the model will focus solely on the one antigen test that was used for all four species of *Plasmodium* for consistency of the results. The antigen test, merozoite protein 1, was used to detect *Plasmodium falciparum*, *P. vivax*, *P. ovale*, and *P. malariae*. It was not logical to test all seven antigen tests for *P. falciparum* because research is still being conducted to determine which antigen test is the most effective at correctly identifying malaria infections.

Analytical Modeling Results: The results from the model (Table 18) indicate that there was no association between the cluster prevalence ratio and the amount of rainfall from August through December after controlling for the average cluster age, average number of bed nets used in the clusters, and region within Ethiopia, for 2011 or 2015. However, temperature was associated with higher prevalence ratios for three of the four antigen tests in 2011 and one of the antigen tests (PfMSP1) in 2015. In 2011, for the *P. falciparum* merozoite protein 1 antigen test, there was an increased risk of positive malaria results at

higher temperatures for all five months tested (August through December). The prevalence ratio of positive PfMSP1 antigen tests indicates that for every one-degree Celsius increase in temperature, the proportion of individuals testing positive for the PfMSP1 antigen test was 1.22 (1.11-1.35) times greater after controlling for the average cluster age, the average number of bed nets used in the clusters, and the region. The same statistically significant association between temperature and prevalence ratios for the PfMSP1 antigen test was observed in September through December, with the risk increasing from 1.24 to 1.30 after controlling for the average cluster age, the average number of bed nets used in the clusters, and the region. During August through September, a one-degree Celsius increase in temperature was associated with an increased risk of testing positive for the *P. vivax* merozoite protein 1; however, the results were only statistically significant in November and December. During those two months, the model indicated that for every one-degree Celsius increase in temperature, the proportion of individuals who tested positive for the PvMSP1 antigen test was 1.12 (1.00-1.25) and 1.13 (1.01-1.26) times greater after controlling for the average cluster age, the average number of bed nets used in the clusters, and the region. The association between temperature and increased risk of malaria was only statistically significant for the last three months in 2011, October, November, and December, for the *P. malariae* merozoite protein 1 antigen test. Again, there was an increased risk of having a positive PmMSP1 antigen test (an increased prevalence ratio) when there was an increase in the atmospheric temperature. For every one-degree Celsius increase in temperature, the proportion of individuals who tested positive for the PmMSP1 antigen test ranged between 1.17 to 1.19 times greater during these three months, after controlling for the average cluster age, the average number of bed nets used in the clusters, and the region. There was no association between temperature in 2011 and the results from the *P. ovale* merozoite protein 1 antigen test.

In 2015, there was a significant association between temperature and the prevalence ratio for one antigen test. This association was seen in all five months, August through December, of 2015 with the PfMSP1 antigen test. The association showed that with every one-degree Celsius increase in temperature, the

proportion of individuals who tested positive results for the PfMSP1 antigen test was between 1.17 to 1.19 times greater after controlling for the average cluster age, the average number of bed nets used in the clusters, and the region. A similar pattern of increased risk of malaria associated with higher temperature was observed for individuals who had results for the PvMSP1, PmMSP1, and PoMSP1 antigen tests was also seen in the five months in 2015, but this association was not statistically significant after controlling for the average cluster age, the average number of bed nets used in the clusters, and the region.

2011		
PfMSP1	Rainfall	Temperature
August	1.00 (1.00-1.01)	1.22 (1.11-1.35)
September	1.00 (1.00-1.01)	1.24 (1.12-1.38)
October	1.00 (1.00-1.01)	1.26 (1.14-1.39)
November	1.00 (1.00-1.01)	1.30 (1.16-1.45)
December	0.98 (0.94-1.03)	1.29 (1.15-1.44)
PvMSP1	Rainfall	Temperature
August	1.00 (1.00-1.01)	1.06 (0.95-1.17)
September	1.00 (1.00-1.01)	1.07 (0.97-1.19)
October	1.00 (1.00-1.01)	1.10 (1.00-1.22)
November	1.00 (1.00-1.01)	1.12 (1.00-1.25)
December	0.98 (0.93-1.03)	1.13 (1.01-1.26)
PmMPS1	Rainfall	Temperature
August	1.00 (0.99-1.01)	1.16 (0.99-1.36)
September	1.00 (0.99-1.01)	1.15 (0.98-1.36)
October	1.00 (0.99-1.01)	1.17 (1.01-1.36)
November	1.00 (0.99-1.01)	1.19 (1.01-1.42)
December	0.96 (0.86-1.08)	1.19 (1.00-1.41)
PoMSP1	Rainfall	Temperature
August	1.00 (0.99-1.01)	1.10 (0.90-1.34)
September	1.00 (0.99-1.01)	1.11 (0.89-1.40)
October	1.00 (0.99-1.02)	1.17 (0.96-1.42)
November	1.00 (0.99-1.01)	1.17 (0.93-1.47)
December	0.98 (0.87-1.10)	1.19 (0.95-1.50)

2015		
PfMSP1	Rainfall	Temperature
August	1.00 (1.00-1.00)	1.18 (1.03-1.36)
September	1.00 (1.00-1.00)	1.19 (1.04-1.36)
October	1.00 (0.99-1.01)	1.19 (1.05-1.35)
November	1.00 (0.99-1.01)	1.17 (1.03-1.32)
December	0.99 (0.97-1.01)	1.18 (1.03-1.34)
PvMSP1	Rainfall	Temperature
August	1.00 (0.99-1.00)	1.10 (0.94-1.28)
September	1.00 (1.00-1.00)	1.09 (0.94-1.27)
October	1.00 (0.99-1.01)	1.10 (0.96-1.27)
November	1.00 (0.99-1.01)	1.10 (0.96-1.26)
December	0.99 (0.97-1.01)	1.10 (0.94-1.28)
PmMPS1	Rainfall	Temperature
August	1.00 (0.99-1.00)	1.10 (0.88-1.37)
September	1.00 (0.99-1.00)	1.10 (0.90-1.35)
October	1.00 (0.99-1.01)	1.08 (0.88-1.32)
November	1.00 (0.99-1.01)	1.05 (0.86-1.30)
December	1.00 (0.98-1.03)	1.07 (0.85-1.34)
PoMSP1	Rainfall	Temperature
August	1.00 (0.99-1.02)	1.13 (0.83-1.54)
September	1.00 (0.99-1.01)	1.11 (0.83-1.50)
October	1.00 (0.99-1.02)	1.12 (0.84-1.50)
November	1.00 (0.97-1.03)	1.10 (0.83-1.47)
December	1.00 (0.95-1.06)	1.11 (0.80-1.54)

Table 18: Risk-Ratio Results of the Log-Binomial Regression Model, indicating that with every one-millimeter increase in rainfall or with every one-degree increase in temperature, the proportion of individuals who tested positive for a specific antigen test* was X times greater during the month and year, after controlling for the average cluster age and the average number of bed nets used in the

Discussion

To briefly refocus on the purpose of this research and the original objectives we hoped to achieve:

> Objective 1: Examine if climate change is occurring in Ethiopia by comparing decadal patterns of rainfall and temperature from 1981 to 2019 using open-source datasets.
>
> Objective 2: Describe changes in rainfall, temperature, and malaria prevalence (as measured by antigen detection tests) between 2011 and 2015.
>
> Objective 3: Examine the association between rainfall changes and temperature changes and the prevalence of positive malaria antigen tests in 2011 and 2015.

Objective 1: Climate Change Exposure #1: Rainfall

1981 to 2019 Long-term Rainfall Observations: The decadal rainfall patterns in each region supported that even with typical fluctuation of rainfall over the years, the longer, decadal pattern of the regions revealed an inconsistent pattern in the rainfall data –most likely contributed by global warming. Without global warming, a more uniform decadal rainfall pattern in each region would be observed. Climate change, in terms of rainfall, was observed in Ethiopia during the period between 1981 to 2019. The differences in the average maximum and average minimum total yearly rainfall measurements for each of the nine tested regions in Ethiopia resulted in statistically significant differences between those values. These results are consistent with our hypothesis that climate change, in terms of rainfall patterns, is occurring in Ethiopia. The variability in rainfall patterns, whether increasing or decreasing rainfall, depending on the region of Ethiopia, indicates an inconsistency in rainfall patterns which could influence the development and growth of the *Anopheles* vector. Observing the decadal patterns of rainfall during the period indicated strong variability in the rainfall patterns in the nine regions. These long-term rainfall

patterns are consistent with other reports[162],[163],[164],[165], which also observed increasing variability of rainfall in different countries around the globe. The inconsistencies surrounding rainfall patterns, currently and in the future, pose a problem when trying to model the burden of malaria and other vector-borne diseases. Uncertainty about whether rainfall will increase or decrease in certain regions, and about the current regional baseline of rainfall, must be taken into consideration when determining the influence of rainfall on malaria or other vector-borne diseases. The difference between an increase in rainfall in a region with low precipitation compared to a region with high precipitation can drastically impact the development and growth of pathogens and vectors[166],[167],[168].

Objective 1: Climate Change Exposure #2: Temperature

1981 to 2019 Long-term Temperature Observations: Similarly, evidence of climate change, in terms of temperature, was also observed in Ethiopia during the period between 1981 to 2019. The linear lines of best fit indicated a correlation between increasing temperatures as the years. Additionally, the differences in the average maximum and average minimum yearly temperature measurements for each of the nine tested regions in Ethiopia resulted in statistically significant differences between those values. This is consistent with our hypothesis that climate change, in terms of temperature, is also occurring in Ethiopia. This increase in temperature in the country is a cause for concern as many pathogens, like *Plasmodium*, may develop or multiply more rapidly at higher temperatures. However, as temperatures continue to

[162] Portela, Maria Manuela, et al. "Long-Term Rainfall Trends and Their Variability in Mainland Portugal in the Last 106 Years." *Climate*, vol. 8, no. 12, 2020, p. 146., https://doi.org/10.3390/cli8120146.
[163] Gebrechorkos, S.H., Hülsmann, S. & Bernhofer, C. Long-term trends in rainfall and temperature using high-resolution climate datasets in East Africa. *Sci Rep* **9,** 11376 (2019). https://doi.org/10.1038/s41598-019-47933-
[164] Alves, Lincoln M., et al. "Assessment of Rainfall Variability and Future Change in Brazil across Multiple Timescales." *International Journal of Climatology*, vol. 41, no. S1, 2020, https://doi.org/10.1002/joc.6818.
[165] Mainuddin, Mohammed, et al. "Long-Term Spatio-Temporal Variability and Trends in Rainfall and Temperature Extremes and Their Potential Risk to Rice Production in Bangladesh." *PLOS Climate*, vol. 1, no. 3, 2022, https://doi.org/10.1371/journal.pclm.0000009.
[166] Wang, Huijun, et al. "Predicting Climate Anomalies: A Real Challenge." *Atmospheric and Oceanic Science Letters*, vol. 15, no. 1, 2022, p. 100115., https://doi.org/10.1016/j.aosl.2021.100115.
[167] Deaton, Jeremy. "Climate Change Could Make Weather Harder to Predict." *The Washington Post*, WP Company, 25 Jan. 2022, https://www.washingtonpost.com/weather/2022/01/25/climate-change-weather-unpredictable/.
[168] "Climate Changes Make Some Aspects of Weather Forecasting Increasingly Difficult." *ScienceDaily*, ScienceDaily, 22 Mar. 2019, https://www.sciencedaily.com/releases/2019/03/190322105718.htm.

climb as a result of climate change, it is also important to consider the optimal temperatures for the vector also. Typically, *Anopheles* mosquitoes cannot perform very well at higher temperatures (90-100° C) depending on the species and other climatic factors—precipitation and humidity. Although increasing temperature conditions might be favorable for the pathogen, the vector may not thrive under the same conditions. The contrasting outcome of temperature increases causes more uncertainty about the direction the burden of malaria, and other vector-borne diseases will progress. Long-term temperature increases as a result of climate change are well documented by multiple climate-change organizations and research[169], [170], [171], [172], [173], [174]. Furthermore, other research has already recorded the shift of mosquito-borne diseases into temperate regions, significantly expanding their global distributions[175],[176],[177],[178]. Temperature is one of the most significant abiotic factors affecting both the vectors and the range of pathogens they transmit in many ways. With great variance depending on vector species, populations, and pathogen strains, temperature influences vector survival, vector population growth, distribution and genetic structure, host contact and feeding behavior, virus susceptibility, extrinsic incubation period, virus structure, and replication[179].

---

[169] Dahlman, Rebecca Lindsey and LuAnn. "Climate Change: Global Temperature." *Climate Change: Global Temperature | NOAA Climate.gov*, https://www.climate.gov/news-features/understanding-climate/climate-change-global-temperature#:~:text=According%20to%20NOAA's%202020%20Annual,more%20than%20twice%20that%20rate.

[170] "What Are the Long-Term Effects of Climate Change?" *What Are the Long-Term Effects of Climate Change? | U.S. Geological Survey*, https://www.usgs.gov/faqs/what-are-long-term-effects-climate-change.

[171] "Climate Change Indicators: Weather and Climate." *EPA*, Environmental Protection Agency, https://www.epa.gov/climate-indicators/weather-climate.

[172] Thompson, Lonnie G. "Climate change: the evidence and our options." *The Behavior analyst* vol. 33,2 (2010): 153-70. doi:10.1007/BF03392211

[173] Lyon, Christopher, et al. "Climate Change Research and Action Must Look beyond 2100." *Global Change Biology*, vol. 28, no. 2, 2021, pp. 349–361., https://doi.org/10.1111/gcb.15871.

[174] Zickfeld, Kirsten, et al. "Long-Term Climate Change Commitment and Reversibility: An Emic Intercomparison." *Journal of Climate*, vol. 26, no. 16, 2013, pp. 5782–5809., https://doi.org/10.1175/jcli-d-12-00584.1.

[175] Bellone, Rachel, and Anna-Bella Failloux. "The Role of Temperature in Shaping Mosquito-Borne Viruses Transmission." *Frontiers in Microbiology*, vol. 11, 2020, https://doi.org/10.3389/fmicb.2020.584846.

[176] Fouque, Florence, and John C. Reeder. "Impact of Past and on-Going Changes on Climate and Weather on Vector-Borne Diseases Transmission: A Look at the Evidence." *Infectious Diseases of Poverty*, vol. 8, no. 1, 2019, https://doi.org/10.1186/s40249-019-0565-1.

[177] Brand, Samuel P C, and Matt J Keeling. "The impact of temperature changes on vector-borne disease transmission: *Culicoides* midges and bluetongue virus." *Journal of the Royal Society, Interface* vol. 14,128 (2017): 20160481. doi:10.1098/rsif.2016.0481

[178] Rohr, Jason R., and Jeremy M. Cohen. "Understanding How Temperature Shifts Could Impact Infectious Disease." *PLOS Biology*, vol. 18, no. 11, 2020, https://doi.org/10.1371/journal.pbio.3000938.

[179] Agarwal, A., Parida, M., and Dash, P. K. (2017). Impact of transmission cycles and vector competence on global expansion and emergence of arboviruses. *Rev. Med. Virol.* doi: 10.1002/rmv.1941 [Epub ahead of print].

Objective 2: Climate Change Exposure #1: Rainfall

2011 and 2015 Short-term Rainfall Observations: The yearly average rainfall in 2011 and 2015 by region (Figure 8) illustrated a consistent short-term decline in rainfall in most of the regions in Ethiopia. Although these declines in rainfall amounts between 2011 and 2015 were not statistically significant at the regional level, they still demonstrate the impact and consistency of climate change on rainfall patterns in Ethiopia. In most of the regions, too, this decline in rainfall, when stratified by the rainfall seasons, was seen during Kiremt (June through September). The statistical analysis for the short-term influence of climate change between 2011 and 2015 revealed a statistically significant difference in the total average yearly rainfall in 2011 compared to 2015 at the country level for Ethiopia. The individual regional-level analyses did not reveal any statistically significant differences in rainfall between the two years. This is possibly due to the smaller sample size at the regional level compared to the large sample size at the country level. Perhaps a larger sample size for some of the regions would have provided a statistically significant difference in the total yearly average rainfall amounts between 2011 and 2015. Analyses of seasonal rainfall indicated significant differences between 2011 and 2015 occurred from June through September, during the Kiremt season, in some regions. The results showed that both Oromiya and SNNPR had statistically significant differences in the total average rainfall from June through September between 2011 and 2015. This suggests that this variability of rainfall due to climate change may not occur year-round but during certain rainfall seasons.

A global analysis of seasonal hydroclimatic regimes supports the finding that climate change will affect precipitation through seasonal changes, rather than a consistent rainfall change year-round[180],[181]. If rainfall patterns are influenced by seasonal climate change effects, then we can expect to see changes in malaria prevalence based on a seasonal pattern. The seasonal changes in rainfall, though, will not be

[180] Konapala, Goutam, et al. "Climate Change Will Affect Global Water Availability through Compounding Changes in Seasonal Precipitation and Evaporation." *Nature Communications*, vol. 11, no. 1, 2020, https://doi.org/10.1038/s41467-020-16757-w.
[181] "Altered Precipitation." *Conservation in a Changing Climate*, 20 Sept. 2015, https://climatechange.lta.org/climate-impacts/changing-water-regimes/altered-precipitation/.

directly related to malaria prevalence during that season, as the reasonable lag time between rainfall and malarial prevalence is two months, with climate factors preceding malaria outcomes[182]. This is rational when considering the time required for the life cycles of the mosquito[183] and parasite[184], and the timing between the date of malarial diagnosis and the date of entry into the system[185]. However, there have been reports of lags greater than two months[186],[187],[188].

Objective 2: Climate Change Exposure #2: Temperature

2011 and 2015 Short-term Temperature Observations: The yearly average temperature in 2011 and 2015 by region (Figure 10) illustrated a consistent short-term increase in temperature in every region in Ethiopia. While, these increases in temperature between 2011 and 2015 were not statistically significant at the regional level, they still demonstrate the impact and consistency of climate change on temperature patterns in Ethiopia. In most of the regions, increased temperature, when stratified by the rainfall seasons, was seen during Belg (February through May). In combination with the stratified rainfall patterns, this trend is reasonable. The temperature increase that was seen in most regions in Ethiopia happened right before there was a decline in rainfall. It is logical that the increased temperatures impacted the rate of evaporation, leading to less precipitation with a lagged effect[189]. When temperature increases, there is a decrease in relative humidity, which results in lower rainfall[190]. The statistical analysis for the short-term

[182] Ikeda, Takayoshi, et al. "Seasonally Lagged Effects of Climatic Factors on Malaria Incidence in South Africa." *Scientific Reports*, vol. 7, no. 1, 2017, https://doi.org/10.1038/s41598-017-02680-6.
[183] Lyons, C. L., Coetzee, M. & Chown, S. L. Stable and fluctuating temperature effects on the development rate and survival of two malaria vectors. *Anopheles arabiensis and Anopheles funestus, Parasites & Vectors* **6**, 1–9 (2013).
[184] Saenz, F. E., Balu, B., Smith, J., Mendonca, S. R. & Adams, J. H. The Transmembrane Isoform of *Plasmodium falciparum* MAEBL Is Essential for the Invasion of *Anopheles* Salivary Glands. *PLoS One* **3**, e2287 (2008).
[185] Gerritsen, Aa. M., Kruger, P., van der Loeff, M. F. S. & Grobusch, M. P. Malaria incidence in Limpopo Province, South Africa, 1998–2007. *Malar. J.* **7**, 162 (2008).
[186] Hashizume, M., Terao, T. & Minakawa, N. The Indian Ocean Dipole and malaria risk in the highlands of western Kenya. *Proc. Natl. Acad. Sci. USA* **106**, 1857–1862 (2009).
[187] Klutse, A. N. B., Aboagye-antwi, F., Owusu, K. & Ntiamoa-baidu, Y. Assessment of Patterns of Climate Variables and Malaria Cases in Two Ecological Zones of Ghana. *Open J. Ecol.* **4**, 764–775 (2014).
[188] Sena, L., Deressa, W. & Ali, A. Correlation of Climate Variability and Malaria: A Retrospective Comparative Study, Southwest Ethiopia. *Ethiop. J. Health Sci.* **25**, 129–38 (2015).
[189] "What Climate Models Tell Us About Future Rainfall." *Carbon Brief*, 18 Jan. 2018, https://www.carbonbrief.org/explainer-what-climate-models-tell-us-about-future-rainfall#:~:text=Temperatures%20also%20impact%20the%20rate,offset%20by%20temperature%2Ddriven%20drying.
[190] Panthou, Gérémy, et al. "Relationship between Surface Temperature and Extreme Rainfalls: A Multi-Time-Scale and Event-Based Analysis*." *Journal of Hydrometeorology*, vol. 15, no. 5, 2014, pp. 1999–2011., https://doi.org/10.1175/jhm-d-14-0020.1.

influence of climate change between 2011 and 2015 revealed a statistically significant difference in the average yearly temperature in 2011 compared to 2015 at the country level for Ethiopia. The individual regional level did not reveal any statistically significant differences in rainfall between the two years. This is possibly due to the smaller sample size provided at the individual level as compared to the large sample size at the country level. Perhaps a larger sample size in some of the regions would have provided a statistically significant difference in the yearly average rainfall amounts between 2011 and 2015.

Since the differences in temperature between 2011 and 2015 occurred from February through May (the rainfall season, Belg), the regions were analyzed again, but solely focusing on these months. However, the results still showed no statistically significant associations between the differences in the average temperature during February through May between 2011 and 2015. This suggests that a difference of four years is probably too short to detect significant temperature changes at such a detailed geographic scale.

On a broader level, statistically, significant differences were still seen at the country level. This supports previous research that has shown increases in temperature are becoming larger over time. In various studies, temperatures between 1900-1950 increased at a rate of 0.2° F per decade. However, between 1950-2015, temperatures increased at a rate of 0.5° F per decade[191]. This indicates that not only are temperatures increasing, but they are also increasing at an even faster rate than in the past. The progressively faster increases in temperature only accelerate any potentially negative consequence of increasing temperatures on the transmission of vector-borne diseases. Global warming is most likely to disturb the delicate equilibrium of current vector-borne diseases and contribute to new epidemics, such as malaria[192]. Research concerning the *Aedes* mosquito, which is responsible for Dengue, Zika, and Yellow

[191] "Climate and Health - Minnesota Dept. of Health." *Climate and Health - Minnesota Dept. of Health*, https://www.health.state.mn.us/communities/environment/climate/.
[192] Brower, V. "Vector-borne diseases and global warming: are both on an upward swing? Scientists are still debating whether global warming will lead to a further spread of mosquitoes and the diseases they transmit." *EMBO reports* vol. 2,9 (2001): 755-7. doi:10.1093/embo-reports/kve193

Fever, suggests that the mosquito is only shifting its geographical range, not expanding. This is an improved outcome; yet, there are still public health concerns about this shift[193],[194].

Objective 2: Malaria Antigen Diagnostic Test Outcomes

Comparing 2011 and 2015 Malaria Prevalence by Antigen Diagnostic Test: Between 2011 and 2015, the entire country of Ethiopia experienced an increase in the proportion of positive *Plasmodium* antigen tests for all 12 antigens. This indicates that, at the country level, malaria prevalence increased between 2011 and 2015. However, different trends were observed on the regional level. The statistically significant differences between 2011 and 2015 in Afar were all a result of declining proportions of positive antigen tests. Yet, in Amhara, differences between 2011 and 2015 were because of an increase in the proportion of positive tests for all 12 antigens. The only statistically significant difference in Benishangul Gumuz was with the PfMSP1 antigen which reduced its proportion of positive antigen tests between 2011 and 2015. Similarly, Dire Dawa had a statistically significant change in the results for only one antigen diagnostic test (chPvMSP1) which decreased from 26% to 9% positive results. 11 of the 12 antigen tests in Oromiya had statistically significantly increases in the proportions of positive results between 2011 and 2015. The majority (10) of antigens in SNNPR also had a statistically significant increase in the proportions of positive test results; only the positive results for the PoMSP1 antigen test declined, though not statistically significant. In Somali, there were significantly fewer positive results for all 12 antigen tests. Lastly, in Tigray, only the results from the PmMSP1 antigen tests were statistically significantly different, with fewer positive results; most of the other antigen test results remained at the same proportion between 2011 and 2015.

[193] "Climate Risk and Spread of Vector-Borne Diseases." *Climate Nexus*, 28 Oct. 2019, https://climatenexus.org/climate-issues/health/climate-change-and-vector-borne-diseases/.
[194] "Climate Change Is Accelerating Vector-Borne Diseases." *NACCHO*, https://www.naccho.org/blog/articles/climate-change-is-accelerating-vector-borne-diseases.

Objective 3: Associations of Climate Change with Prevalence of Positive Malaria Antigen Tests

Geographic Comparisons of Climate Change: Rainfall and Temperature: From the geographic comparison of the nine regions with the 12 different antigen tests the rainfall climatic factor illustrated a stronger correlation with the proportion of positive antigen test results during Kiremt as compared to Bega. Since the MIS blood samples were collected during Bega, this result demonstrates that the rainfall patterns prior to the collection were more significantly associated with the prevalence of malaria than the rainfall patterns during the time of sample collection. There was a lag effect of rainfall on the prevalence of malaria in Ethiopia. This lag effect of rainfall was seen in every region analyzed in Ethiopia.

The geographic comparison of the 12 different antigen tests and temperature across the nine regions demonstrated a stronger correlation with the proportion of positive antigen test results during Bega as compared to Kiremt. This is the opposite of what was observed for the rainfall trends. Since the MIS blood samples were collected during Bega, this result demonstrates that the temperature patterns during the time of sample collection were more significantly associated with the prevalence of malaria than the temperature patterns prior to collection. There is a direct effect of temperature on malaria prevalence, as compared to a lag effect observed for rainfall in Ethiopia. This pattern was seen in each region in Ethiopia included in the analysis. Since the *Anopheles* vector develops prior to being infected with the pathogen, the impact of rainfall should have a lag effect, which gives the *Anopheles* vector time to lay its eggs and develop. Water is a critical environmental factor for laying eggs and the development of the larvae[195],[196]. After the mosquitoes are fully developed, temperature becomes the more important climatic factor for the development and replication of *Plasmodium* inside the vector[197],[198]. Thus, our observations of the stronger

[195] Akpodiete, Nwamaka O., et al. "Effect of Water Source and Feed Regime on Development and Phenotypic Quality in Anopheles Gambiae (S.l.): Prospects for Improved Mass-Rearing Techniques towards Release Programmes." *Parasites & Vectors*, vol. 12, no. 1, 2019, https://doi.org/10.1186/s13071-019-3465-0.
[196] *Weather, Water and Malaria Mosquito Larvae - Wur*. Meteorology and Air Quality Group, https://edepot.wur.nl/4348.
[197] Bi, Yan, et al. "Impact of Climate Variability on Plasmodium Vivax and Plasmodium Falciparum Malaria in Yunnan Province, China." *Parasites & Vectors*, vol. 6, no. 1, 2013, https://doi.org/10.1186/1756-3305-6-357.
[198] Noden, B H et al. "The impact of variations in temperature on early Plasmodium falciparum development in Anopheles stephensi." *Parasitology* vol. 111 (Pt 5) (1995): 539-45. doi:10.1017/s0031182000077003

correlation with rainfall during the time prior to malaria diagnostic testing and the stronger correlation with temperature during the time period of the diagnostic testing are consistent with the biological factors that affect the development of the vector and pathogen.

Log-Binomial Regression Model: When examining the cluster prevalence of each antigen test result in August through December of 2011 and 2015 overlayed with the rainfall and temperature distributions, it was difficult to observe any statistically significant associations between the climatic factors and the prevalence of malaria detected with the various antigen tests. Thus, the log-binomial regression model was beneficial to test these associations. From the statistical analysis with the log-binomial regression model, there was no significant interaction between rainfall and the cluster prevalence ratios for the PfMSP1, PvMSP1, PoMSP1, or PmMSP1 antigen tests. While we expected to see an association between rainfall and the prevalence ratios of these antigen tests, based on the importance of water for *Anopheles* development, it is possible that the decreases in rainfall in areas with 100+ mm of rainfall each year created more stable breeding grounds for the mosquitoes and increased the positive cluster prevalence ratios (less chance of flooding and washing away of the breeding sites with less water). However, in other areas where rainfall was only <30 mm each year, the decreased rainfall resulted in droughts in the areas which were not suitable for mosquitoes to breed, thus, decreasing the positive cluster prevalence ratios. The net change, then, in mosquito prevalence and positive antigen test results was zero and resulted in a null association between the exposure variable and the expected outcome.

In future research, we should improve upon the stratification of these geographic locations to account for the differences in annual rainfall across the country. Perhaps then it would be possible to observe a protective influence of rainfall against malaria infections in certain areas and harmful influences in other areas as climate change affects the geographic distribution of malaria. As climate change continues, some locations will experience increases in rainfall and others a decrease. It is essential though to consider these rainfall changes in the context of the baseline rainfall amounts to understand what the effects of

changes in rainfall are likely to be in various regions and how these effects may support or limit breeding sites of mosquitoes and other insect vectors.

For the statistical analysis with the log-binomial regression model, there were statistically significant associations between temperature and the cluster prevalence ratios of PfMSP1, PvMSP1, and PoMSP1 in 2011. Yet, in 2015 there were only statistically significant associations between temperature and the cluster prevalence ratios of PfMSP1. We expected to see a harmful impact of temperature on the risk of malaria and this was observed for the prevalence ratios for some of the antigen tests in 2011. Though, in 2015, we were unsure whether there would be an increase in those prevalence ratios due to the favorable conditions for *Plasmodium*, or a decrease in the prevalence, as the increase in temperature in 2015 could have been harmful to *Anopheles*.

In 2015, the temperature was still statistically significant associated with the cluster prevalence ratios for the PfMSP1 antigen test. However, the prevalence ratios were slightly reduced as compared to the prevalence ratios seen in 2011. This small decline in the 2015 prevalence ratios could indicate the start of a negative impact of temperature on the ability of *Anopheles* to transmit malaria. Similarly, it is possible that the lack of association seen in 2015 with PvMSP1 and PmMSP1 antigen tests was the result of the temperature increasing above the optimal range of the mosquitoes. Unlike the *Plasmodium* species that develop better in hotter temperatures, the mosquito vector is negatively influenced by increasing temperatures. If the small temperature increases between 2011 and 2015 forced *Anopheles* out of their optimal temperature range, this could explain the prevalence ratios not being statistically significant. The results from the PoMSP1 antigen test were not statistically significantly associated with rainfall or temperature in 2011 or 2015, and this is most likely due to this *Plasmodium* species not being largely present in Ethiopia. *P. falciparum* is the most common species in Ethiopia, and *P. ovale* is much rarer. The smaller proportions of positive antigen tests for this species could have masked any association between rainfall and temperature that might be present.

Strengths and Limitations

This research on the influence of climatic factors—rainfall and temperature—on the cluster prevalence of malaria antigen tests has many strengths, including the data collection and the descriptive and analytical approaches used to examine the data. First, the MIS data collected at the household level was done through a randomization process which increased the diversity of the sample population. This was done in both 2011 and 2015 for the collection process. Additionally, the data collected came from a wide representation of the geographic topography in Ethiopia—from nine different regions in Ethiopia. Similarly, these MIS datasets were rich databases to analyze because they collected data on multiple antigen diagnostic tests for four species of *Plasmodium.* From this, we were able to explore the more common species responsible for malaria in Ethiopia (*P. falciparum* and *P. vivax*) as compared to the less common species (*P. ovale* and *P. malariae*). The rainfall and temperature data were reported on a monthly level which increased the granularity of those measurements as compared to yearly collection levels.

However, this paper is not without its limitations, there was room for improvement in the available data and the analysis of the research. Primarily, this data did not include microscopy results from the blood samples for malaria. Microscopy is the gold standard method for diagnosing malaria; without having the gold standard results, we were limited in understanding the accuracy of the antigen diagnostic tests. Additionally, the original datasets only had limited contextual information on the study participants and communities that could be included as confounding variables in the analysis. Many other factors like humidity, wind, insecticide use, nearby bodies of water, rice cultivation, days with rain, extreme precipitation events, and minimum and maximum daily temperatures, should have been controlled for in the model, but unfortunately, this data was not available. While the original research objectives were modified to explore spatial differences in rainfall and temperature across the geographic locations as well as compare differences between 2011 and 2015, our examination of climate change effects were limited by the relatively short four-year difference between rounds of blood sample collection and changes in

climate due to climate change. Climate change is more noticeable at the decadal scale rather than individual years, and therefore limited our ability to examine the effects of climate change on the prevalence of malaria in Ethiopia. Furthermore, our exploration of climate change was limited to rainfall and temperature patterns. Other factors, such as humidity, wind, and UV exposure, should be explored in future research to account for other climatic factors that will be impacted by climate change and can influence the prevalence of *Anopheles* and malaria.

Conclusions

Although the results of this research did not show obvious impacts of climate change on malaria prevalence, especially at a regional level, continued research in this field is imperative to understand the burden of malaria in the future. The results of this paper showed an initial association of temperature with the prevalence of malaria in Ethiopia, which is consistent with other research[199],[200],[201] showing that temperature will play a crucial role in the burden of malaria. Temperatures around the globe are increasing due to global warming, this can lead to an increased burden of malaria in certain regions through the re-emergence of malaria or a completely new emergence of the disease. Though, other regions might experience a reduction in malaria prevalence as the temperatures move out of the optimal range of mosquito survival[202]. It is imperative to continue understanding the path of climate change and how temperatures around the globe will increase and, thus, how that affects the burden of malaria. On an even larger scale, climate change will not only affect malaria but many other vector-borne diseases. Similar research is needed for other pathogens, vectors, and climatic factors to understand likely trends in the burden of diseases as a result of climate change. The same can be said of rainfall patterns. Our

[199] Mordecai, Erin A et al. "Optimal temperature for malaria transmission is dramatically lower than previously predicted." *Ecology letter*s vol. 16,1 (2013): 22-30. doi:10.1111/ele.12015
[200] Lunde, Torleif Markussen, et al. "How Malaria Models Relate Temperature to Malaria Transmission." *Parasites & Vectors*, vol. 6, no. 1, 2013, https://doi.org/10.1186/1756-3305-6-20.
[201] Patz, Jonathan A., and Sarah H. Olson. "Malaria Risk and Temperature: Influences from Global Climate Change and Local Land Use Practices." *Proceedings of the National Academy of Sciences*, vol. 103, no. 15, 2006, pp. 5635–5636., https://doi.org/10.1073/pnas.0601493103.
[202] Mordecai, Erin A et al. "Optimal temperature for malaria transmission is dramatically lower than previously predicted." *Ecology letter*s vol. 16,1 (2013): 22-30. doi:10.1111/ele.12015

analyses did not reveal any associations between malaria prevalence and rainfall but the results from other studies[203],[204],[205],[206] suggest that rainfall patterns can both increase and decrease malaria prevalence. Depending on the variability of rainfall patterns and the current baseline of rainfall measurements, increases in rainfall could increase the breeding grounds of mosquitoes, or with enough rain, possibly wash them away. Similarly, decreases in rainfall could support more stable breeding grounds, or create drought conditions that could not sustain mosquito larvae.

Finally, other climatic factors must be considered in addition to temperature and rainfall, and it is necessary to consider these variables in relation to each other. The combination of multiple changing variables could result in patterns that were not seen with an examination of the independent variables. Likewise, future research on malaria should also be contextualized for other vector-borne diseases[207],[208],[209],[210]. Climate change is a threat to the environment, animal, and human health; any research that can be conducted to assist in our understanding of the future burden of climate change should be done in order to best plan and implement mitigation strategies for vector-borne diseases.

[203] T.H. Jetten, W.J. Martens, W. Takken, "Model stimulations to estimate malaria risk under climate change", Journal of Medical Entomology, 33(3) (1996): p.361-71.
[204] "Climate Change and Malaria - a Complex Relationship." *United Nations*, United Nations, https://www.un.org/en/chronicle/article/climate-change-and-malaria-complex-relationship#:~:text=An%20increase%20in%20temperature%2C%20rainfall,it%20was%20not%20reported%20earlier.
[205] Odongo-Aginya, E et al. "Relationship between malaria infection intensity and rainfall pattern in Entebbe peninsula, Uganda." *African health sciences* vol. 5,3 (2005): 238-45. doi:10.5555/afhs.2005.5.3.238
[206] Emeto, Theophilus I et al. "Disparities in Risks of Malaria Associated with Climatic Variability among Women, Children and Elderly in the Chittagong Hill Tracts of Bangladesh." *International journal of environmental research and public health* vol. 17,24 9469. 17 Dec. 2020, doi:10.3390/ijerph17249469
[207] Tran, Bao-Linh et al. "Estimating the Threshold Effects of Climate on Dengue: A Case Study of Taiwan." *International journal of environmental research and public health* vol. 17,4 1392. 21 Feb. 2020, doi:10.3390/ijerph17041392
[208] Tesla, Blanka et al. "Temperature drives Zika virus transmission: evidence from empirical and mathematical models." *Proceedings. Biological sciences* vol. 285,1884 20180795. 15 Aug. 2018, doi:10.1098/rspb.2018.0795
[209] Brownstein, John S et al. "Effect of Climate Change on Lyme Disease Risk in North America." *EcoHealth* vol. 2,1 (2005): 38-46. doi:10.1007/s10393-004-0139-x
[210] Yang, Guo-Jing, and Robert Bergquist. "Potential Impact of Climate Change on Schistosomiasis: A Global Assessment Attempt." *Tropical medicine and infectious disease* vol. 3,4 117. 3 Nov. 2018, doi:10.3390/tropicalmed3040117

Recommendations

For the Centers for Disease Control Data Collection

- Collection of data on other potential confounding variables
    - Insecticide use
        - Would decrease mosquito populations in certain areas, and decrease transmission
        - Could, over time, allow mosquito populations to increase again due to insecticide-resistance
    - Landscape descriptions
        - Any standing water? Buckets or tires for water collection?
    - Agricultural practices
        - Rice cultivation
            - Attract mosquitoes for breeding, increase the density of mosquito populations
    - Housing information
        - Cracks in dwellings or windows/doors without screens
        - Could allow mosquitoes into the home, increasing exposure to biting and potential transmission

For Future Research with this data

- Utilization of daily temperature measurements
    - Minimum and maximum daily temperatures
- Utilization of daily rainfall measurements
    - Total number of days with rainfall
    - Extreme rainfall events (length)
        - Flooding
        - Drought
- Examination of these climate factors at a subregional level
    - Administrative council data

For Future Research on Climate Change

- Inclusion of other climate variables
    - Humidity, Wind, atmospheric pressure

Appendix A: Average Rainfall--Climate Change

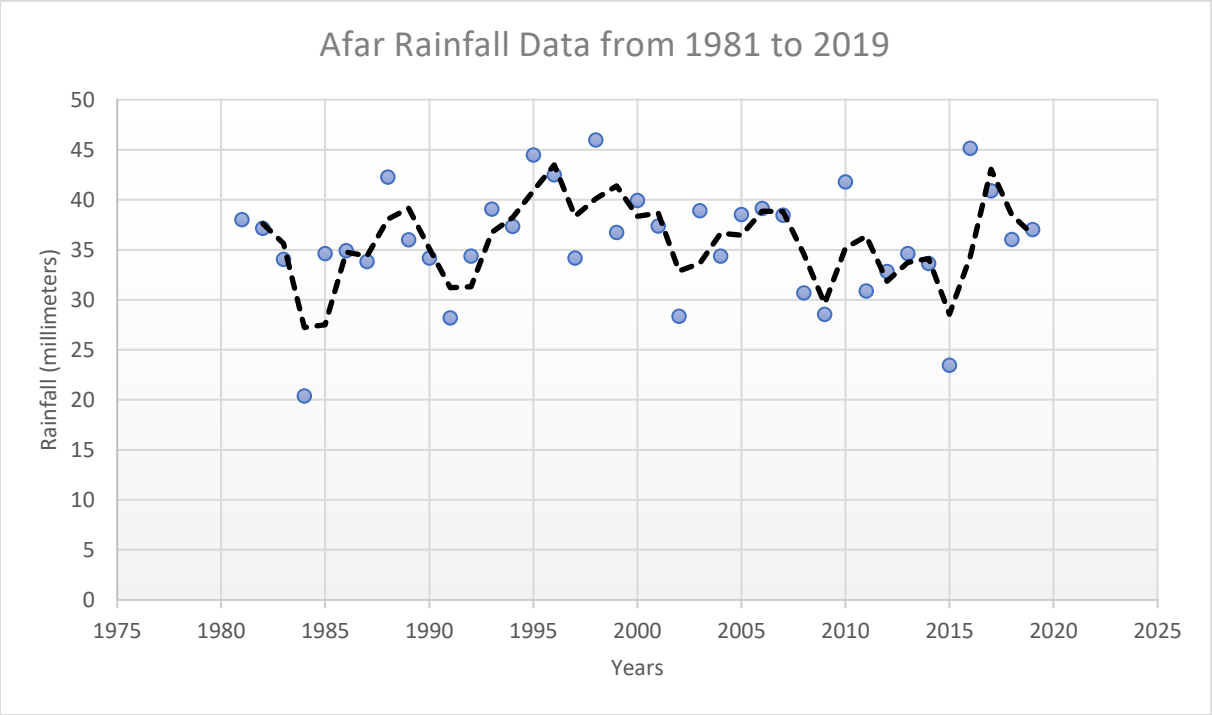

Figure A1.1: Yearly Average Rainfall distribution in Afar, Ethiopia from 1981 to 2019

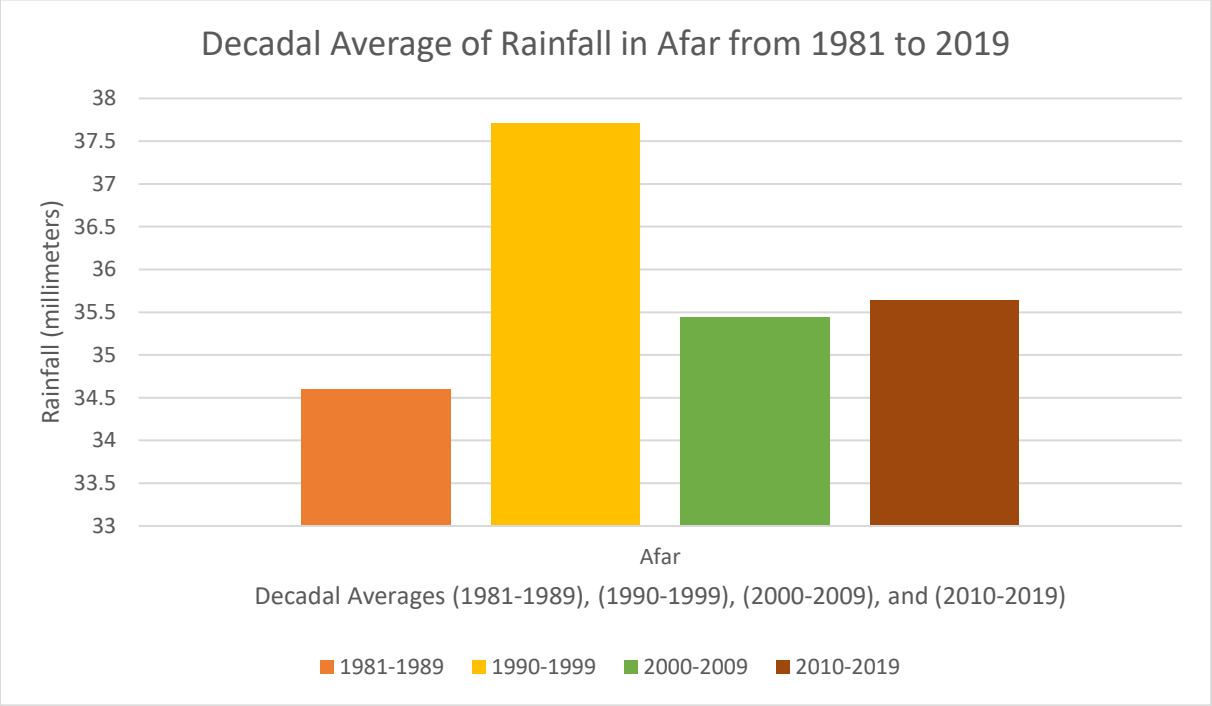

Figure A1.2: Decadal Average Rainfall distribution in Afar, Ethiopia from (1981-1989), (1990-1999), (2000-2009), and (2010-2019)

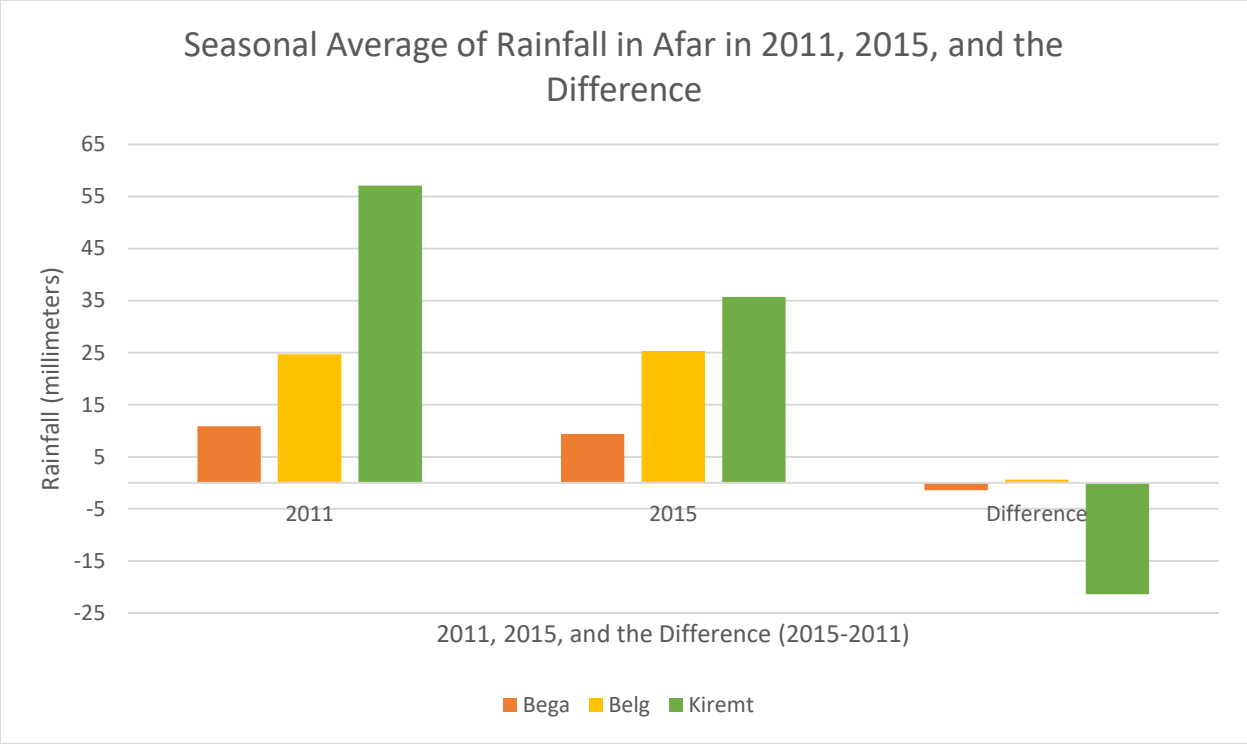

Figure A1.3: Seasonal Average Rainfall Distribution in Afar, Ethiopia from 2011, 2015, and the Difference Between the Two Years during Bega, Belg, and Kiremt

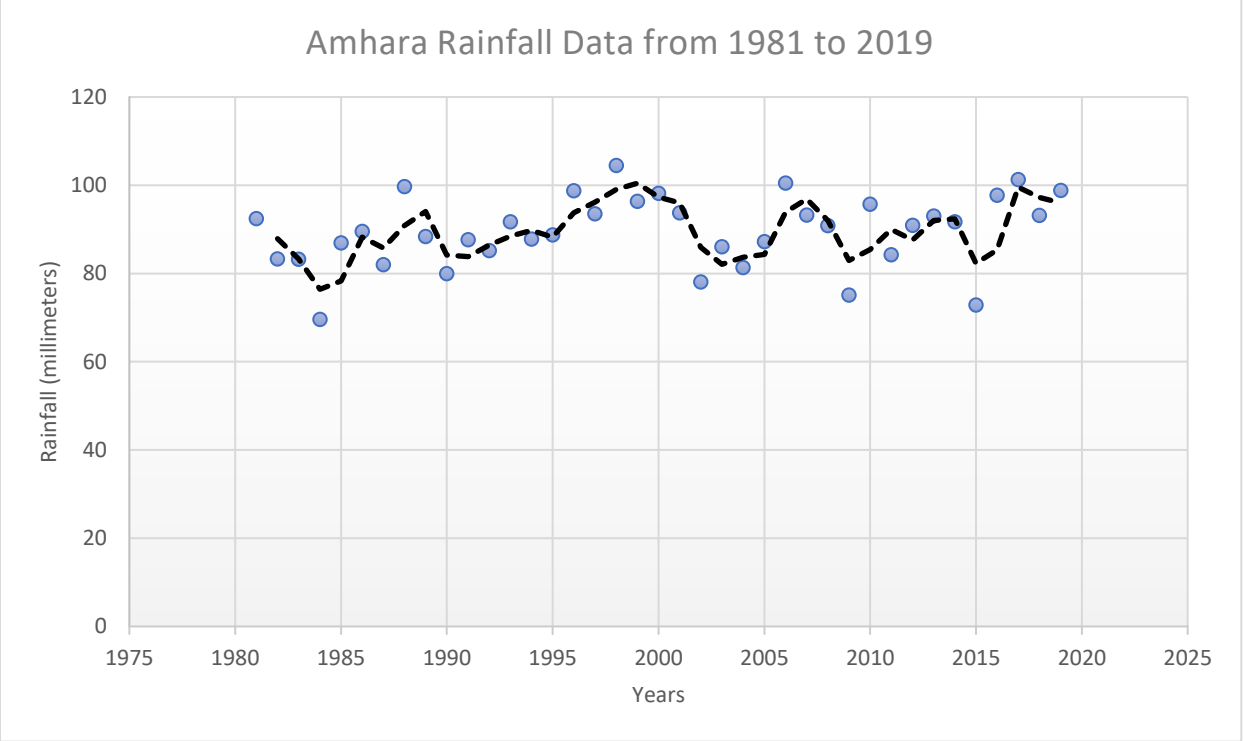

Figure A2.1: Yearly Average Rainfall distribution in Amhara, Ethiopia from 1981 to 2019

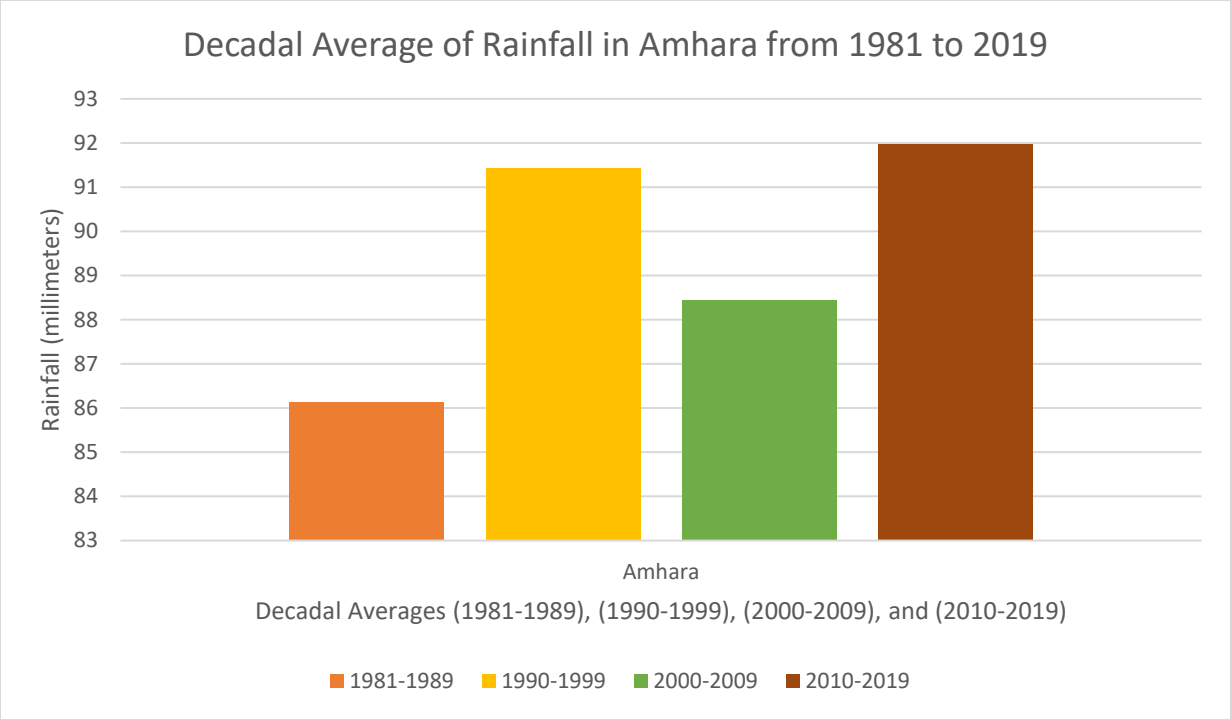

Figure A2.2: Decadal Average Rainfall distribution in Amhara, Ethiopia from (1981-1989), (1990-1999), (2000-2009), and (2010-2019)

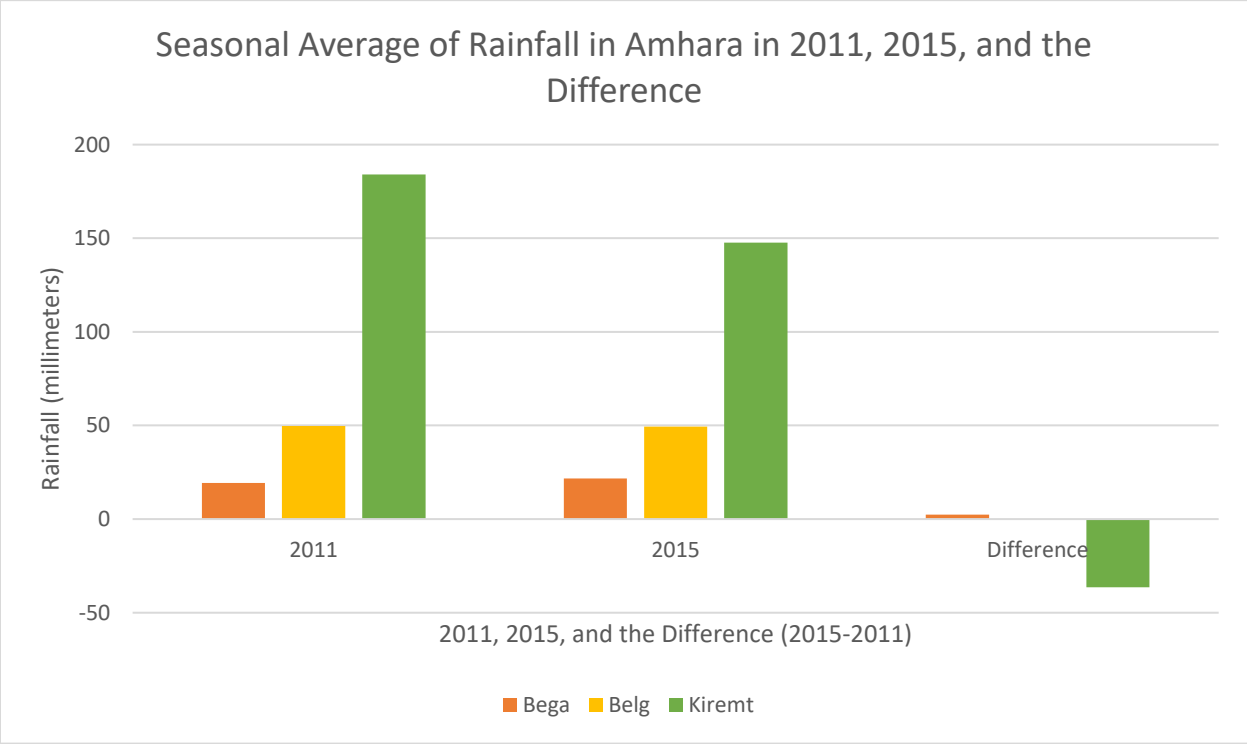

Figure A2.3: Seasonal Average Rainfall Distribution in Amhara, Ethiopia from 2011, 2015, and the Difference Between the Two Years Bega, Belg, and Kiremt

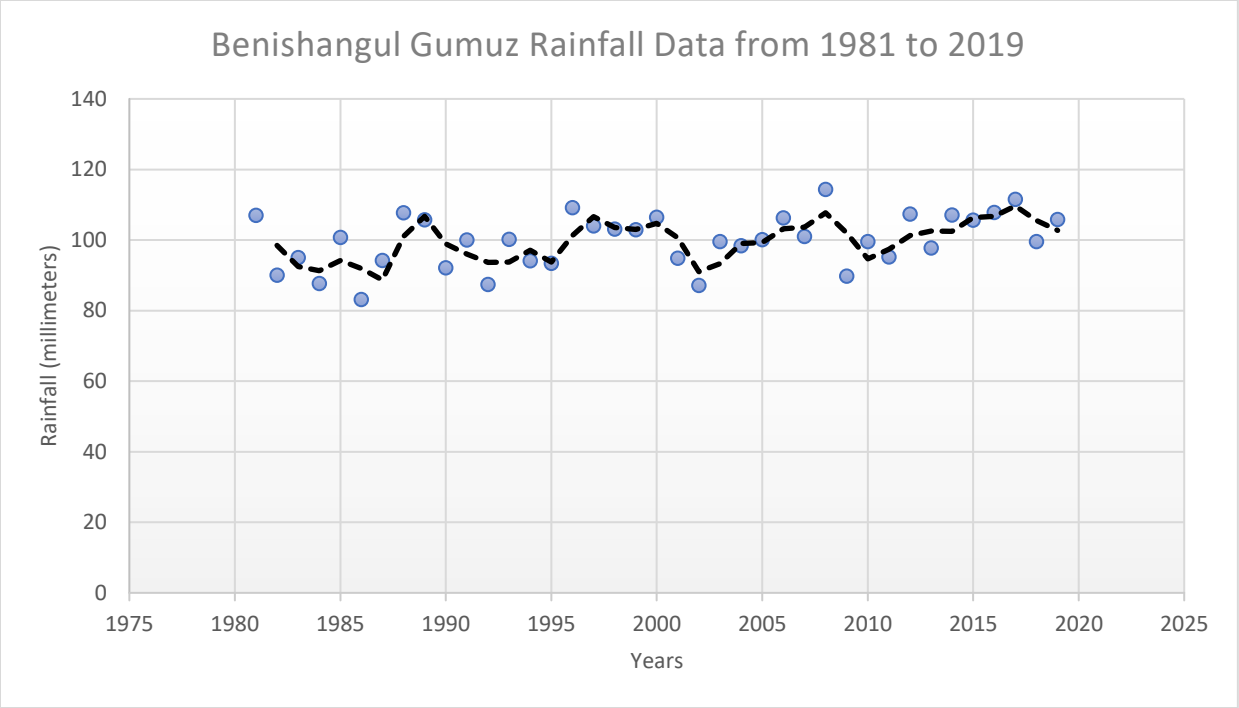

Figure A3.1: Yearly Average Rainfall distribution in Benishangul Gumuz, Ethiopia from 1981 to 2019

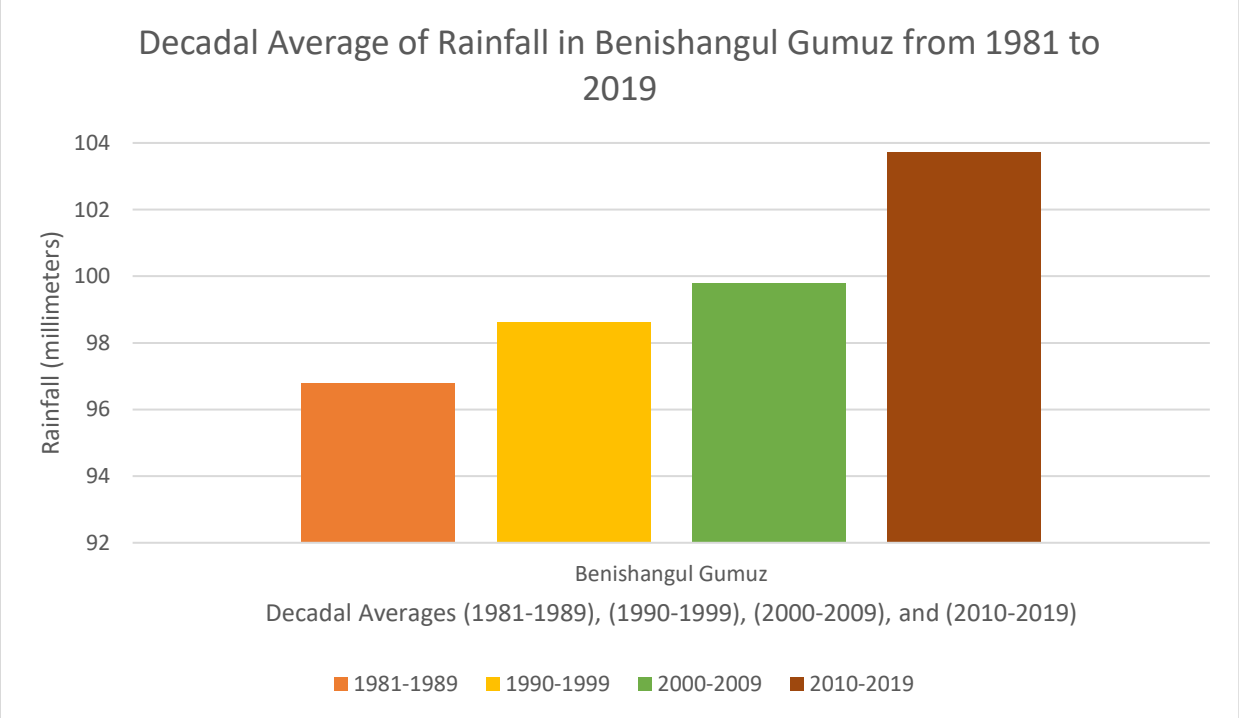

Figure A3.2: Decadal Average Rainfall distribution in Benishangul Gumuz, Ethiopia from (1981-1989), (1990-1999), (2000-2009), and (2010-2019)

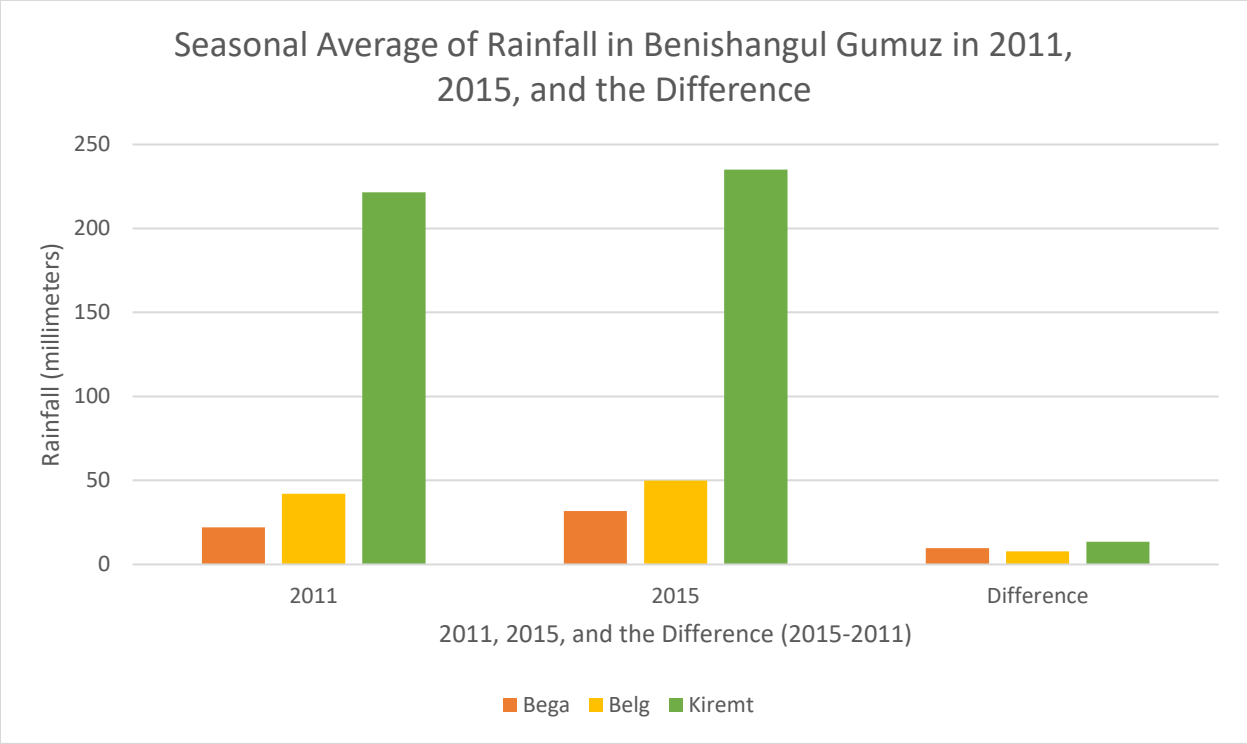

Figure A3.3: Seasonal Average Rainfall Distribution in Benishangul Gumuz, Ethiopia from 2011, 2015, and the Difference Between the Two Years Bega, Belg, and Kiremt

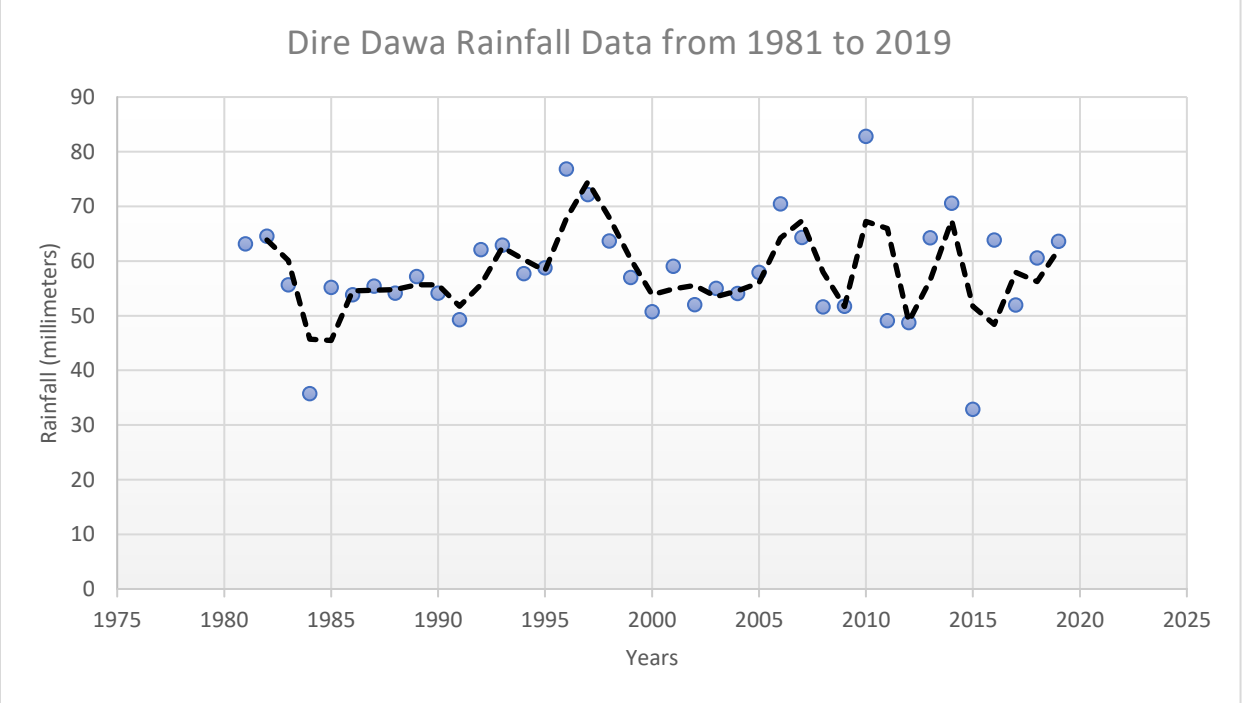

Figure A4.1: Yearly Average Rainfall distribution in Dire Dawa, Ethiopia from 1981 to 2019

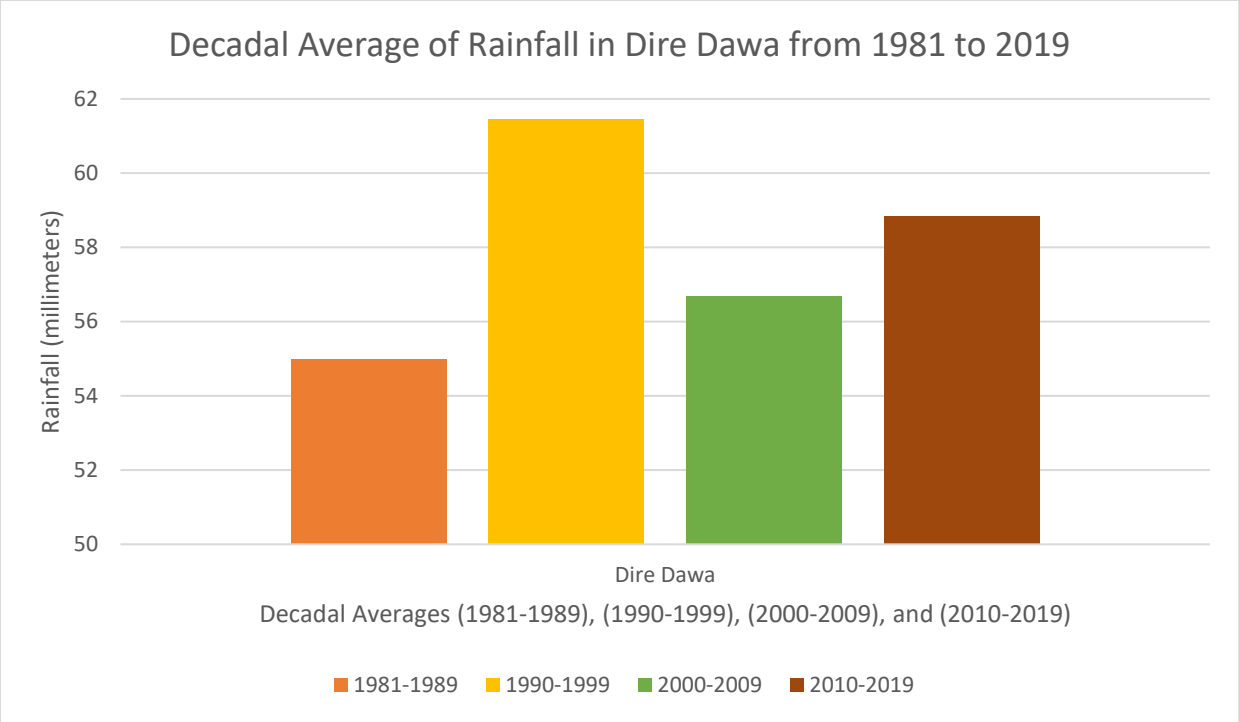

Figure A4.2: Decadal Average Rainfall distribution in Dire Dawa, Ethiopia from (1981-1989), (1990-1999), (2000-2009), and (2010-2019)

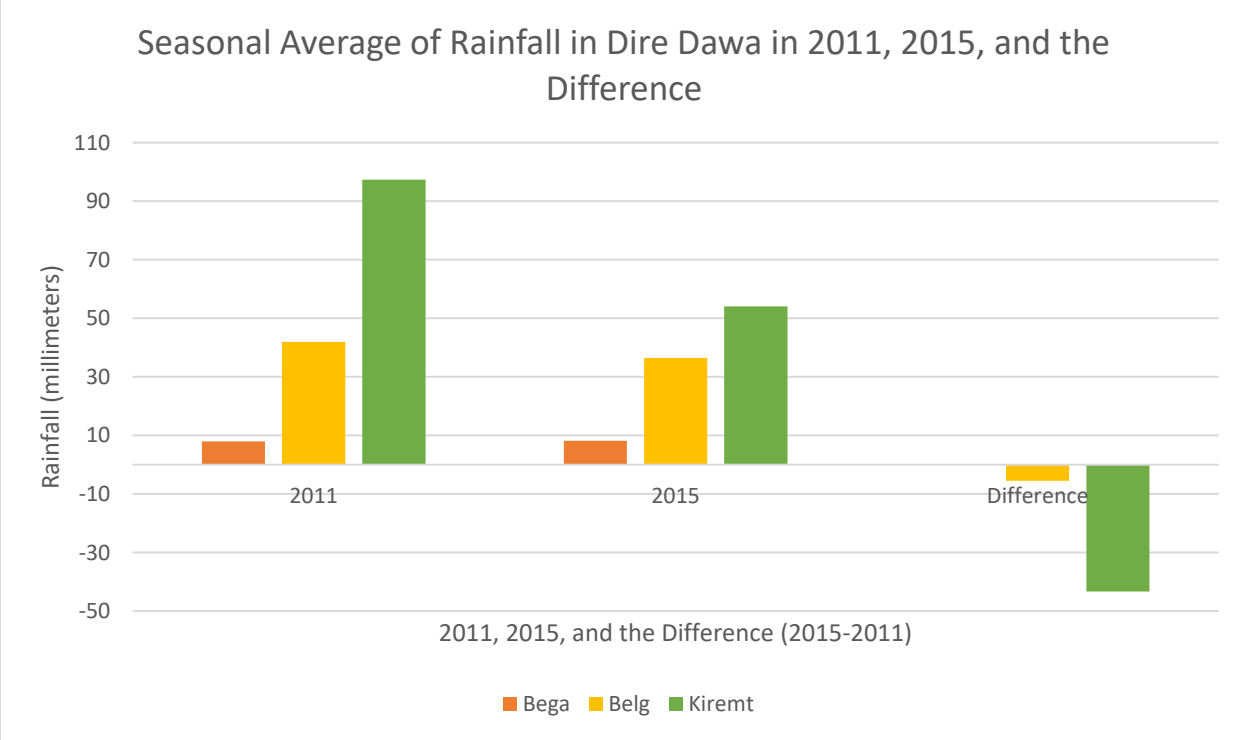

Figure A4.3: Seasonal Average Rainfall Distribution in Dire Dawa, Ethiopia from 2011, 2015, and the Difference Between the Two Years Bega, Belg, and Kiremt

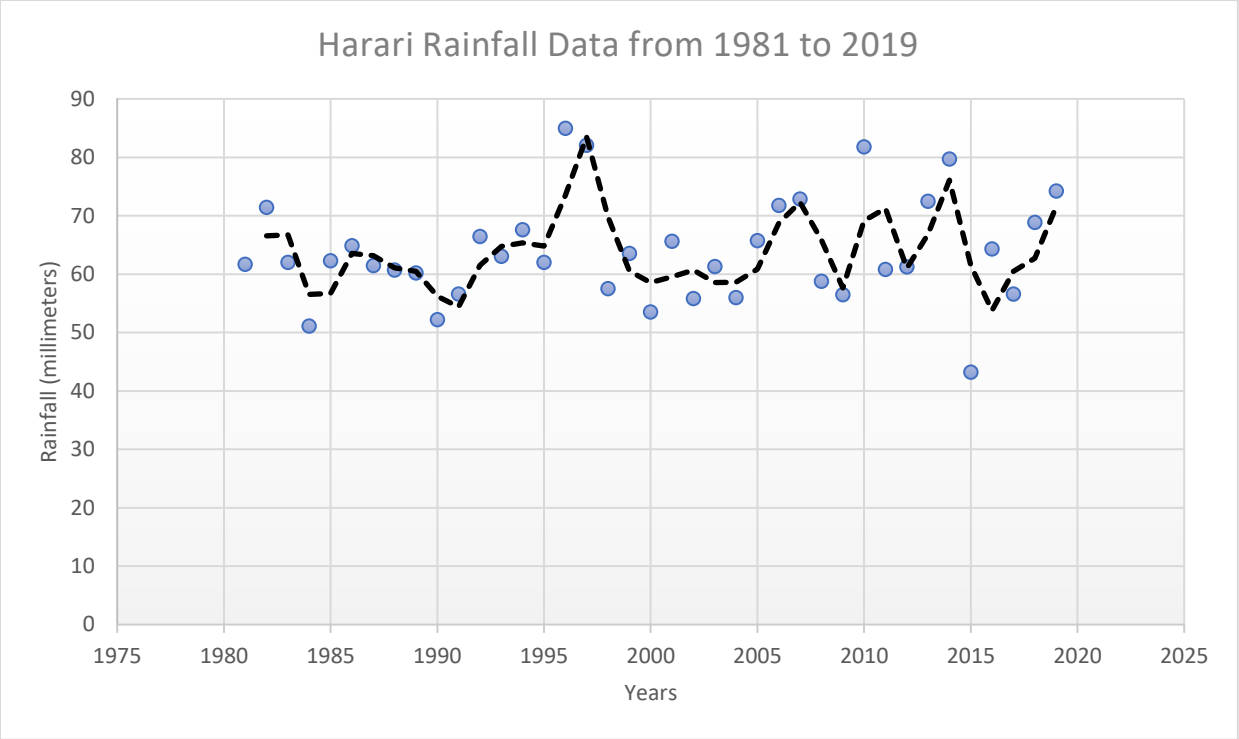

Figure A5.1: Yearly Average Rainfall distribution in Harari, Ethiopia from 1981 to 2019

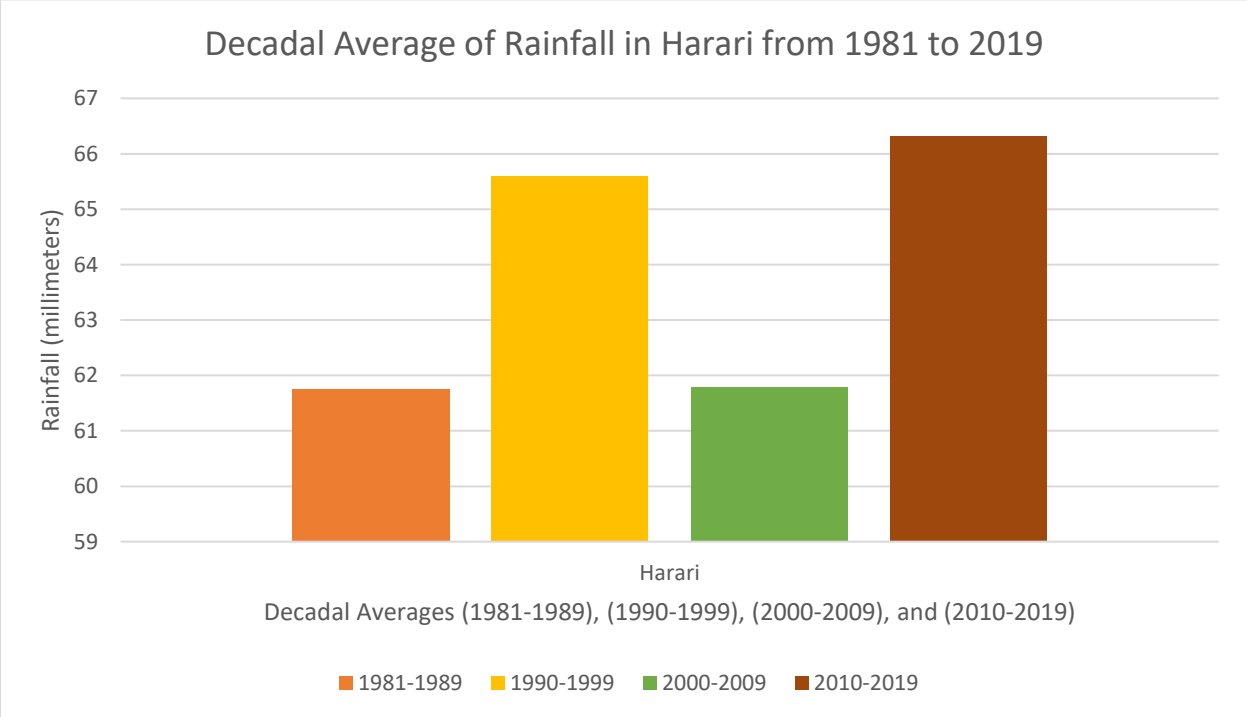

Figure A5.2: Decadal Average Rainfall distribution in Harari, Ethiopia from (1981-1989), (1990-1999), (2000-2009), and (2010-2019)

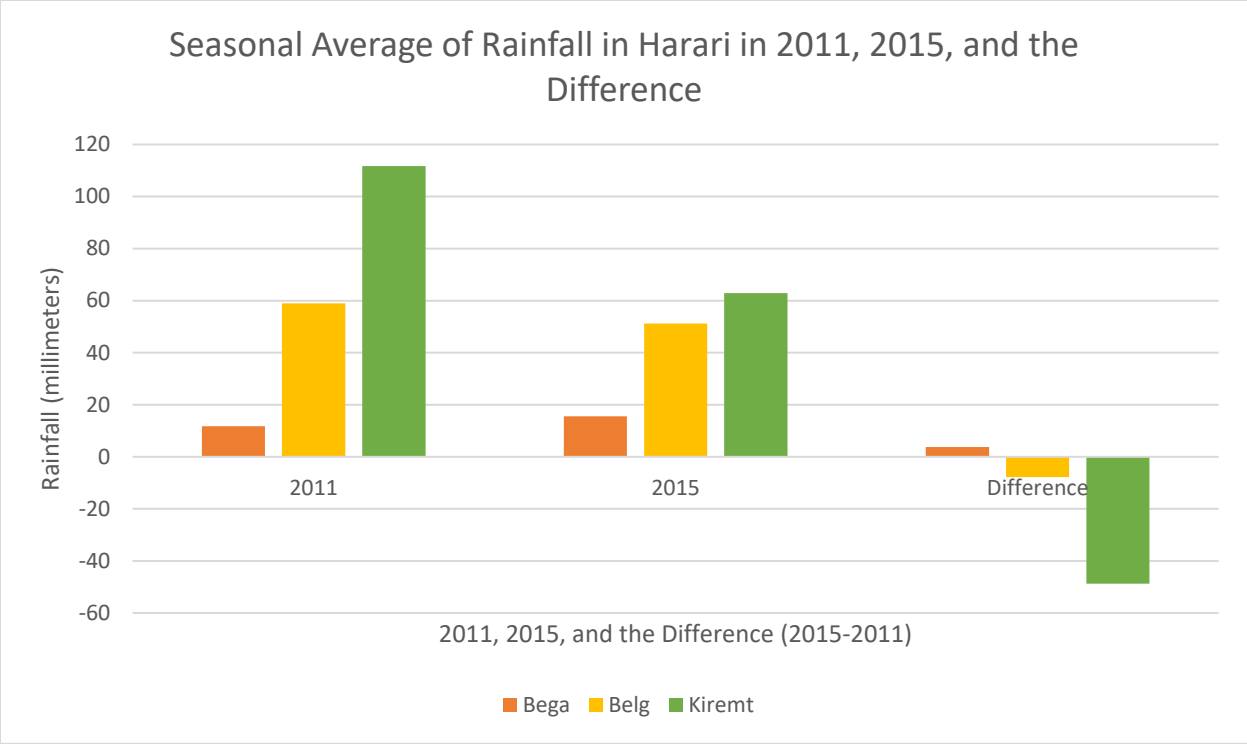

Figure A5.3: Seasonal Average Rainfall Distribution in Harari, Ethiopia from 2011, 2015, and the Difference Between the Two Years Bega, Belg, and Kiremt

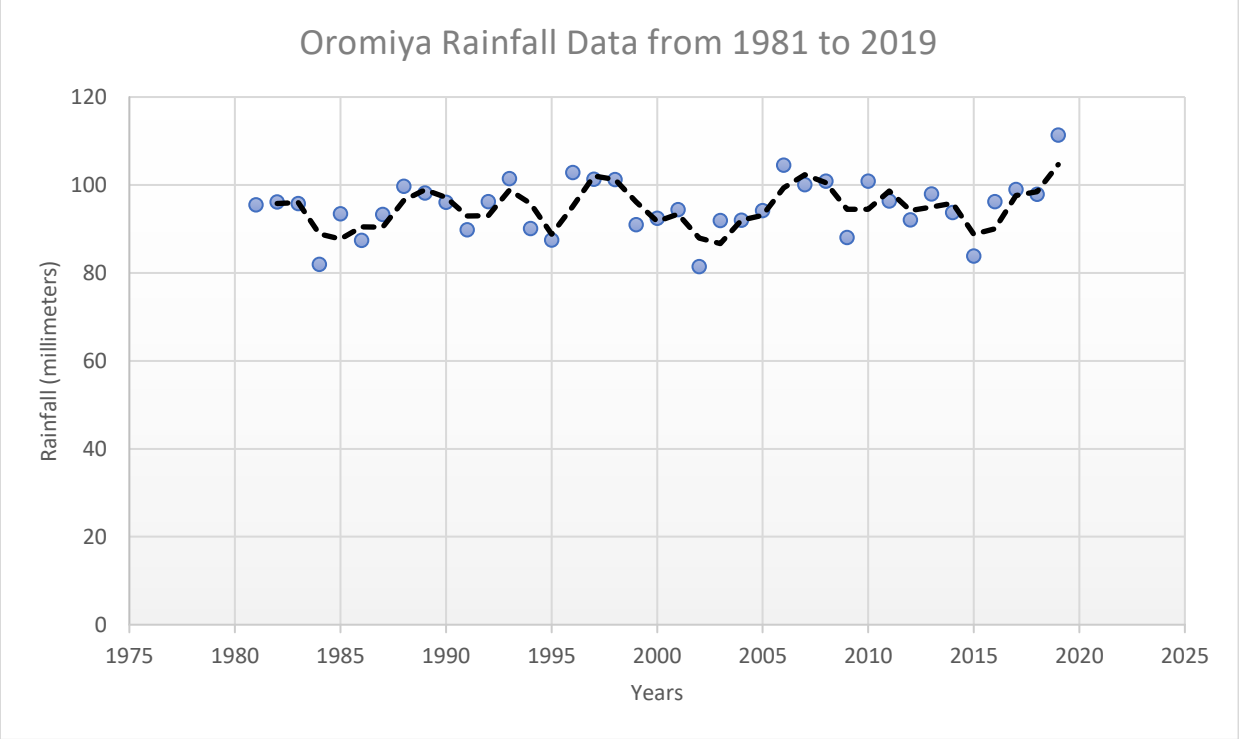

Figure A6.1: Yearly Average Rainfall distribution in Oromiya, Ethiopia from 1981 to 2019

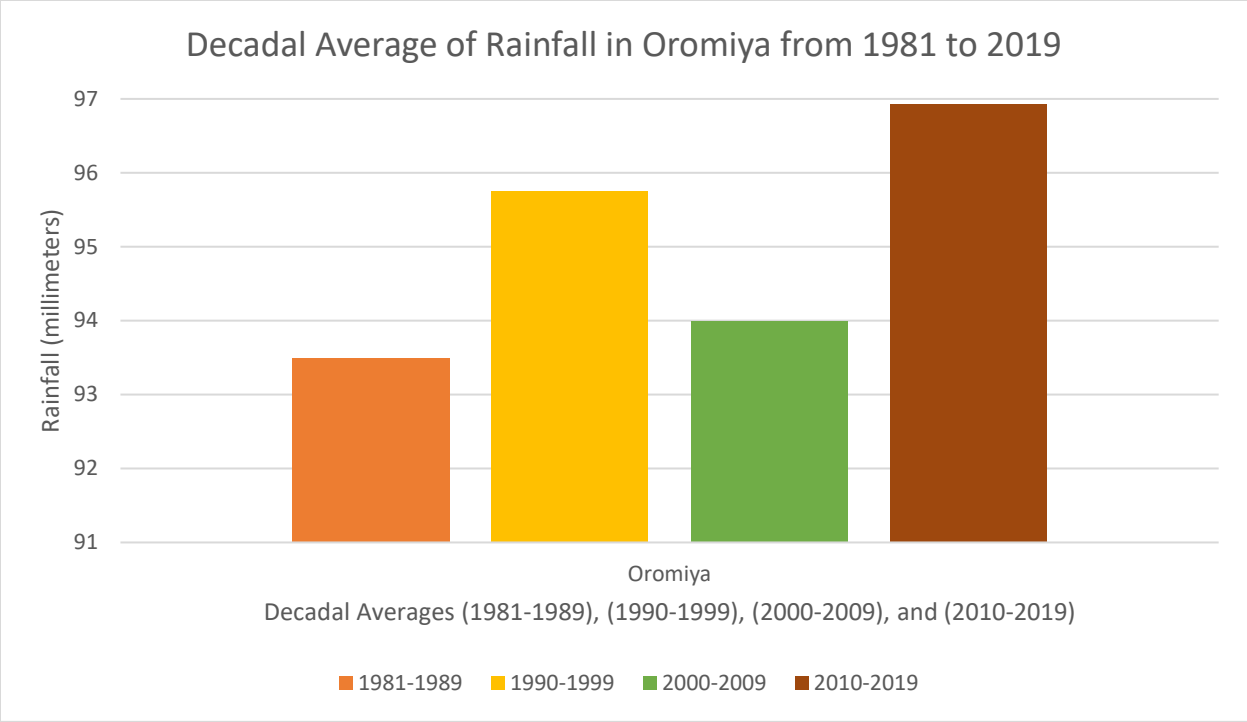

Figure A6.2: Decadal Average Rainfall distribution in Oromiya, Ethiopia from (1981-1989), (1990-1999), (2000-2009), and (2010-2019)

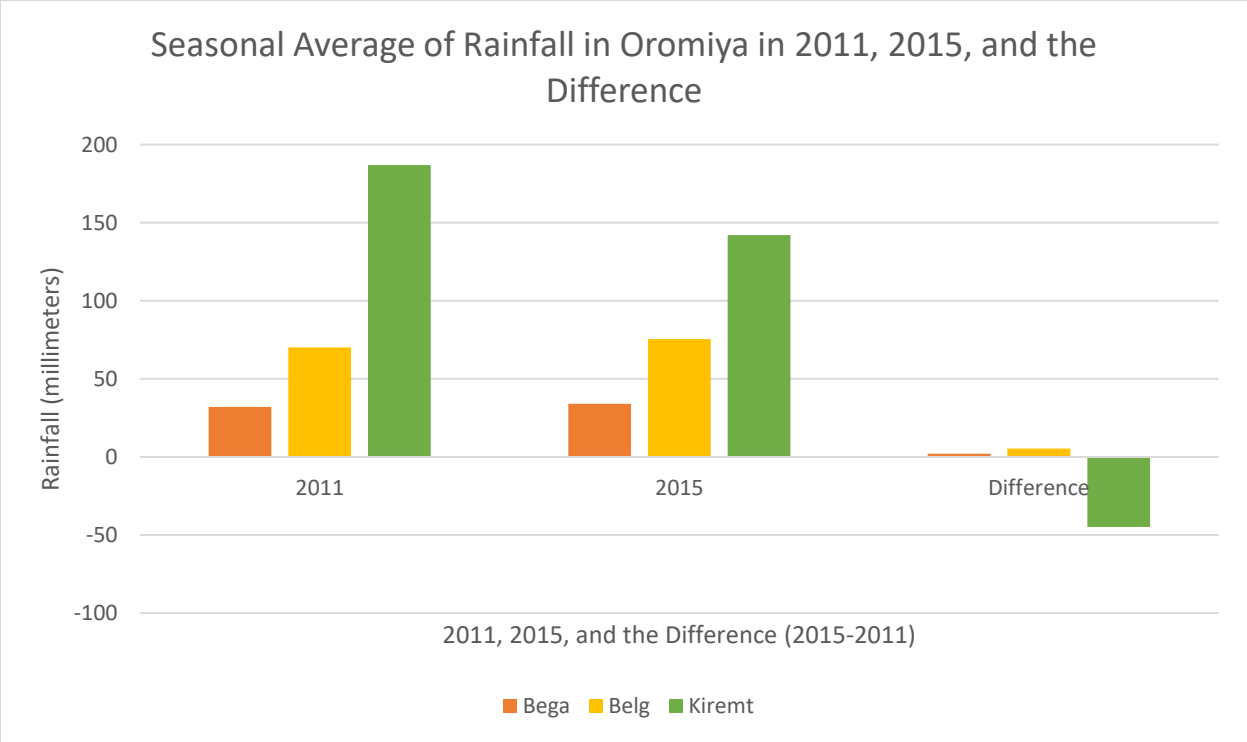

Figure A6.3: Seasonal Average Rainfall Distribution in Oromiya, Ethiopia from 2011, 2015, and the Difference Between the Two Years Bega, Belg, and Kiremt

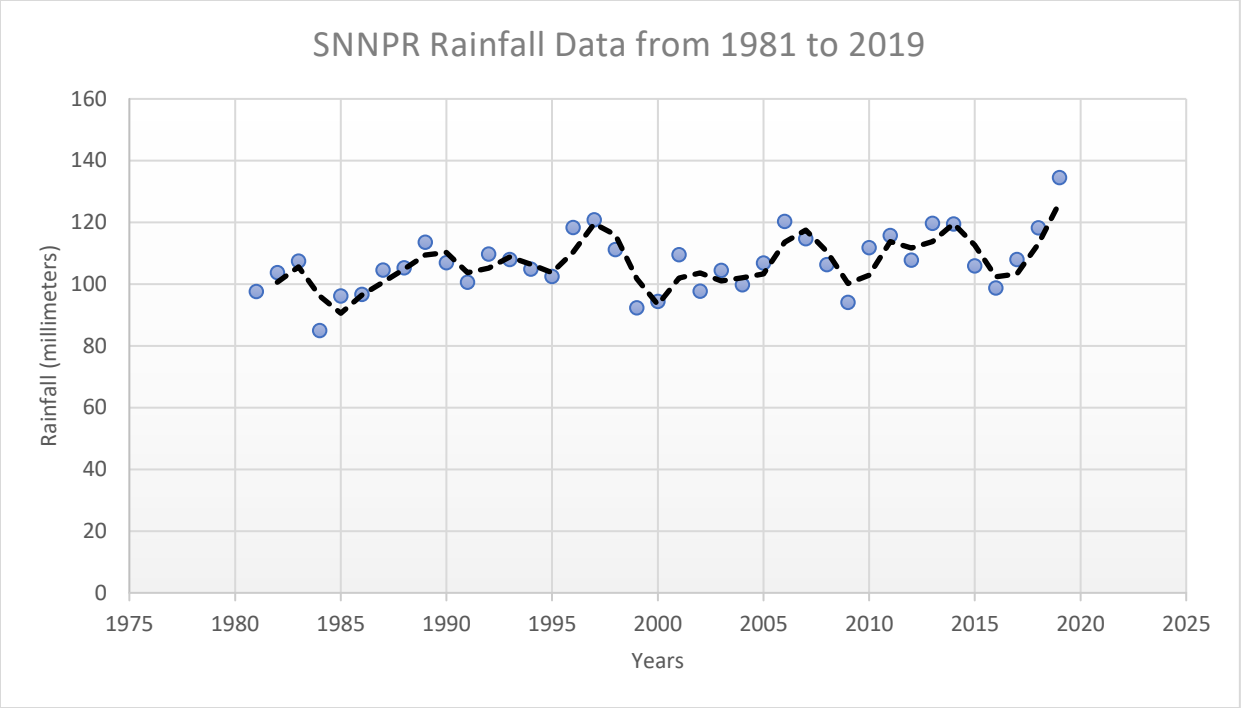

Figure A7.1: Yearly Average Rainfall distribution in SNNPR, Ethiopia from 1981 to 2019

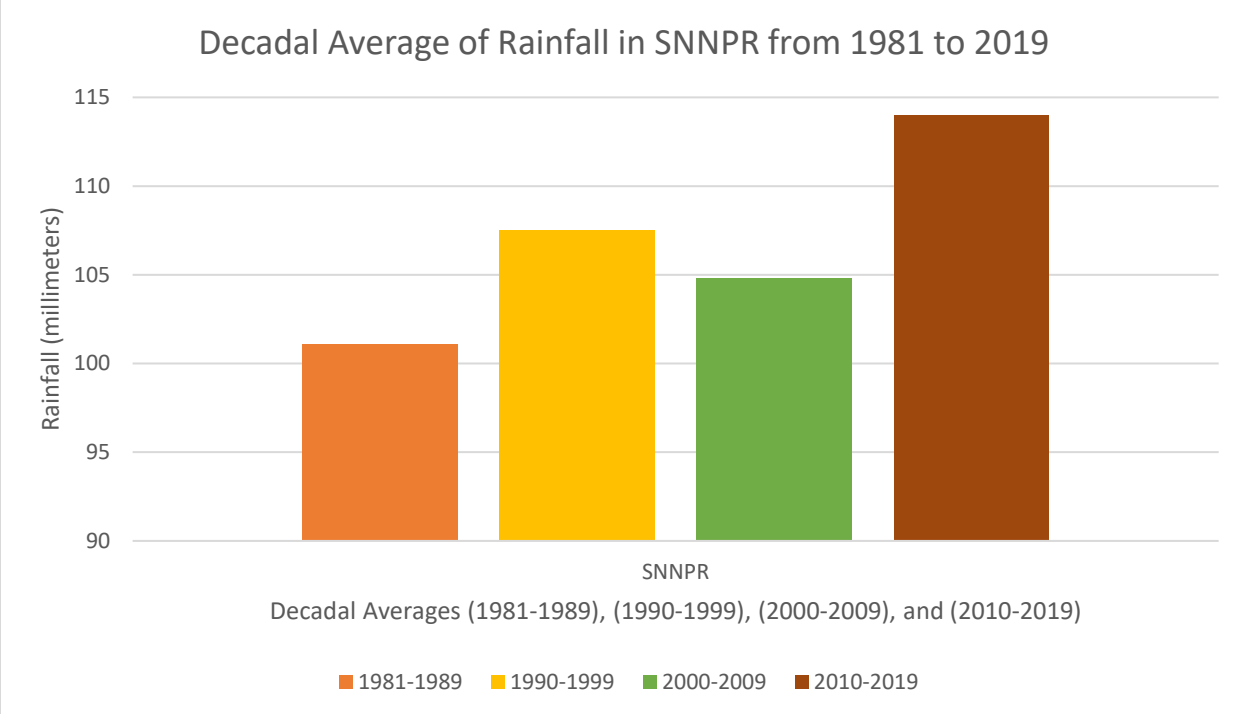

Figure A7.2: Decadal Average Rainfall distribution in SNNPR, Ethiopia from (1981-1989), (1990-1999), (2000-2009), and (2010-2019)

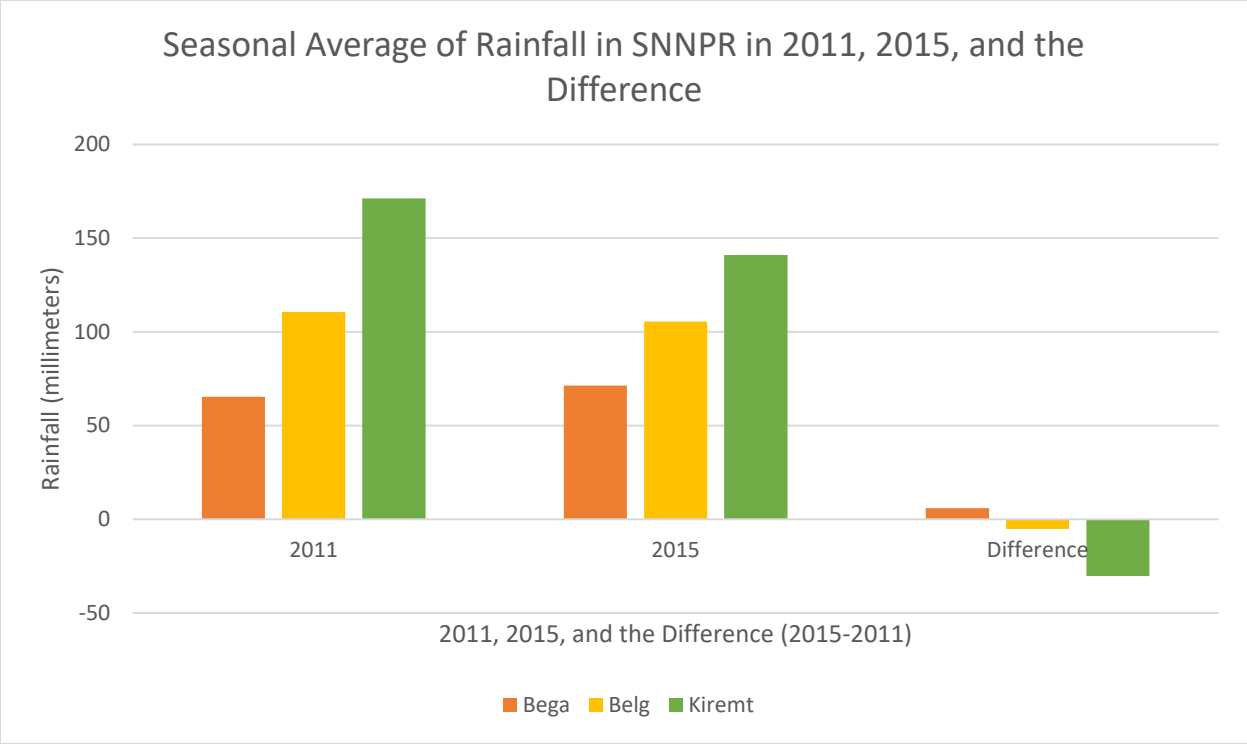

Figure A7.3: Seasonal Average Rainfall Distribution in SNNPR, Ethiopia from 2011, 2015, and the Difference Between the Two Years Bega, Belg, and Kiremt

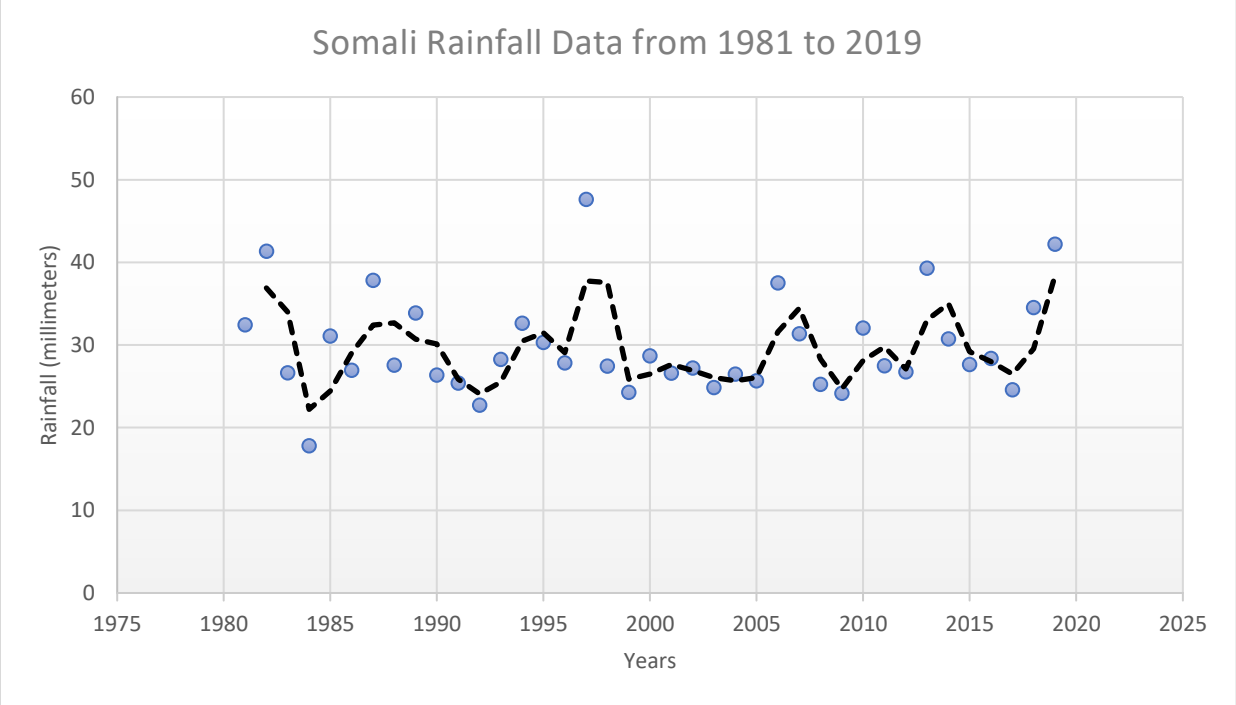

Figure A8.1: Yearly Average Rainfall distribution in Somali, Ethiopia from 1981 to 2019

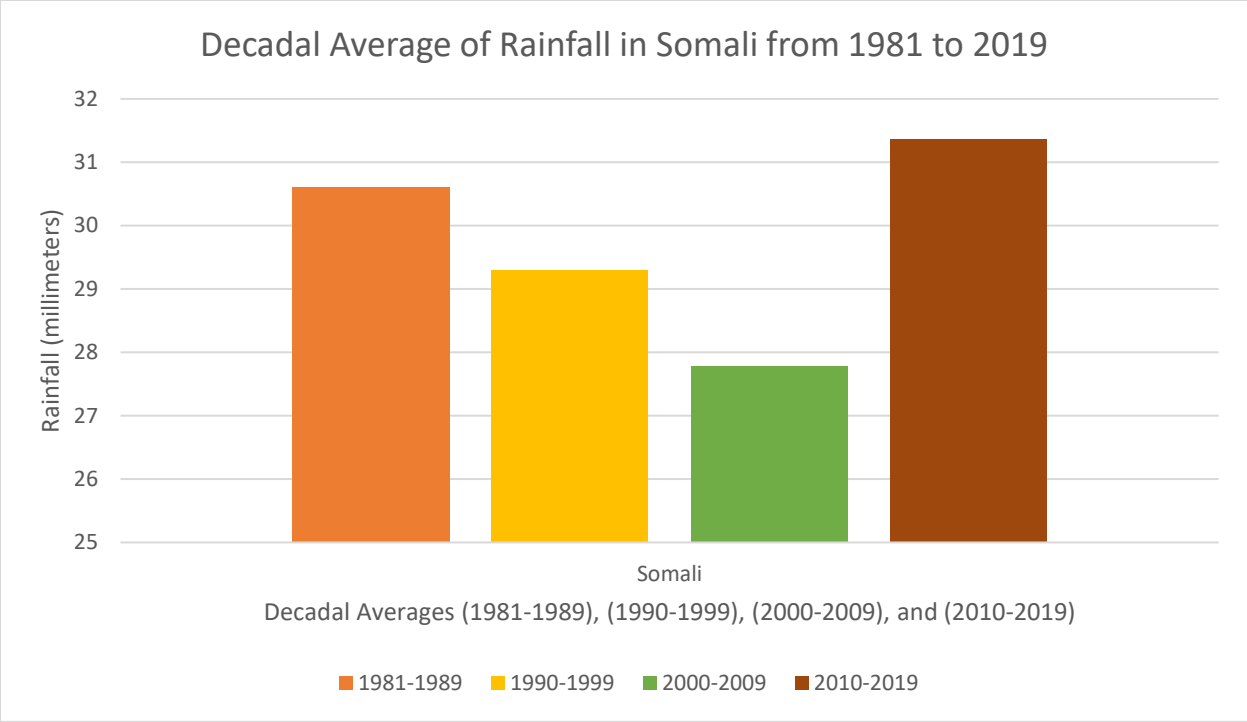

Figure A8.2: Decadal Average Rainfall distribution in Somali, Ethiopia from (1981-1989), (1990-1999), (2000-2009), and (2010-2019)

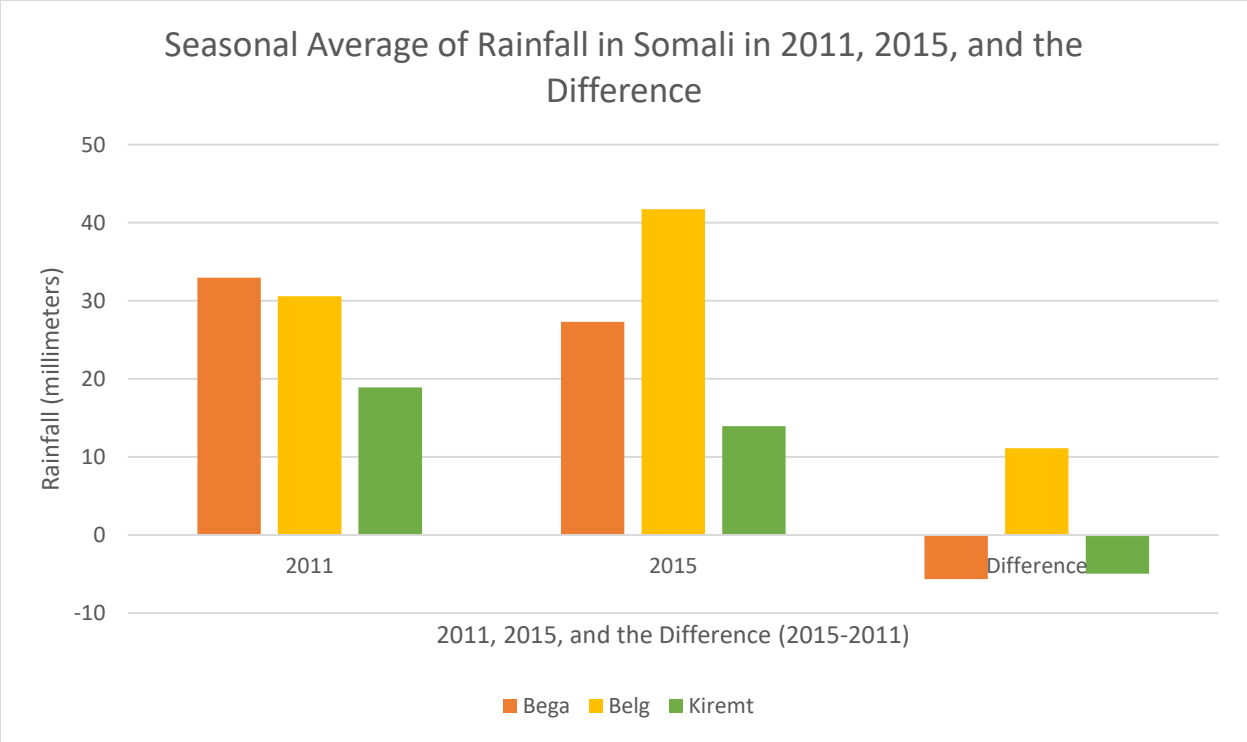

Figure A8.3: Seasonal Average Rainfall Distribution in Somali, Ethiopia from 2011, 2015, and the Difference Between the Two Years Bega, Belg, and Kiremt

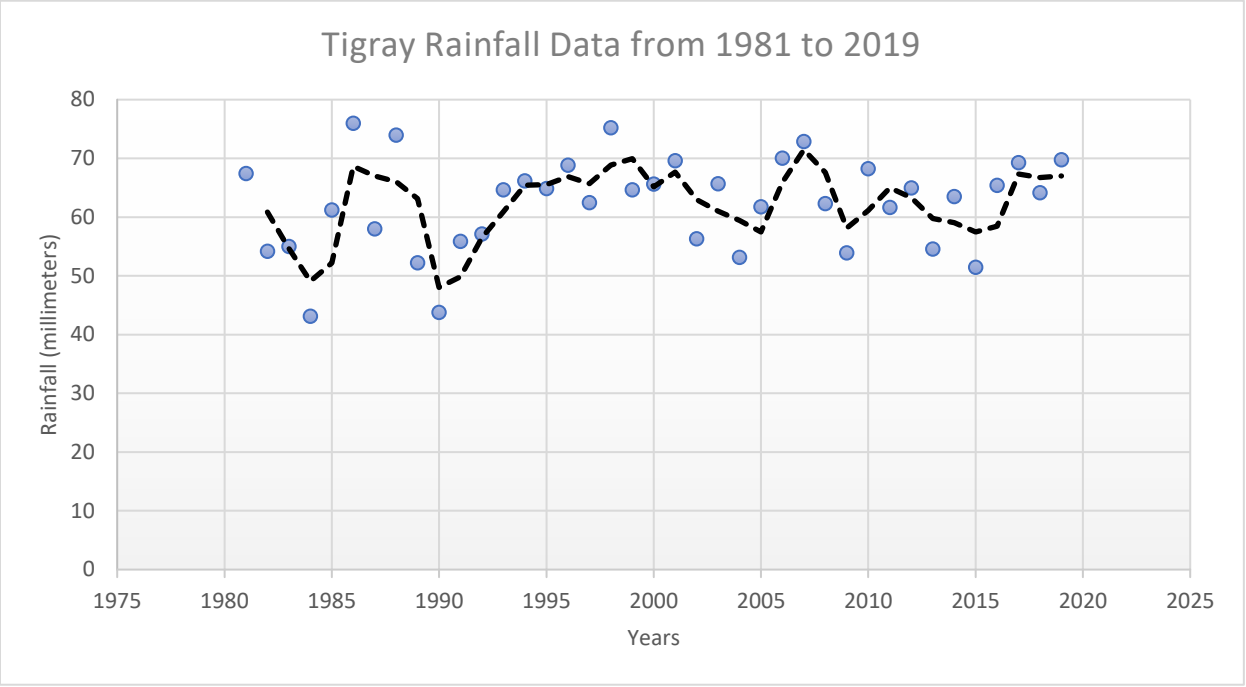

Figure A9.1: Yearly Average Rainfall distribution in Tigray, Ethiopia from 1981 to 2019

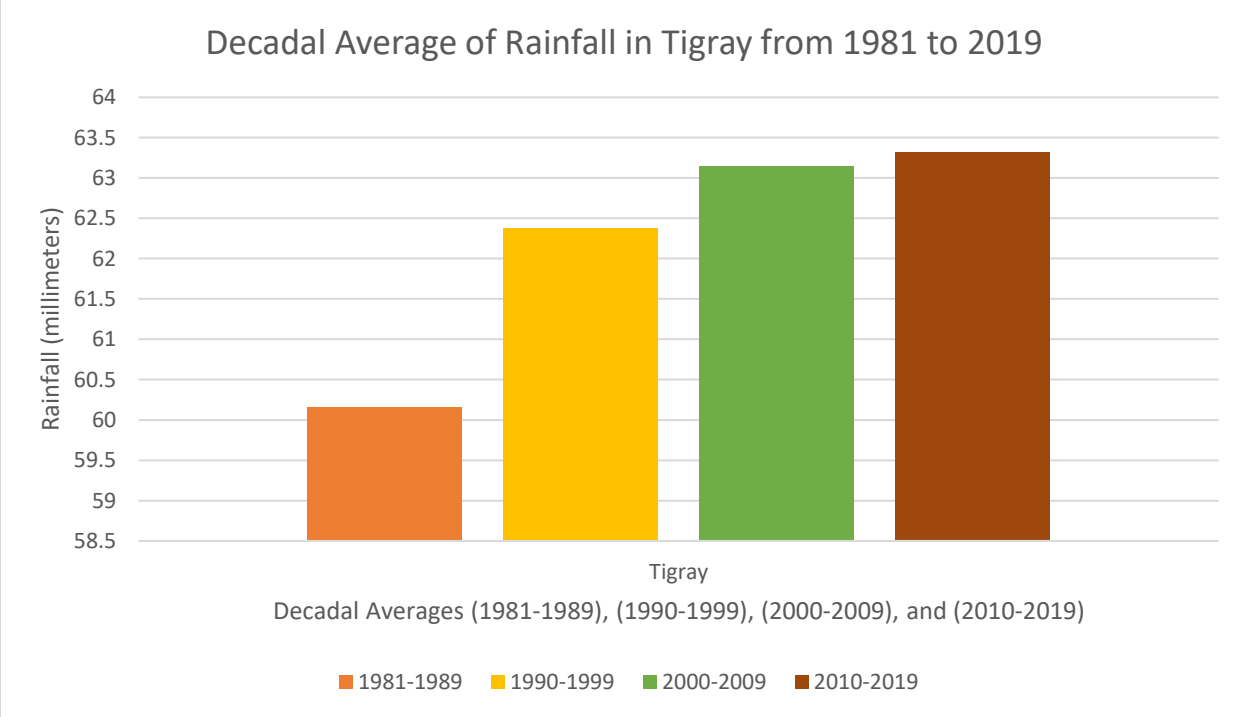

Figure A9.2: Decadal Average Rainfall distribution in Tigray, Ethiopia from (1981-1989), (1990-1999), (2000-2009), and (2010-2019)

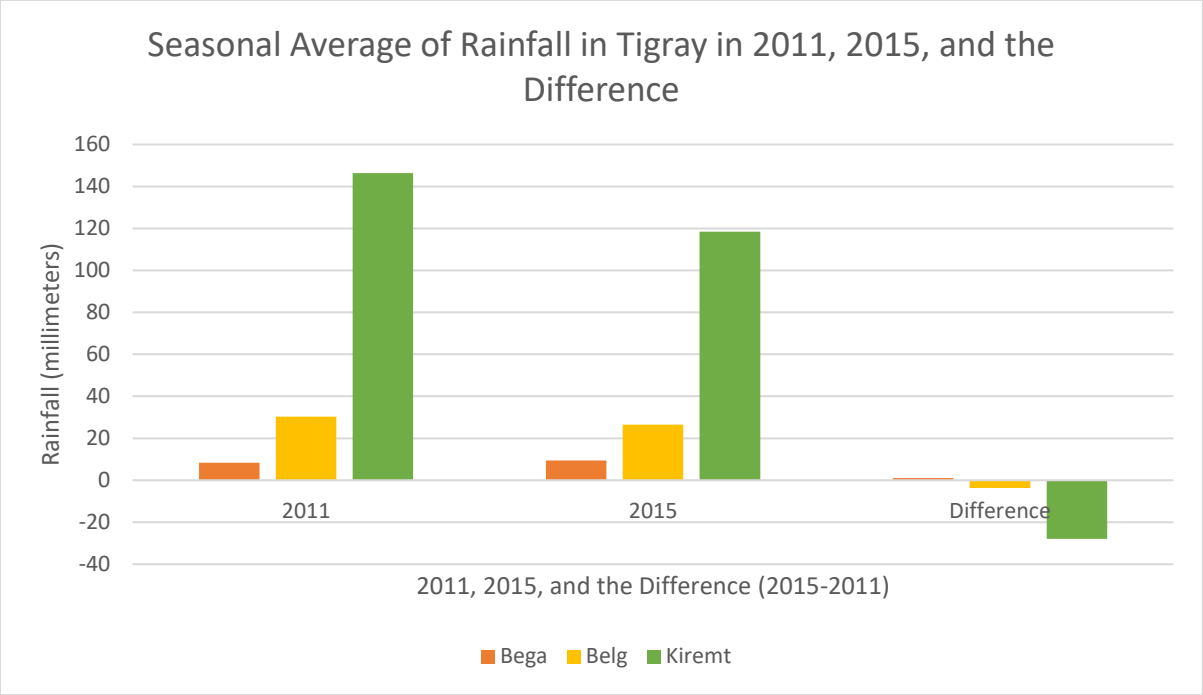

Figure A9.3: Seasonal Average Rainfall Distribution in Tigray, Ethiopia from 2011, 2015, and the Difference Between the Two Years Bega, Belg, and Kiremt

Appendix B: Average Temperature--Climate Change

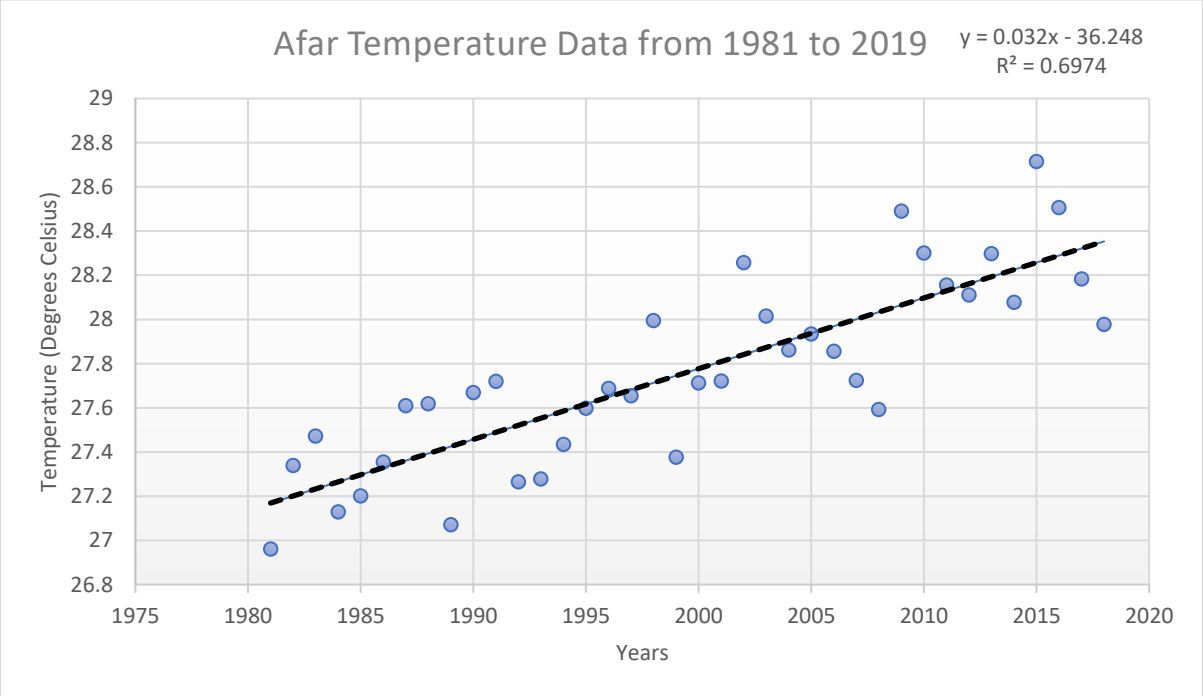

Figure B1: Yearly Average Temperature distribution in Afar, Ethiopia from 1981 to 2019 with a linear regression line, (R^2 = 0.70)

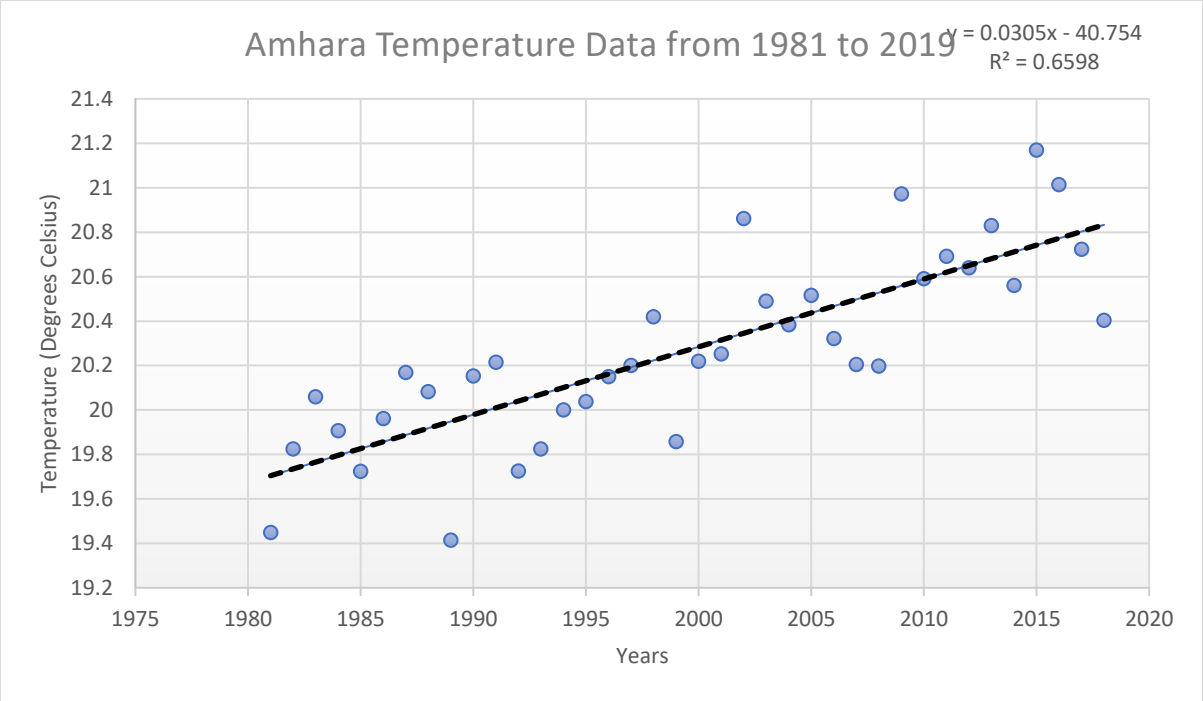

Figure B2: Yearly Average Temperature distribution in Amhara, Ethiopia from 1981 to 2019 with a linear regression line, (R^2 = 0.66)

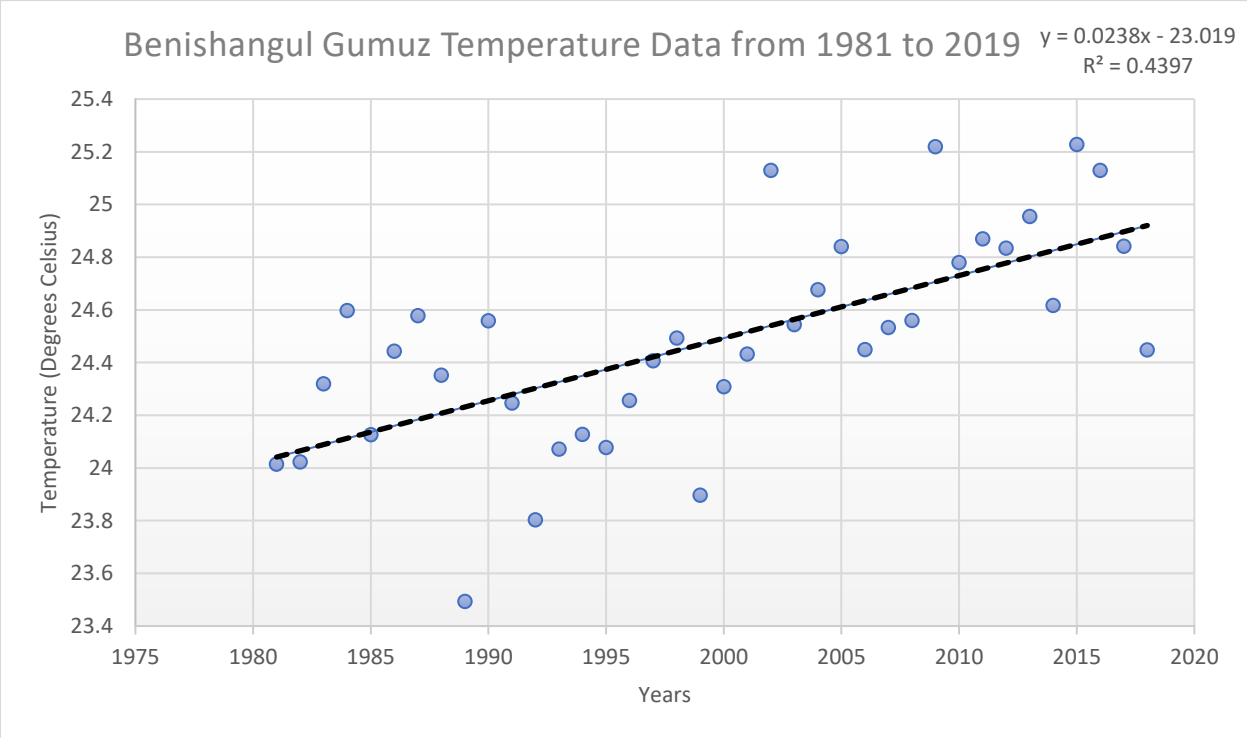

Figure B3: Yearly Average Temperature distribution in Benishangul Gumuz, Ethiopia from 1981 to 2019 with a linear regression line, (R^2 = 0.44)

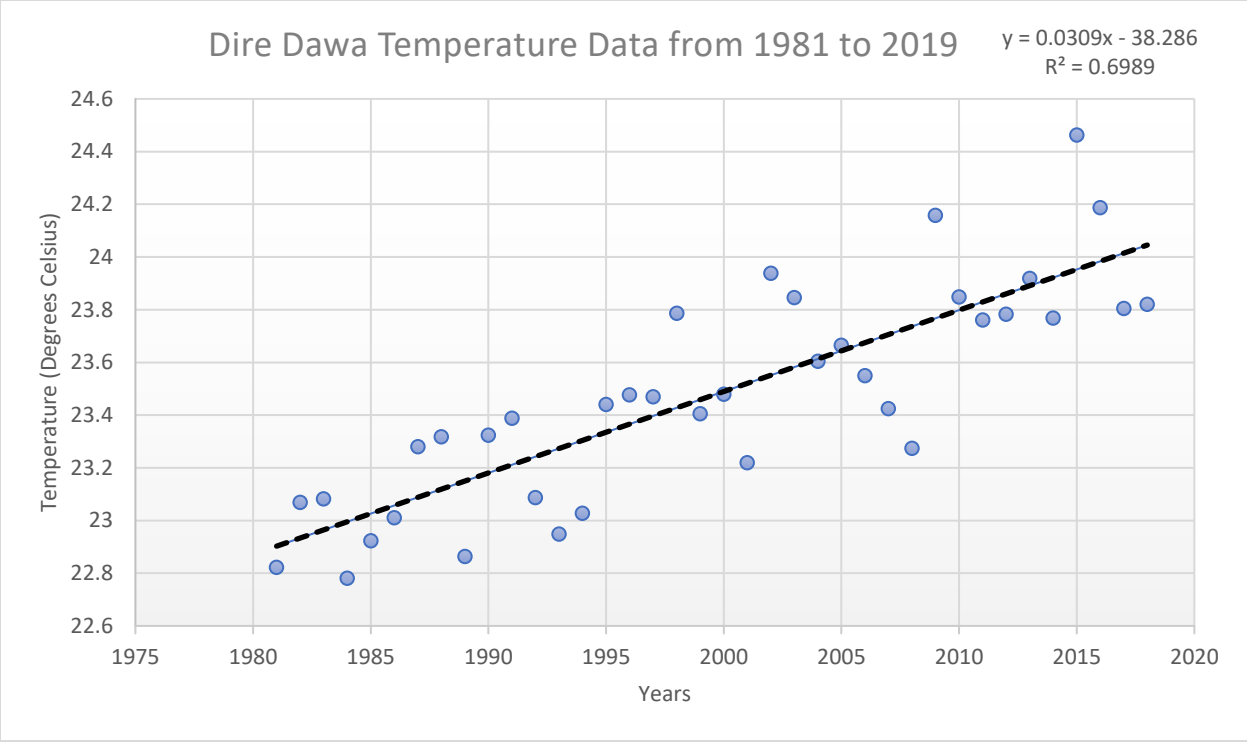

Figure B4: Yearly Average Temperature distribution in Dire Dawa, Ethiopia from 1981 to 2019 with a linear regression line, (R^2 = 0.70)

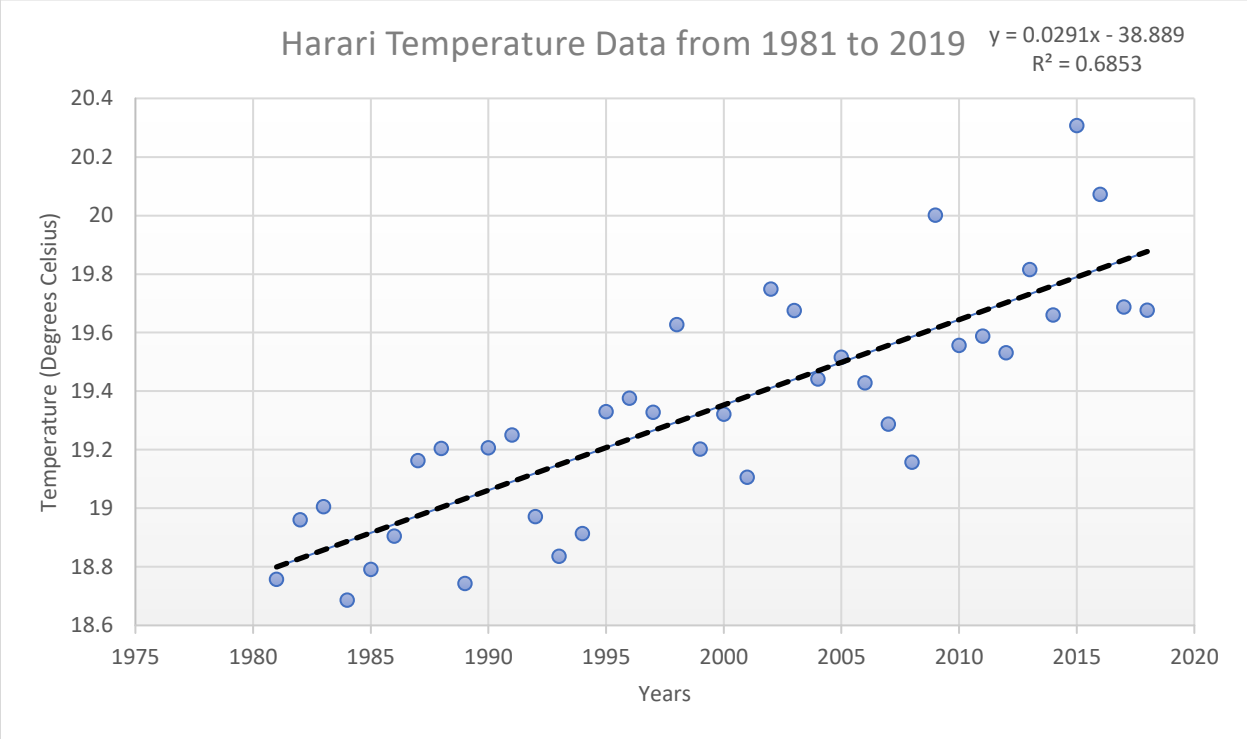

Figure B5: Yearly Average Temperature distribution in Harari, Ethiopia from 1981 to 2019 with a linear regression line, (R^2 = 0.69)

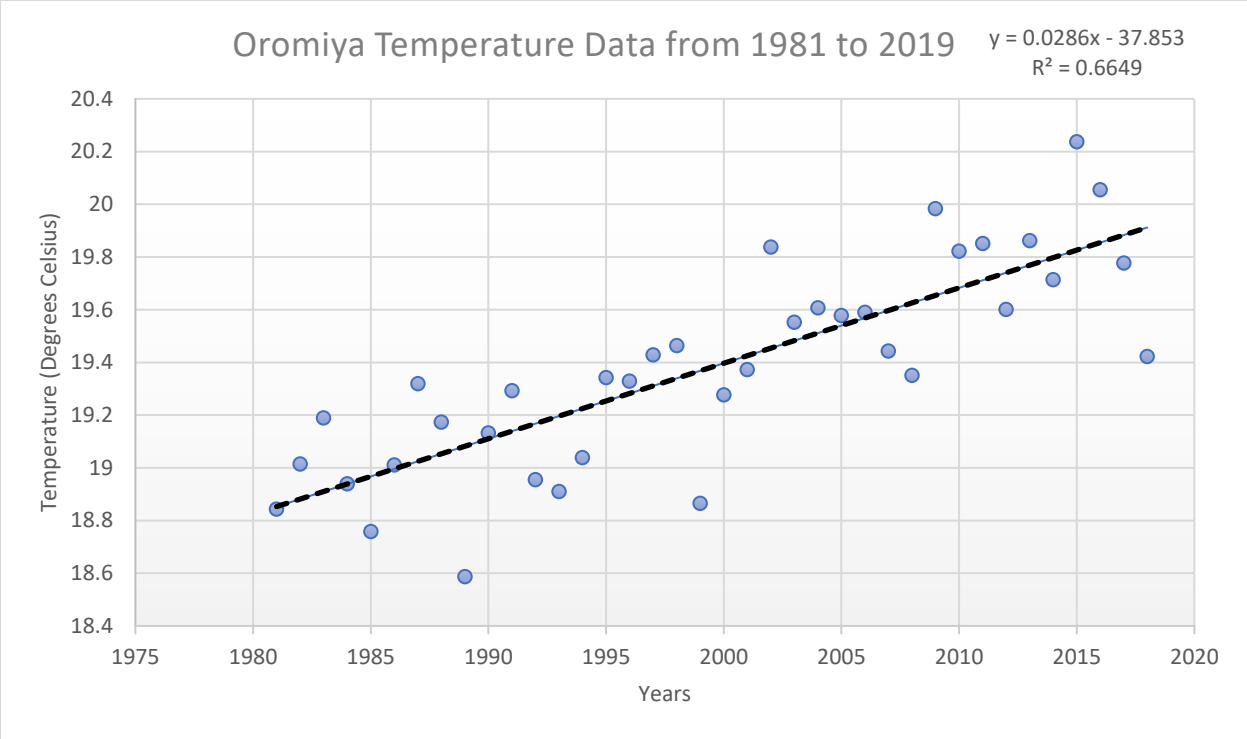

Figure B6: Yearly Average Temperature distribution in Oromiya, Ethiopia from 1981 to 2019 with a linear regression line, (R^2 = 0.66)

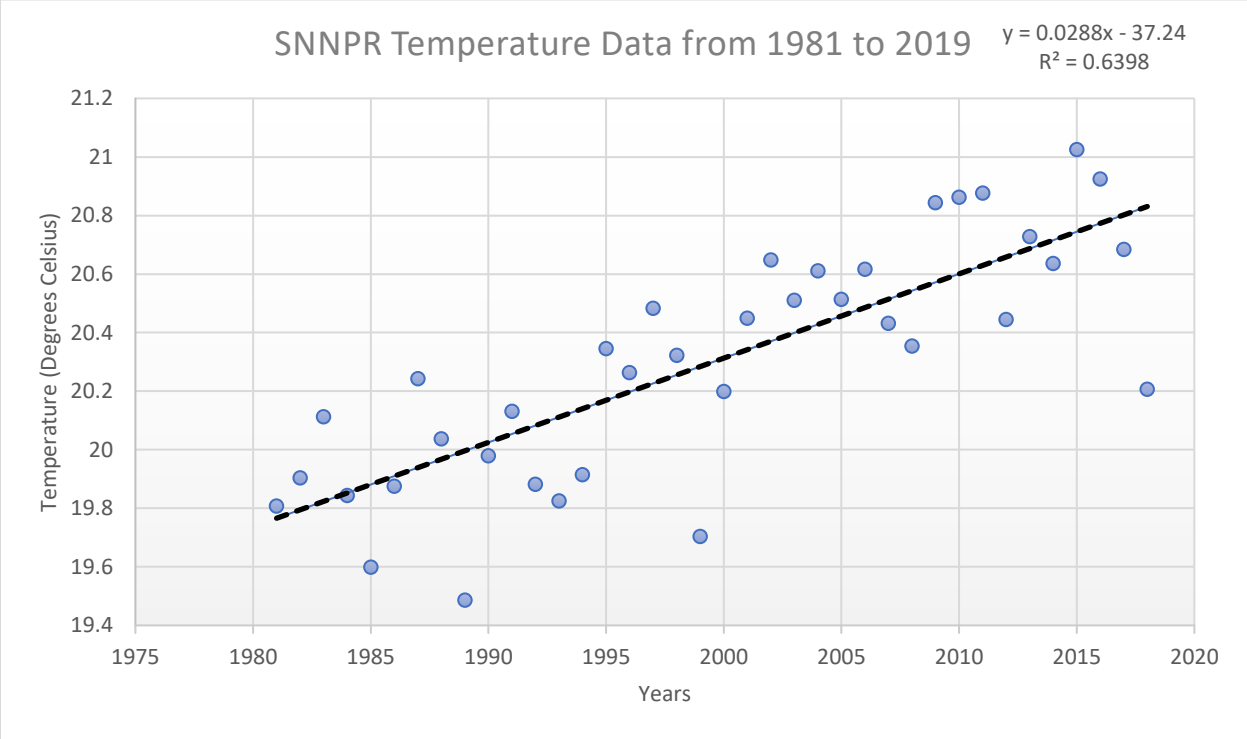

Figure B7: Yearly Average Temperature distribution in SNNPR, Ethiopia from 1981 to 2019 with a linear regression line, (R^2 = 0.64)

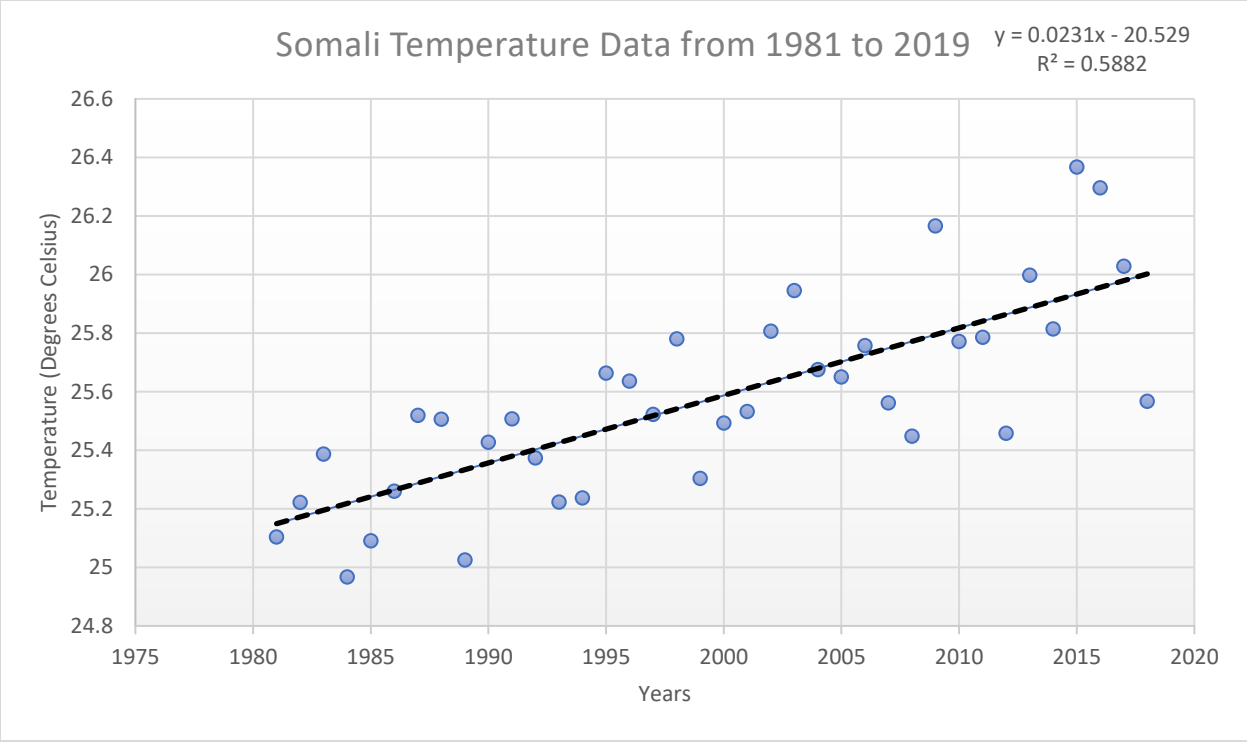

Figure B8: Yearly Average Temperature distribution in Somali, Ethiopia from 1981 to 2019 with a linear regression line, (R^2 = 0.59)

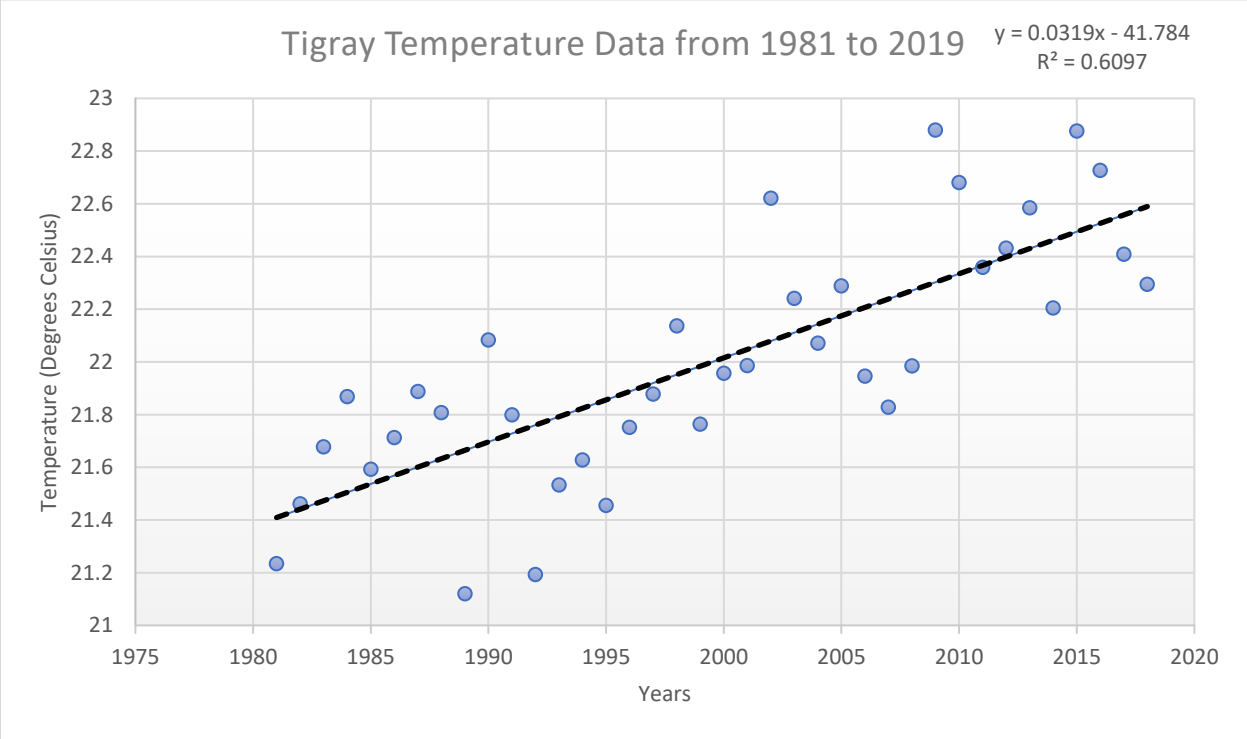

Figure B9: Yearly Average Temperature distribution in Tigray, Ethiopia from 1981 to 2019 with a linear regression line, (R^2 = 0.61)

Appendix C: Proportions of Positive Antigen Test Detection

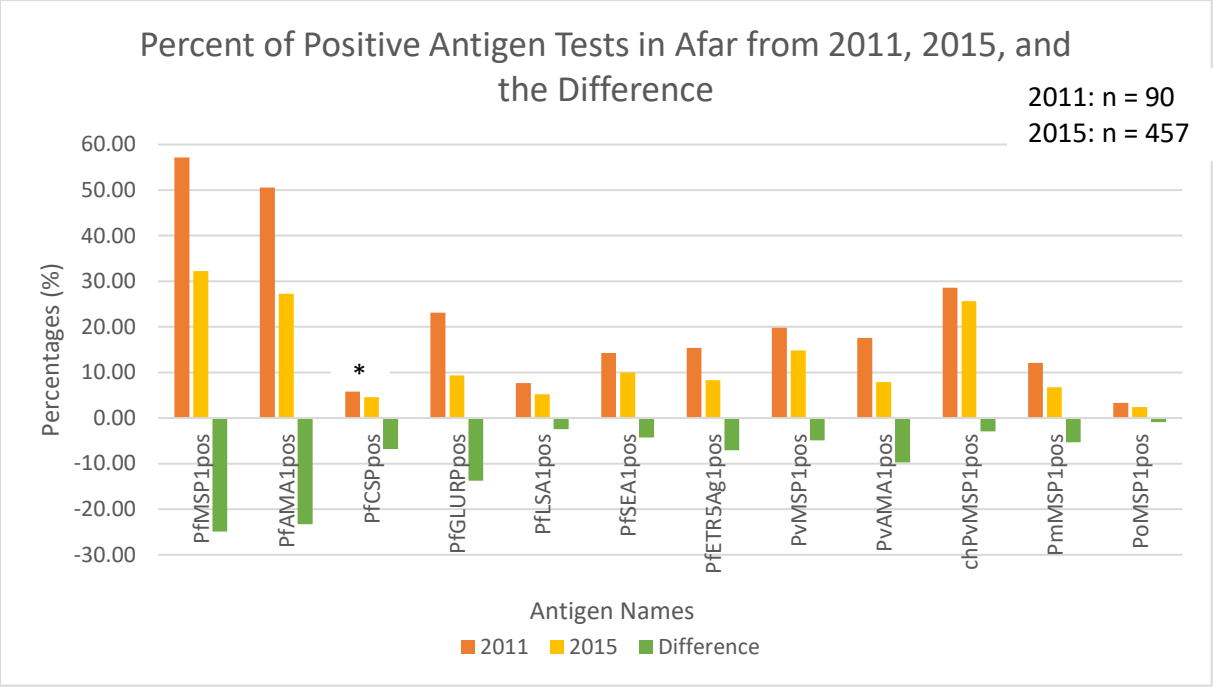

Figure C1: Positive Antigen Test Proportions of Malaria Cases in Afar, Ethiopia from 2011, 2015, and the Difference Between the Two Years; PfCSPpos in 2011, n= 79

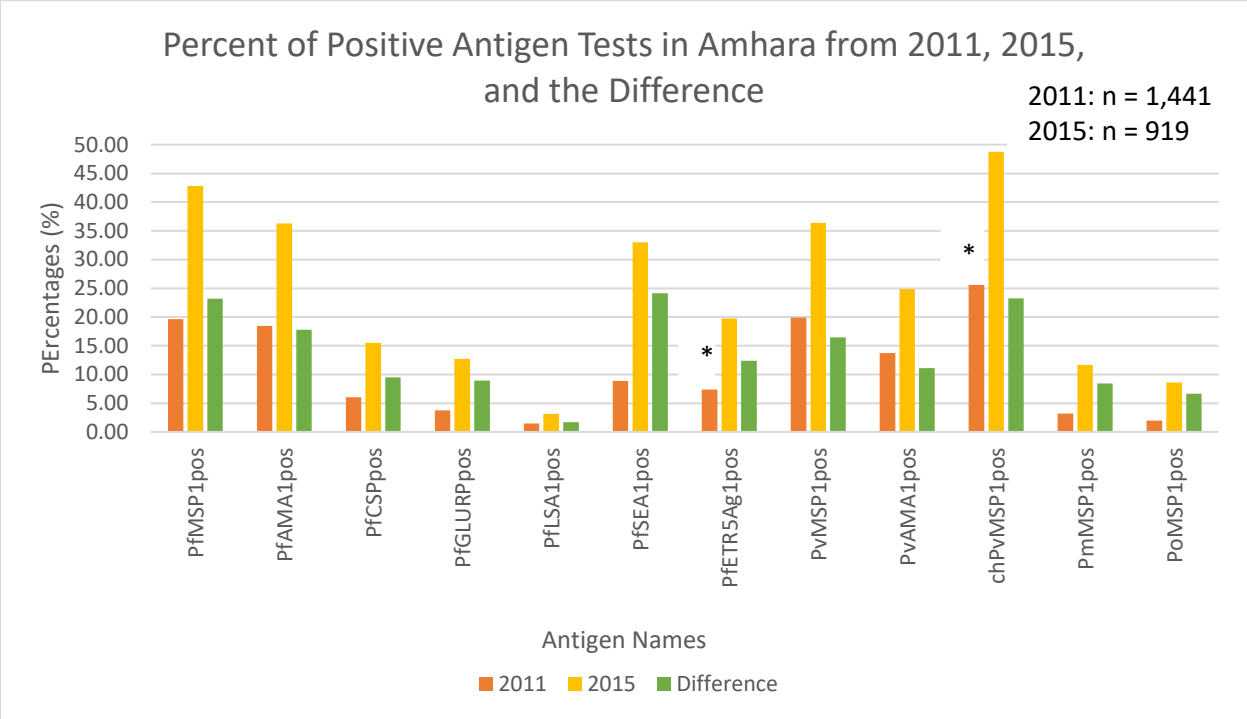

Figure C2: Positive Antigen Test Proportions of Malaria Cases in Amhara, Ethiopia from 2011, 2015, and the Difference Between the Two Years; PfETR5Ag1pos in 2011, n= 584; chPvMSP1pos in 2011, n= 1,440

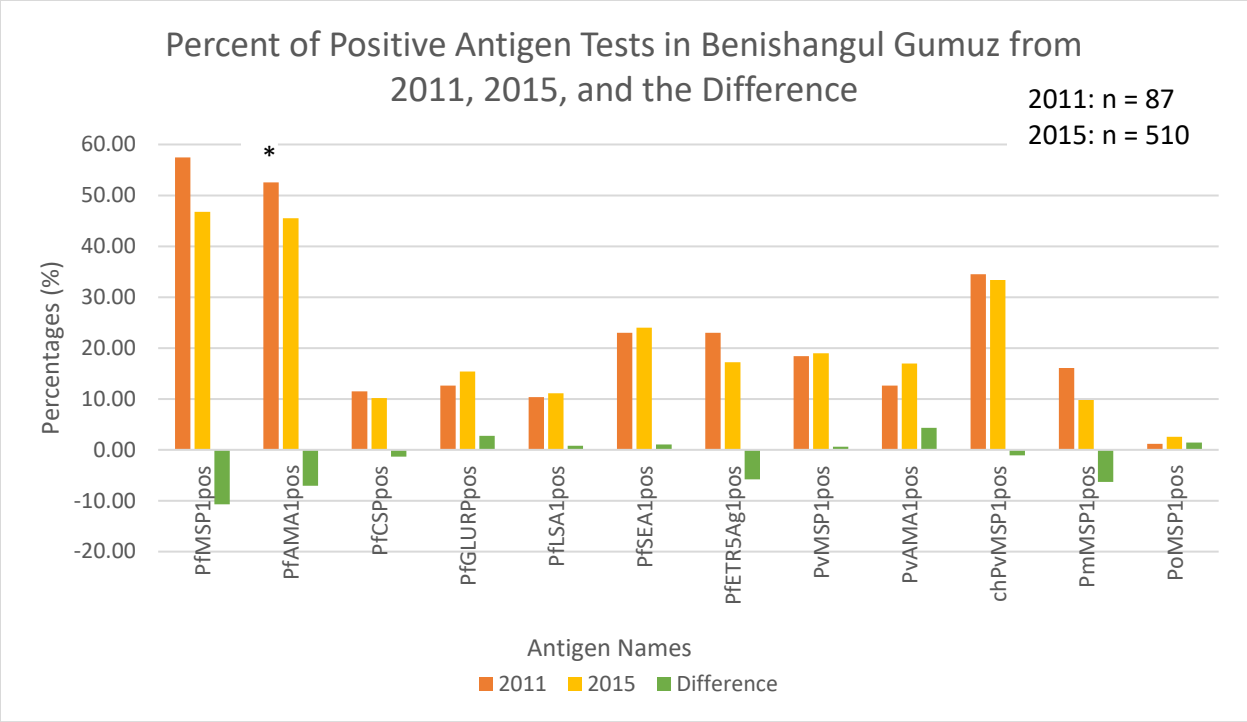

Figure C3: Positive Antigen Test Proportions of Malaria Cases in Benishangul Gumuz, Ethiopia from 2011, 2015, and the Difference Between the Two Years; PfAMA1pos in 2011, n= 86

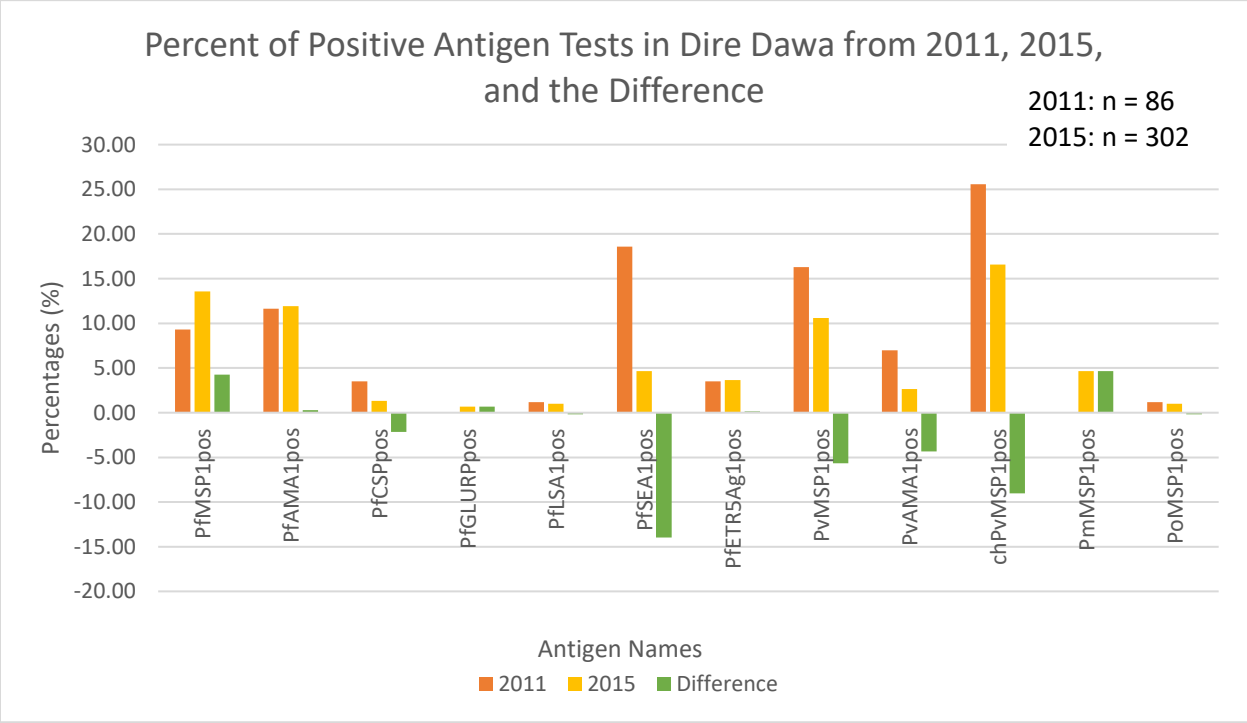

Figure C4: Positive Antigen Test Proportions of Malaria Cases in Dire Dawa, Ethiopia from 2011, 2015, and the Difference Between the Two Years

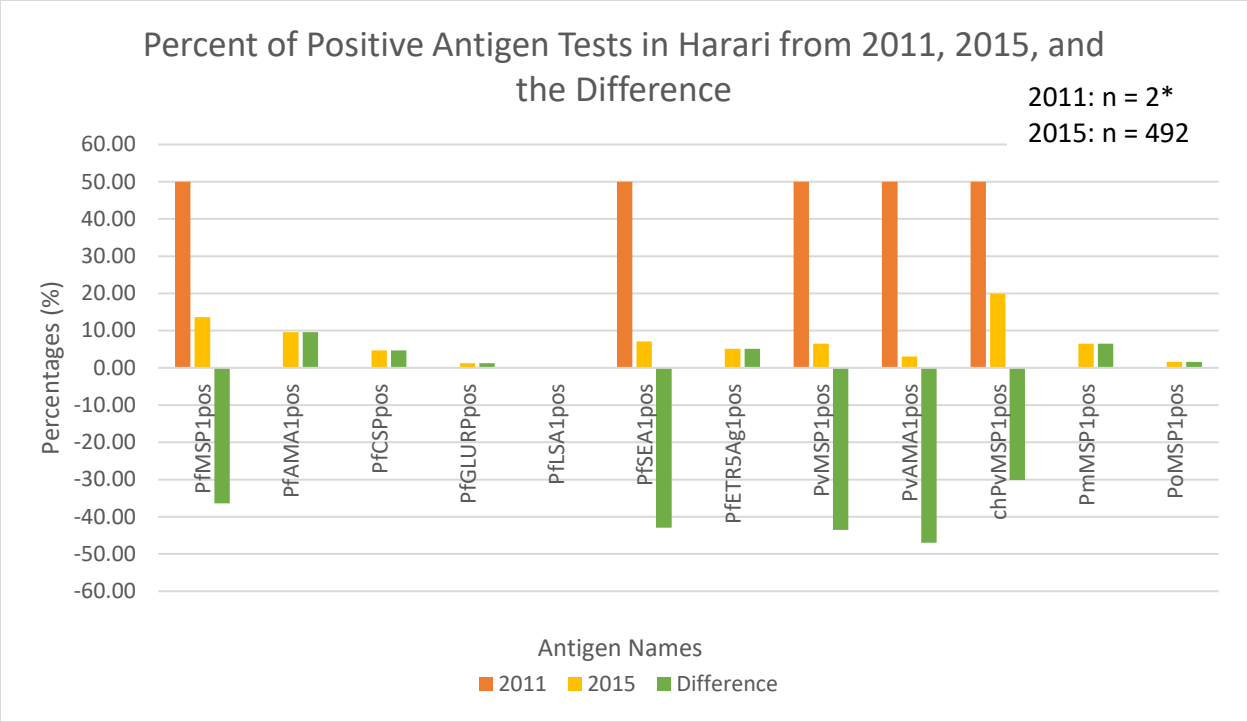

Figure C5: Positive Antigen Test Proportions of Malaria Cases in Harari, Ethiopia from 2011, 2015, and the Difference Between the Two Years *Harari was excluded from analysis due to sample size

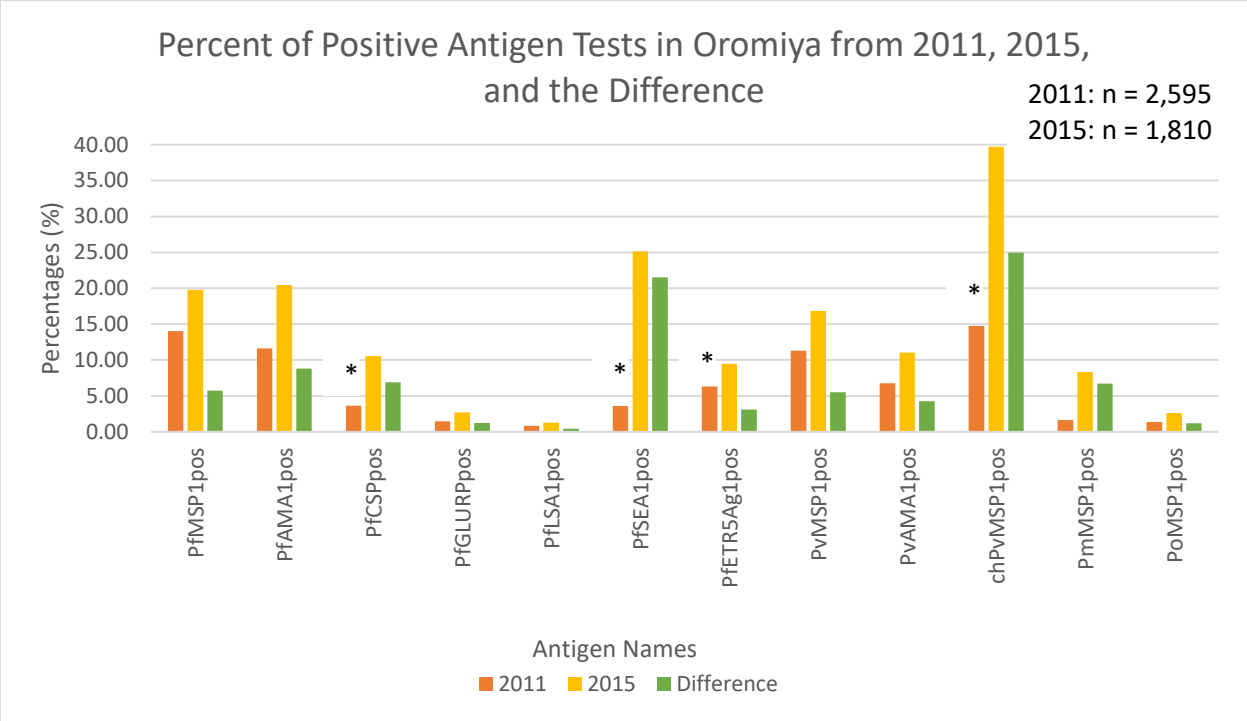

Figure C6: Positive Antigen Test Proportions of Malaria Cases in Oromiya, Ethiopia from 2011, 2015, and the Difference Between the Two Years; PfCSPpos in 2011, n= 2,077; PfSEA1pos in 2011, n= 2,594; PfETR5Ag1pos in 2011, n= 711; chPvMSP1pos in 2011, n= 2,594

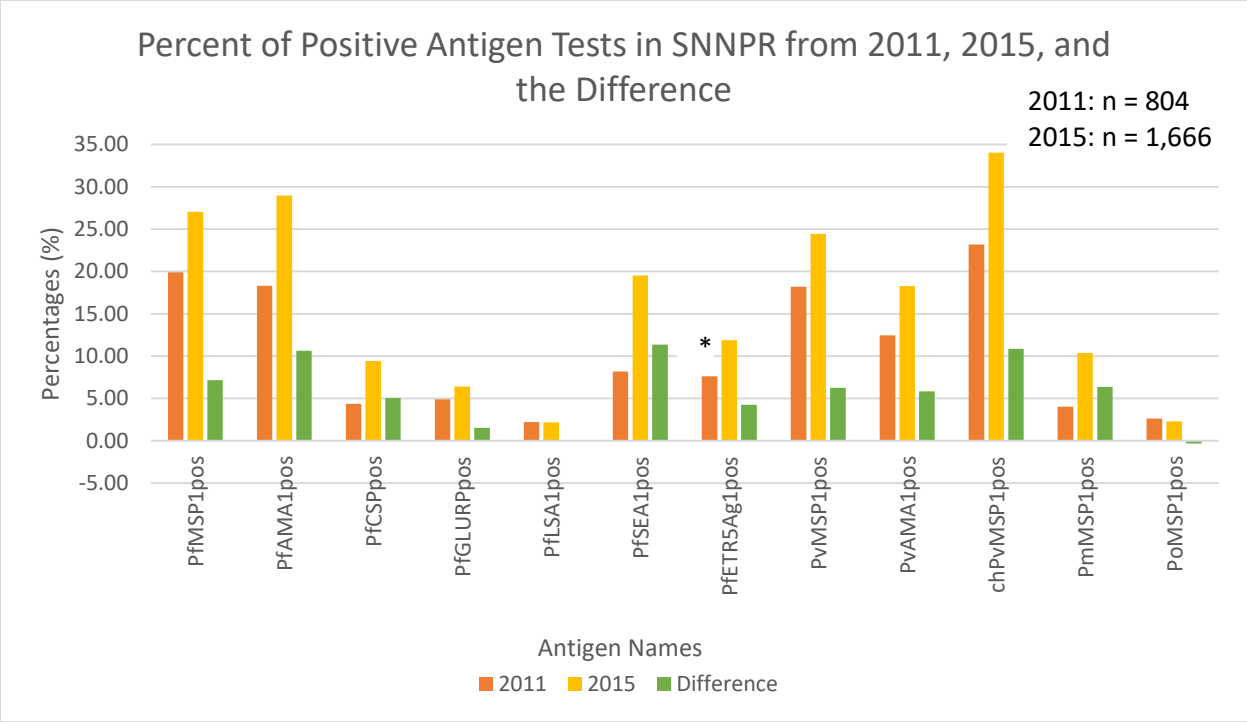

Figure C7: Positive Antigen Test Proportions of Malaria Cases in SNNPR, Ethiopia from 2011, 2015, and the Difference Between the Two Years

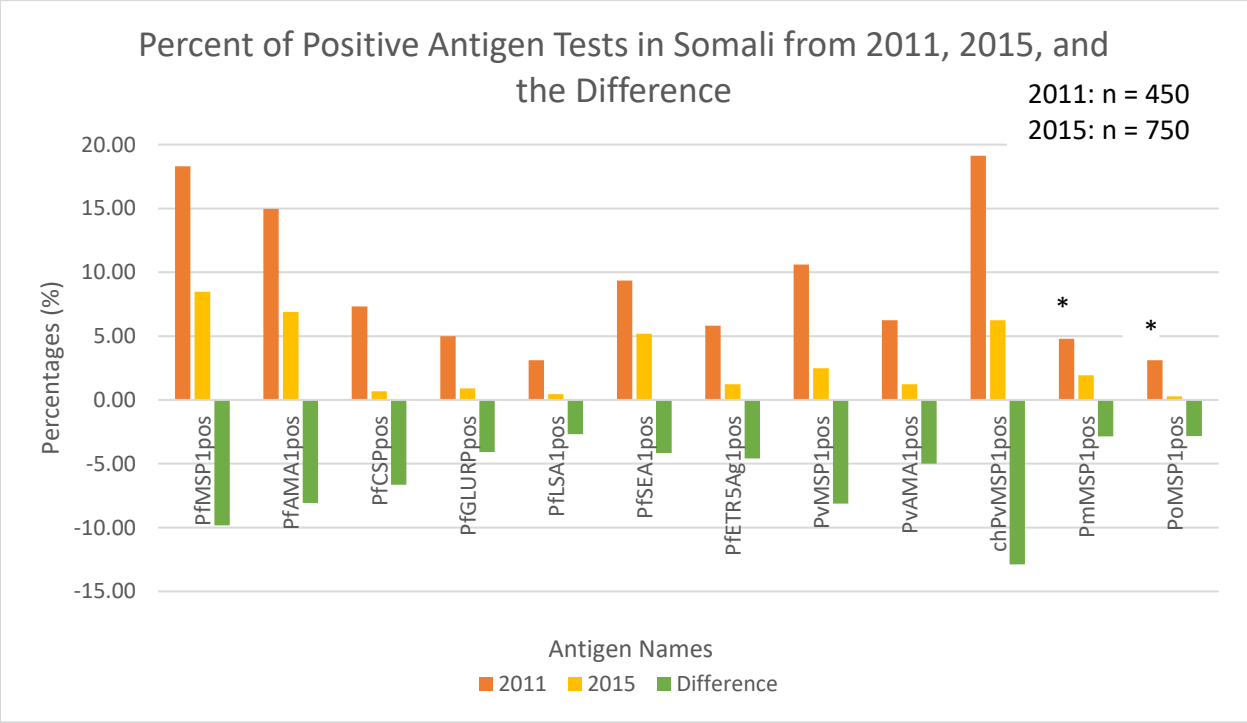

Figure C8: Positive Antigen Test Proportions of Malaria Cases in Somali, Ethiopia from 2011, 2015, and the Difference Between the Two Years; PmMSP1pos in 2011, n= 449; PoMSP1pos in 2011, n= 451

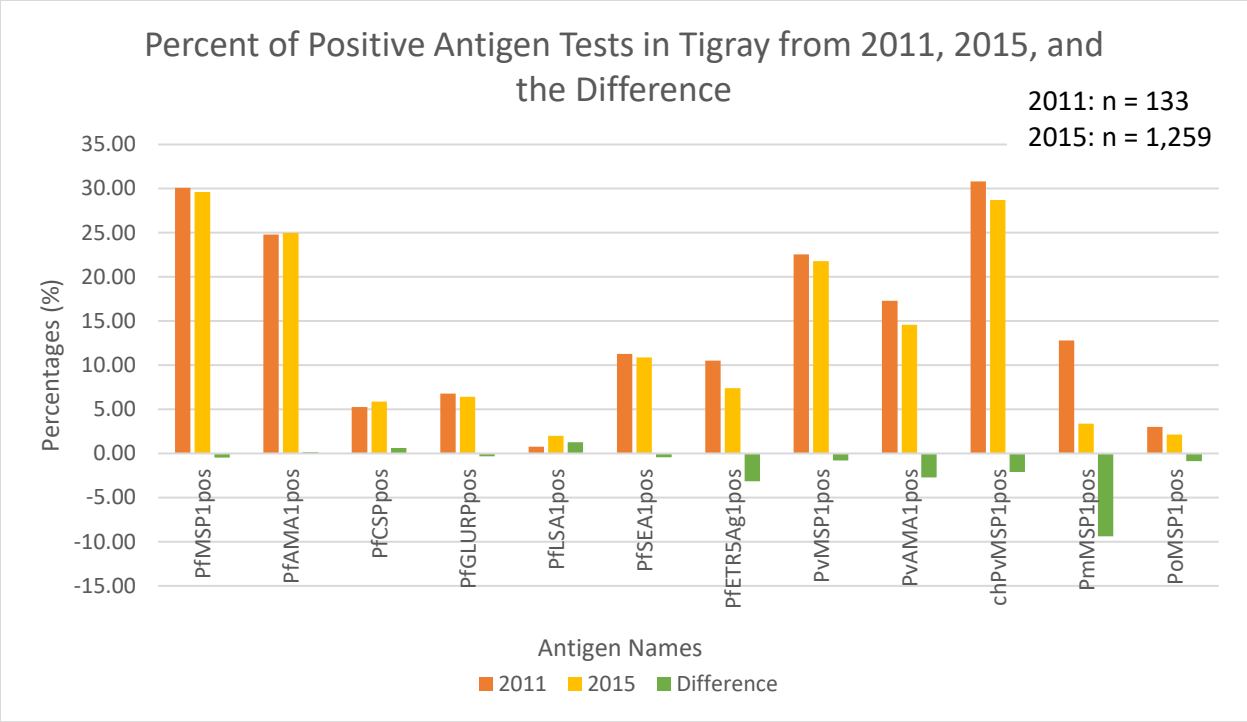

Figure C9: Positive Antigen Test Proportions of Malaria Cases in Tigray, Ethiopia from 2011, 2015, and the Difference Between the Two Years

Appendix D: Geographic Association between Climate Change and Proportions of Positive Antigens

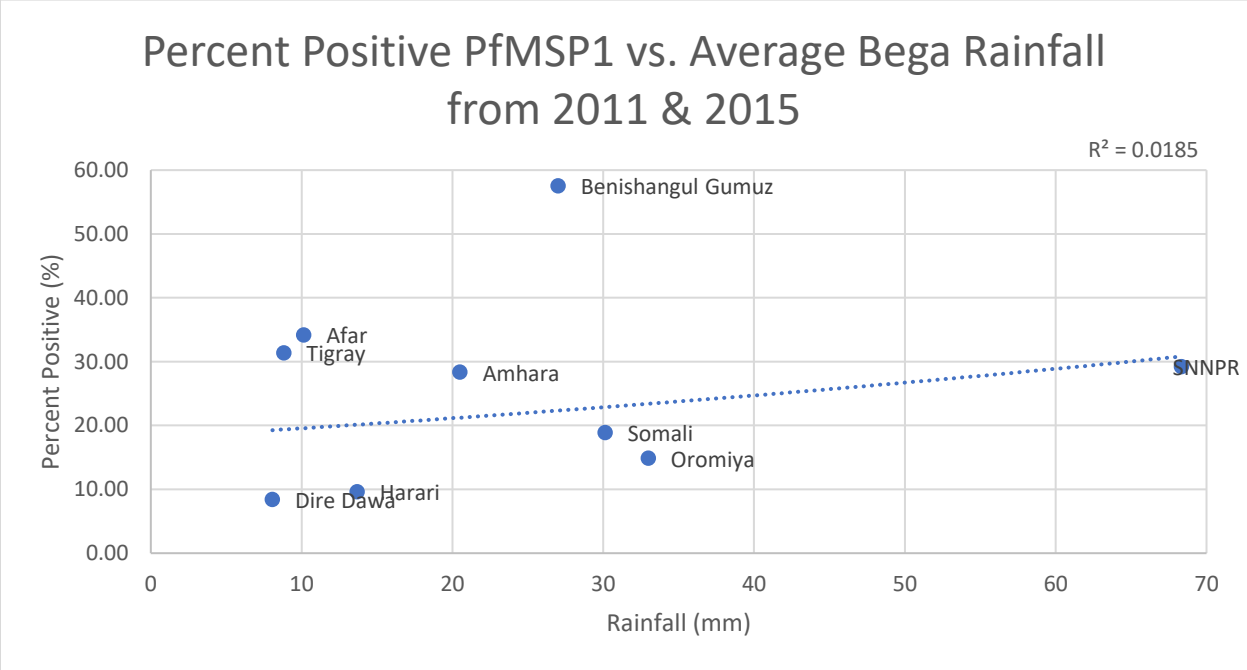

Figure D1: Percent Positive *P. falciparum* merozoite protein 1 Plotted with the 2011 and 2015 Average Bega (October to December) Rainfall for Ethiopia; R^2 = 0.06 from an Exponential Curve.

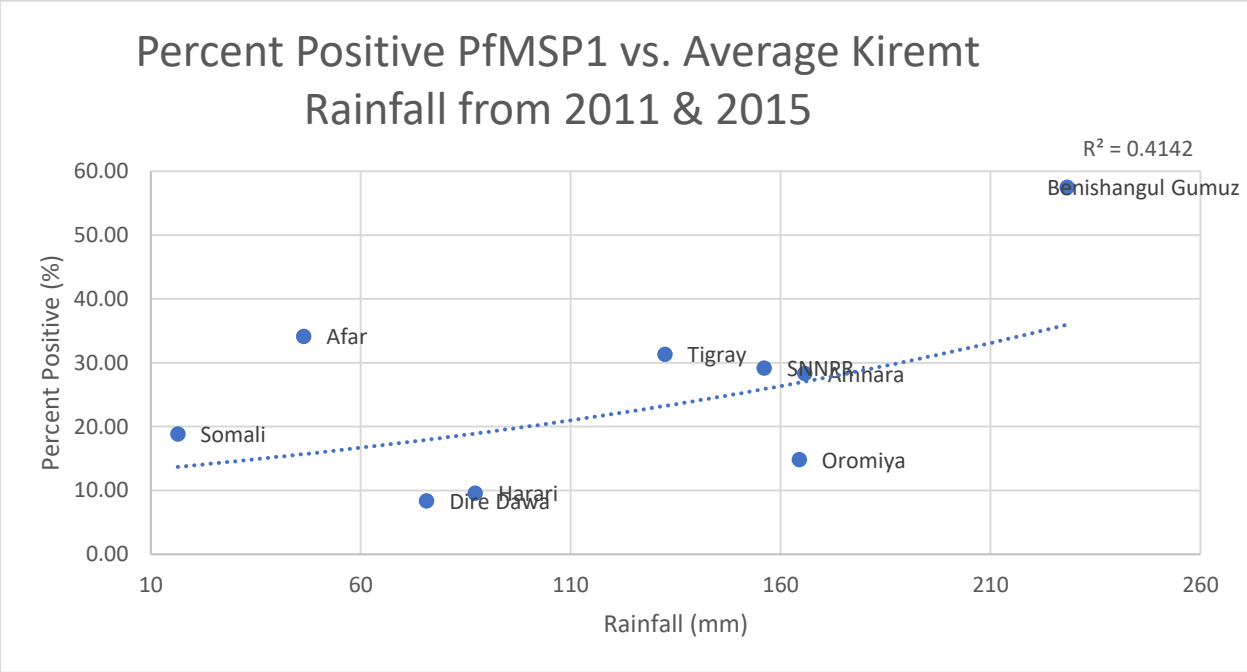

Figure D2: Percent Positive *P. falciparum* merozoite protein 1 Plotted with the 2011 and 2015 Average Kiremt (June to September) Rainfall for Ethiopia; R^2 = 0.24 from an Exponential Curve.

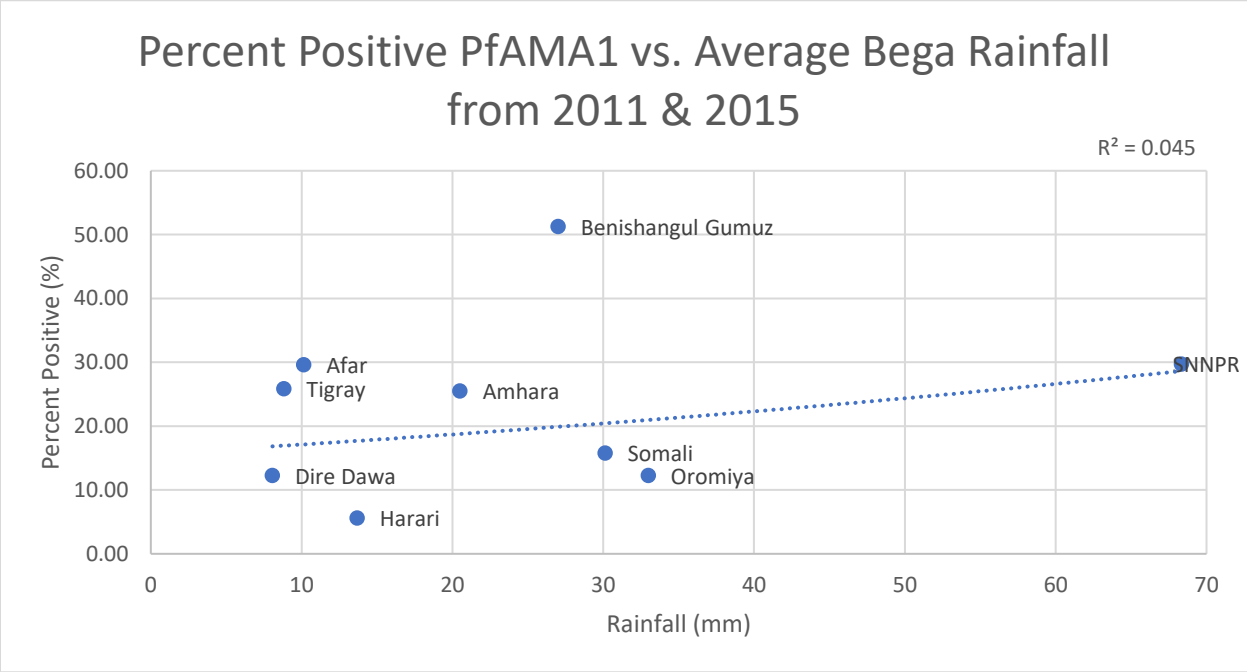

Figure D3: Percent Positive *P. falciparum* apical membrane antigen 1 Plotted with the 2011 and 2015 Average Bega (October to December) Rainfall for Ethiopia; R^2 = 0.06 from an Exponential Curve.

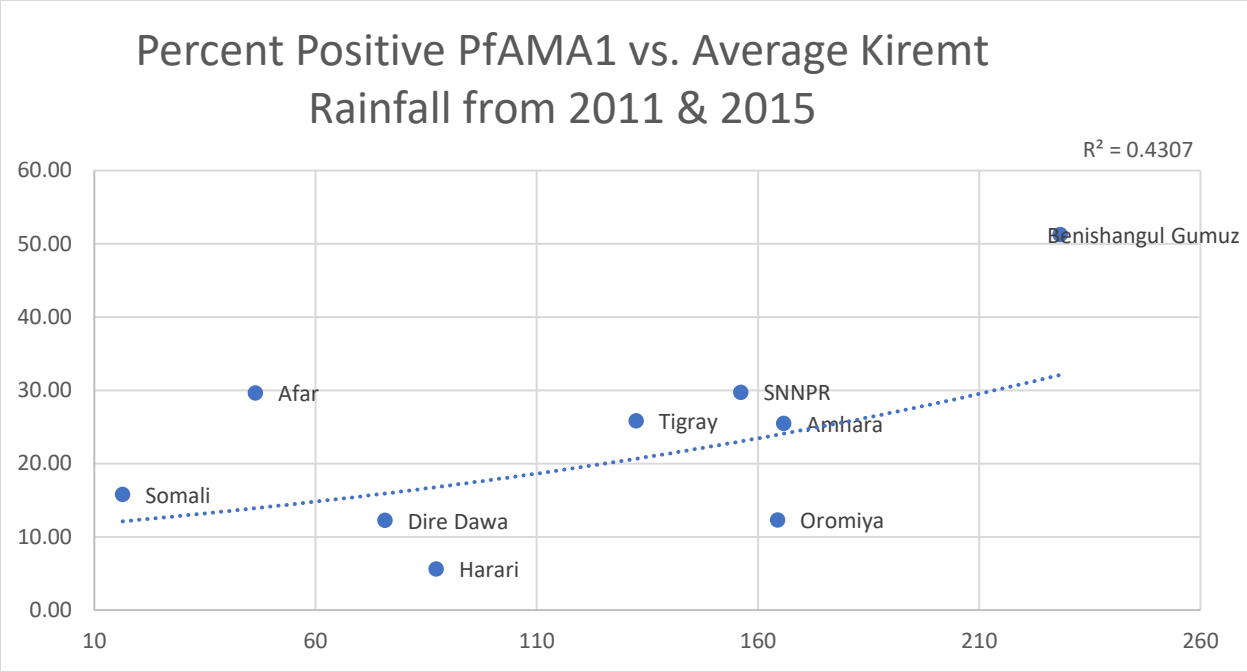

Figure D4: Percent Positive *P. falciparum* apical membrane antigen 1 Plotted with the 2011 and 2015 Average Kiremt (June to September) Rainfall for Ethiopia; R^2 = 0.22 from an Exponential Curve.

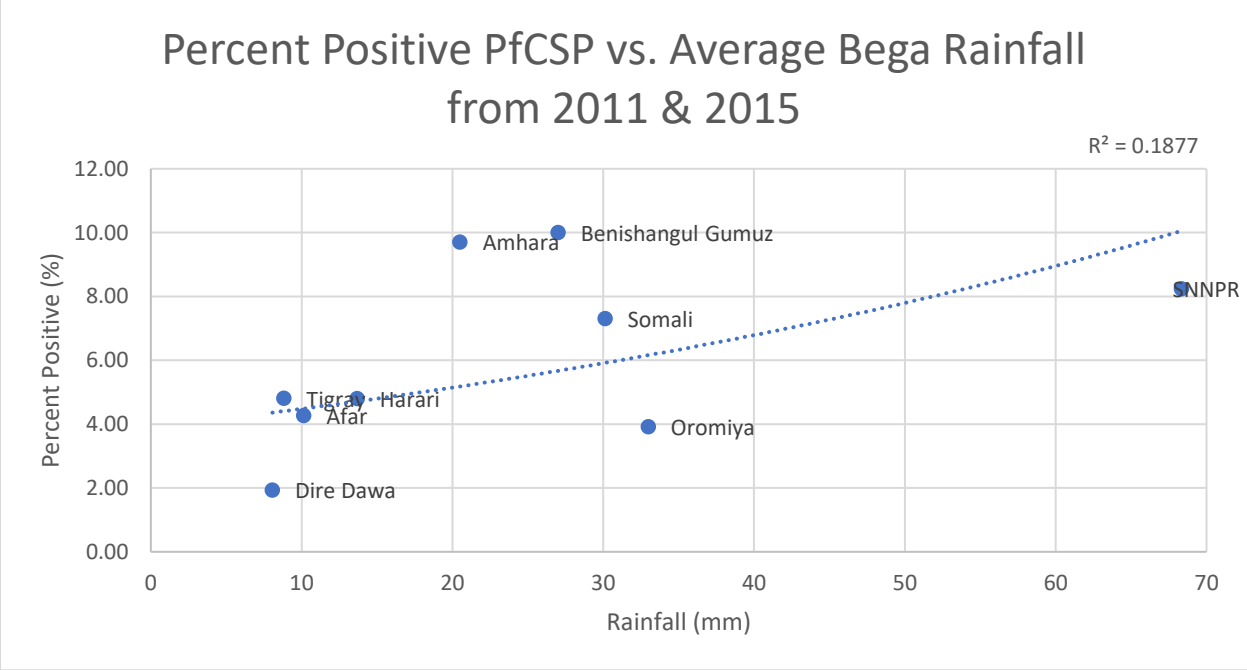

Figure D5: Percent Positive *P. falciparum* circumsporozoite protein Plotted with the 2011 and 2015 Average Bega (October to December) Rainfall for Ethiopia; R^2 = 0.25 from an Exponential Curve.

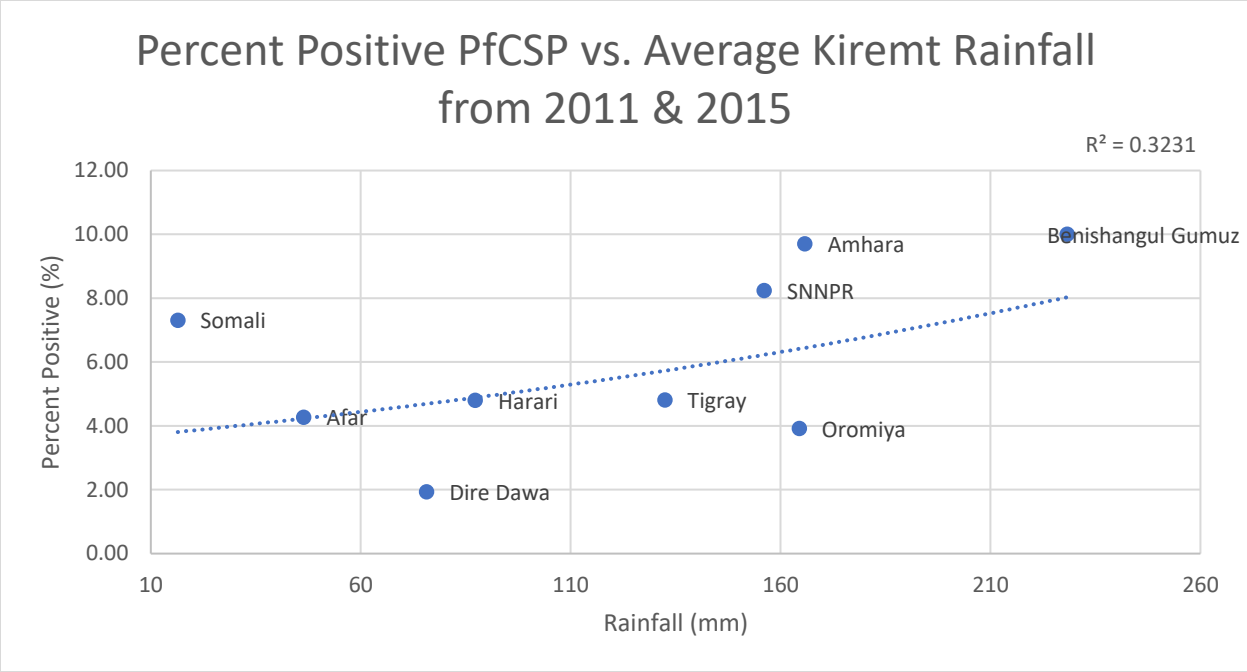

Figure D6: Percent Positive *P. falciparum* circumsporozoite protein Plotted with the 2011 and 2015 Average Kiremt (June to September) Rainfall for Ethiopia; R^2 = 0.20 from an Exponential Curve.

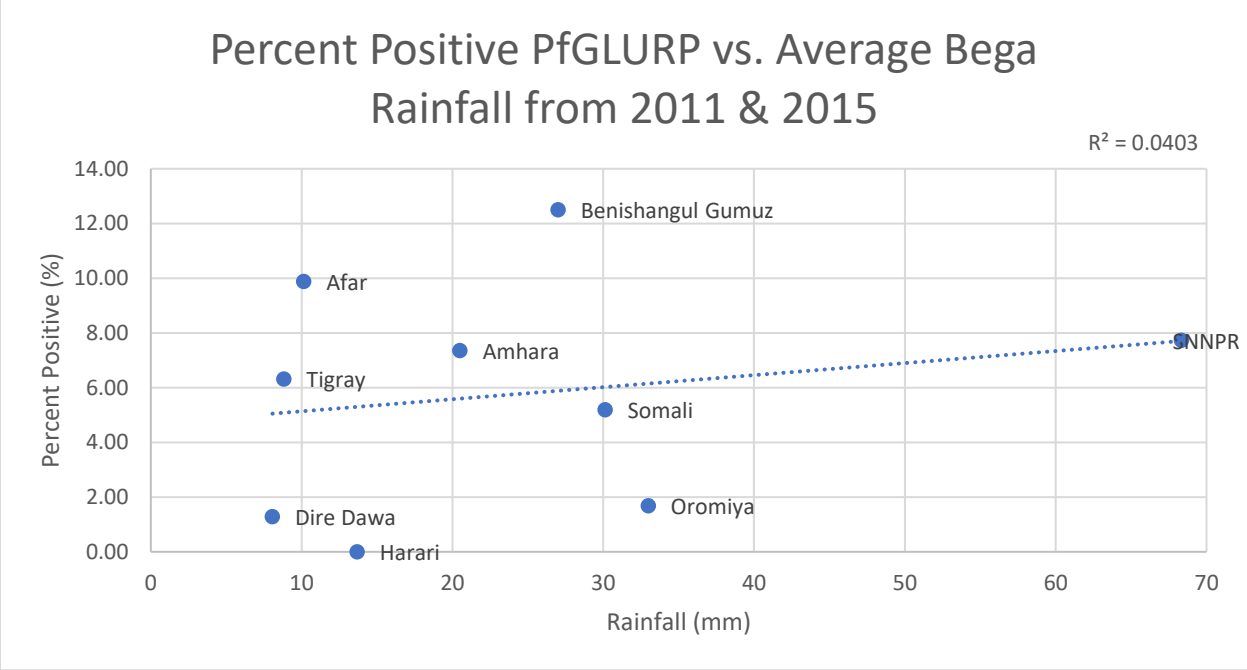

Figure D7: Percent Positive *P. falciparum* glutamate-rich protein, Ro fragment Plotted with the 2011 and 2015 Average Bega (October to December) Rainfall for Ethiopia; R^2 = 0.04 from an Exponential Curve.

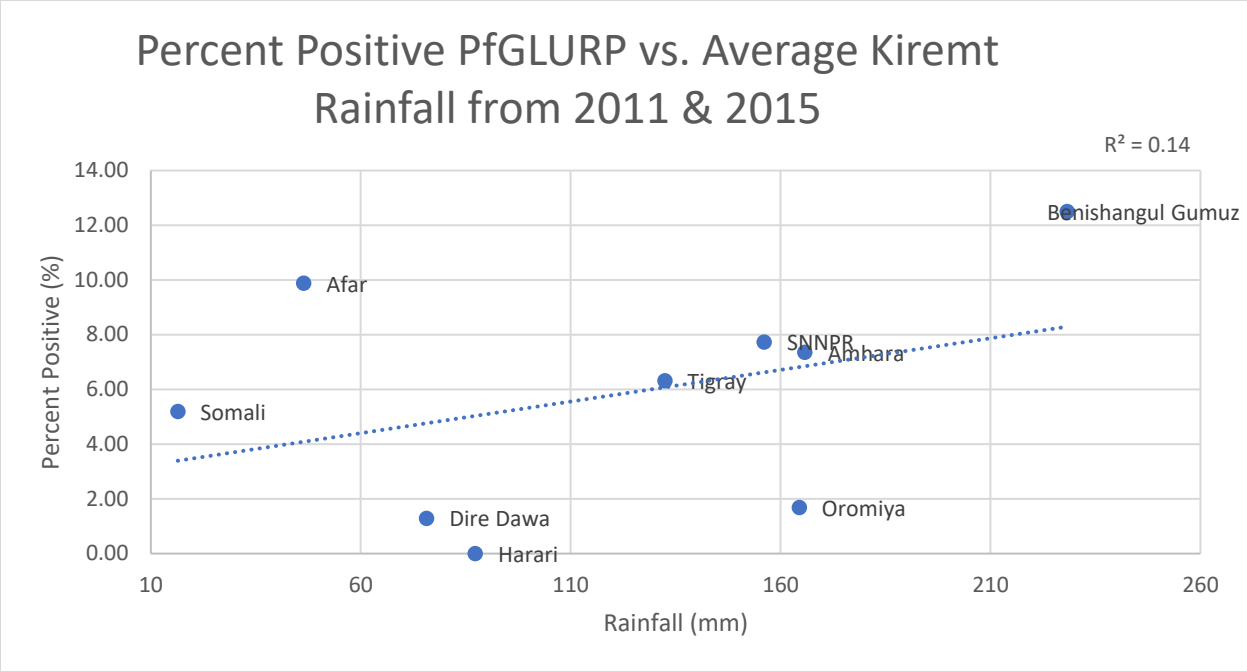

Figure D8: Percent Positive *P. falciparum* glutamate-rich protein, Ro fragment Plotted with the 2011 and 2015 Average Kiremt (June to September) Rainfall for Ethiopia; R^2 = 0.14 from an Exponential Curve.

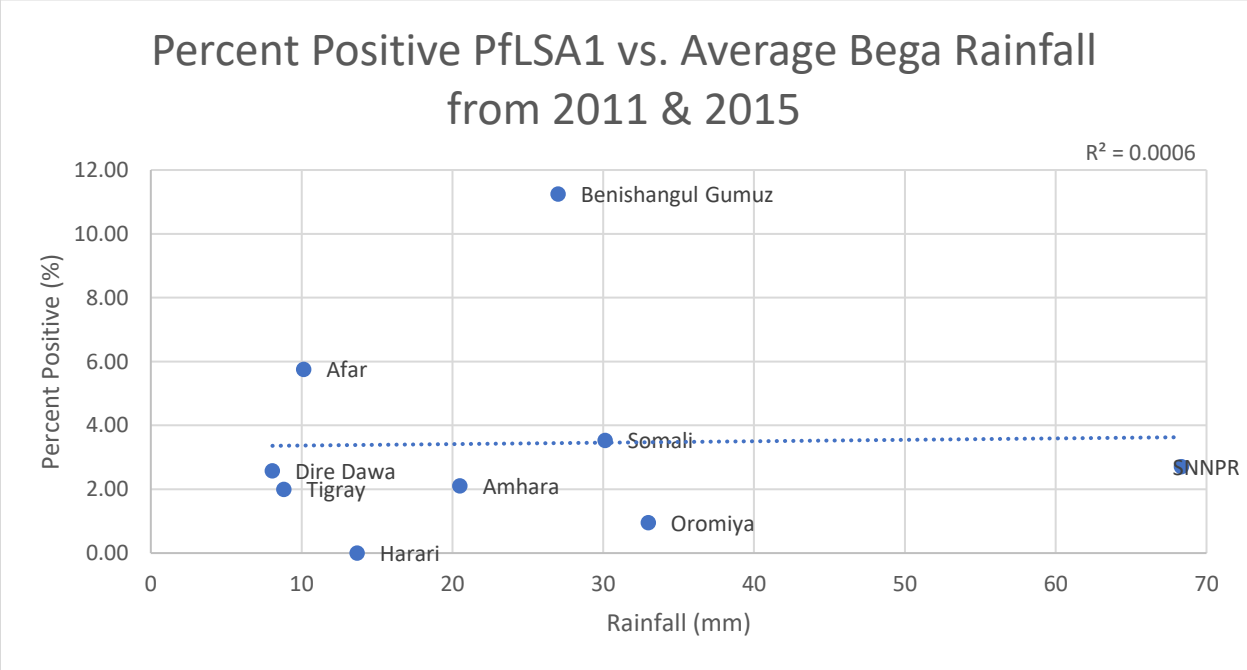

Figure D9: Percent Positive *P. falciparum* liver stage antigen 1 Plotted with the 2011 and 2015 Average Bega (October to December) Rainfall for Ethiopia; R^2 = 0.0006 from an Exponential Curve.

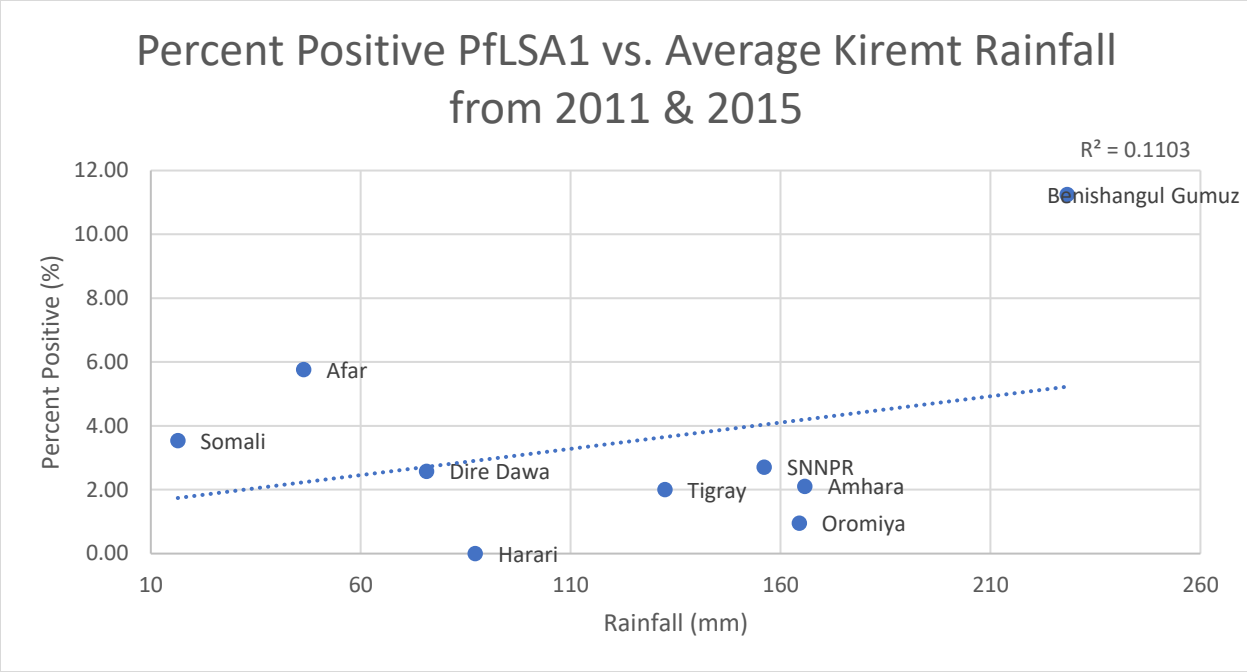

Figure D10: Percent Positive *P. falciparum* liver stage antigen 1 Plotted with the 2011 and 2015 Average Kiremt (June to September) Rainfall for Ethiopia; R^2 = 0.11 from an Exponential Curve.

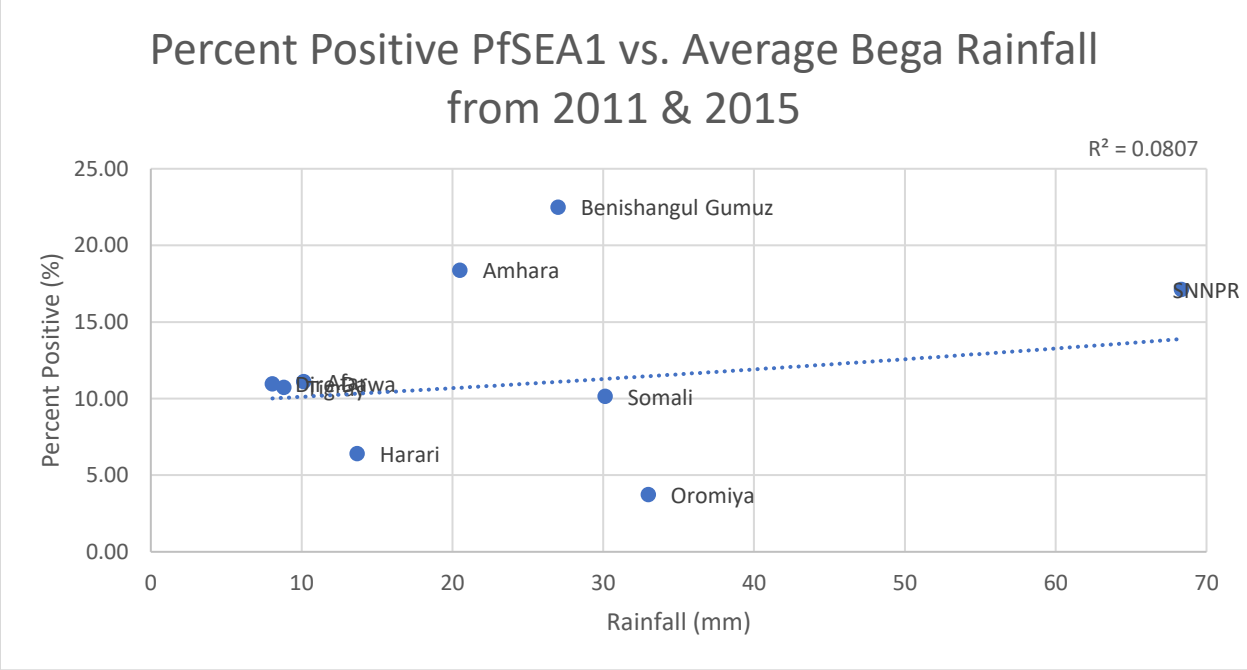

Figure D11: Percent Positive *P. falciparum* schizont egress antigen 1 Plotted with the 2011 and 2015 Average Bega (October to December) Rainfall for Ethiopia; R^2 = 0.03 from an Exponential Curve.

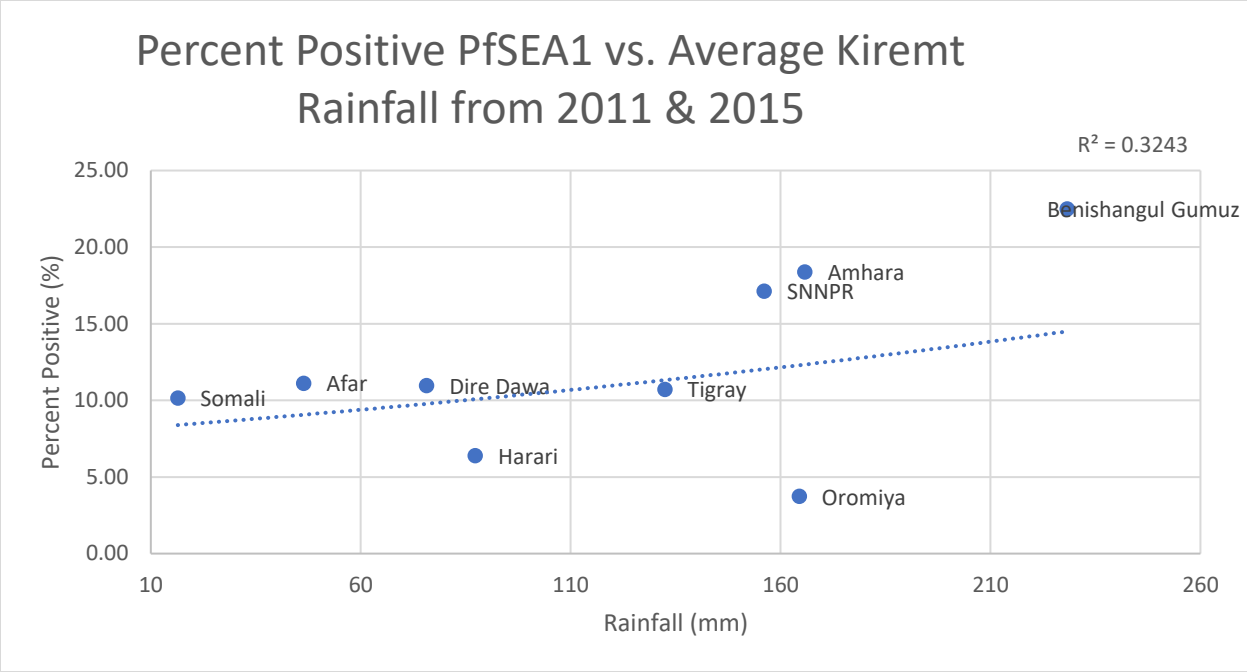

Figure D12: Percent Positive *P. falciparum* schizont egress antigen 1 Plotted with the 2011 and 2015 Average Kiremt (June to September) Rainfall for Ethiopia; R^2 = 0.10 from an Exponential Curve.

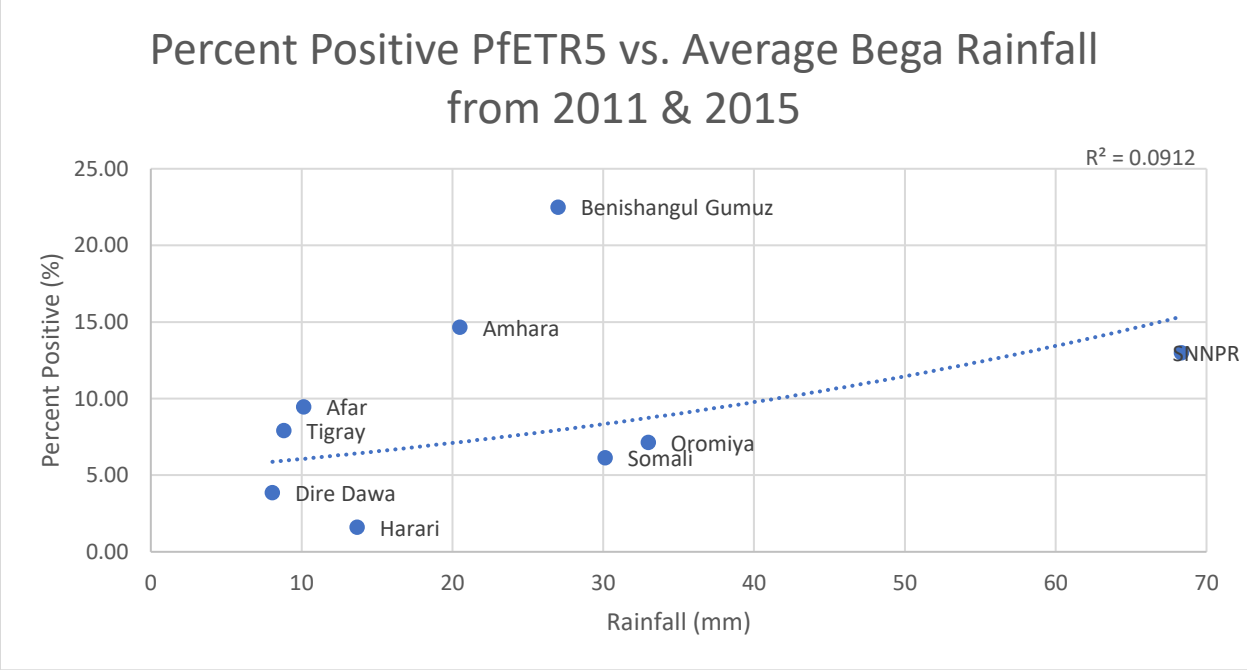

Figure D13: Percent Positive *P. falciparum* ETRAMP 5 antigen 1 Plotted with the 2011 and 2015 Average Bega (October to December) Rainfall for Ethiopia; R^2 = 0.15 from an Exponential Curve.

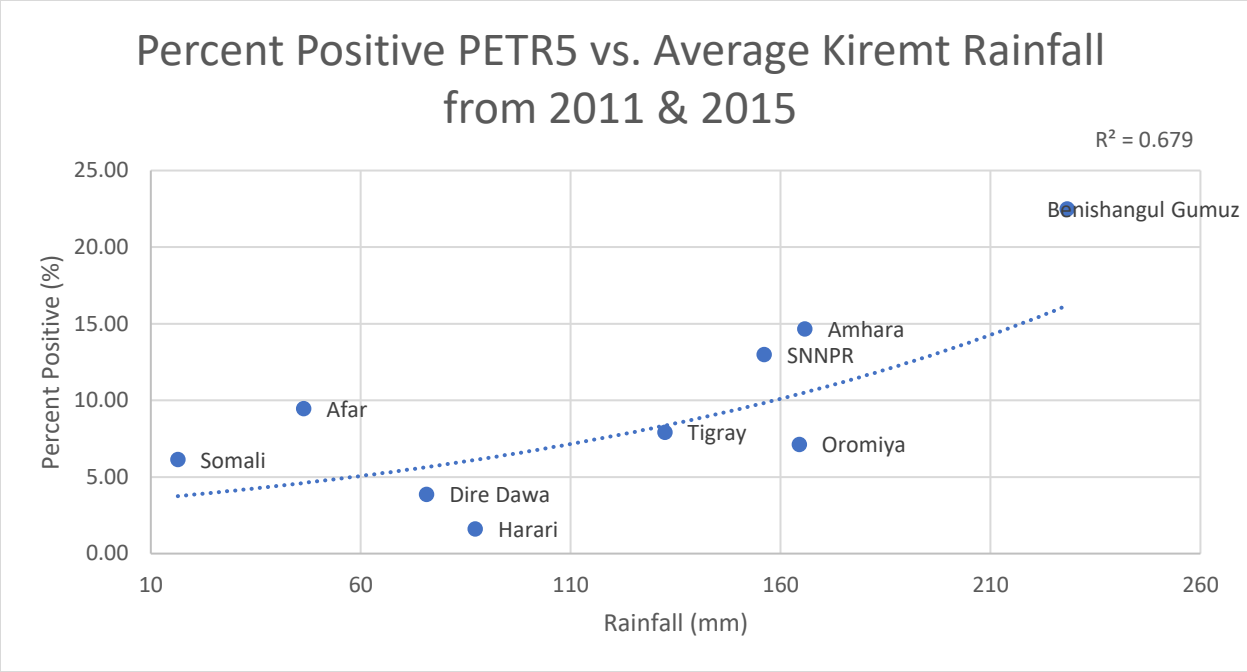

Figure D14: Percent Positive *P. falciparum* ETRAMP 5 antigen 1 Plotted with the 2011 and 2015 Average Kiremt (June to September) Rainfall for Ethiopia; R^2 = 0.36 from an Exponential Curve.

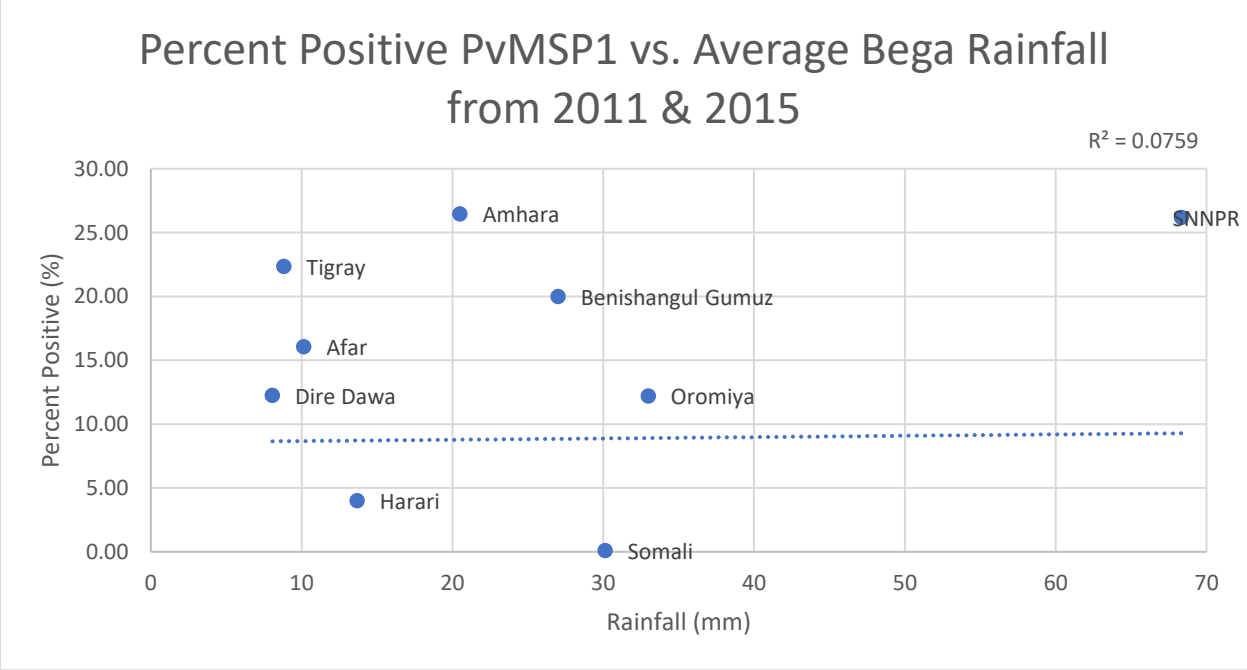

Figure D15: Percent Positive *P. vivax* merozoite protein 1 Plotted with the 2011 and 2015 Average Bega (October to December) Rainfall for Ethiopia; R^2 = 0.0002 from an Exponential Curve.

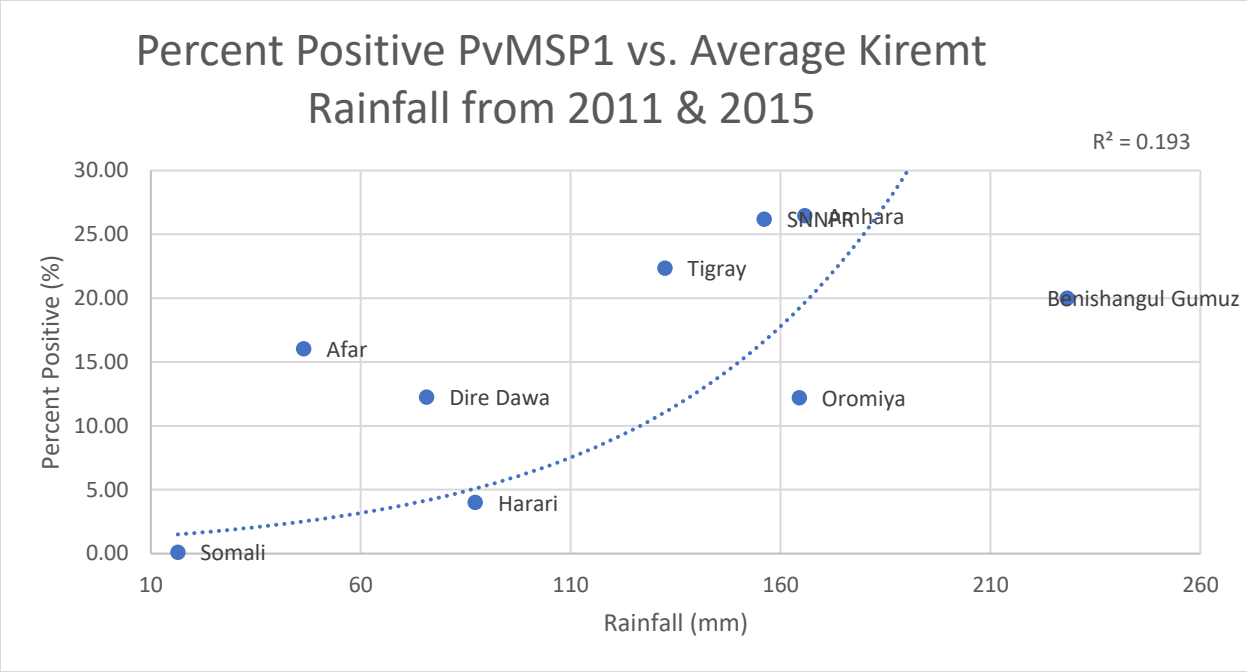

Figure D16: Percent Positive *P. vivax* merozoite protein 1 Plotted with the 2011 and 2015 Average Kiremt (June to September) Rainfall for Ethiopia; R^2 = 0.44 from an Exponential Curve.

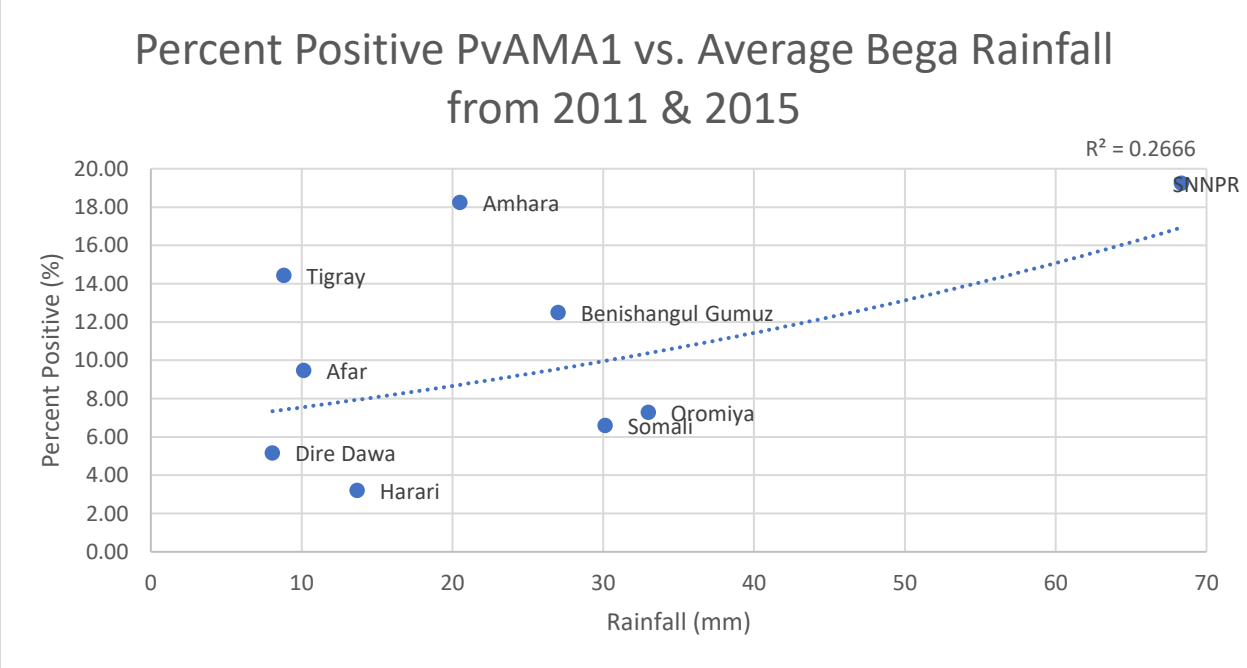

Figure D17: Percent Positive *P. vivax* apical membrane antigen 1 Plotted with the 2011 and 2015 Average Bega (October to December) Rainfall for Ethiopia; R^2 = 0.19 from an Exponential Curve.

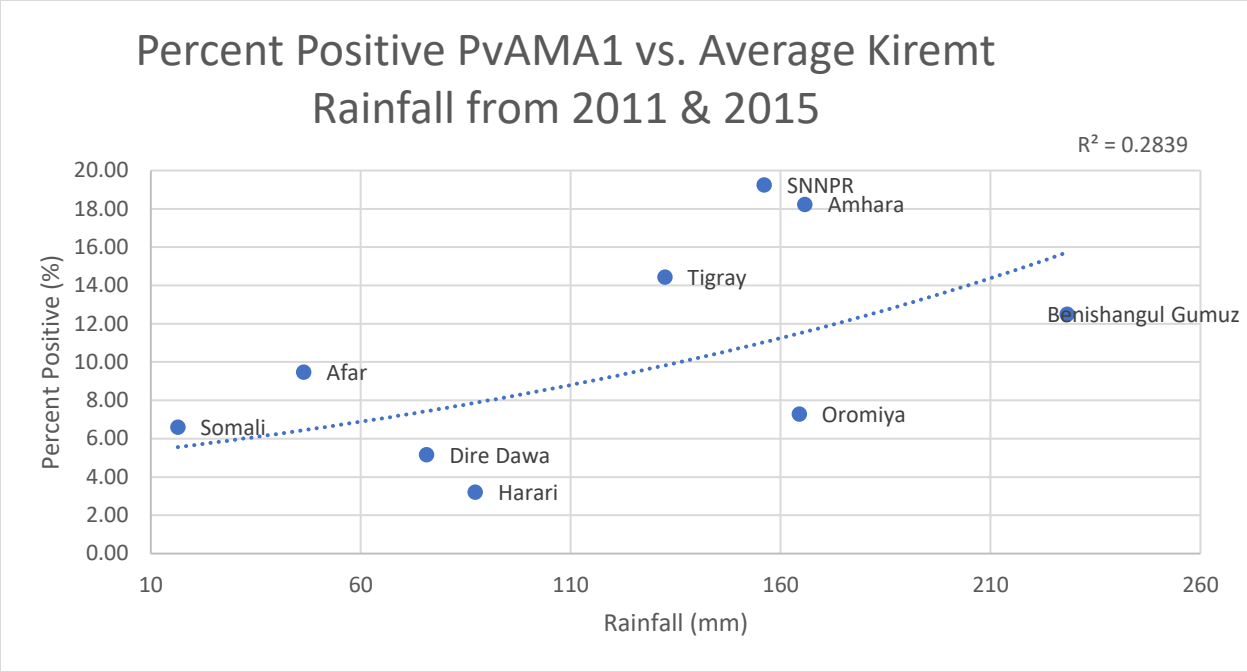

Figure D18: Percent Positive *P. vivax* apical membrane antigen 1 Plotted with the 2011 and 2015 Average Kiremt (June to September) Rainfall for Ethiopia; R^2 = 0.30 from an Exponential Curve.

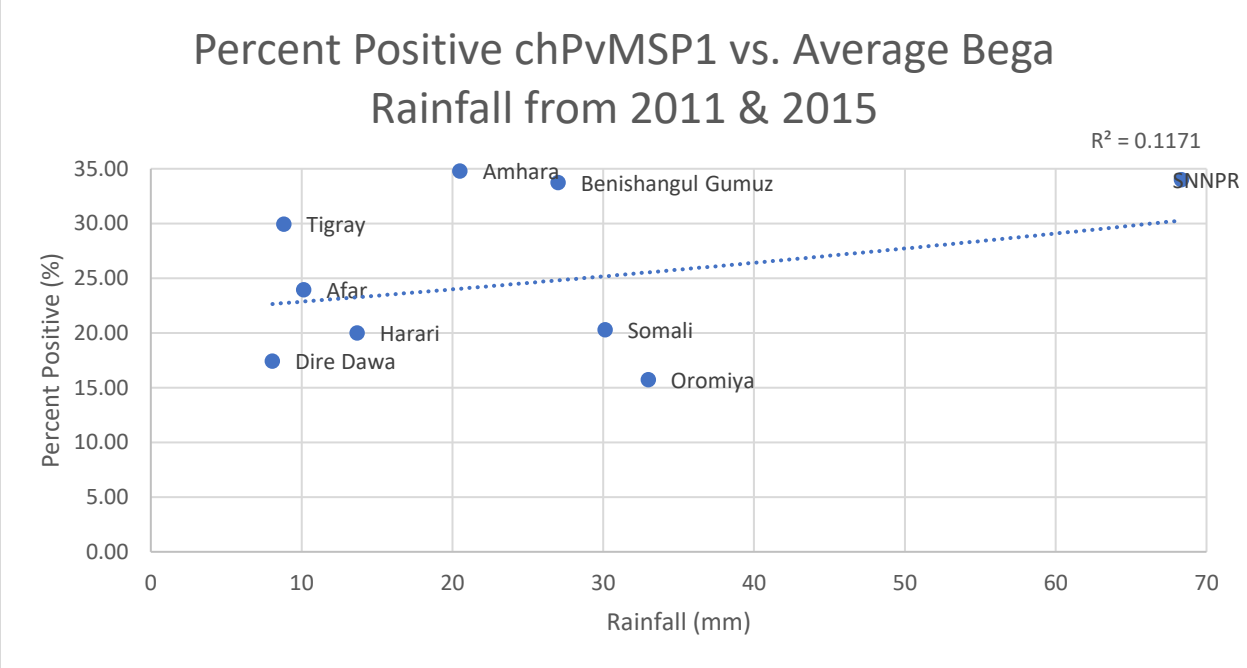

Figure D19: Percent Positive chimeric *P. vivax* merozoite protein 1, including additional B and T cell epitopes Plotted with the 2011 and 2015 Average Bega (October to December) Rainfall for Ethiopia; R^2 = 0.09 from an Exponential Curve.

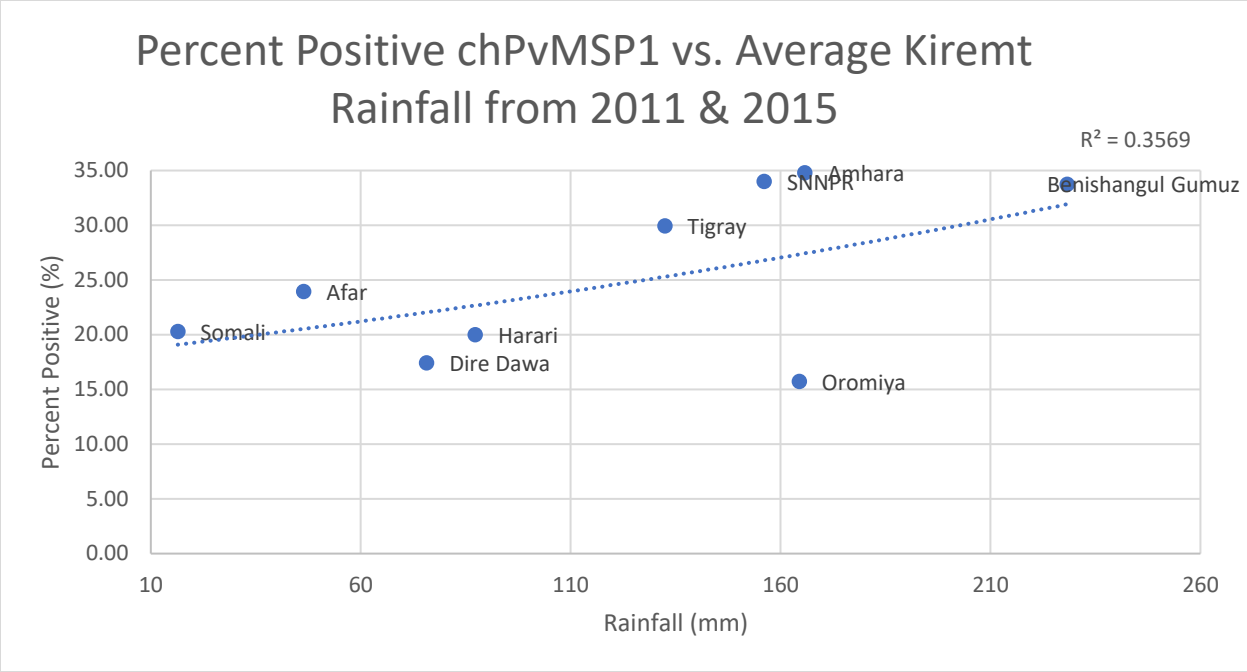

Figure D20: Percent Positive chimeric *P. vivax* merozoite protein 1, including additional B and T cell epitopes Plotted with the 2011 and 2015 Average Kiremt (June to September) Rainfall for Ethiopia; R^2 = 0.28 from an Exponential Curve.

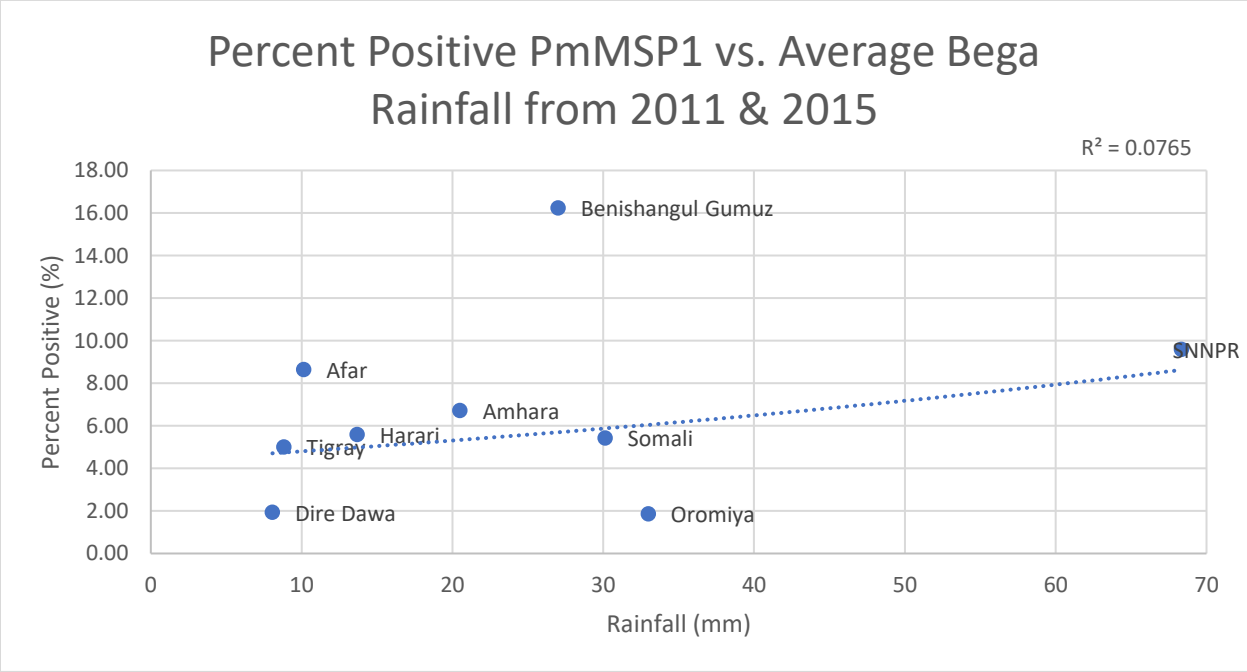

Figure D21: Percent Positive *P. malariae* merozoite protein 1 Plotted with the 2011 and 2015 Average Bega (October to December) Rainfall for Ethiopia; R^2 = 0.07 from an Exponential Curve.

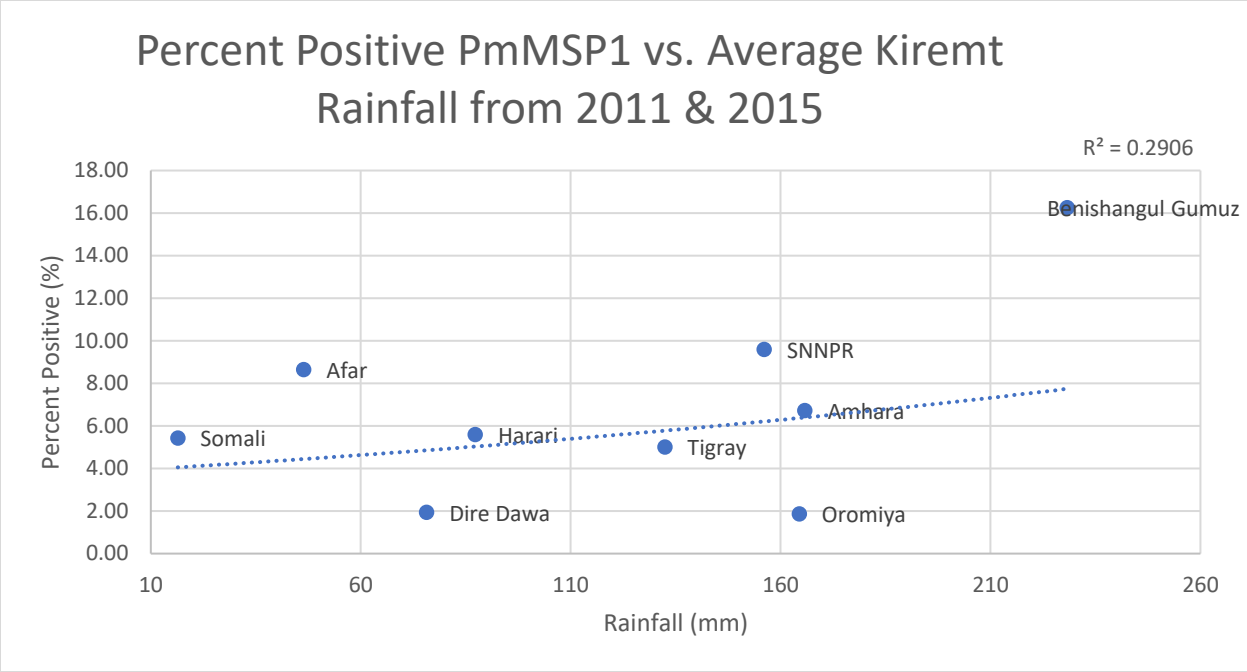

Figure D22: Percent Positive *P. malariae* merozoite protein 1 Plotted with the 2011 and 2015 Average Kiremt (June to September) Rainfall for Ethiopia; R^2 = 0.09 from an Exponential Curve.

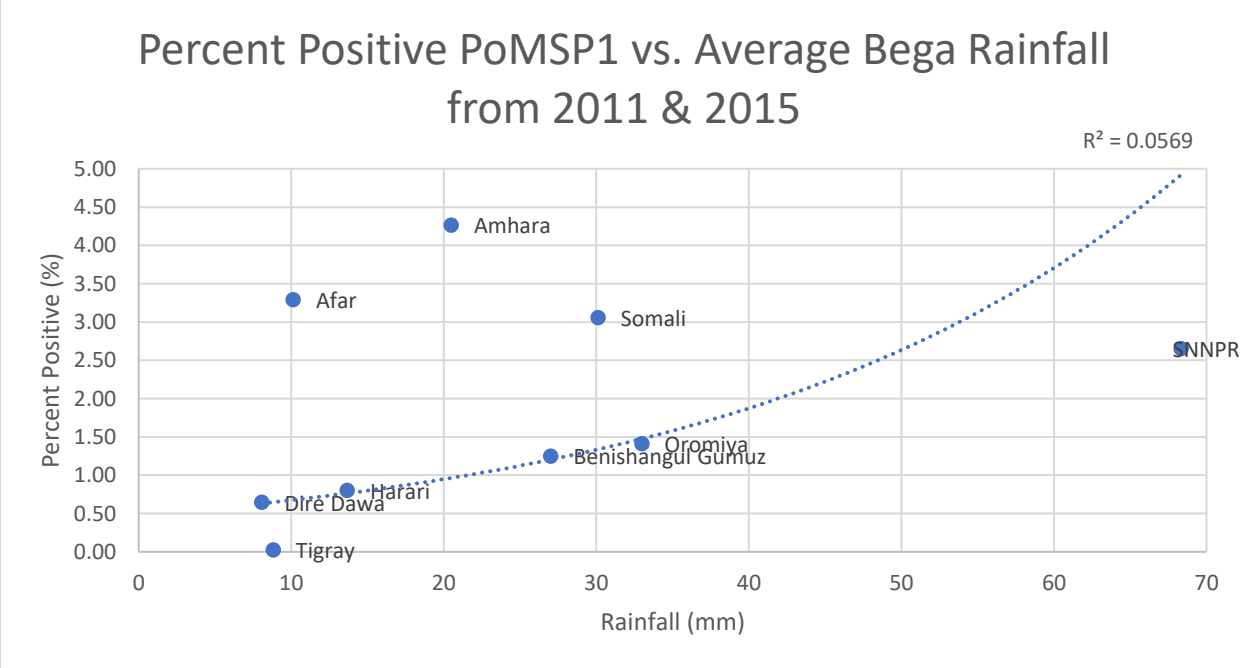

Figure D23: Percent Positive *P. ovale* merozoite protein 1 Plotted with the 2011 and 2015 Average Bega (October to December) Rainfall for Ethiopia; R^2 = 0.17 from an Exponential Curve.

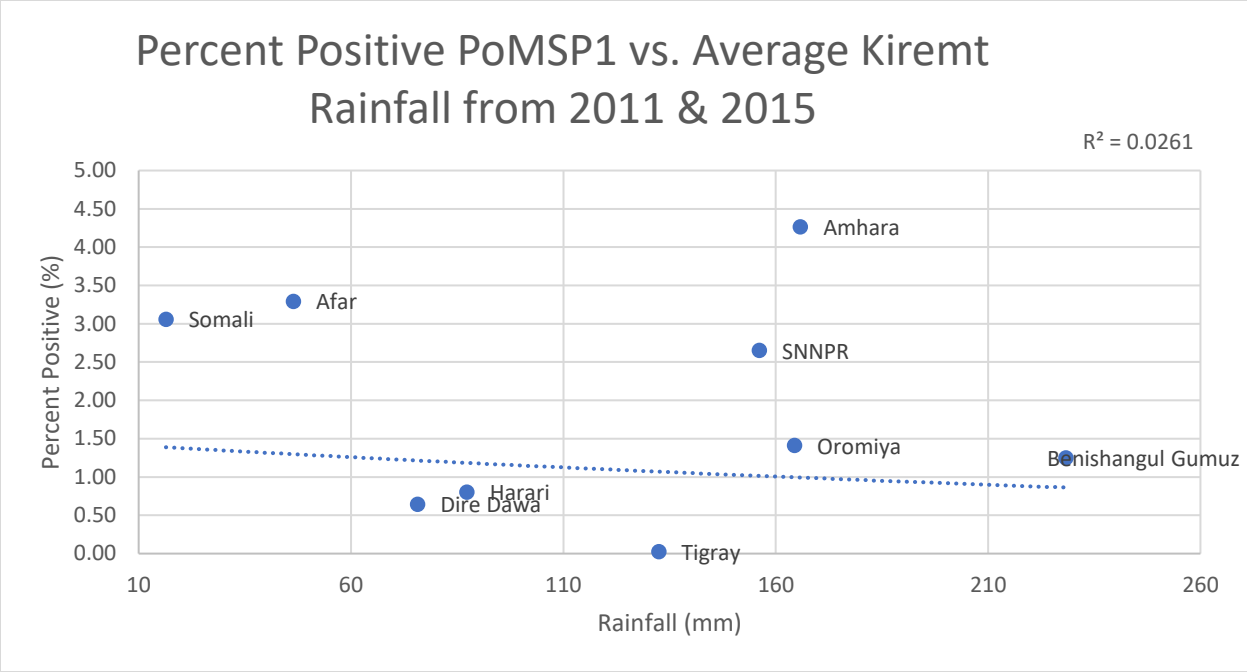

Figure D24: Percent Positive *P. ovale* merozoite protein 1 Plotted with the 2011 and 2015 Average Kiremt (June to September) Rainfall for Ethiopia; R^2 = 0.009 from an Exponential Curve.

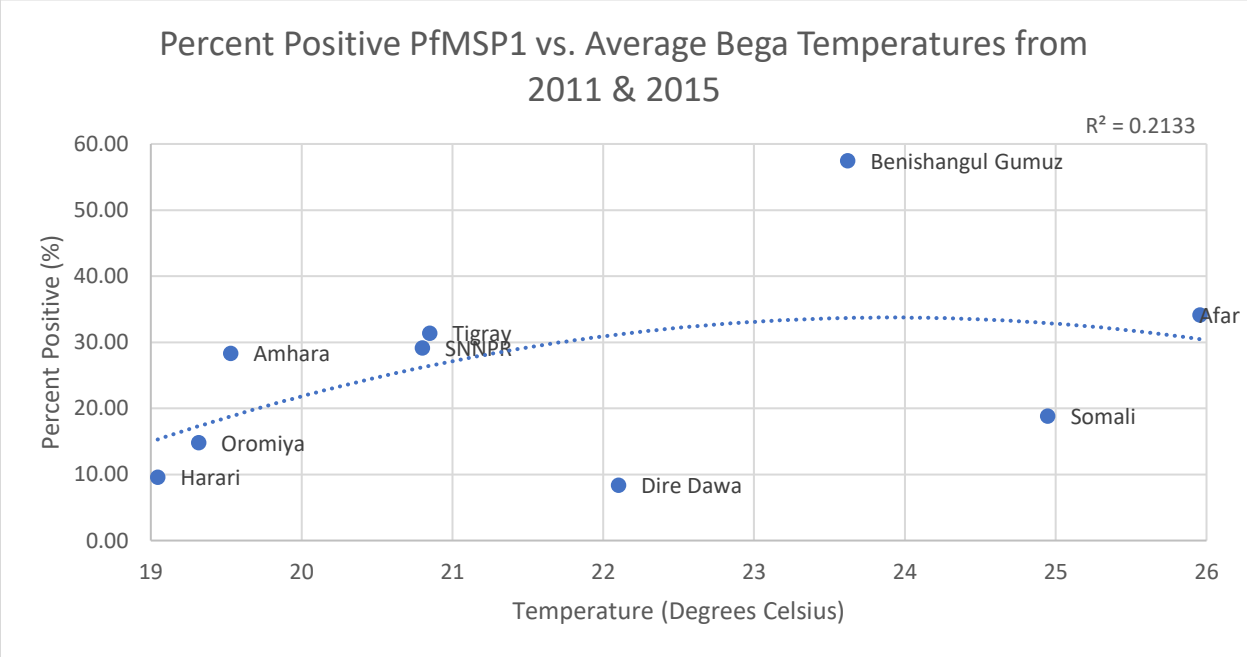

Figure D25: Percent Positive *P. falciparum* merozoite protein 1 Plotted with the 2011 and 2015 Average Bega (October to December) Temperatures for Ethiopia; R^2 = 0.21 from a Polynomial Curve.

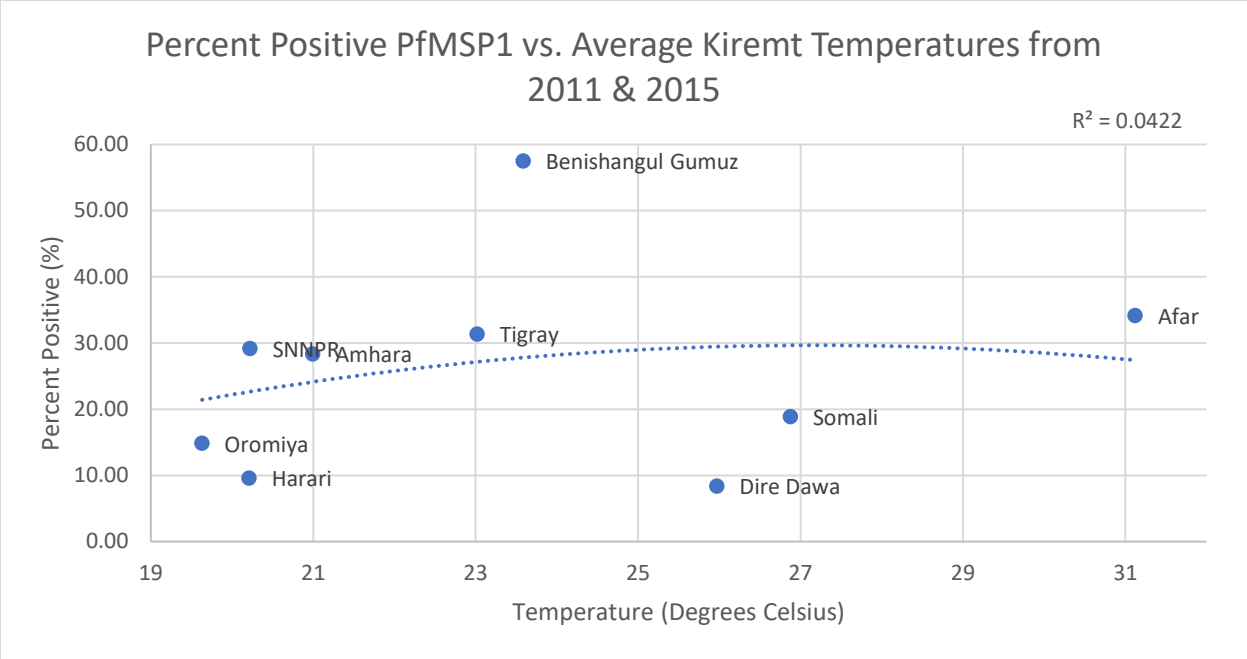

Figure D26: Percent Positive *P. falciparum* merozoite protein 1 Plotted with the 2011 and 2015 Average Kiremt (June to September) Temperatures for Ethiopia; R^2 = 0.04 from a Polynomial Curve.

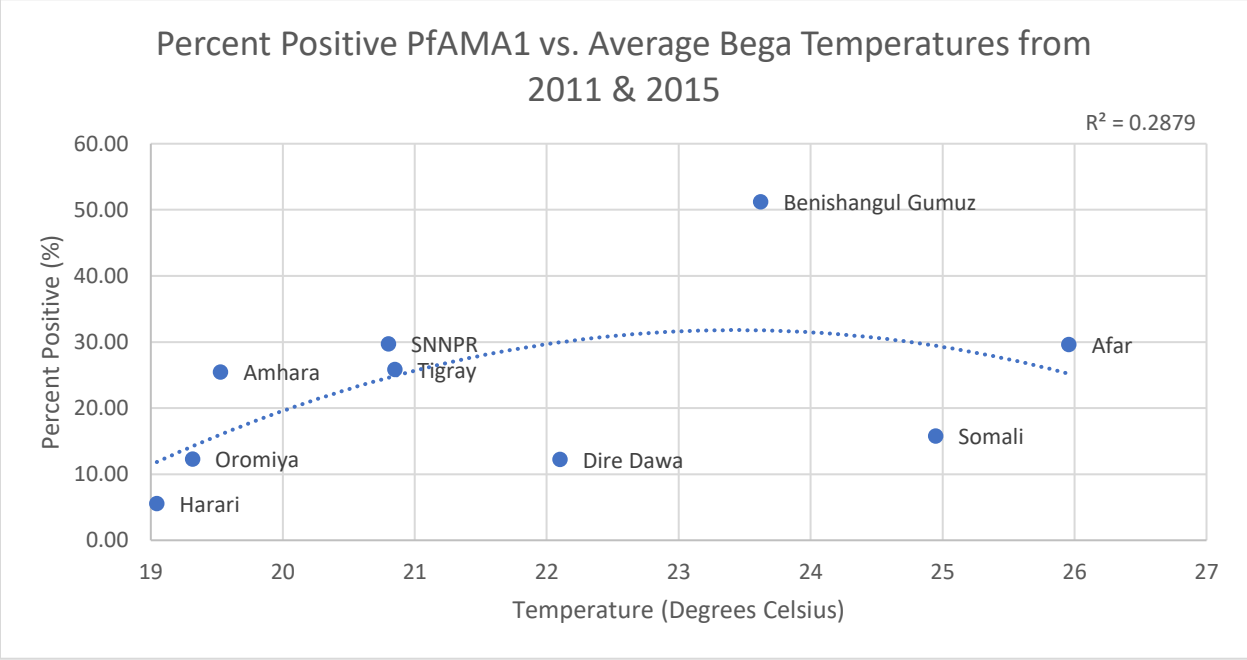

Figure D27: Percent Positive *P. falciparum* apical membrane antigen 1 Plotted with the 2011 and 2015 Average Bega (October to December) Temperatures for Ethiopia; R^2 = 0.29 from a Polynomial Curve.

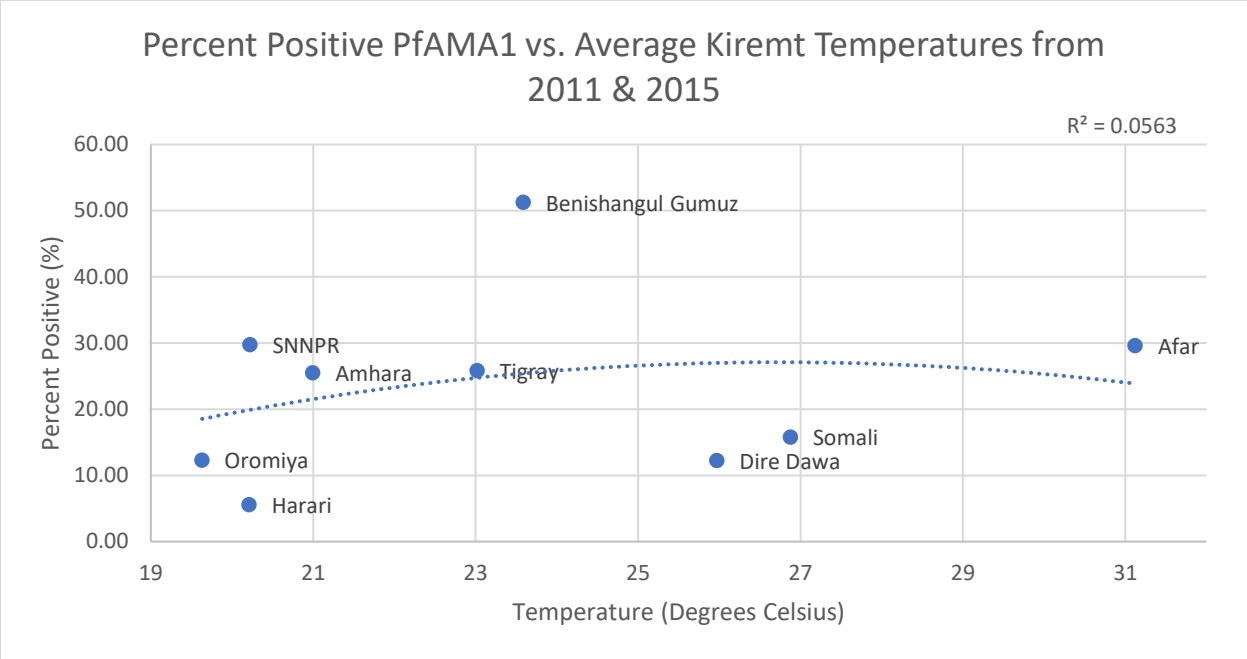

Figure D28: Percent Positive *P. falciparum* apical membrane antigen 1 Plotted with the 2011 and 2015 Average Kiremt (June to September) Temperatures for Ethiopia; R^2 = 0.06 from a Polynomial Curve.

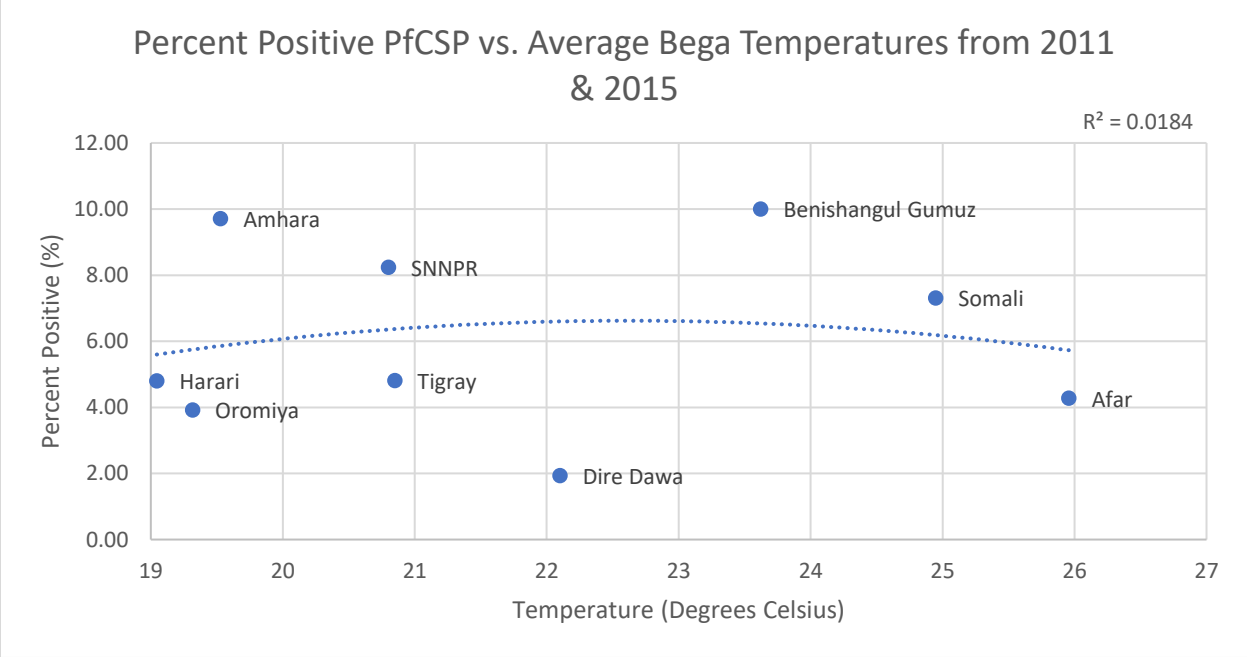

Figure D29: Percent Positive *P. falciparum* circumsporozoite protein Plotted with the 2011 and 2015 Average Bega (October to December) Temperatures for Ethiopia; R^2 = 0.02 from a Polynomial Curve.

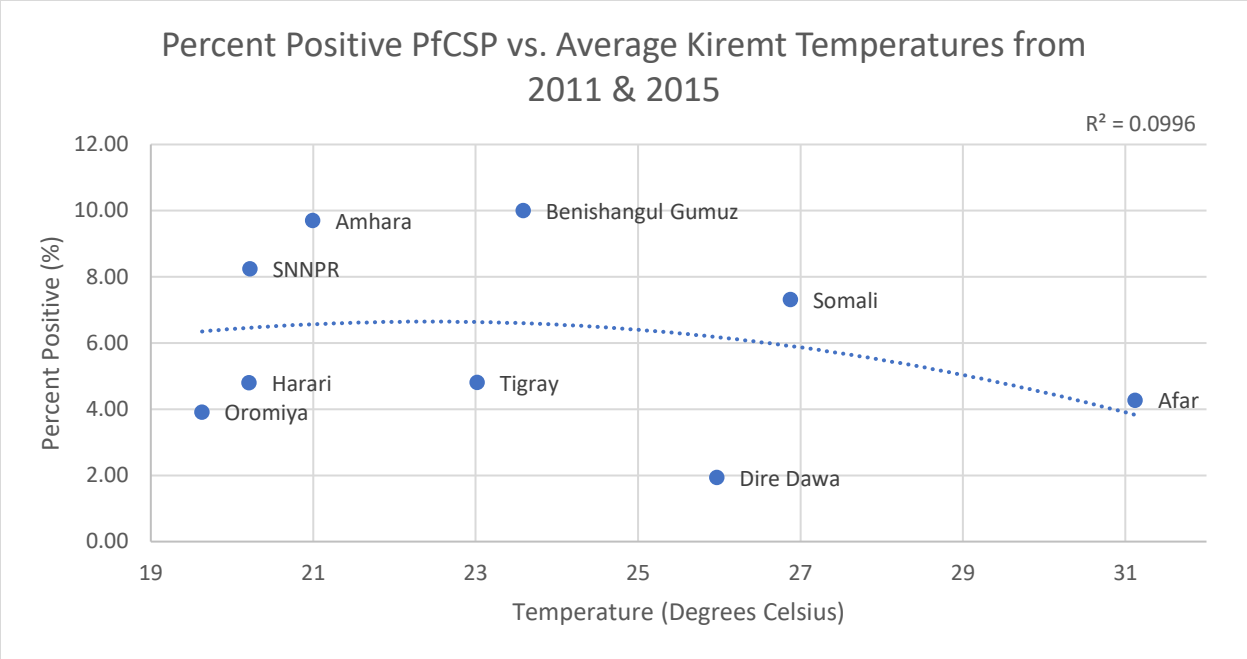

Figure D30: Percent Positive *P. falciparum* circumsporozoite protein Plotted with the 2011 and 2015 Average Kiremt (June to September) Temperatures for Ethiopia; R^2 = 0.10 from a Polynomial Curve.

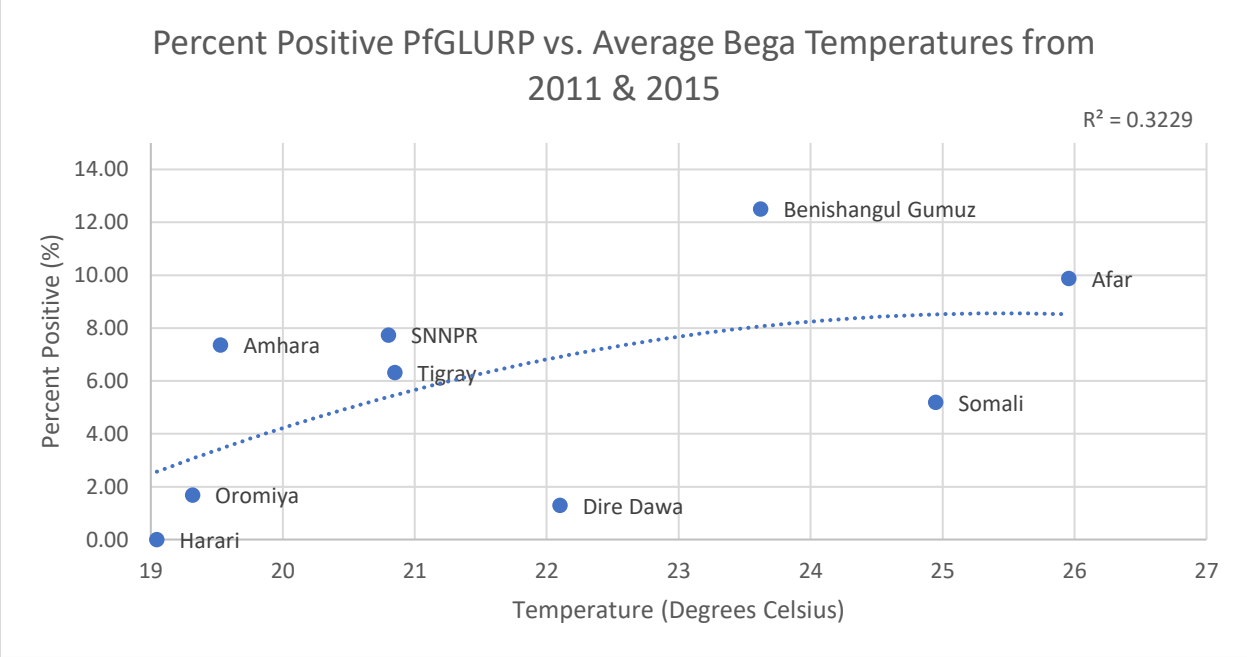

Figure D31: Percent Positive *P. falciparum* glutamate-rich protein, Ro fragment Plotted with the 2011 and 2015 Average Bega (October to December) Temperatures for Ethiopia; R^2 = 0.32 from a Polynomial Curve.

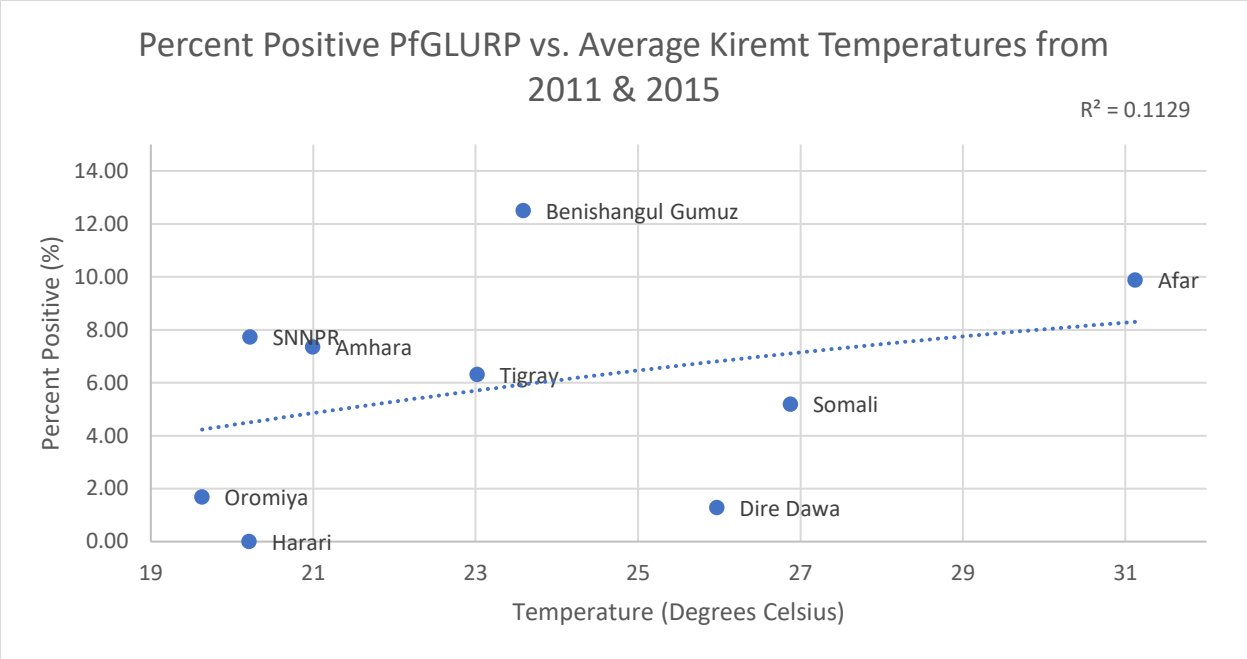

Figure D32: Percent Positive *P. falciparum* glutamate-rich protein, Ro fragment Plotted with the 2011 and 2015 Average Kiremt (June to September) Temperatures for Ethiopia; R^2 = 0.11 from a Polynomial Curve.

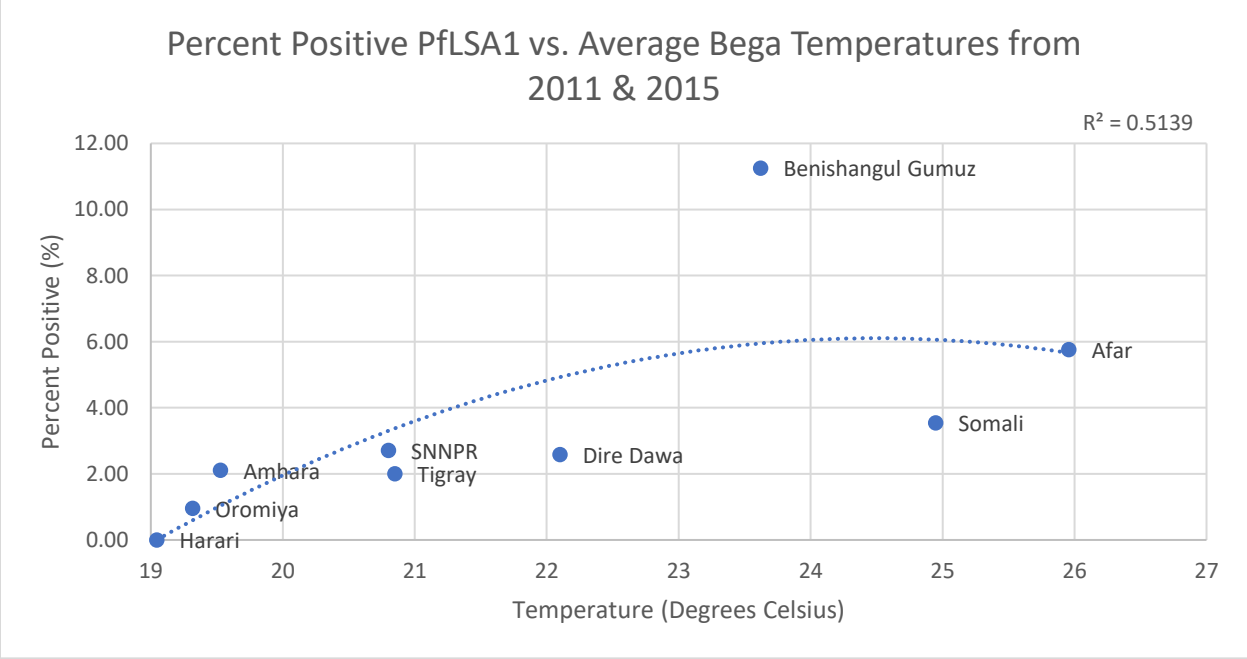

Figure D33: Percent Positive *P. falciparum* liver stage antigen 1 Plotted with the 2011 and 2015 Average Bega (October to December) Temperatures for Ethiopia; R^2 = 0.51 from a Polynomial Curve.

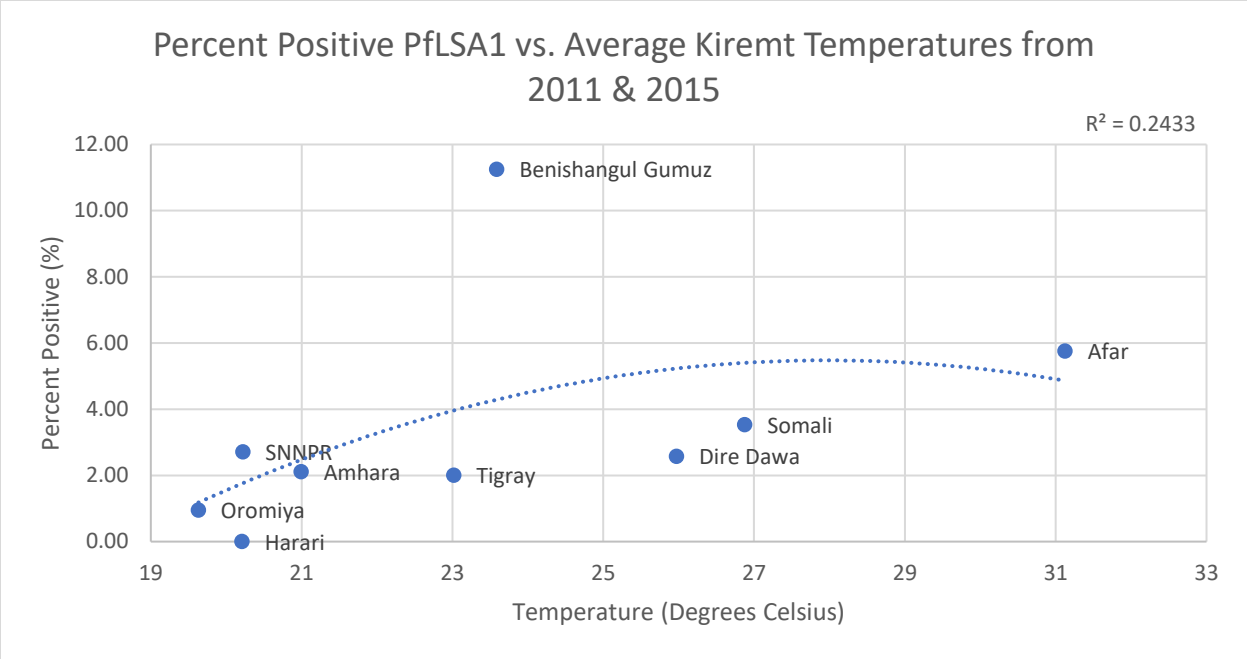

Figure D34: Percent Positive *P. falciparum* liver stage antigen 1 Plotted with the 2011 and 2015 Average Kiremt (June to September) Temperatures for Ethiopia; R^2 = 0.24 from a Polynomial Curve.

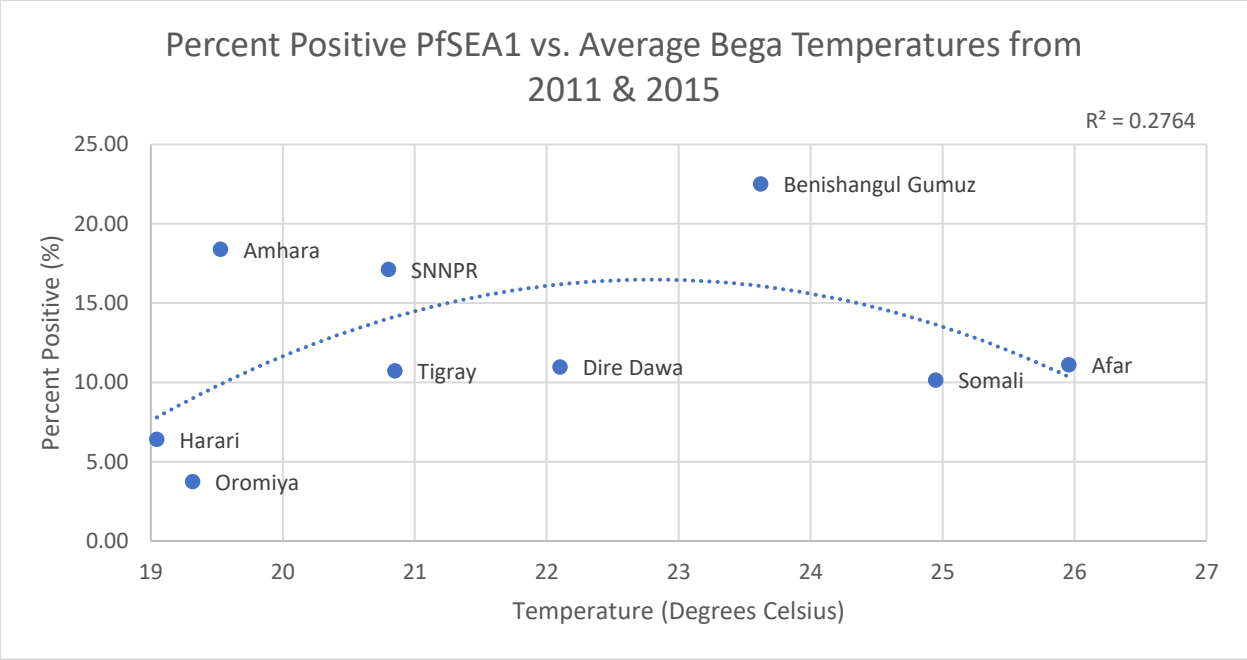

Figure D35: Percent Positive *P. falciparum* schizont egress antigen 1 Plotted with the 2011 and 2015 Average Bega (October to December) Temperatures for Ethiopia; R^2 = 0.28 from a Polynomial Curve.

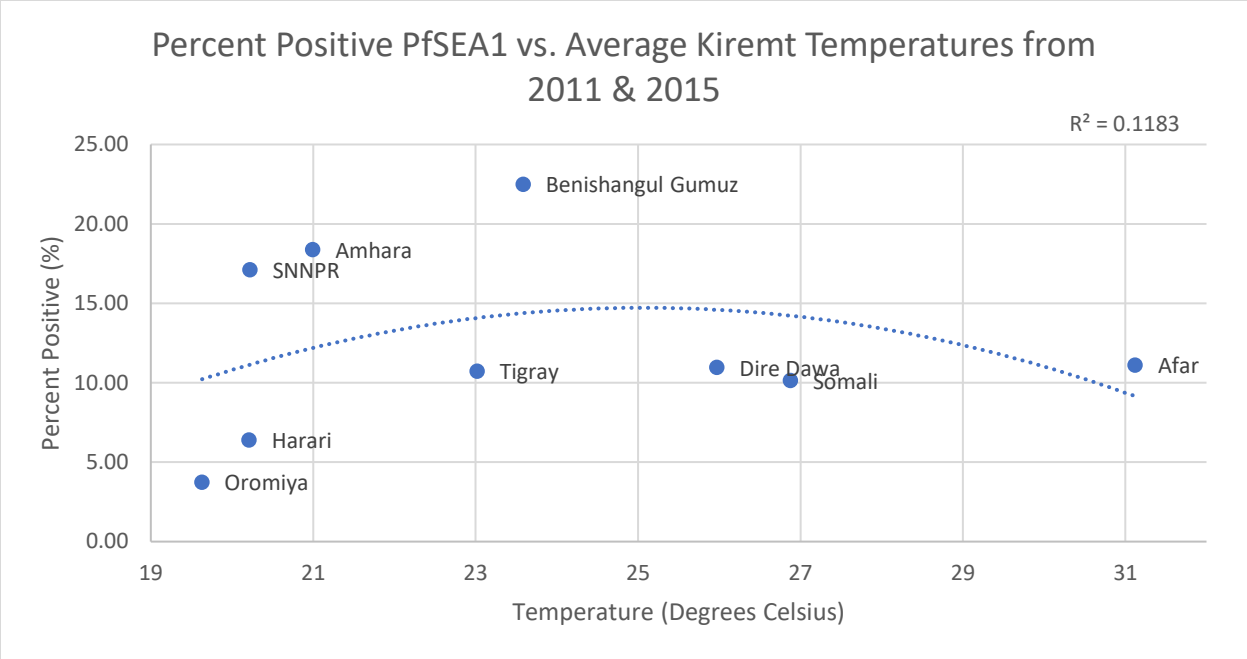

Figure D36: Percent Positive *P. falciparum* schizont egress antigen 1 Plotted with the 2011 and 2015 Average Kiremt (June to September) Temperatures for Ethiopia; R^2 = 0.12 from a Polynomial Curve.

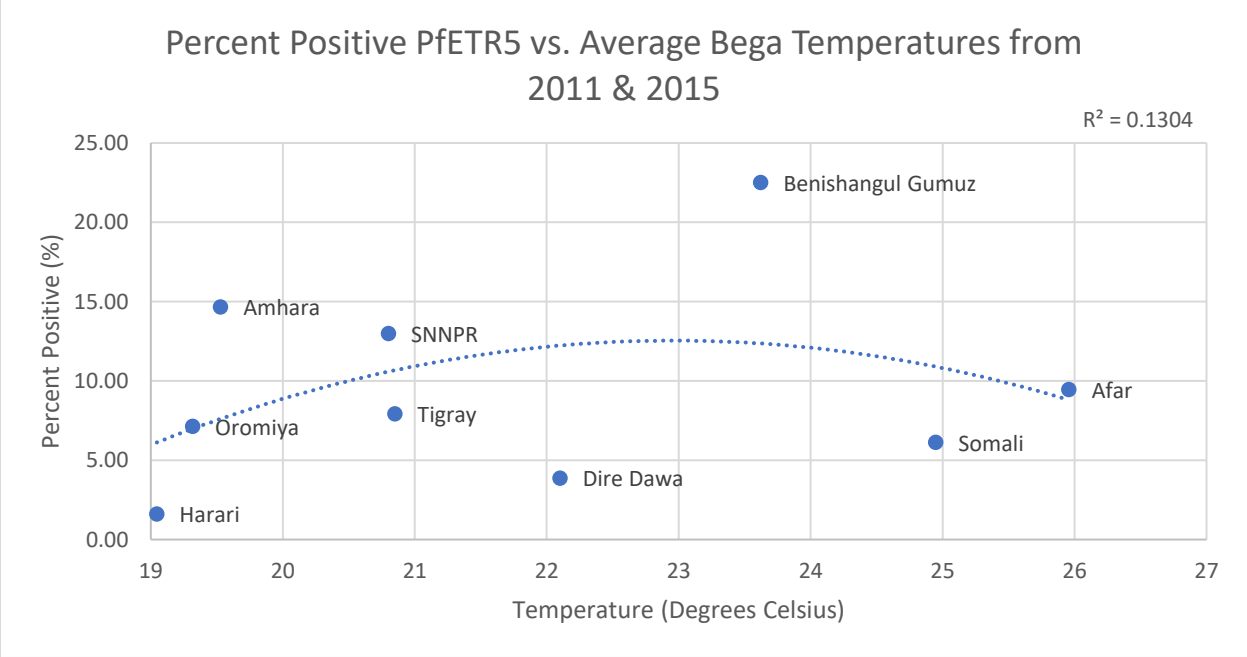

Figure D37: Percent Positive *P. falciparum* ETRAMP 5 antigen 1 Plotted with the 2011 and 2015 Average Bega (October to December) Temperatures for Ethiopia; R^2 = 0.13 from a Polynomial Curve.

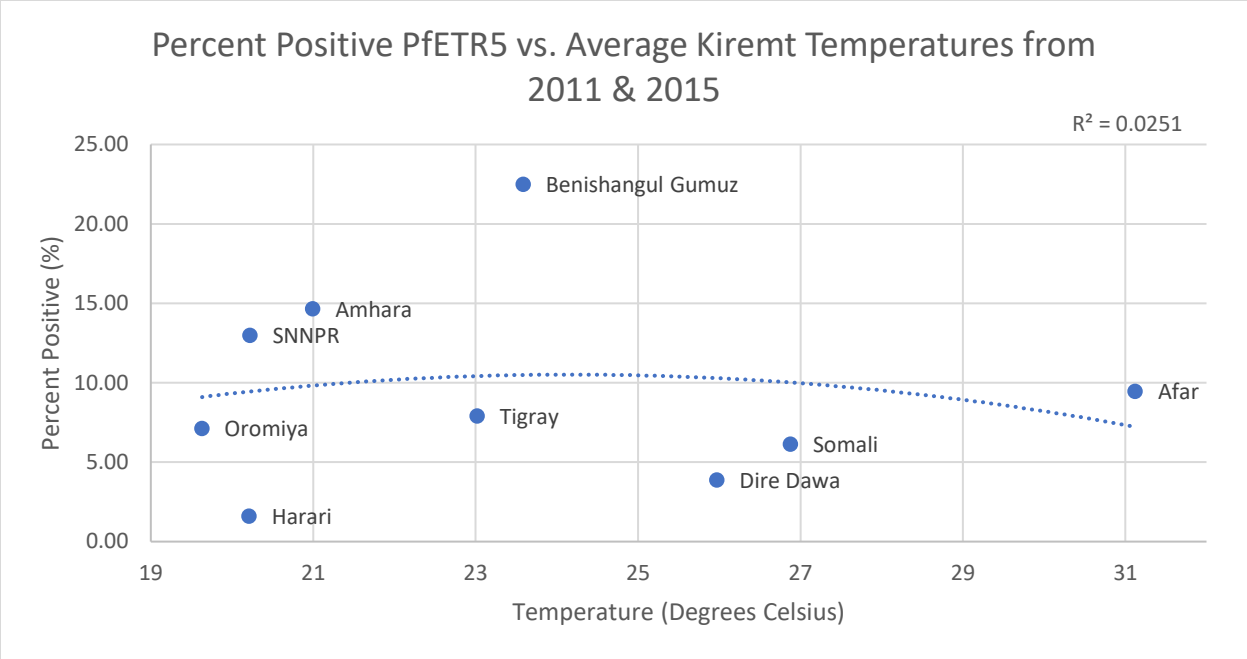

Figure D38: Percent Positive *P. falciparum* ETRAMP 5 antigen 1 Plotted with the 2011 and 2015 Average Kiremt (June to September) Temperatures for Ethiopia; R^2 = 0.03 from a Polynomial Curve.

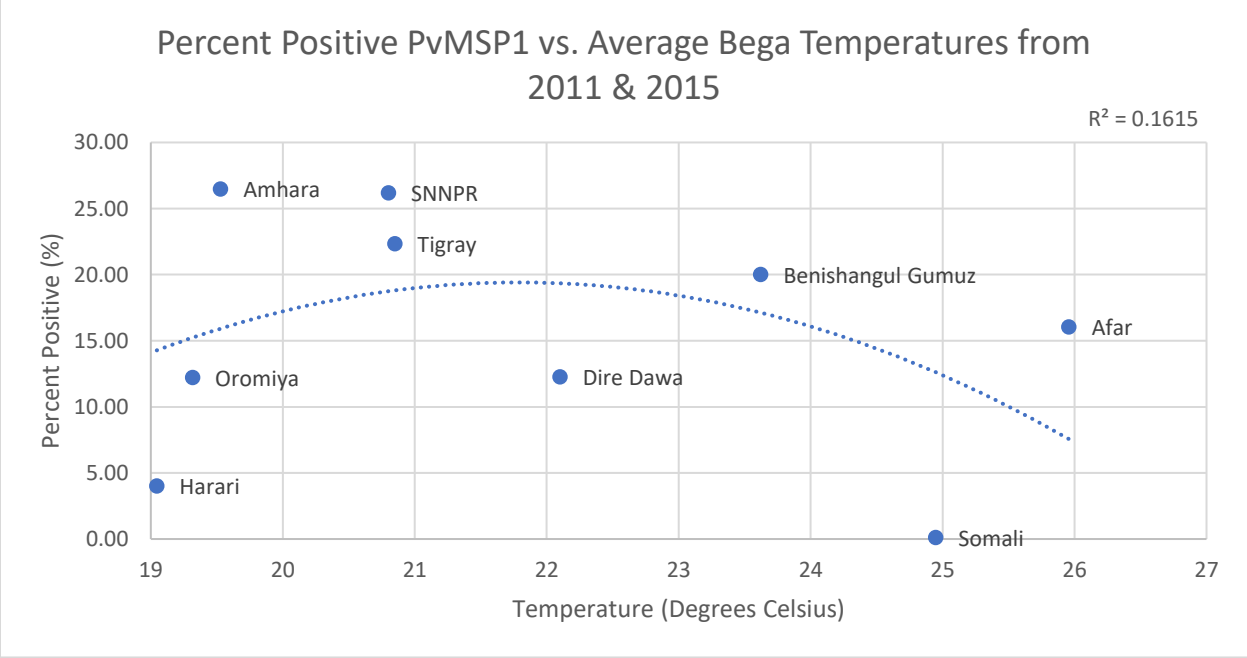

Figure D39: Percent Positive *P. vivax* merozoite protein 1 Plotted with the 2011 and 2015 Average Bega (October to December) Temperatures for Ethiopia; R^2 = 0.16 from a Polynomial Curve.

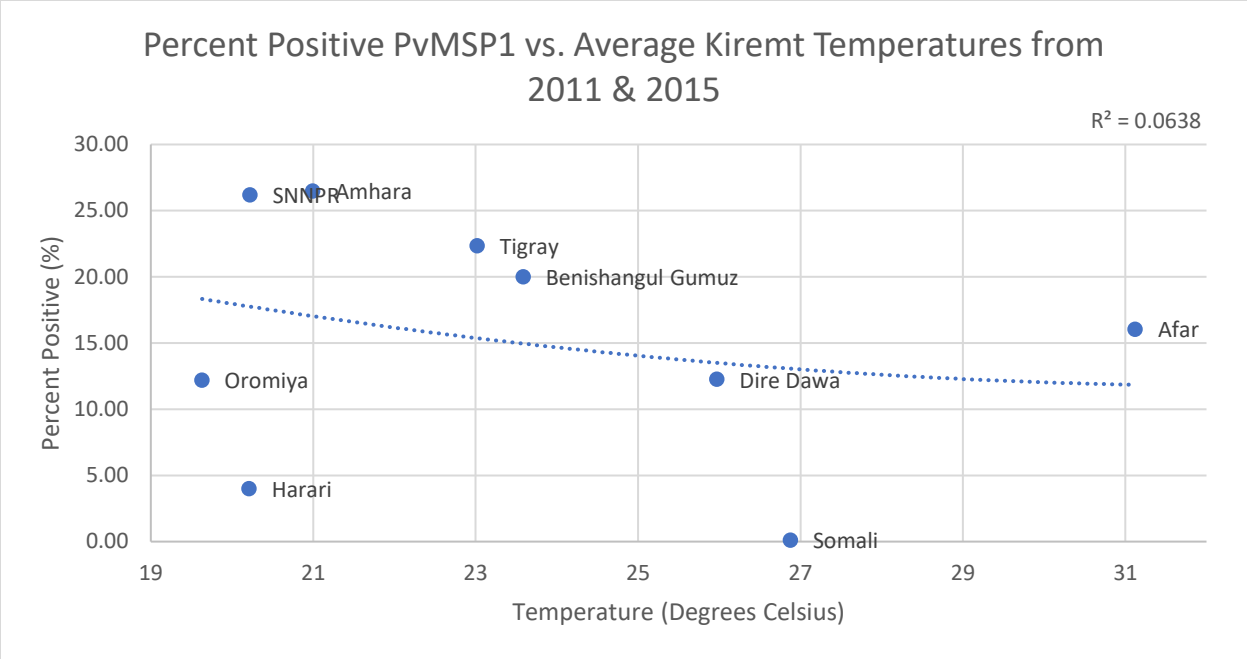

Figure D40: Percent Positive *P. vivax* merozoite protein 1 Plotted with the 2011 and 2015 Average Kiremt (June to September) Temperatures for Ethiopia; R^2 = 0.06 from a Polynomial Curve.

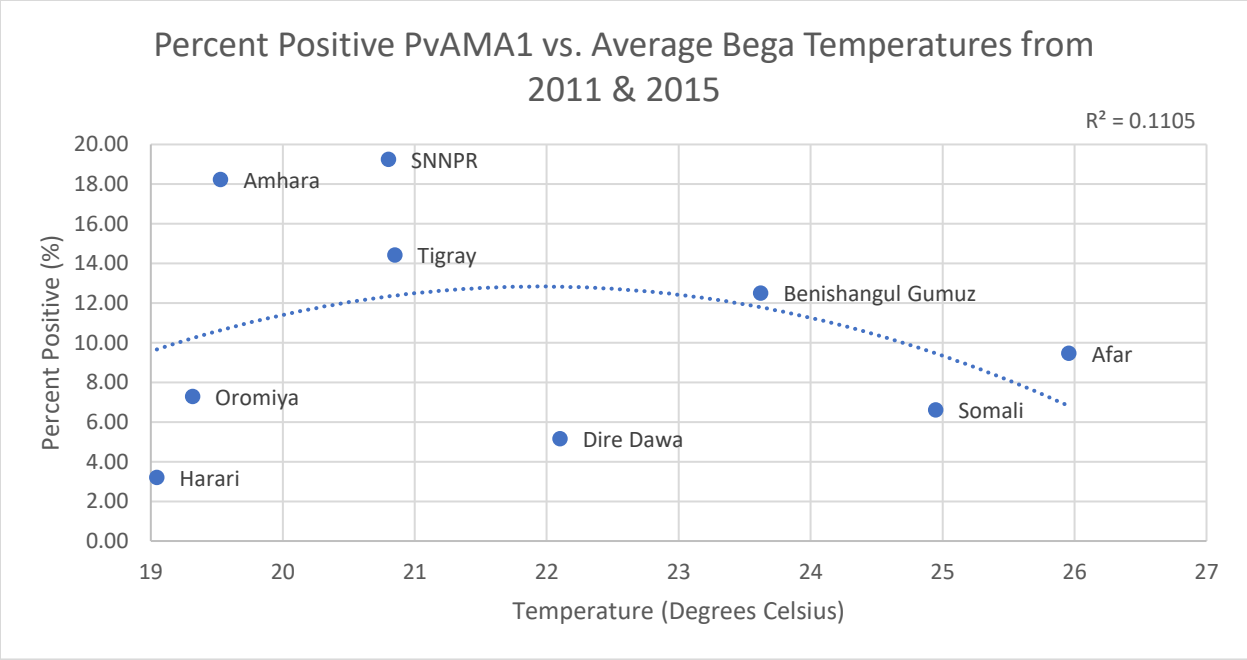

Figure D41: Percent Positive *P. vivax* apical membrane antigen 1 Plotted with the 2011 and 2015 Average Bega (October to December) Temperatures for Ethiopia; R^2 = 0.11 from a Polynomial Curve.

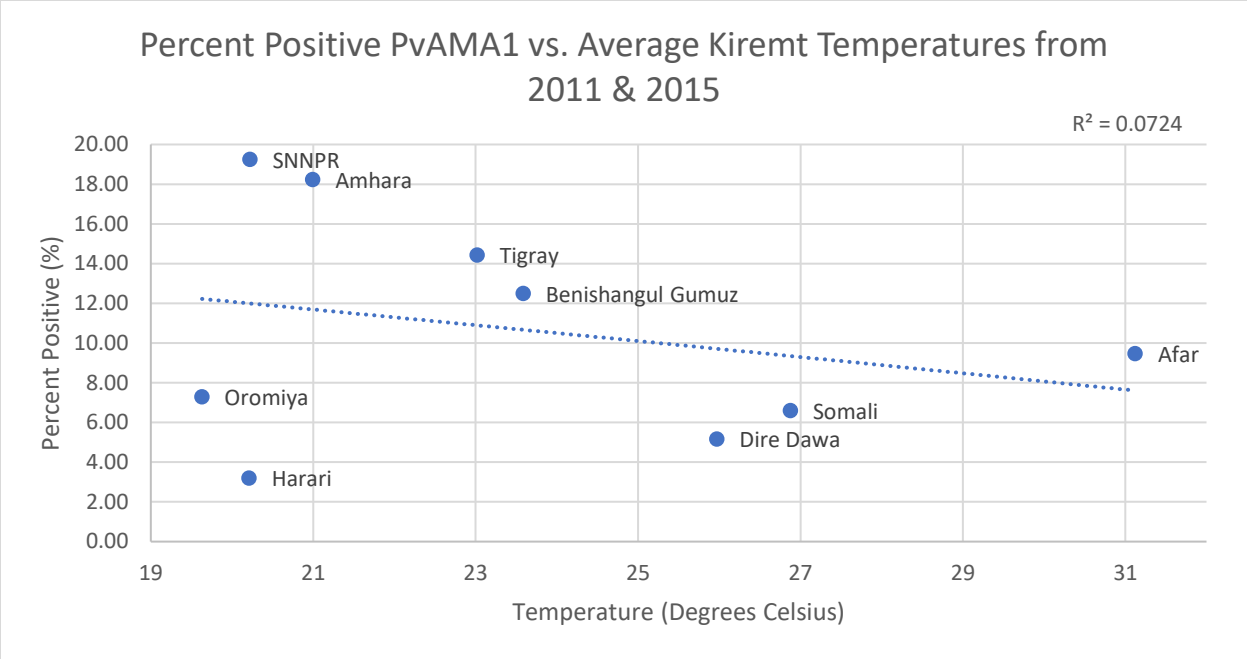

Figure D42: Percent Positive *P. vivax* apical membrane antigen 1 Plotted with the 2011 and 2015 Average Kiremt (June to September) Temperatures for Ethiopia; R^2 = 0.07 from a Polynomial Curve.

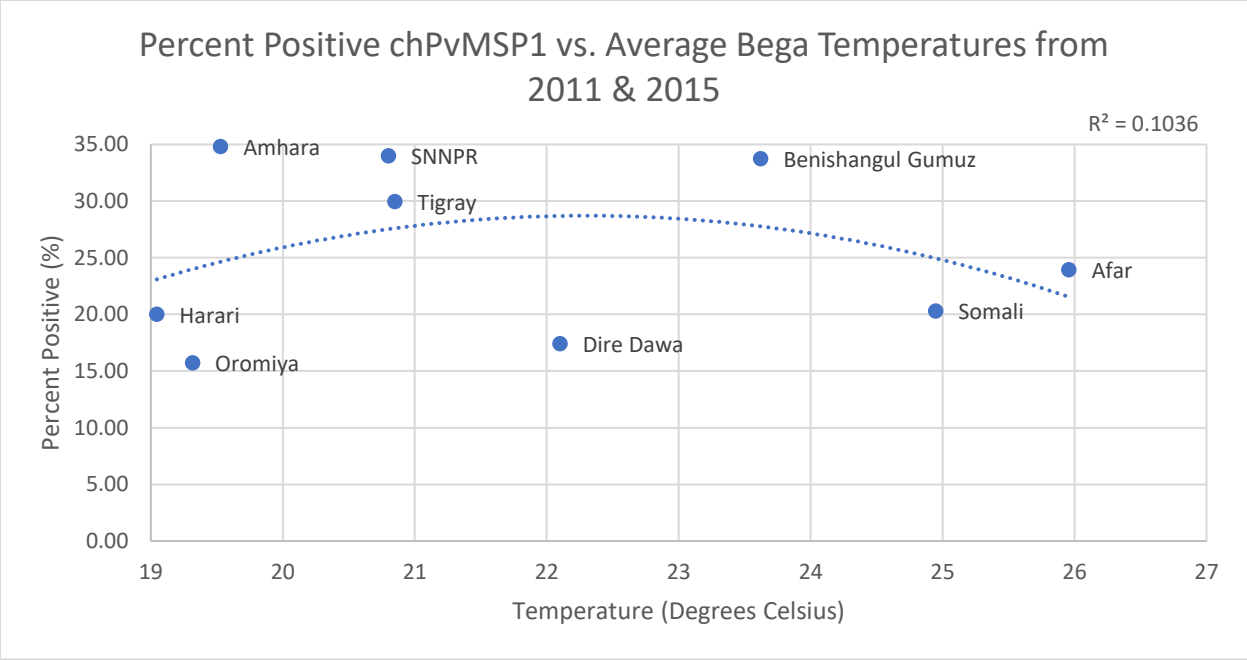

Figure D43: Percent Positive chimeric *P. vivax* merozoite protein 1, including additional B and T cell epitopes Plotted with the 2011 and 2015 Average Bega (October to December) temperatures for Ethiopia; R^2 = 0.10 from a Polynomial Curve.

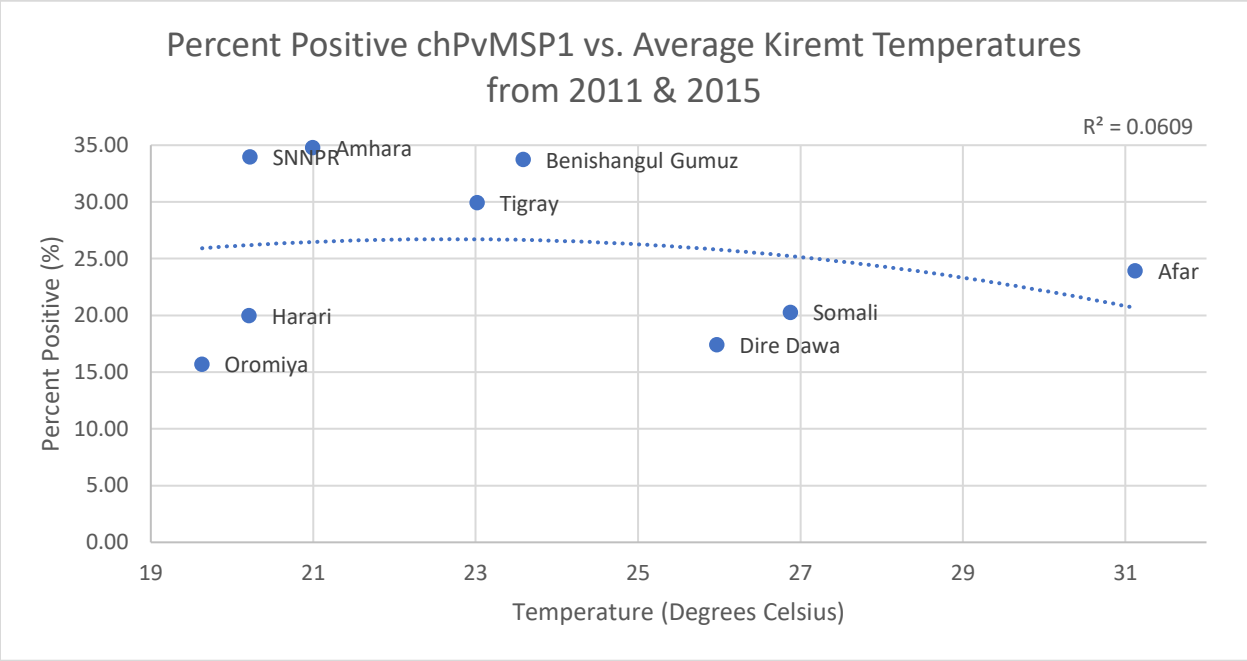

Figure D44: Percent Positive chimeric *P. vivax* merozoite protein 1, including additional B and T cell epitopes Plotted with the 2011 and 2015 Average Kiremt (June to September) Temperatures for Ethiopia; R^2 = 0.06 from a Polynomial Curve.

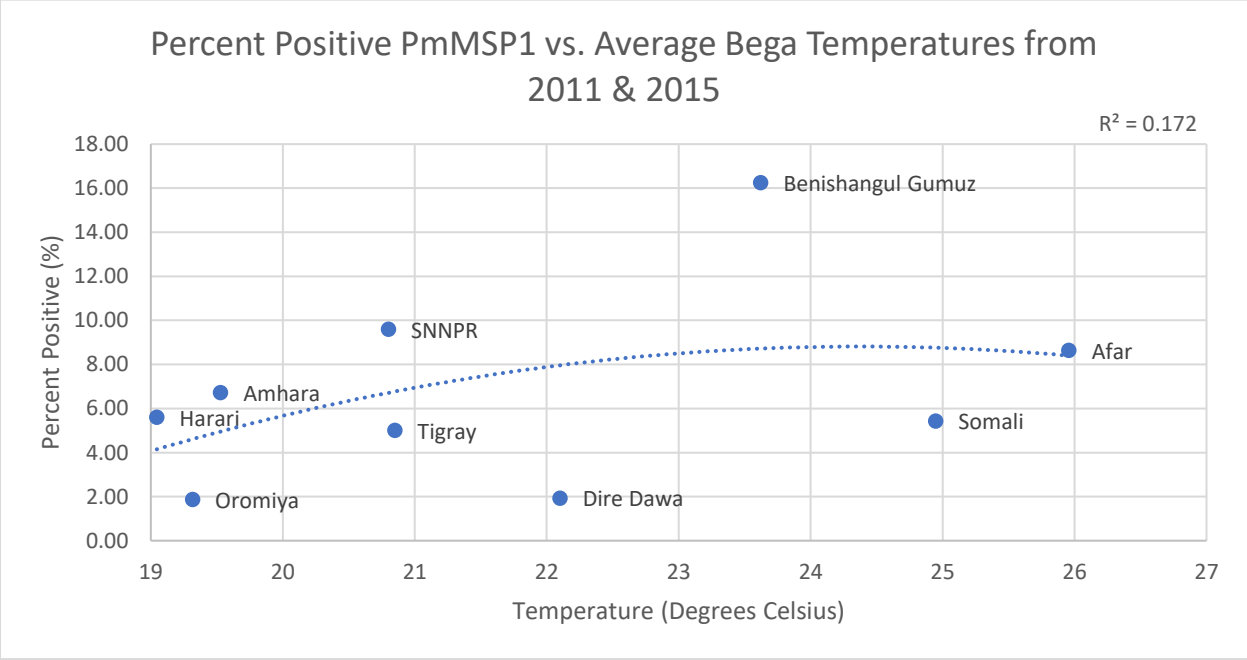

Figure D45: Percent Positive *P. malariae* merozoite protein 1 Plotted with the 2011 and 2015 Average Bega (October to December) Temperatures for Ethiopia; R^2 = 0.17 from a Polynomial Curve.

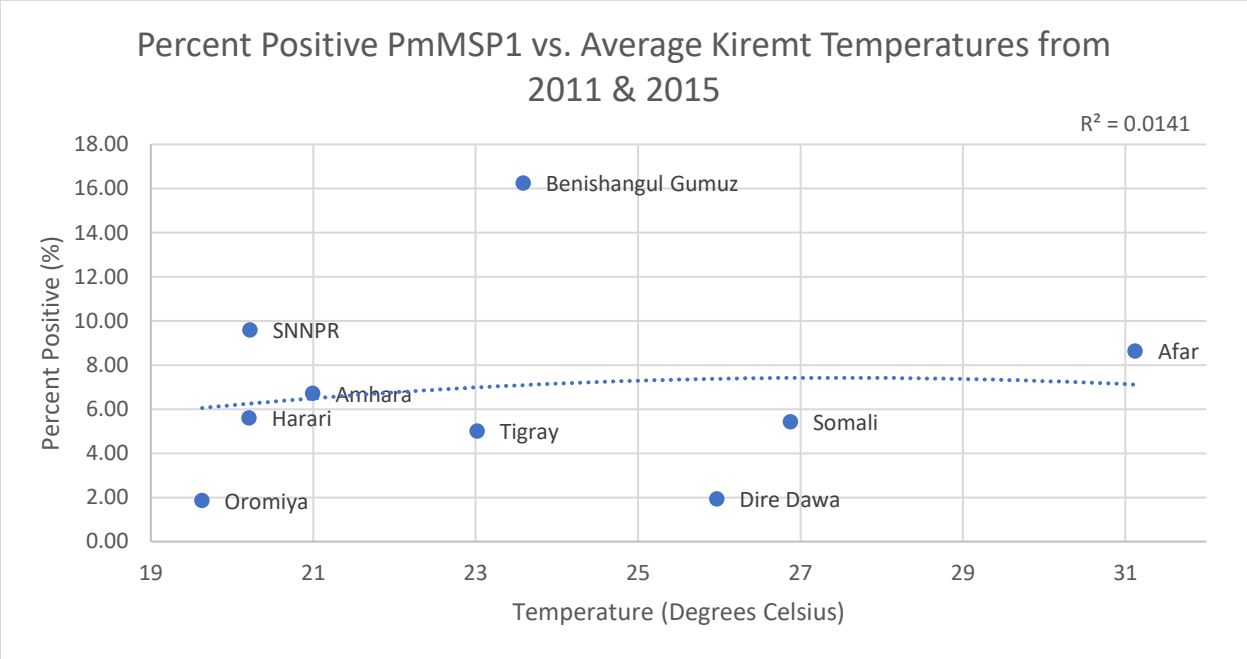

Figure D46: Percent Positive *P. malariae* merozoite protein 1 Plotted with the 2011 and 2015 Average Kiremt (June to September) Temperatures for Ethiopia; R^2 = 0.01 from a Polynomial Curve.

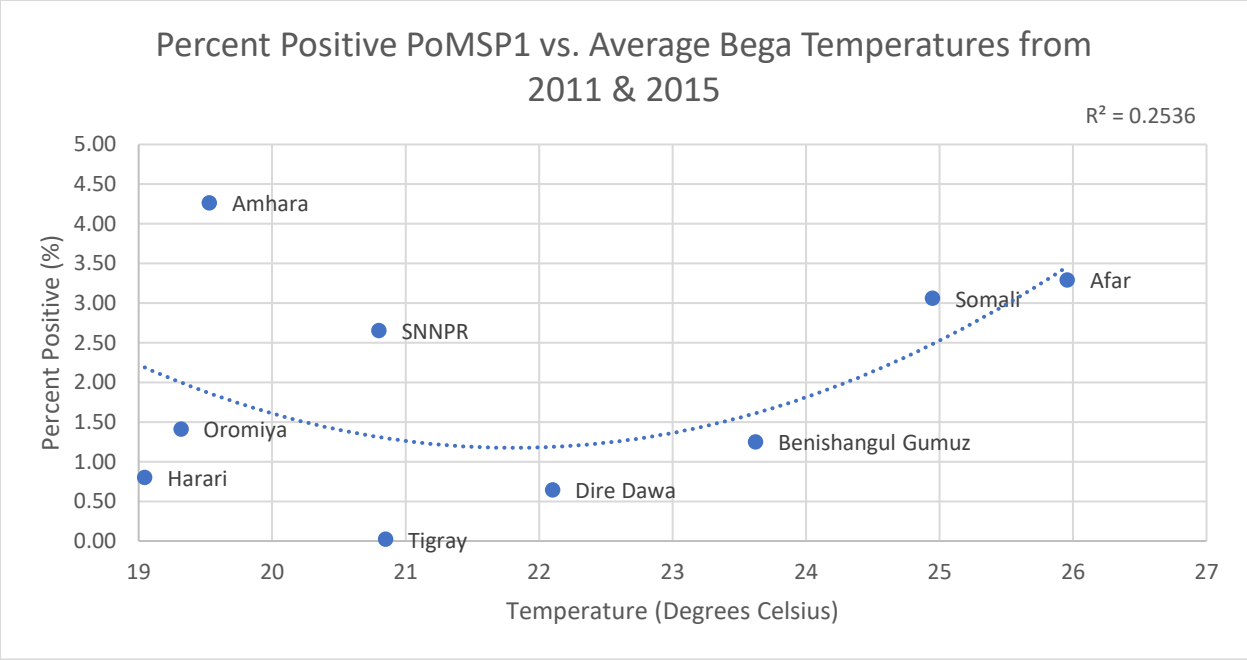

Figure D47: Percent Positive *P. ovale* merozoite protein 1 Plotted with the 2011 and 2015 Average Bega (October to December) Temperatures for Ethiopia; R^2 = 0.25 from a Polynomial Curve.

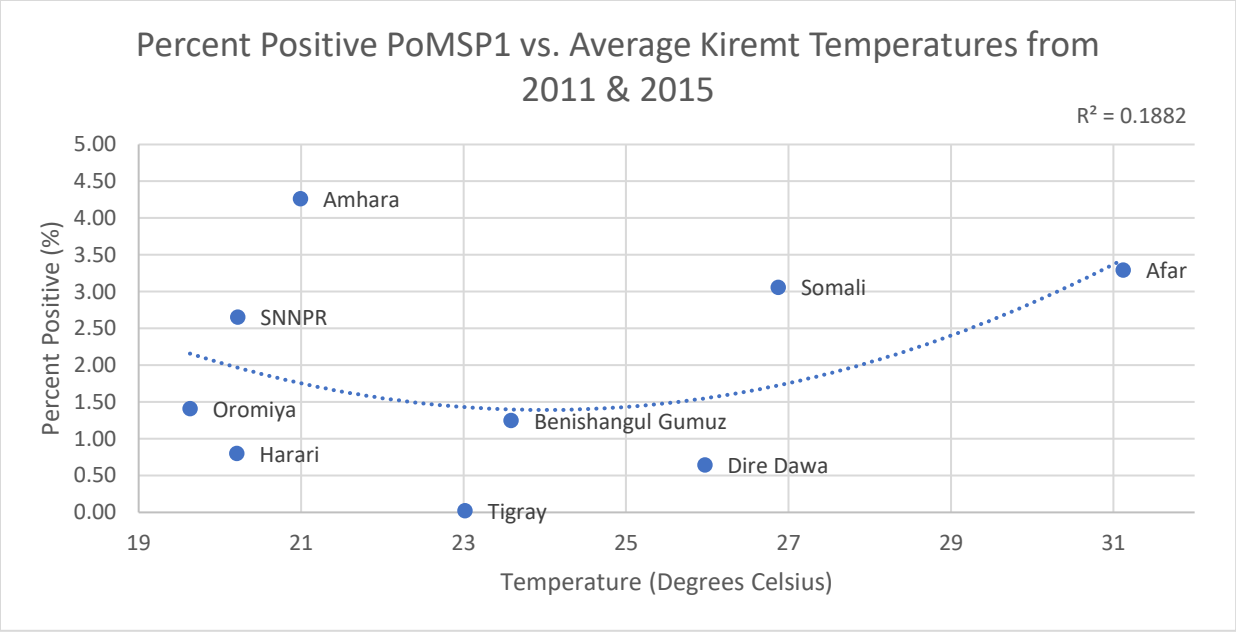

Figure D48: Percent Positive *P. ovale* merozoite protein 1 Plotted with the 2011 and 2015 Average Kiremt (June to September) Temperatures for Ethiopia; R^2 = 0.19 from a Polynomial Curve.

Appendix E: Geographic Depiction of Regional Boundaries in Ethiopia

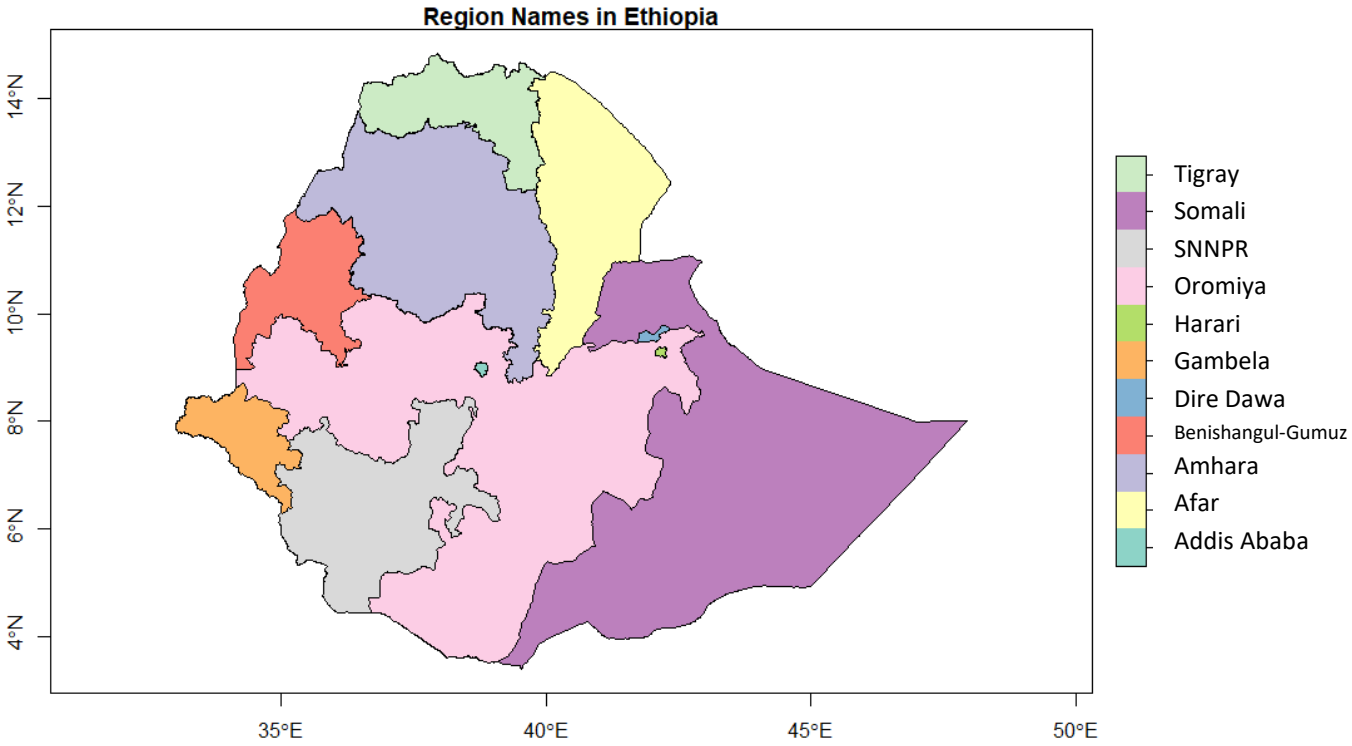

Figure E1: Shapefile of Ethiopia and Regions Color-coded According to the Legend with Latitude and Longitude lines.

Appendix F: Geographic Layers of Rainfall in Ethiopia—2011 and 2015

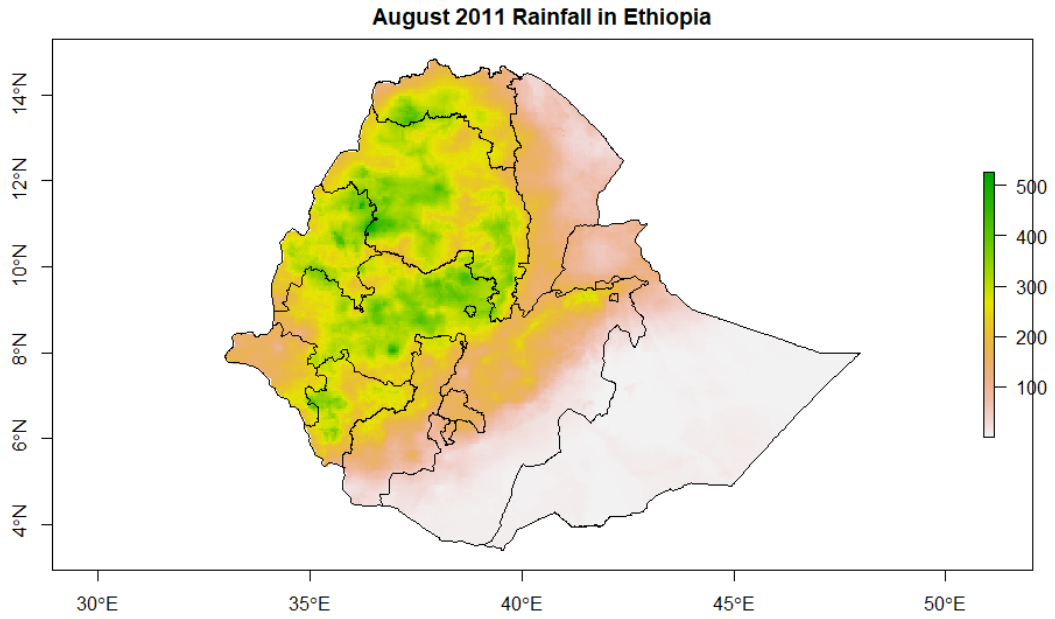

Figure F1: Shapefile of Ethiopia with regional borders and monthly rainfall amount from August 2011, legend on the right from 0 mm to 500 mm with Latitude and Longitude Lines

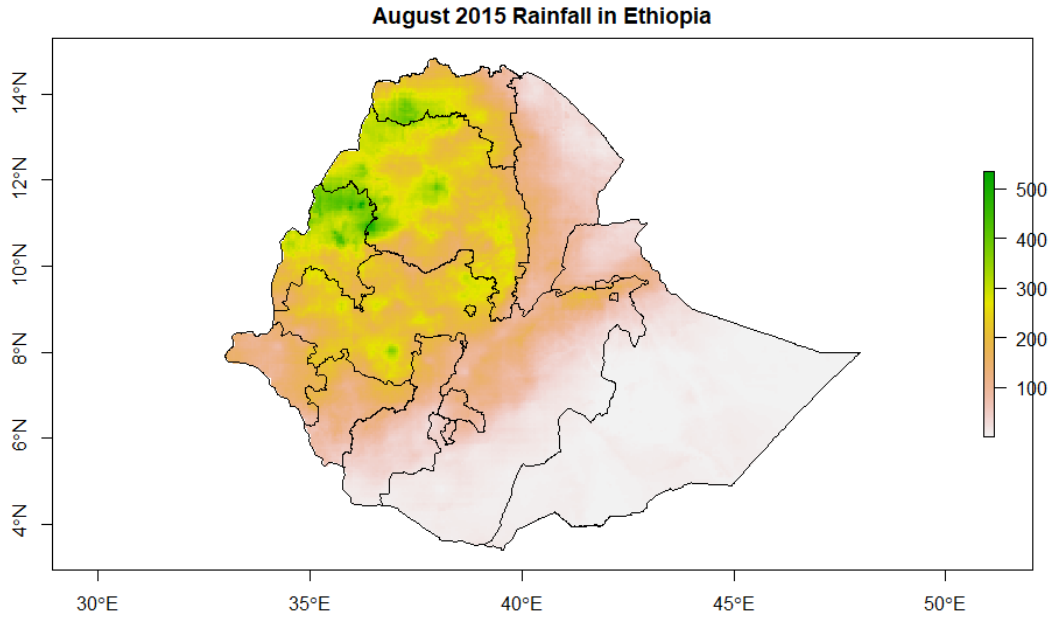

Figure F2: Shapefile of Ethiopia with regional borders and monthly rainfall amount from August 2015, legend on the right from 0 mm to 500 mm with Latitude and Longitude Lines

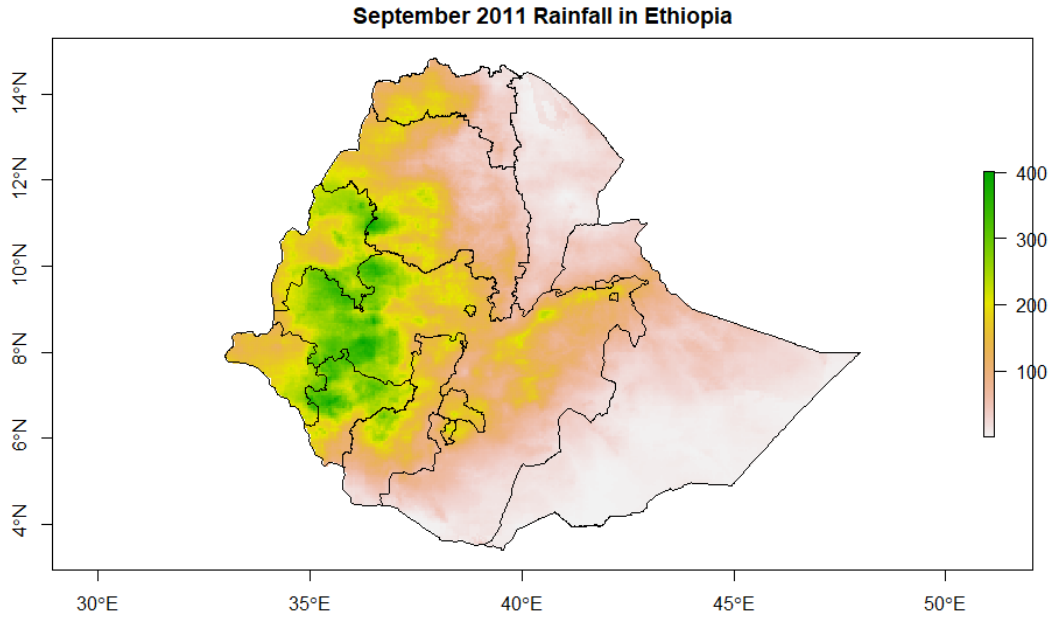

Figure F3: Shapefile of Ethiopia with regional borders and monthly rainfall amount from September 2011, legend on the right from 0 mm to 400 mm with Latitude and Longitude Lines

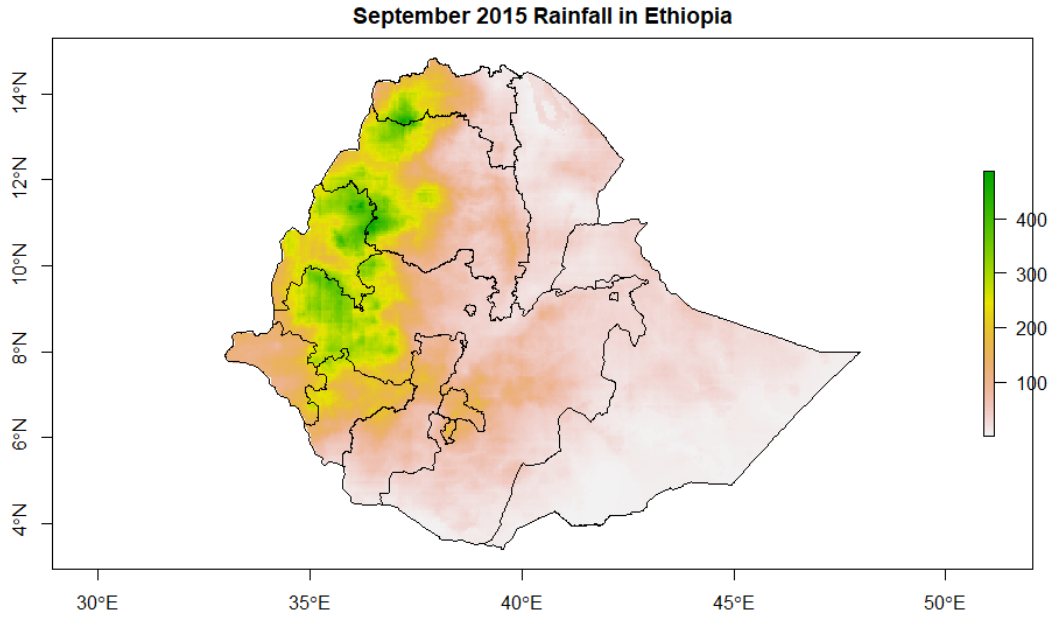

Figure F4: Shapefile of Ethiopia with regional borders and monthly rainfall amount from September 2015, legend on the right from 0 mm to 400 mm with Latitude and Longitude Lines

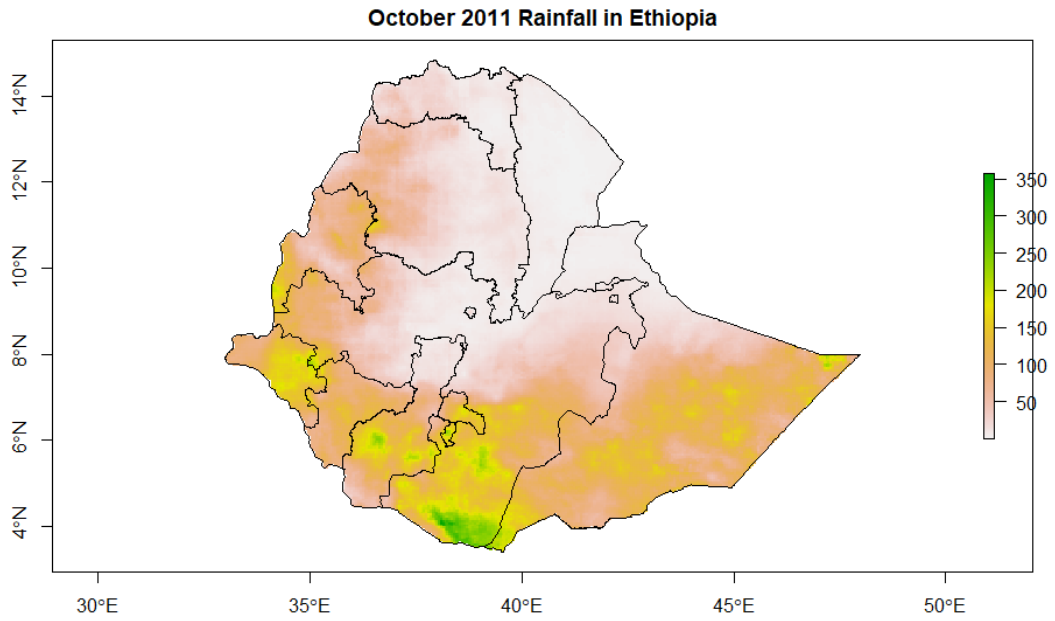

Figure F5: Shapefile of Ethiopia with regional borders and monthly rainfall amount from October 2011, legend on the right from 0 mm to 350 mm with Latitude and Longitude Lines

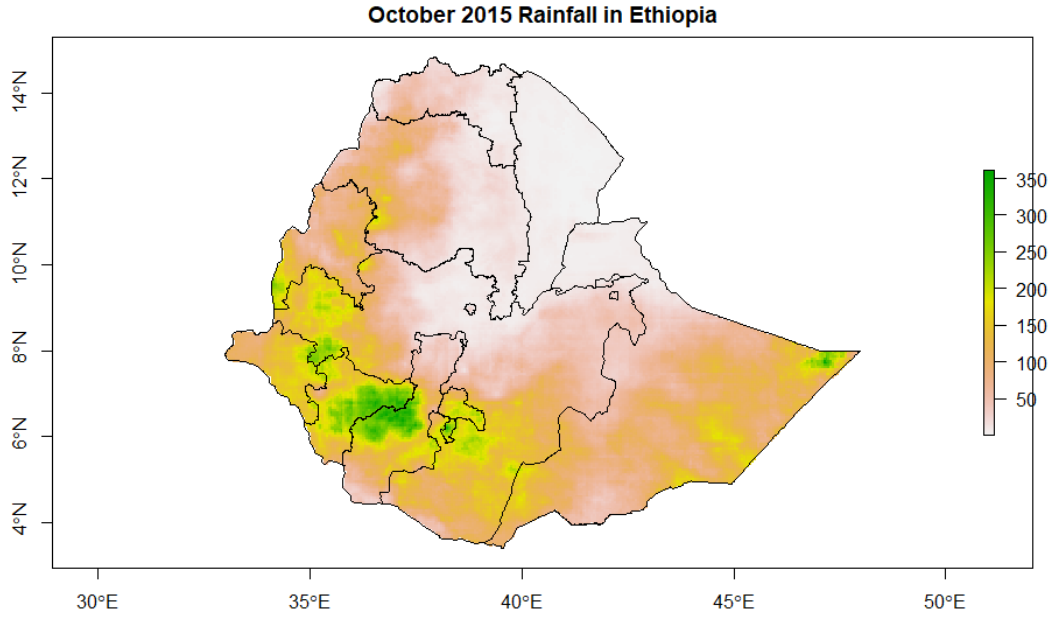

Figure F6: Shapefile of Ethiopia with regional borders and monthly rainfall amount from October 2015, legend on the right from 0 mm to 350 mm with Latitude and Longitude Lines

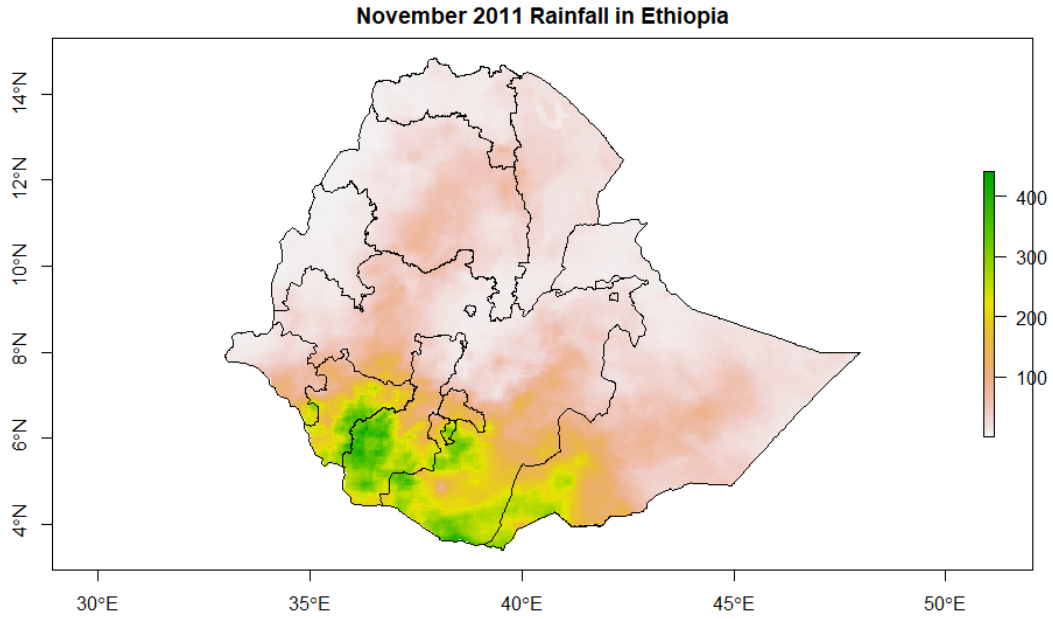

Figure F7: Shapefile of Ethiopia with regional borders and monthly rainfall amount from November 2011, legend on the right from 0 mm to 400 mm with Latitude and Longitude Lines

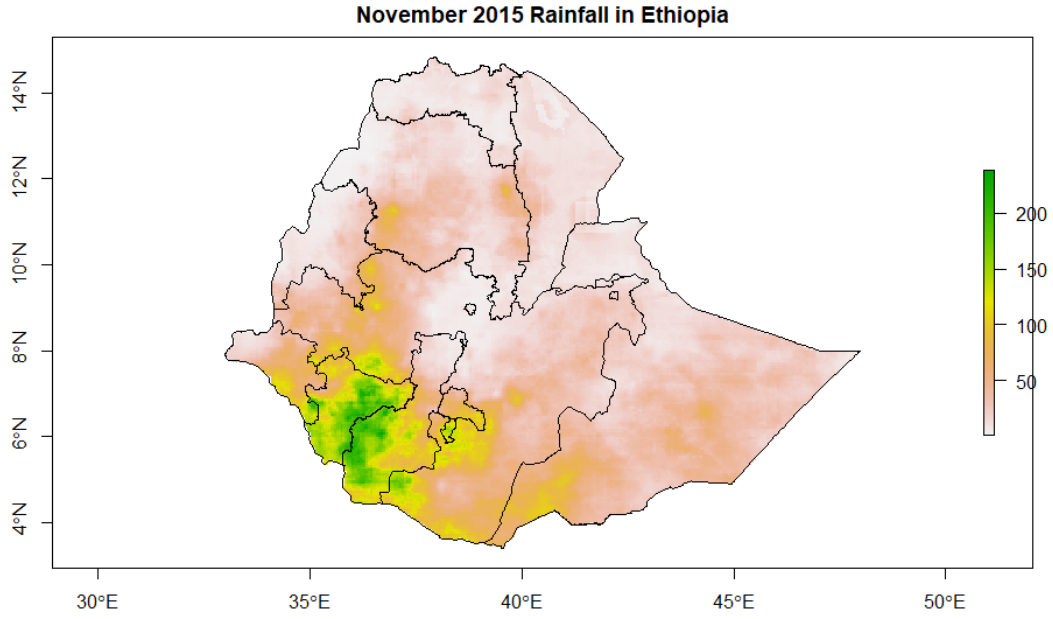

Figure F8: Shapefile of Ethiopia with regional borders and monthly rainfall amount from November 2015, legend on the right from 0 mm to 200 mm with Latitude and Longitude Lines

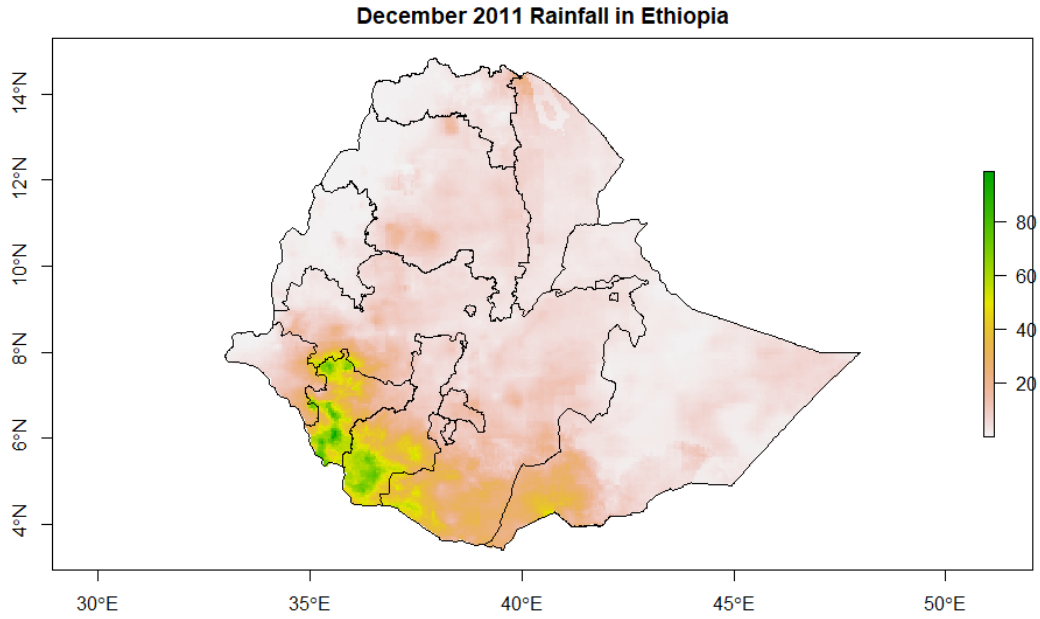

Figure F9: Shapefile of Ethiopia with regional borders and monthly rainfall amount from December 2011, legend on the right from 0 mm to 80 mm with Latitude and Longitude Lines

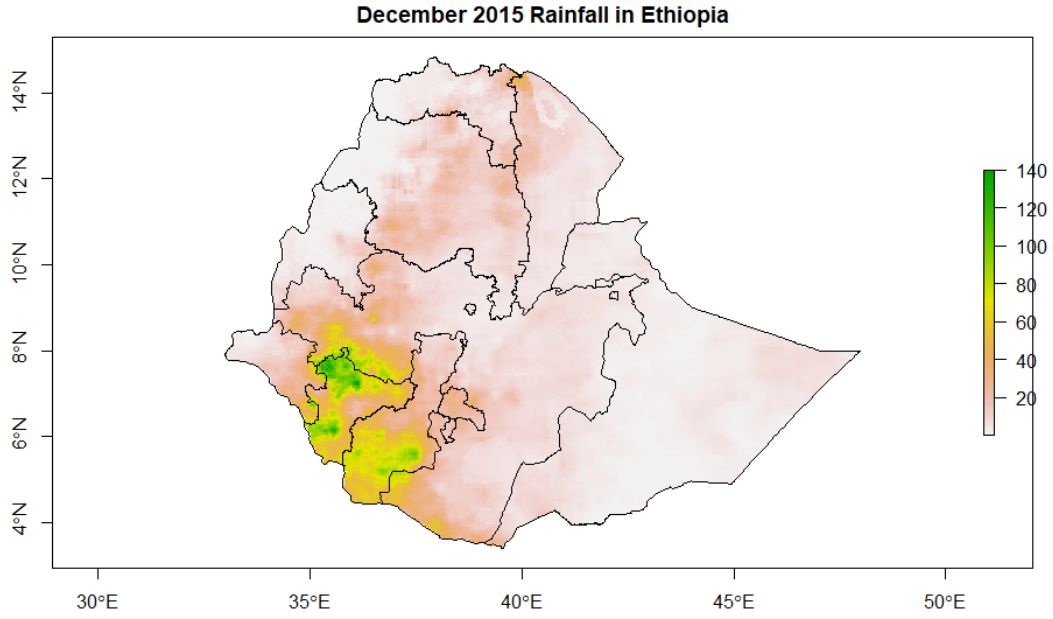

Figure F10: Shapefile of Ethiopia with regional borders and monthly rainfall amount from December 2015, legend on the right from 0 mm to 140 mm with Latitude and Longitude Lines

Appendix G: Geographic Layers of Temperature in Ethiopia—2011 and 2015

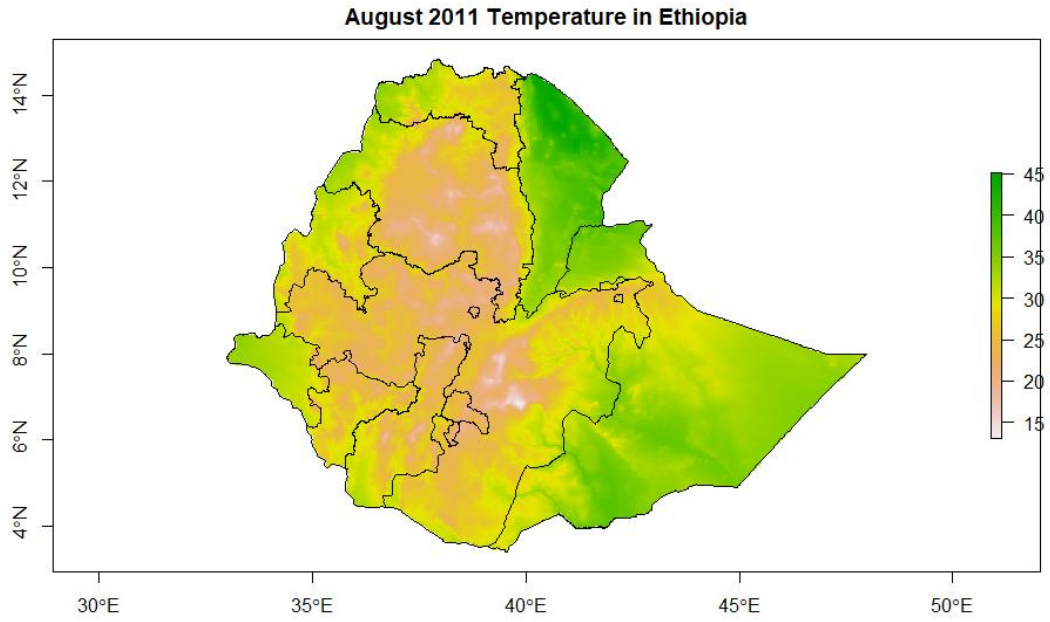

Figure G1: Shapefile of Ethiopia with regional borders and average temperature from August 2011, legend on the right from 15° C to 45° C with Latitude and Longitude Lines

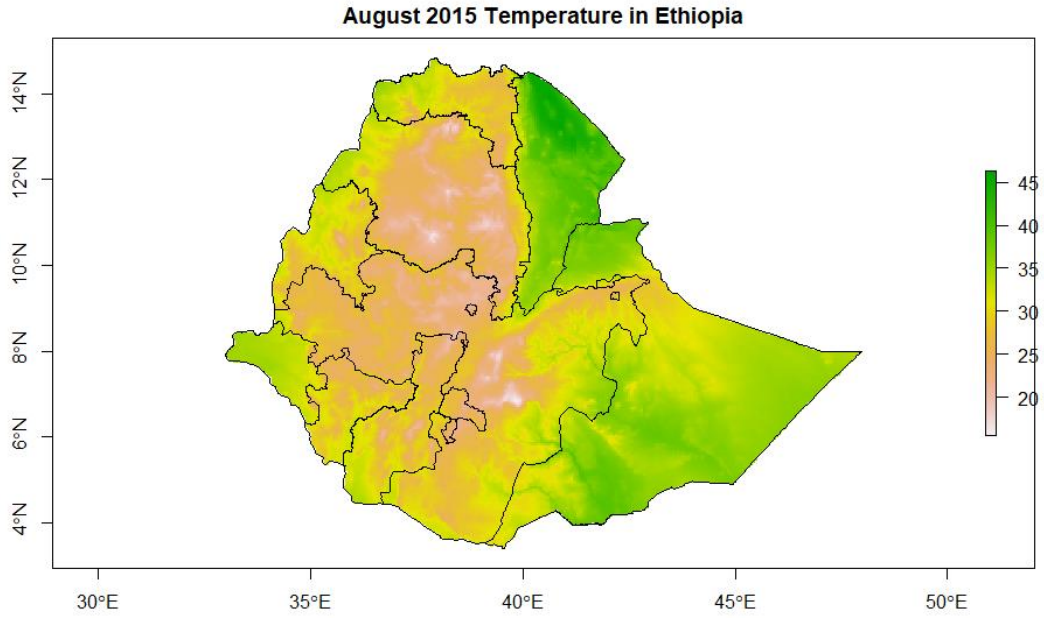

Figure G2: Shapefile of Ethiopia with regional borders and average temperature from August 2015, legend on the right from 15° C to 45° C with Latitude and Longitude Lines

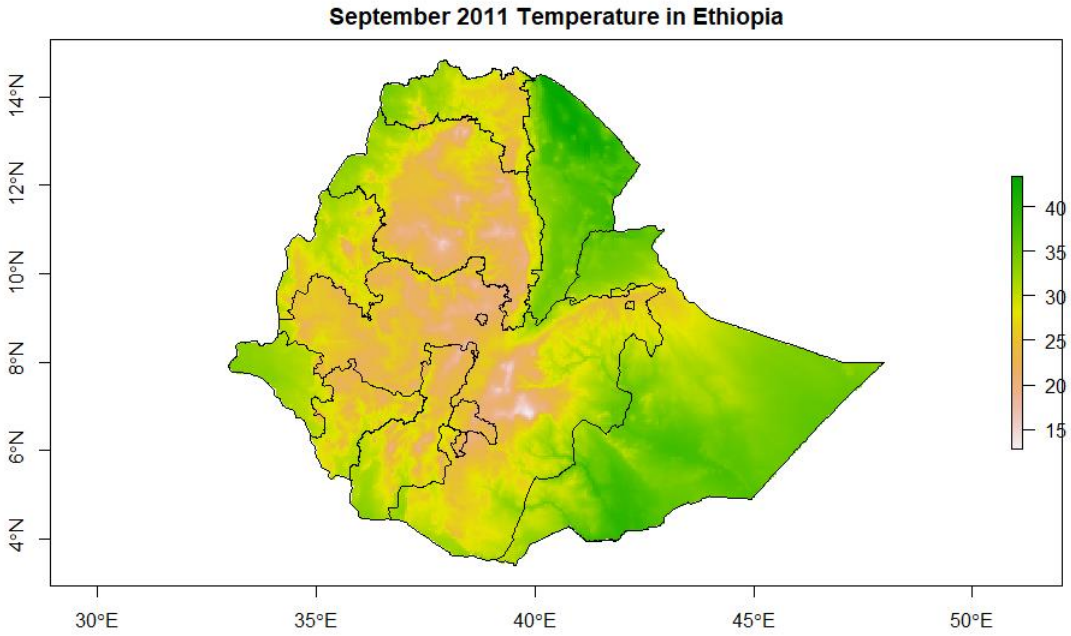

Figure G3: Shapefile of Ethiopia with regional borders and average temperature from September 2011, legend on the right from 15° C to 40° C with Latitude and Longitude Lines

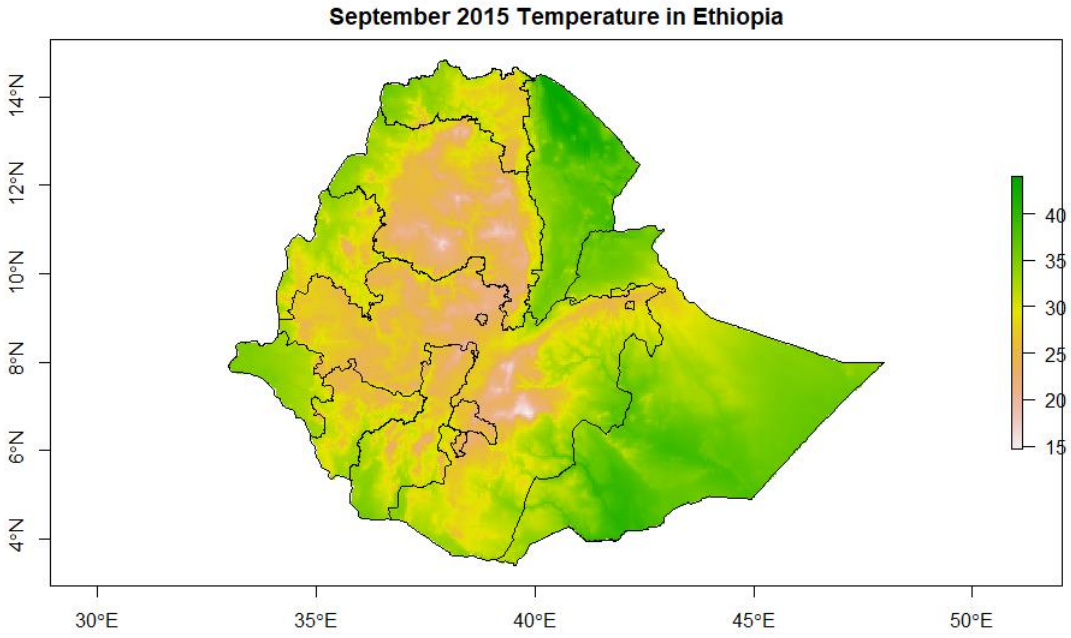

Figure G4: Shapefile of Ethiopia with regional borders and average temperature from September 2011, legend on the right from 15° C to 40° C with Latitude and Longitude Lines

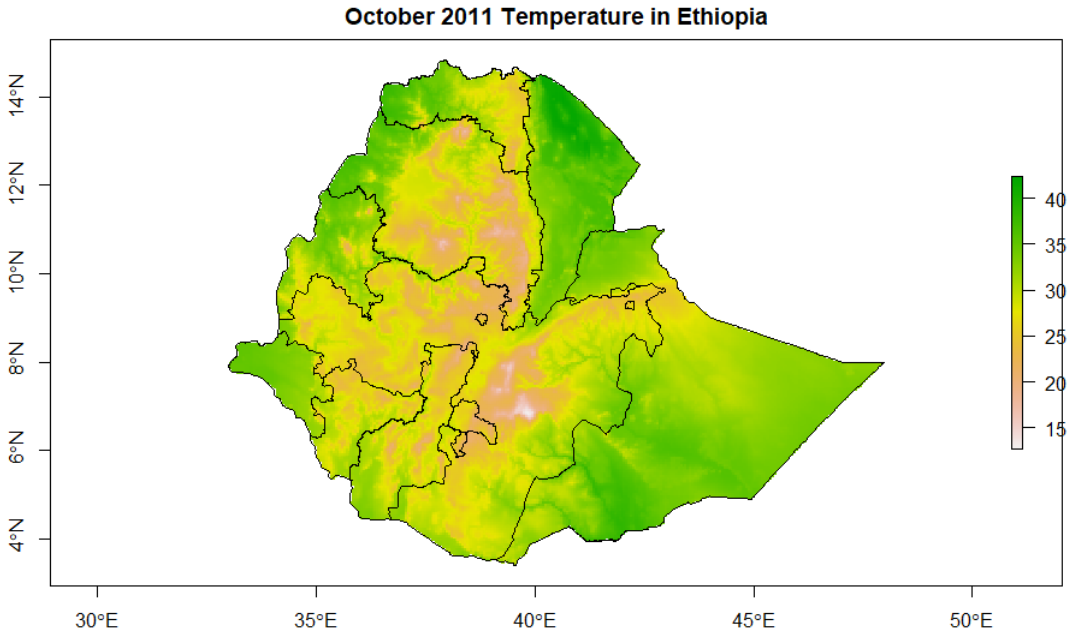

Figure G5: Shapefile of Ethiopia with regional borders and average temperature from October 2011, legend on the right from 15° C to 40° C with Latitude and Longitude Lines

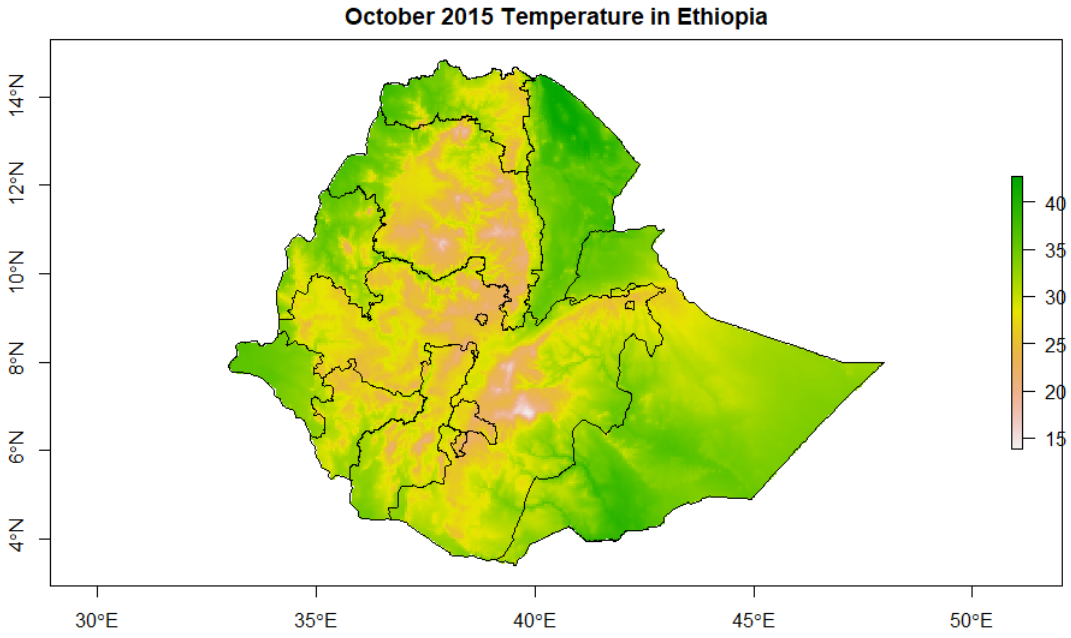

Figure G6: Shapefile of Ethiopia with regional borders and average temperature from October 2011, legend on the right from 15° C to 40° C with Latitude and Longitude Lines

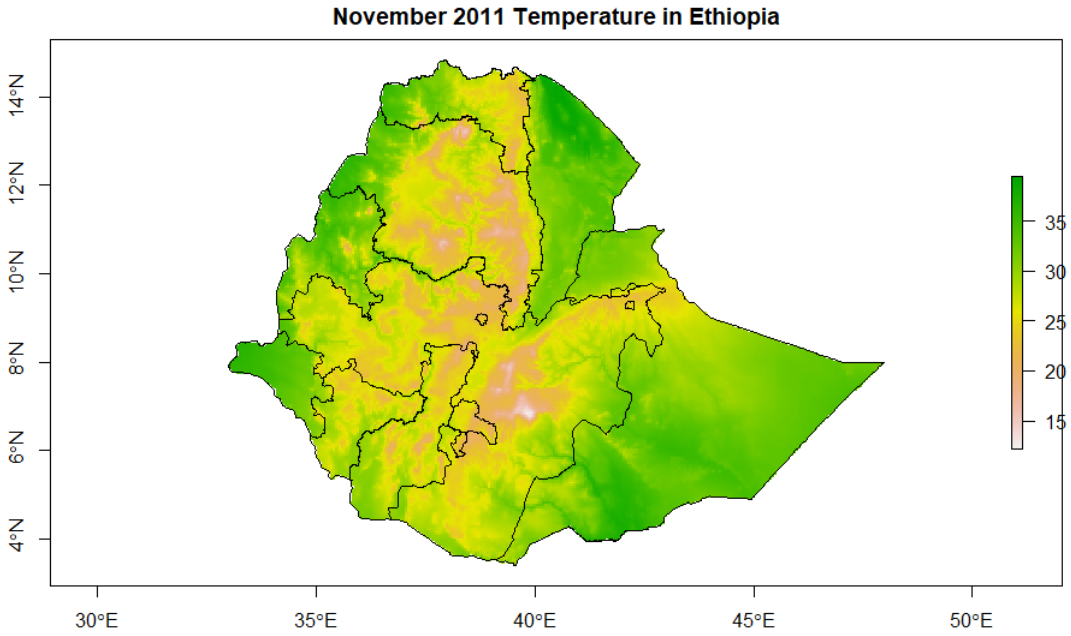

Figure G7: Shapefile of Ethiopia with regional borders and average temperature from November 2011, legend on the right from 15° C to 35° C with Latitude and Longitude Lines

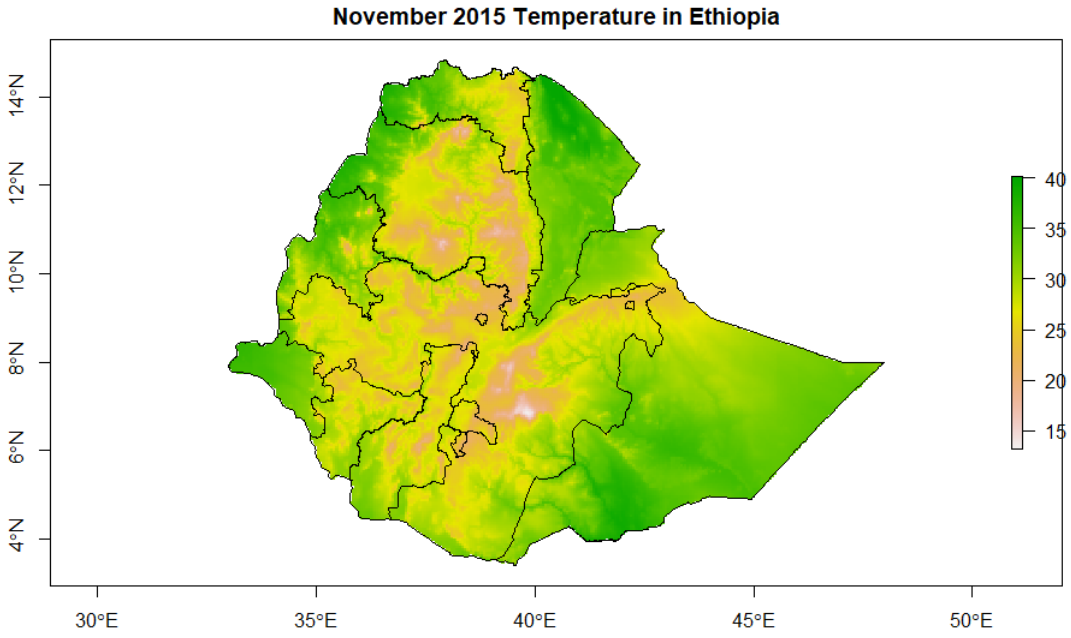

Figure G8: Shapefile of Ethiopia with regional borders and average temperature from November 2011, legend on the right from 15° C to 40° C with Latitude and Longitude Lines

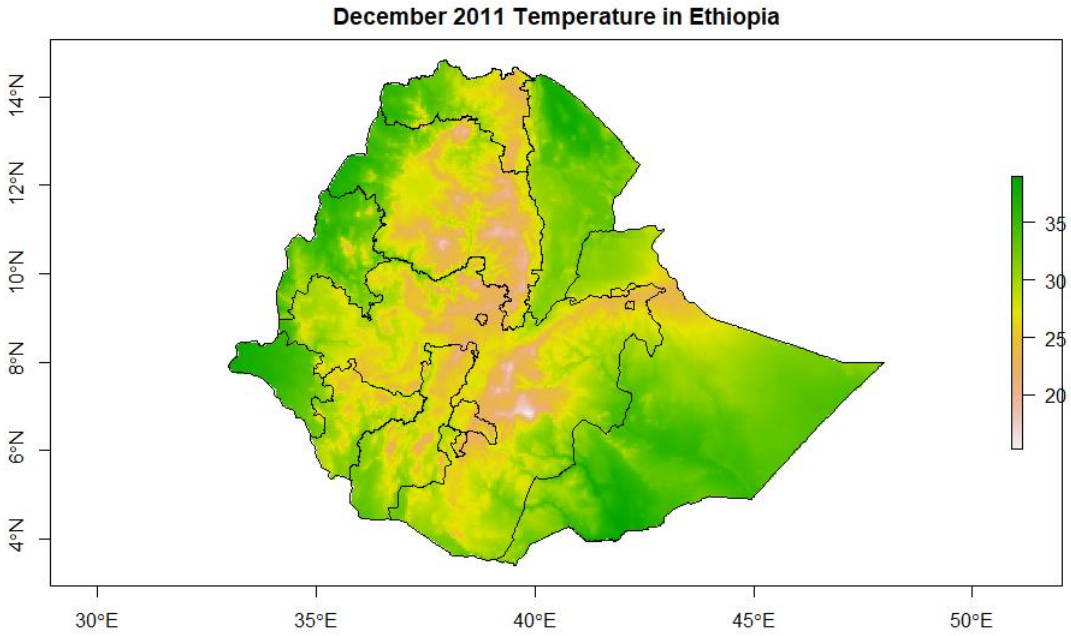

Figure G9: Shapefile of Ethiopia with regional borders and average temperature from December 2011, legend on the right from 15° C to 35° C with Latitude and Longitude Lines

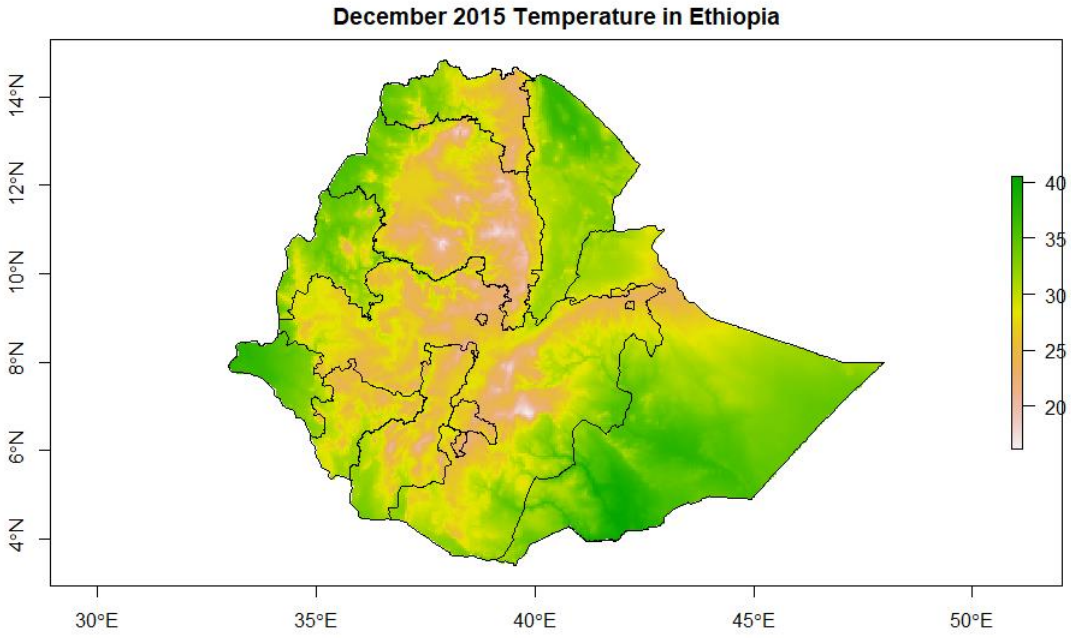

Figure G10: Shapefile of Ethiopia with regional borders and average temperature from December 2011, legend on the right from 15° C to 40° C with Latitude and Longitude Lines

Appendix H: Cluster Prevalence of Antigens Legend

Figure H1: Cluster Prevalence Legend to Reference for the following 24 graphs

Appendix I: Geographic Layers of Cluster Prevalence of Antigens in Ethiopia

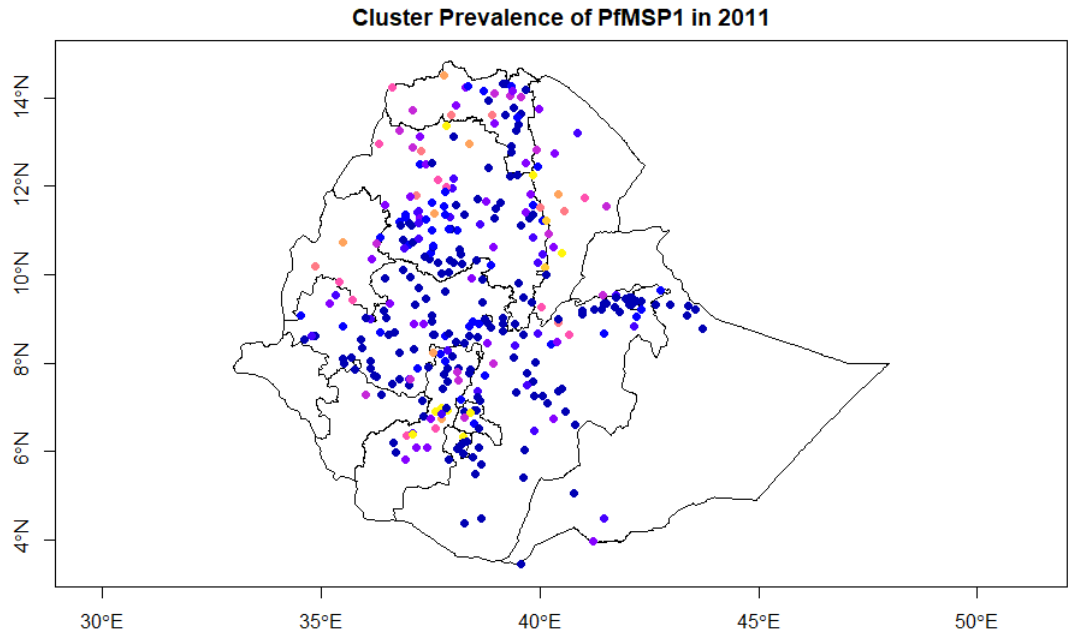

Figure I1: Shapefile of Ethiopia with regional borders and cluster prevalence of *P. falciparum* merozoite protein 1 in 2011 with Latitude and Longitude Lines

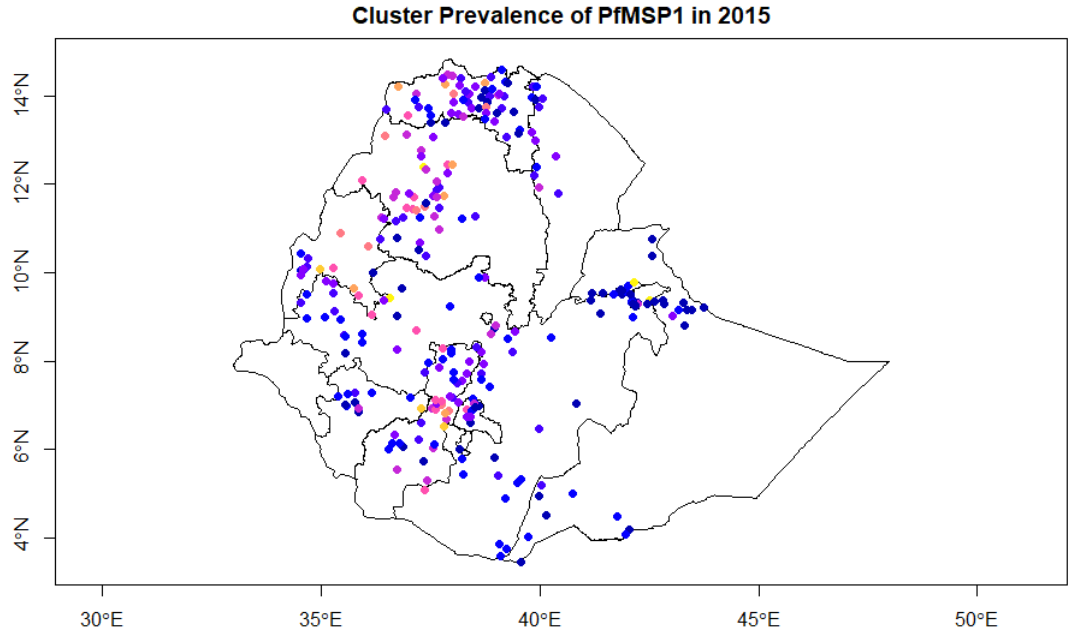

Figure I2: Shapefile of Ethiopia with regional borders and cluster prevalence of *P. falciparum* merozoite protein 1 in 2015 with Latitude and Longitude Lines

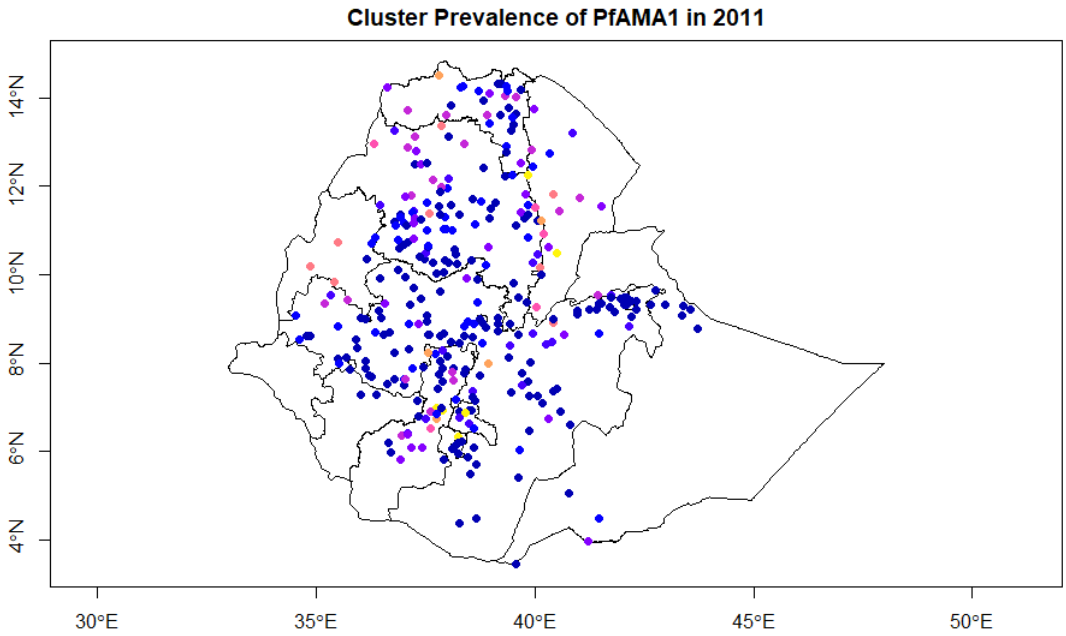

Figure I3: Shapefile of Ethiopia with regional borders and cluster prevalence *P. falciparum* apical membrane antigen 1 in 2011 with Latitude and Longitude Lines

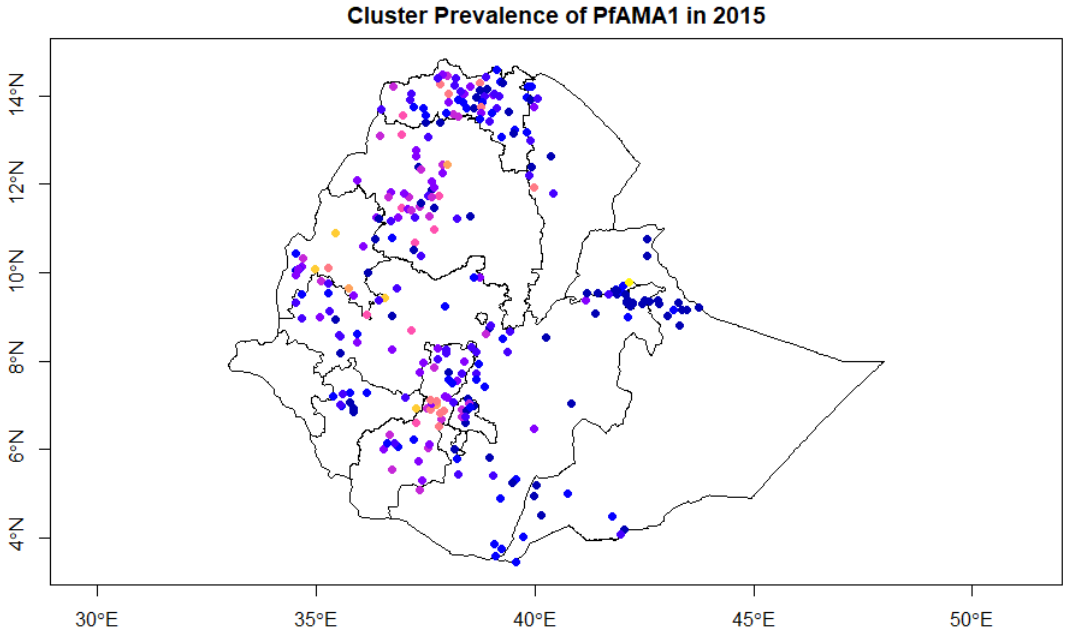

Figure I4: Shapefile of Ethiopia with regional borders and cluster prevalence of *P. falciparum* apical membrane antigen 1 in 2015 with Latitude and Longitude Lines

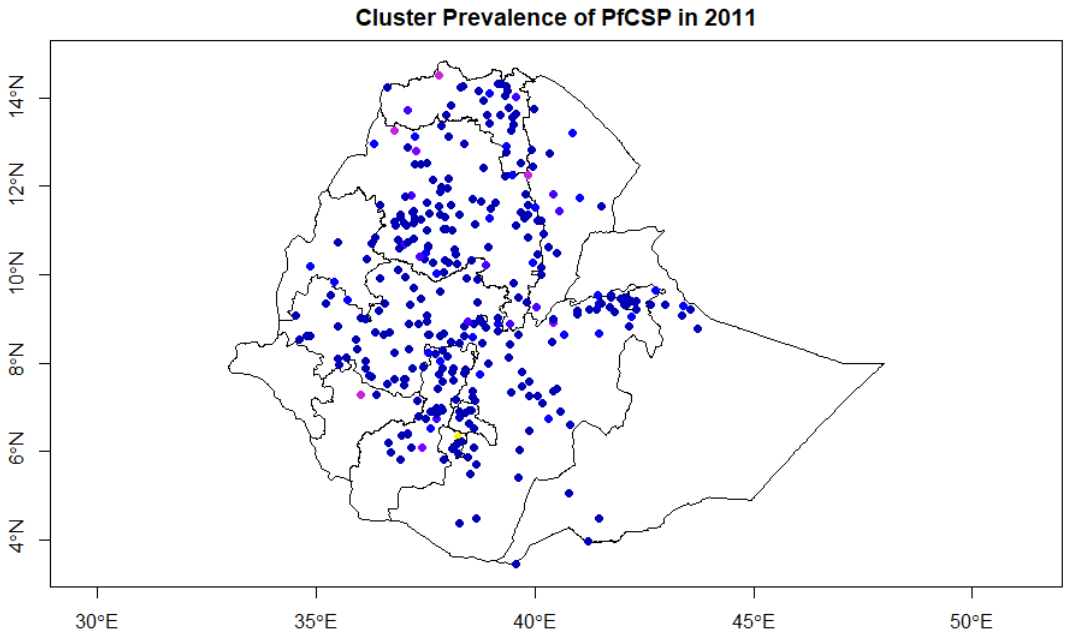

Figure I5: Shapefile of Ethiopia with regional borders and cluster prevalence of *P. falciparum* circumsporozoite protein in 2011 with Latitude and Longitude Lines

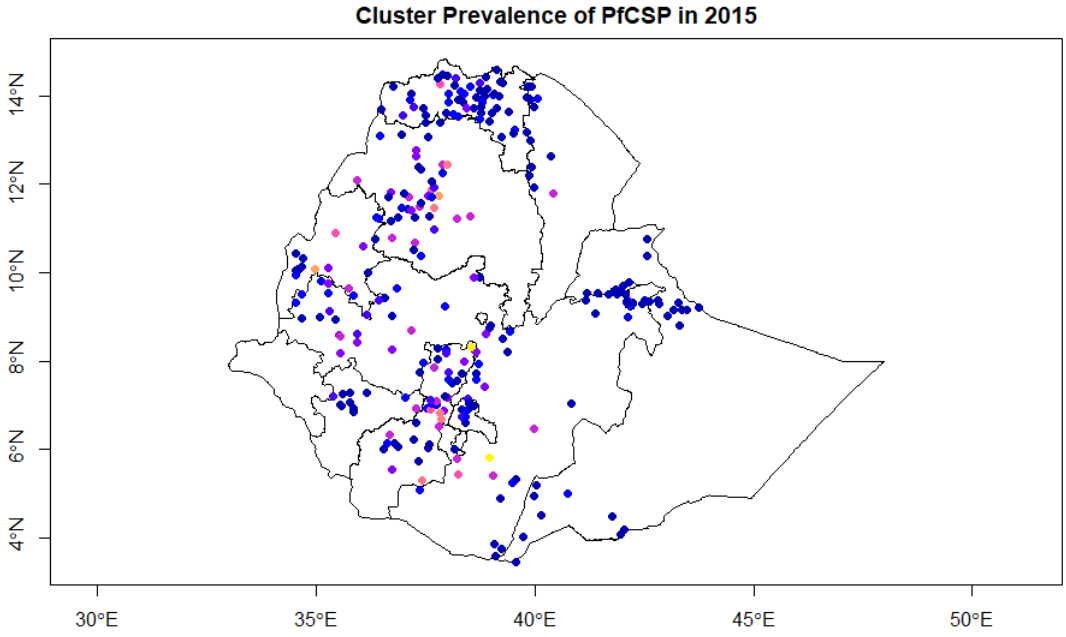

Figure I6: Shapefile of Ethiopia with regional borders and cluster prevalence of *P. falciparum* circumsporozoite protein in 2015 with Latitude and Longitude Lines

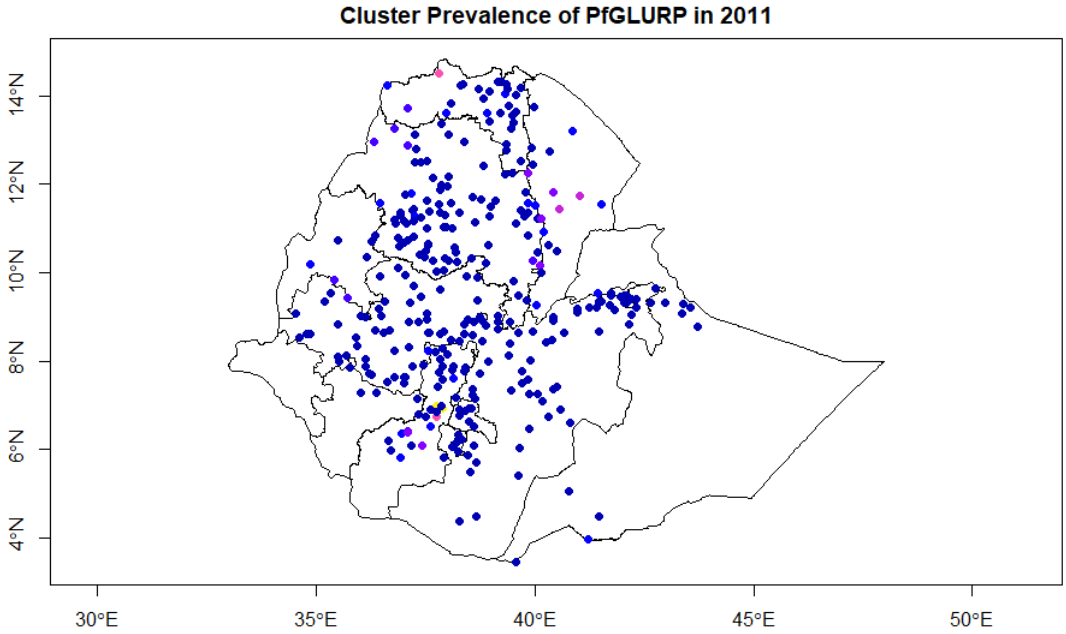

Figure I7: Shapefile of Ethiopia with regional borders and cluster prevalence of *P. falciparum* glutamate-rich protein, Ro fragment in 2011 with Latitude and Longitude Lines

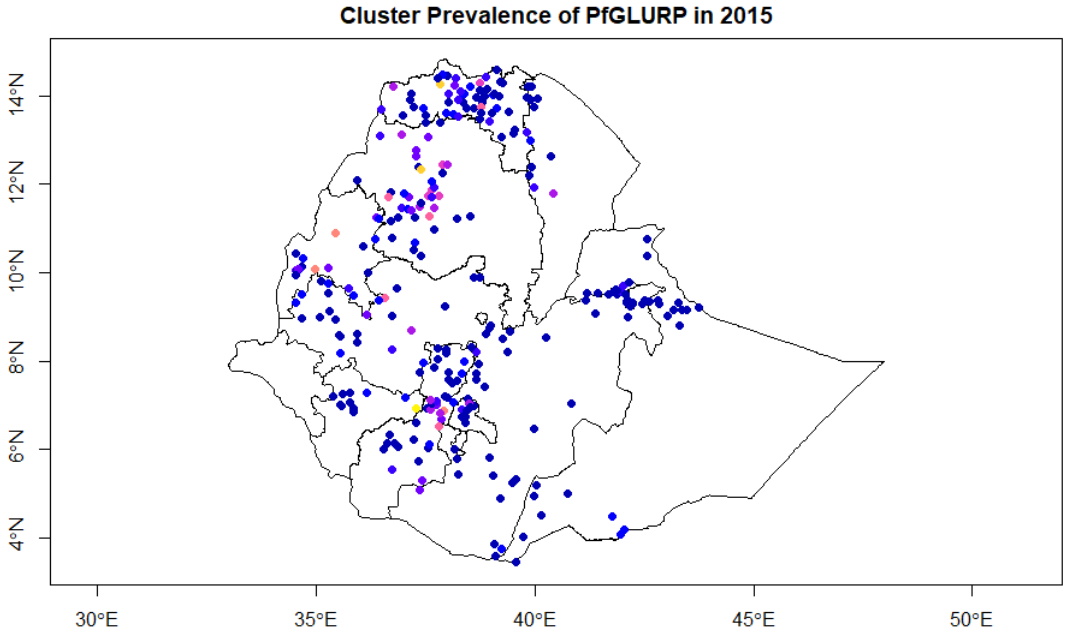

Figure I8: Shapefile of Ethiopia with regional borders and cluster prevalence of *P. falciparum* glutamate-rich protein, Ro fragment in 2015 with Latitude and Longitude Lines

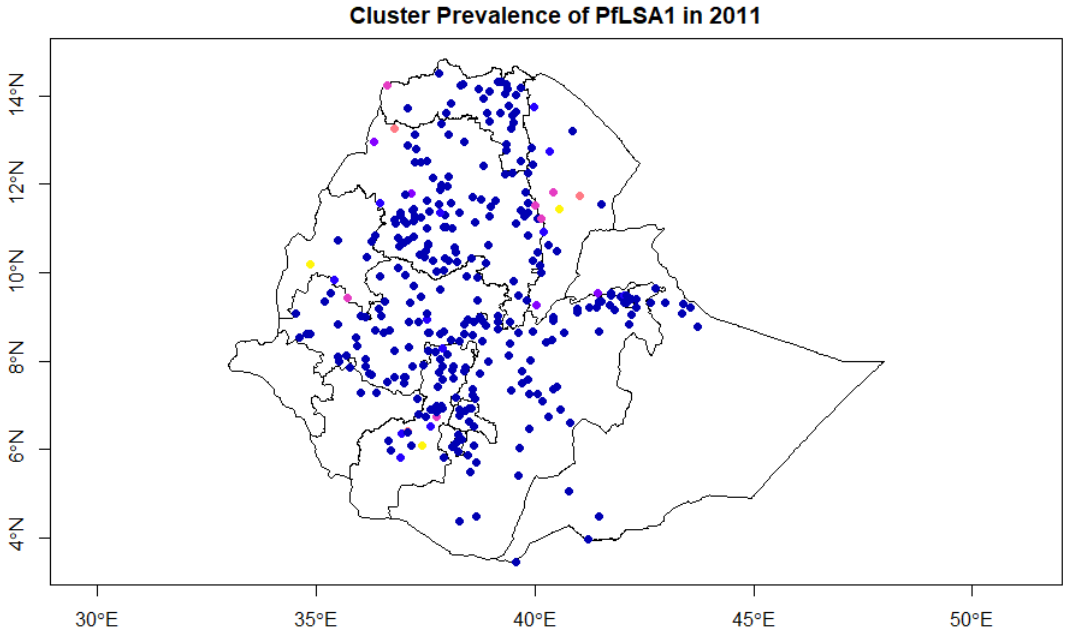

Figure I9: Shapefile of Ethiopia with regional borders and cluster prevalence of *P. falciparum* liver stage antigen 1 in 2011 with Latitude and Longitude Lines

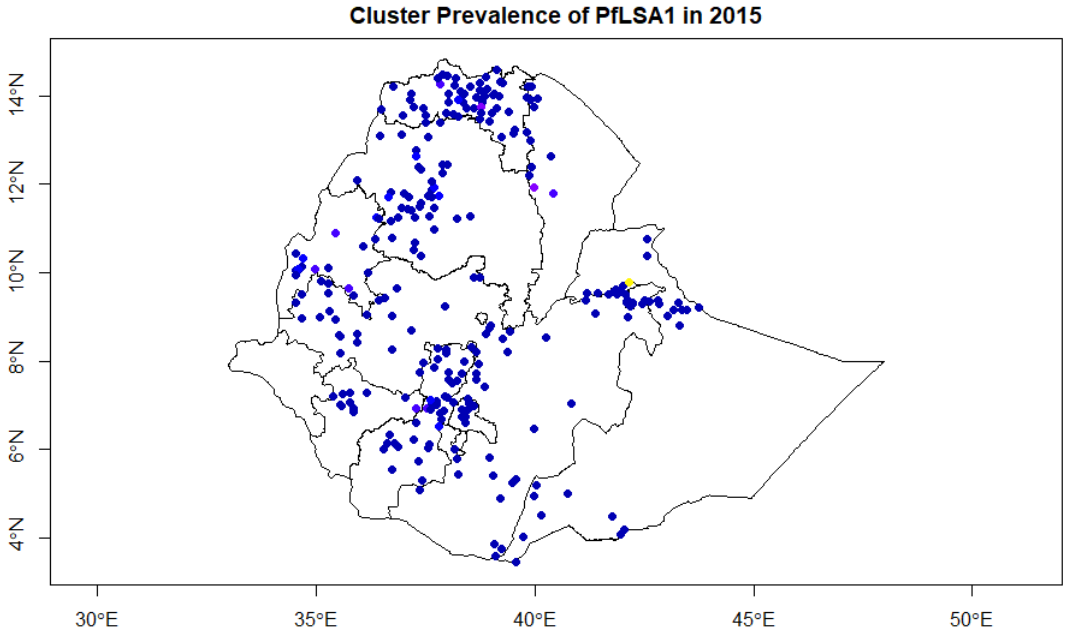

Figure I10: Shapefile of Ethiopia with regional borders and cluster prevalence of *P. falciparum* liver stage antigen 1 in 2015 with Latitude and Longitude Lines

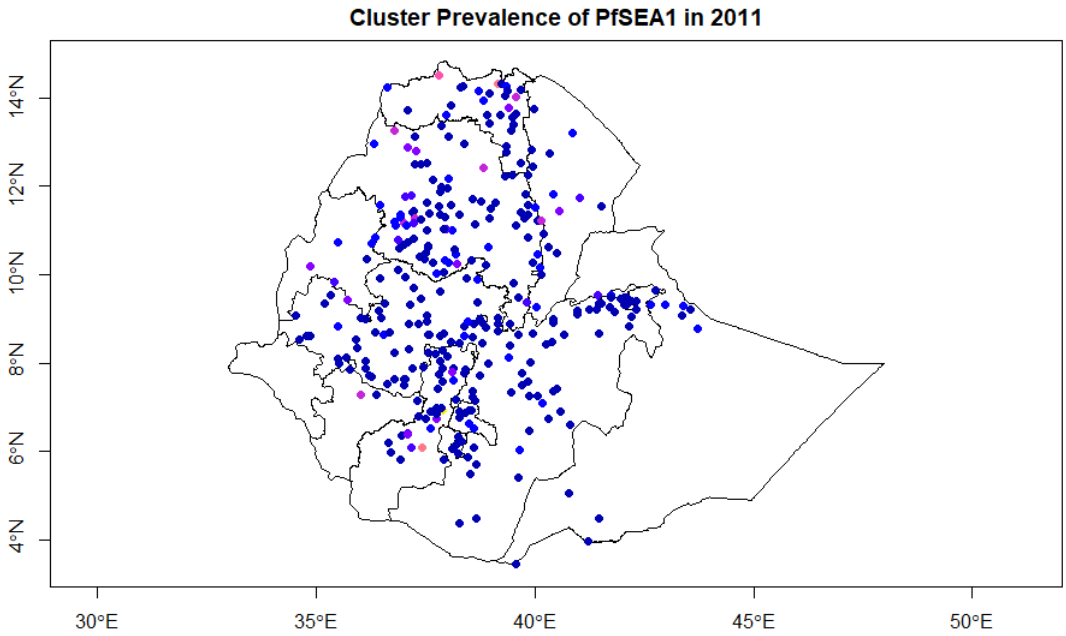

Figure I11: Shapefile of Ethiopia with regional borders and cluster prevalence of *P. falciparum* schizont egress antigen 1 in 2011 with Latitude and Longitude Lines

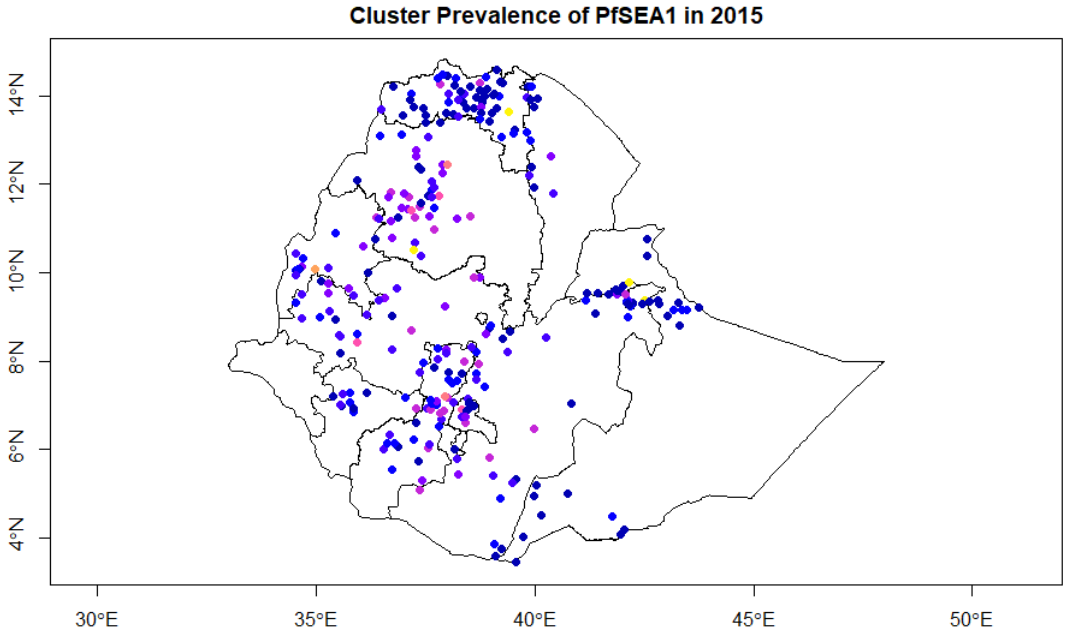

Figure I12: Shapefile of Ethiopia with regional borders and cluster prevalence of *P. falciparum* schizont egress antigen 1 in 2015 with Latitude and Longitude Lines

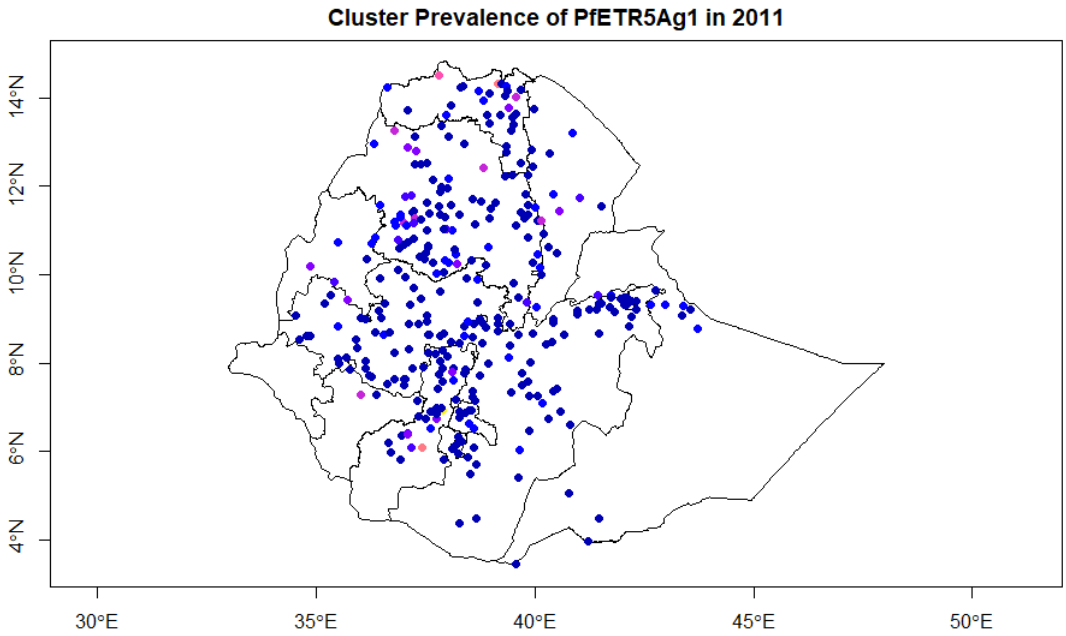

Figure I13: Shapefile of Ethiopia with regional borders and cluster prevalence of *P. falciparum* ETRAMP5 antigen 1 in 2011 with Latitude and Longitude Lines

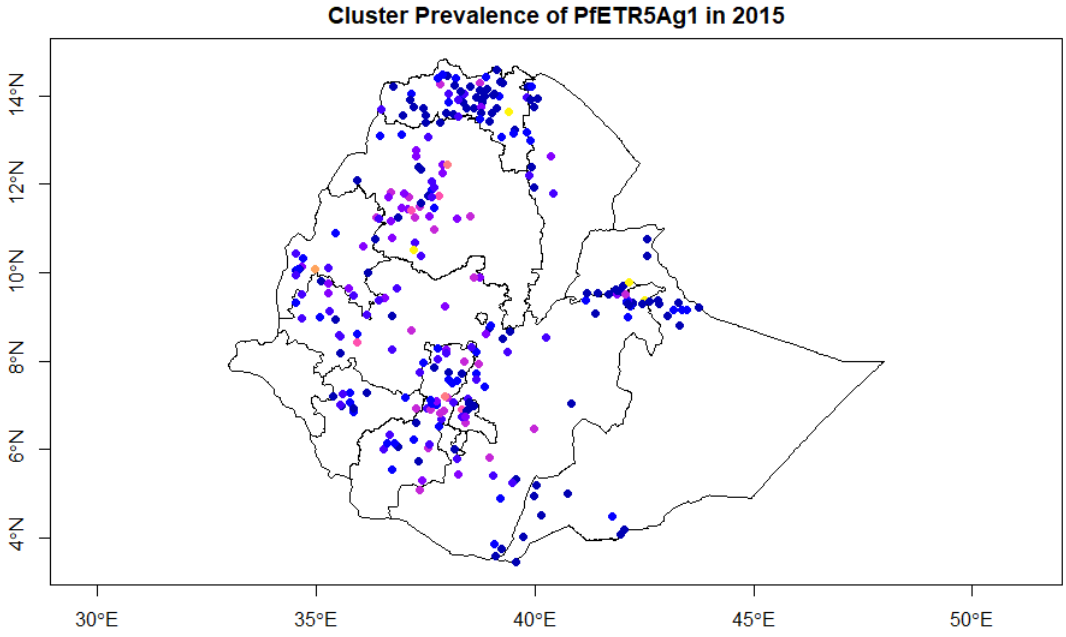

Figure I14: Shapefile of Ethiopia with regional borders and cluster prevalence of *P. falciparum* ETRAMP5 antigen 1 in 2015 with Latitude and Longitude Lines

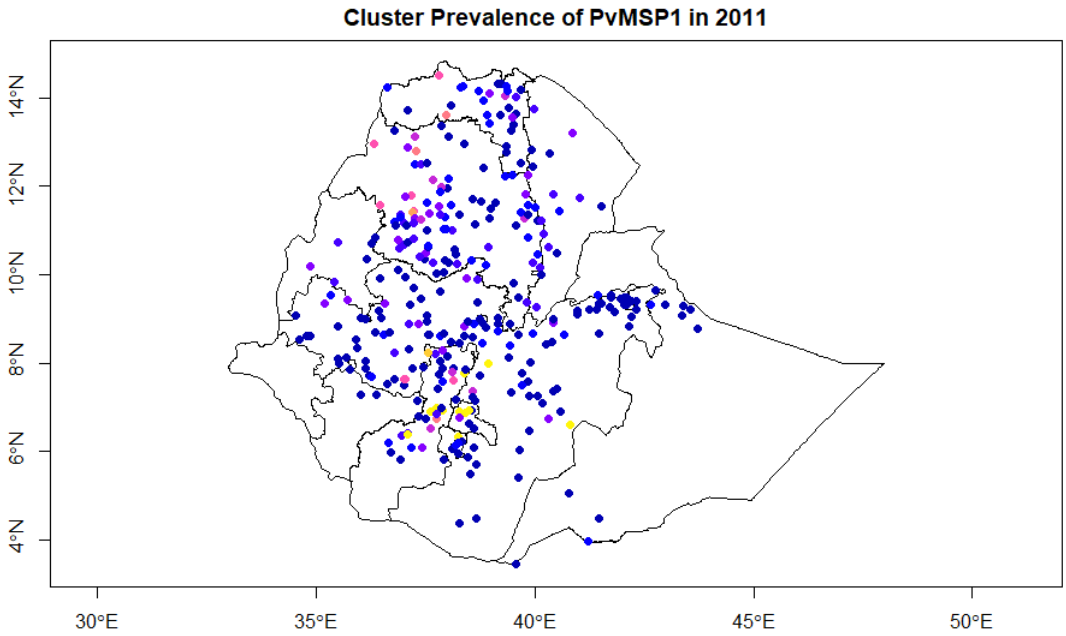

Figure I15: Shapefile of Ethiopia with regional borders and cluster prevalence of *P. vivax* merozoite protein 1 in 2011 with Latitude and Longitude Lines

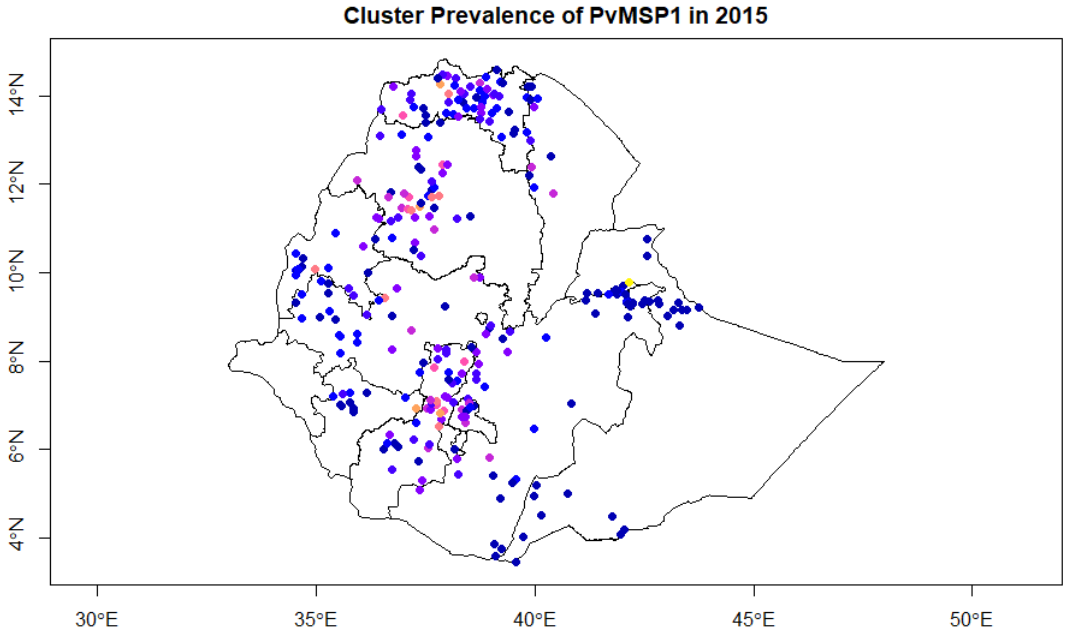

Figure I16: Shapefile of Ethiopia with regional borders and cluster prevalence of *P. vivax* merozoite protein 1 in 2015 with Latitude and Longitude Lines

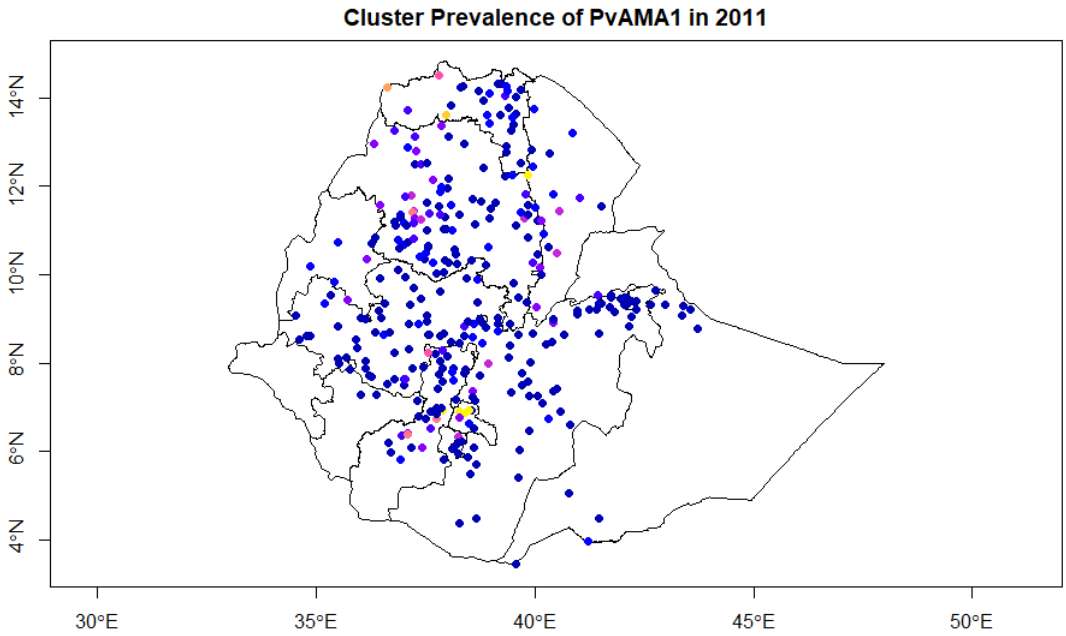

Figure I17: Shapefile of Ethiopia with regional borders and cluster prevalence of *P. vivax* apical membrane antigen 1 in 2011 with Latitude and Longitude Lines

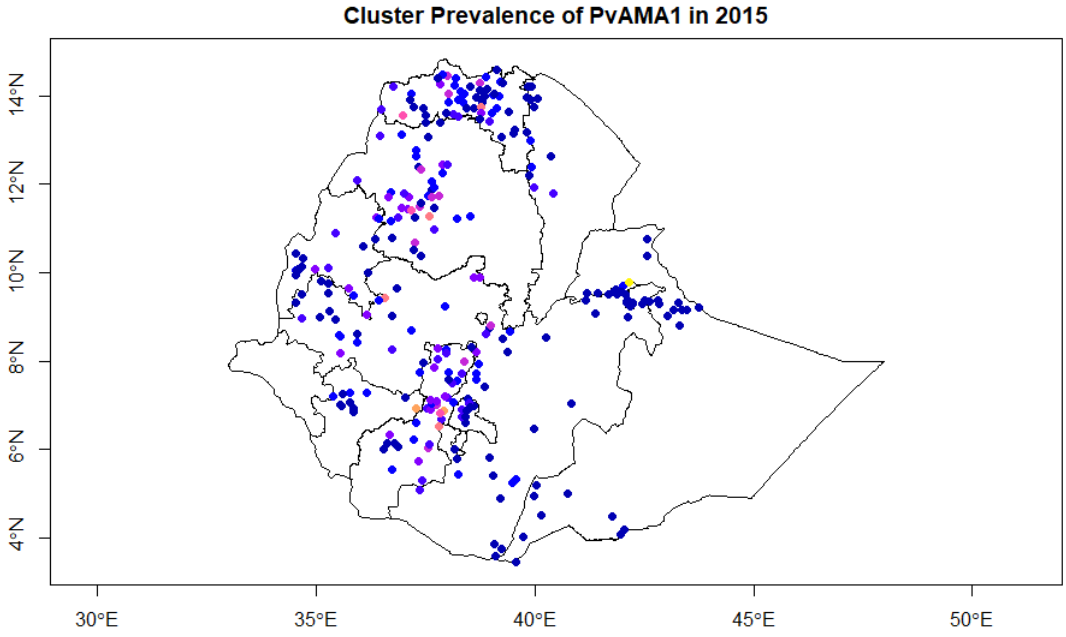

Figure I18: Shapefile of Ethiopia with regional borders and cluster prevalence *P. vivax* apical membrane antigen 1 in 2015 with Latitude and Longitude Lines

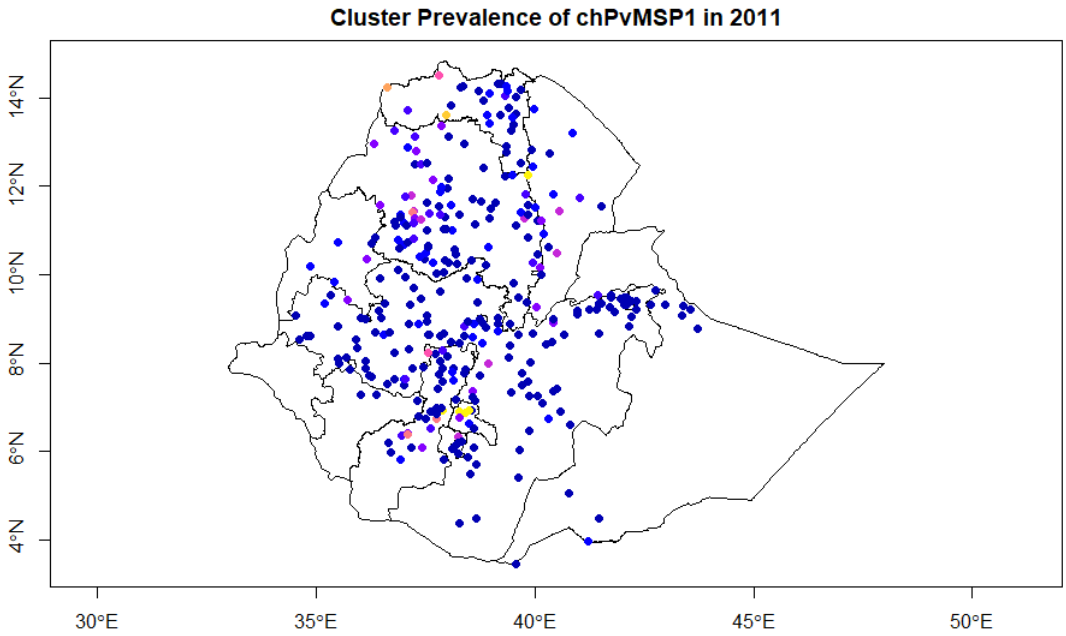

Figure I19: Shapefile of Ethiopia with regional borders and cluster prevalence of chimeric *P. vivax* merozoite protein 1 in 2011 with Latitude and Longitude Lines

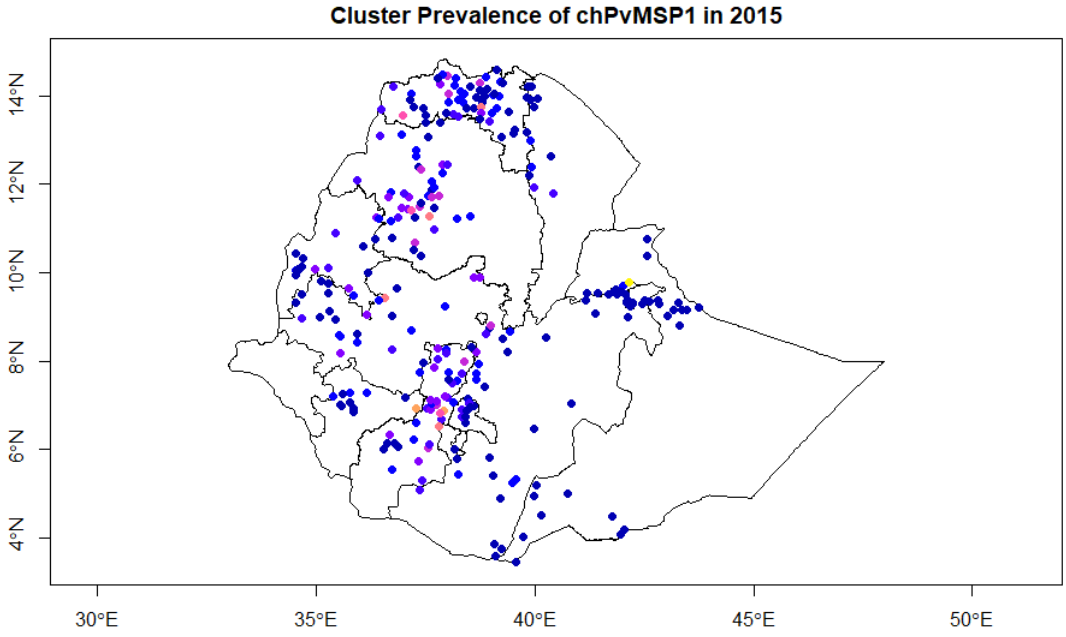

Figure I20: Shapefile of Ethiopia with regional borders and cluster prevalence chimeric *P. vivax* merozoite protein 1 in 2015 with Latitude and Longitude Lines

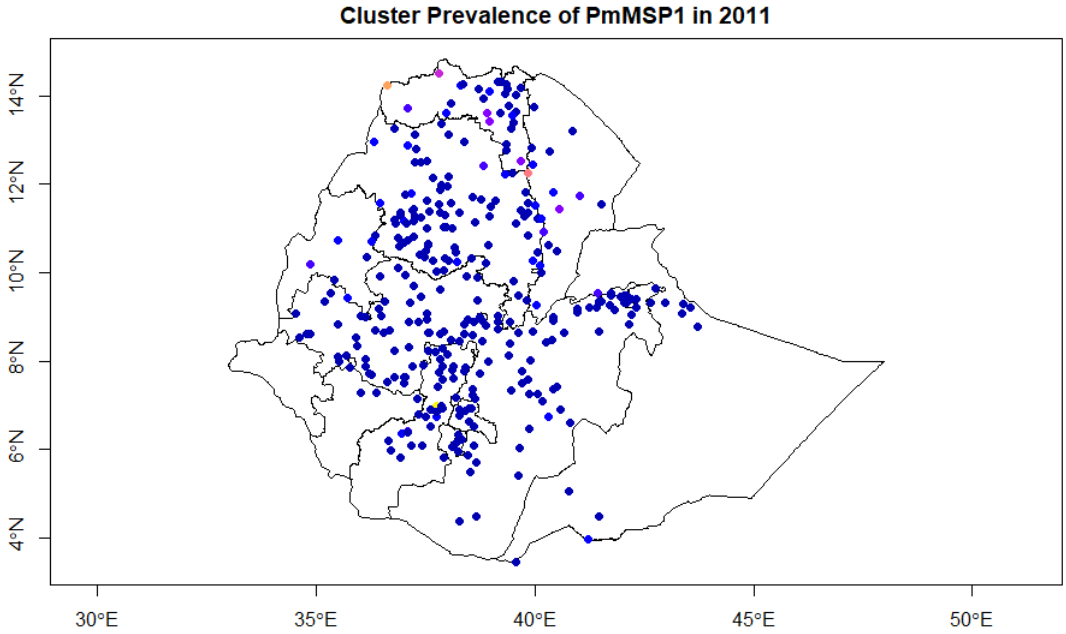

Figure I21: Shapefile of Ethiopia with regional borders and cluster prevalence of *P. malariae* merozoite protein 1 in 2011 with Latitude and Longitude Lines

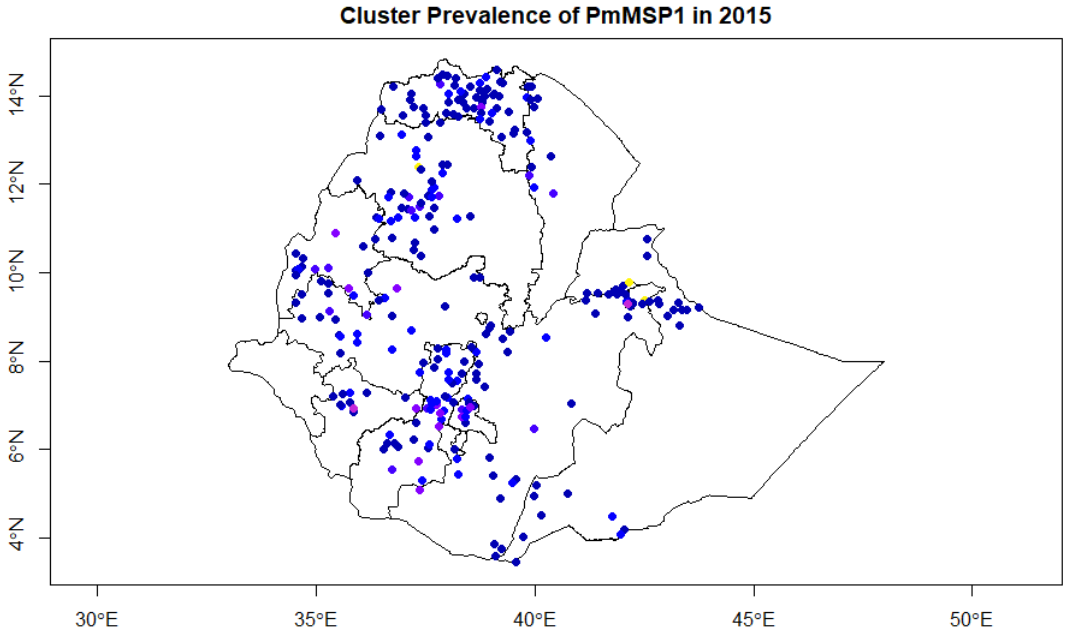

Figure I22: Shapefile of Ethiopia with regional borders and cluster prevalence *P. malariae* merozoite protein 1 in 2015 with Latitude and Longitude Lines

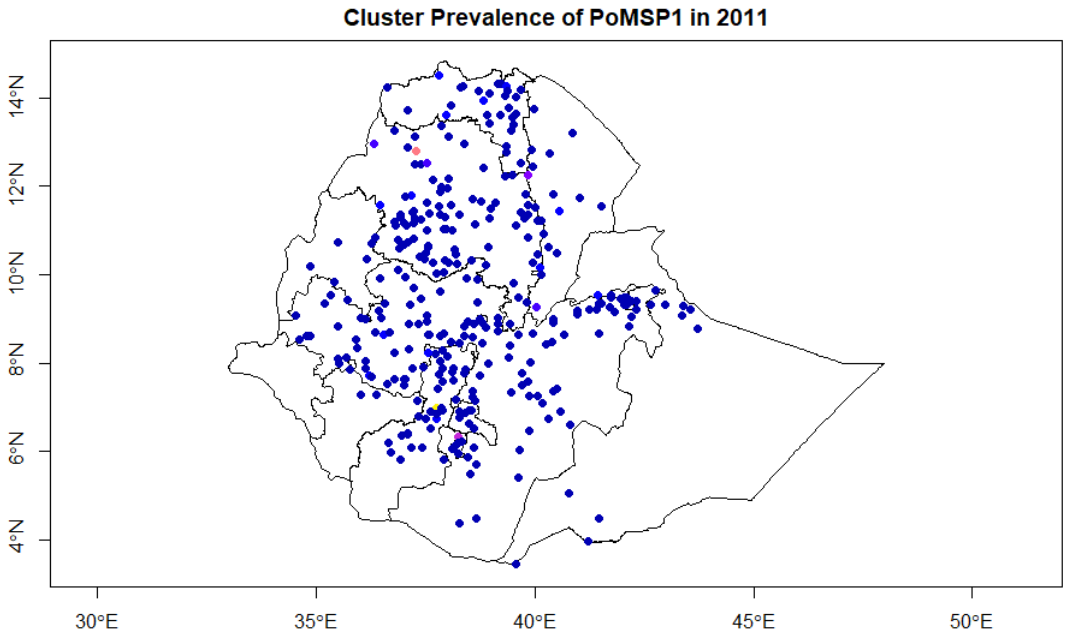

Figure I23: Shapefile of Ethiopia with regional borders and cluster prevalence of *P. ovale* merozoite protein 1 in 2011 with Latitude and Longitude Lines

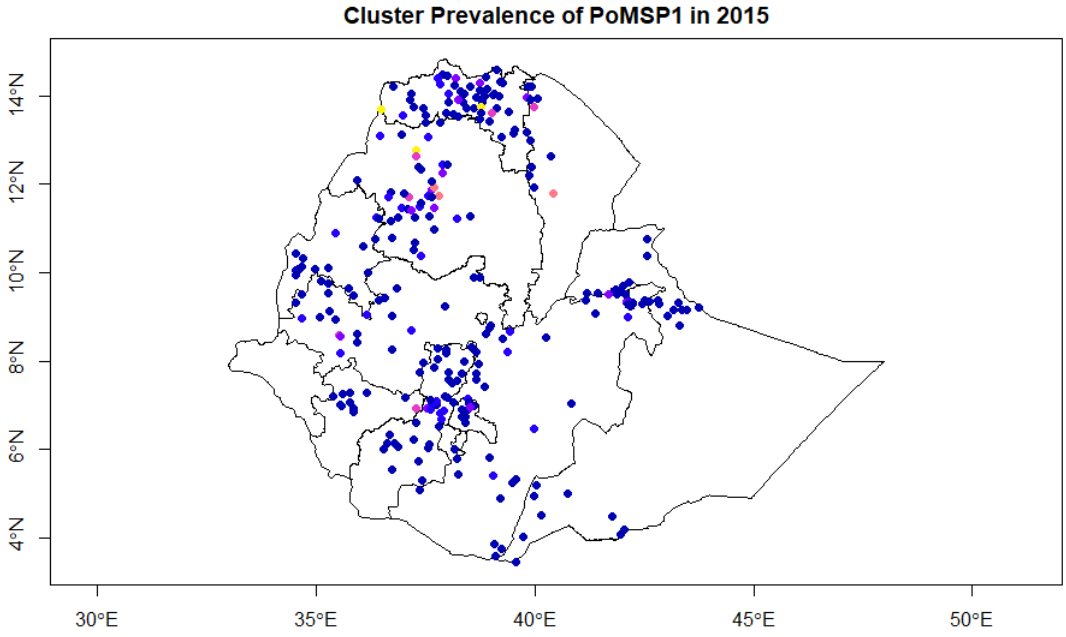

Figure I24: Shapefile of Ethiopia with regional borders and cluster prevalence of *P. ovale* merozoite protein 1 in 2015 with Latitude and Longitude Lines